NASA SP-6008

OFFICE OF MANNED SPACE FLIGHT

APOLLO PROGRAM

STRUCTURAL SYSTEMS AND PROGRAM DECISIONS

Volume 1

Prepared by
APOLLO
PROGRAM OFFICE

NATIONAL AERONAUTICS AND SPACE ADMINISTRATION
Washington, D.C. 20546

NASA SP-6008

APOLLO PROGRAM

OFFICE OF MANNED SPACE FLIGHT

STRUCTURAL SYSTEMS AND PROGRAM DECISIONS

Volume 1

Prepared by
APOLLO PROGRAM OFFICE

NATIONAL AERONAUTICS AND SPACE ADMINISTRATION
Washington, D.C. 20546

For sale by the Clearinghouse for Federal Scientific and Technical Information
Springfield, Virginia 22151 – Price $4.50

FOREWORD

This document, though an official release of the Apollo Program Office, is furnished for information purposes only. Its purpose is to create awareness, stimulate interest and further promote understanding in the art and science of making real-life forecasts and their subsequent utilization in the control of space vehicle weight and performance throughout the Apollo Program.

This book is primarily intended for those in the Apollo Program who are responsible for the administration, design, development, manufacture, and test of the Apollo System. New theorems have been developed, as well as application of proven techniques but more importantly, a weight/performance forecasting methodology has been developed and automated. The text emphasizes the utilization of forecasting devices as applied to space vehicle weight and performance since these two parameters are of vital interest to all levels of management as well as technical personnel. Further, weight is tangible and readily measurable and can be readily related to performance.

The text provides, to those who wish to apply the developed methodology, all details necessary to do so and includes the mathematical development, computer program user's manuals and necessary instructions and procedures.

Forecasts and Appraisals for Management Evaluation text is intended to be a constructive aid to the NASA Apollo team in assisting them in the weight and performance area.

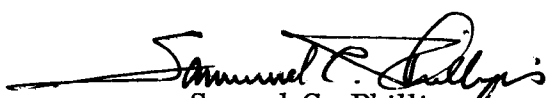

Samuel C. Phillips
Major General, USAF
Director, Apollo Program

ACKNOWLEDGMENT

It is important to recognize those individuals who have contributed to this work, and to assure others who have aided in no less important way that omission is unintentional.

The Apollo Program Office, Major General Samuel C. Phillips, USAF, Director and Mr. Gilbert L. Roth and Mr. Carl R. Liebermann provided overall basic development and technical supervision. The detailed development, computer programming and checkout was provided by the General Electric Company's Apollo Support Department in Daytona Beach, Florida and the Re-Entry Systems Department in Philadelphia.

Finally, material and ideas have been extracted from numerous references which are listed at the end of this manual.

List of Nomenclature is Included in Applicable Sections

TABLE OF CONTENTS

List of Nomenclature is Included in Applicable Sections

TABLE OF CONTENTS (Cont.)

List of Nomenclature is Included in Applicable Sections

TABLE OF CONTENTS (Cont.)

List of Nomenclature is Included in Applicable Sections

LIST OF ILLUSTRATIONS

List of Nomenclature is Included in Applicable Sections

LIST OF ILLUSTRATIONS (Cont.)

List of Nomenclature is Included in Applicable Sections

LIST OF ILLUSTRATIONS (Cont.)

List of Nomenclature is Included in Applicable Sections

LIST OF TABLES

List of Nomenclature is Included in Applicable Sections

LIST OF TABLES (Cont.)

PREFACE

This book describes a program which is designed to provide a means of rapidly assessing the impact of design criteria changes on launch vehicle structural weight. The program is kept as flexible as possible with necessary specialization of techniques or usage aimed at the Saturn V Launch Vehicle. To accomplish this a computer program has been developed which is capable of operating on the GE 625/635, IBM 7044 or IBM 7094 computers.

The material presented in this book is organized into two volumes. Volume 1 contains the general description, typical results, and recommendations for future work. Enough of the details are included in Volume 1 to allow a general understanding of the analysis and its use within the present scope of the program.

Volume 2 provides additional information about the programming aspects and the flow of logic within the computer program. This volume will be of particular use to those personnel in the computer facilities where this program will be used.

SECTION 1

INTRODUCTION

1.1 GENERAL

This book is written for those decision-makers who assimilate, validate, and interpret changes in baseline requirements on space vehicle programs. It provides results and "tools" which support the decision-making process when design criteria, design philosophy, geometrical constraints or environmental considerations are to be examined for their effect on the structural system of a given space vehicle. The procedures and techniques are applicable regardless of size or type of program, from the proposal to the operational phase.

Space program managers who have the responsibility for the management of complex research and development efforts such as the Apollo Program must be capable of making decisions in many technical and administrative areas. In maintaining control of total program performance, an acute awareness of schedule, cost, and technical performance must be maintained at all times; for these are the baseline requirements against which progress is measured and upon which decisions will be made. Because of the intricate relationships between the countless elements of a space program, a single decision may affect more of the program than just that one problem it is solving. Accordingly, most decisions can only be made after considerable study and detail analysis of possible side-effects. This presents a manager with the monumental task of making the optimal decision in view of the many technical and administrative considerations.

To make good decisions and provide proper direction a manager must have an excellent source of factual information. The capacious scope of modern technology with its resultant reports almost defies a manager's ability to comprehend the total picture. He is forced to put an increasing reliance on assessment techniques which are readily adaptable to the management processes of decision making and problem solving. Many management tools are available for immediate application to schedule and cost problems, but very few are available in the technical performance area, and yet every program manager must make technical decisions.

At the program management level, as well as down through the successive management levels, on through to the designer and shop mechanic, there are baseline requirements which must be met. Such requirements are normally described by engineering drawings, and in project and program specifications. Throughout the development of a program, changes are made in design criteria, design philosophy, geometrical constraints and environmental considerations. Such changes when fully justified are reflected in revised engineering releases, and through specification revisions. As in all systematically organized programs, all changes in baseline requirements must go through an approval cycle (normally a change control board) to assure that all aspects of a change are fully assessed for possible program impacts. If a manager is to approve a proposed change, he must have the assurance that the objective of the change will be met. Neither he nor his subordinates are expected to conduct detail analyses to check the results supporting the change proposal, but he must have a management tool which allows the rapid validation of such results.

There are many types of technical tools, for example a pound of launch vehicle hardware can readily be expressed in terms of equivalent payload. Similarly, a change in engine performance can easily be related to propellant requirements. These are tools of the trade, so to speak, but they are elementary and do not allow a manager to examine the effects a change in the design criteria of one system may have on the physical parameters of another system. These reasons are more than sufficient to justify the development of the techniques described herein, and fill a major part of the gap in the technical performance-management decision area.

The importance of the structural system to overall space vehicle performance becomes readily apparent when it is considered that launch vehicle stage performance or efficiency is directly related to stage mass fraction (the ratio of stage propellant to total stage weight), values of which normally range between 0.85 and 0.95. Except for refined propellant loading techniques, little else can be done to improve stage performance through the propellant. Thus, 85 to 95 percent of a stage is not subject to more than minor changes once loading techniques have been optimized. Of the remaining 5 to 15 percent of the stage weight, approximately one-half is structural weight and the remaining half (exclusive of instrumentation) is attributable to the propulsion system including engines, plumbing residuals, reserves, etc. Since the propellant loading is relatively

fixed, the structural weight is a logical place to improve stage performance, even though a lesser percentage of the total stage weight is involved. Accordingly, frequent recommendations to improve stage efficiency are made on the basis of structural design criteria refinements. If design criteria are changed, a resultant impact on the launch vehicle can easily occur, since changes are normally reflected in additional engineering hours, design drawings, tooling, and testing. Therefore, from a management, decision-program impact viewpoint, it is very important that proposed design criteria changes be assessed in a rapid and efficient manner to provide management with an early assurance that the indicated performance gain can be achieved. This can best be accomplished with the aid of a digital computer program which synthesizes a structure for loads which are imposed on a launch vehicle for a specified mission, and then calculates the total weight or the change in the weight of the structure, and ultimately expresses this change in terms of payload or other suitable parameters.

The Apollo Program Office in Washington, D. C., has developed a computerized procedure which cannot only assess changes but will optimize structural systems similar to those of the Saturn V launch vehicle. The program is capable of handling the materials normally used in aerospace launch vehicle construction and the following structural configurations: monocoque, semi-monocoque, 90° waffle, 45° waffle, integral stringer and ring, corrugation, and honeycomb sandwich construction. A prime goal was to keep the program as general and flexible as possible within the general constraints of funding and scheduling, but, if necessary, any specialization of techniques or usage was aimed toward the Saturn V launch vehicle as it is used for the Apollo mission.

1.2 OBJECTIVE

The objective of the Weight/Performance Constraint Analyses Structures Task is tied closely with the needs of program management, and this is the ability to assess quickly the impact upon the program of various changes in design, criteria, etc. With respect to structural weight, this objective can best be reached through the use of a computer program for structural optimization which is applicable to the Saturn V launch vehicle and, at the same time, has the following capabilities:

a. Compare various structural configurations to determine the minimum weight construction for the specific application.

b. Compare weights of "optimum design" structures made from various materials which are acceptable for the specific application.

c. Determine the approximate weight of the above.

d. Assess the change in structural weight due to changes in loads or design criteria.

1.3 SCOPE

The decision of how much detail should be considered in defining the loads on the launch vehicle components was based, to a great extent, upon the objectives of this task. This is true also of the question of which types of construction to include in the program; how refined should the stress analysis be, i.e., whether or not to include such things as discontinuity stresses, thermal stress, inelastic properties, etc.

Table 1-1 gives a brief outline of the capability chosen to be included in the loads definition. Essentially, the process of load calculation is that tank volumes are calculated and then liquid levels are determined at the time of interest. The hydrostatic and internal pressure stress resultants are then calculated and combined with the resultants of bending moment and axial loads due to aerodynamic and control considerations.

Table 1-1

Summary of Items Considered by the STRESS Program

	Shell Analyses			
	Right Circular Cylinder	Conical	Spherical	Ellipsoidal
Axial Load	Yes	Yes	No	No
Gas Pressure Loading	Yes	Yes	Yes	Yes
Hydrostatic Loading	Yes	Yes	Yes	Yes
Beam Bending Moment	Yes	Yes	No	No
Non-Axisymmetric Loads	No	No	No	No
Axisymmetric Loads	Yes	Yes	Yes	Yes
Tank Volume Calculations	Yes	Yes	Yes	Yes
Liquid Level Determination	Yes	Yes	Yes	Yes

1.4 TECHNICAL CONSIDERATIONS

The Weight/Performance Constraint Analyses Structural Program is composed of three major elements. These are (1) the Generalized AeroSpace Program (GASP), (2) the Loads Analysis for Saturn Structures (LASS-1), and (3) the Structural Weight Optimization Program (SWOP). The general organization of these programs with respect to one another, as well as the important input and output parameters, are shown in Figure 1-1. The GASP is a rigid-body analysis which uses the overall normal and axial aerodynamic force coefficients. The vehicle is subjected to a synthetic wind profile while the control system is attempting to keep the vehicle on a nominal trajectory. The outputs of GASP (such as accelerations, angle of attack, engine gimbal angle, etc.) are used as inputs to the LASS-1 Program. In the LASS-1 Program, the vehicle is considered as a non-uniform beam along which the aerodynamic and inertia forces are distributed. The force distributions are integrated numerically to find the axial force and bending moment distributions at the preselected times of interest. Input and output summaries of GASP and LASS-1 are presented in Table 1-2, and the major elements included in these two programs are summarized in Table 1-3.

The SWOP program considers the launch vehicle to be composed of elliptical and conical shells. This program contains several subprograms controlled by an executive control program as shown in Figure 1-2. One of the subprograms which is of primary importance in SWOP is the STRESS subprogram. STRESS calculates the hydrostatic, hydrodynamic, and ullage pressure loadings in the propellant tanks and combines the pressure loads with the force and moment distributions from LASS-1. These total loads are then resolved into orthogonal stress resultants in the plane of the structural components. This procedure of load calculation is repeated for every time point in the mission selected for investigation. The other subprograms can then use the stress resultants from STRESS to calculate the structural weight for several types of construction. The types of construction presently included in the SWOP program are illustrated in Figure 1-3. The optimum structure required to withstand this "time" catalog of stress resultants is then determined by suboptimization analyses for each type of construction. The minimum weight configuration for each type of construction can be compared, showing the relative advantages between different types of construction for the given application. It is possible in some applications that it will not be convenient to select the parameters or various types of construction arbitrarily such that an optimum design occurs. For instance, if the total thickness of a waffle section is to be held fixed, while varying some

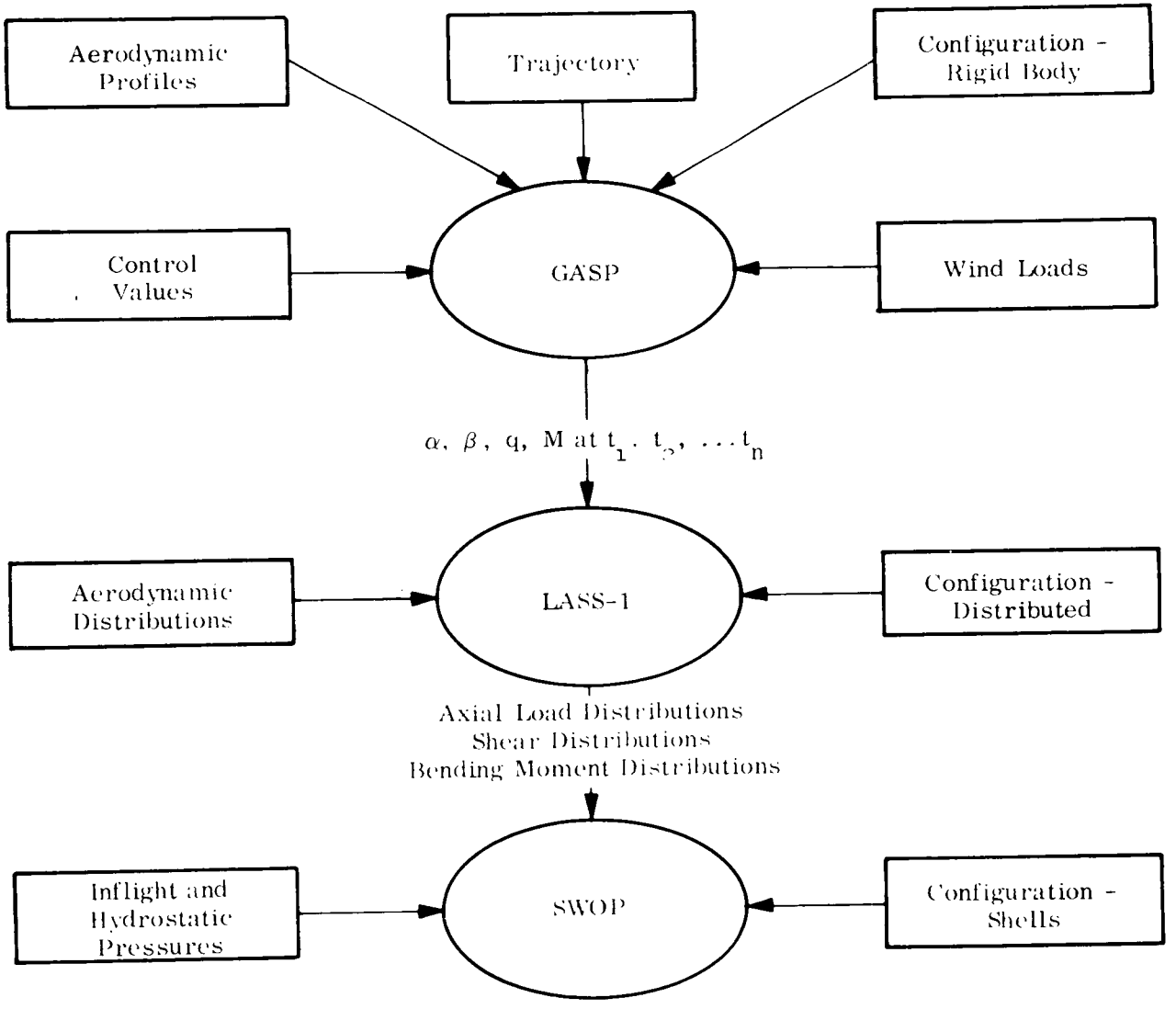

Figure 1-1. Organization of Programs

Table 1-2

Input and Output Summaries

GASP	LASS-1
Input Parameters • Overall normal aerodynamic force coefficient versus mach number. • Overall axial aerodynamic force coefficient versus mach number. • Center of pressure location versus mach number. • Rigid body polar inertia versus flight time. • Control system gains versus flight time. • Wind profile. • Total initial weight and nominal weight rate. • Nominal thrust of engines. • Number of fixed engines. • Number of movable engines. • Nozzle exhaust area. • Reference diameter of vehicle. • Radius of earth. • Acceleration of gravity. • Universal gravitational constant. • ARDC atmosphere model. • Pitch rate profile. • Integration time step.	Input Parameters • Normal force coefficient distributions for several fixed mach numbers. • Non-linear normal force coefficient distributions. • Ground wind profile. • Lateral bending stiffness distribution. • Axial force coefficient distributions for several fixed mach numbers. • Dry weight distribution of vehicle. • Propellant weight distribution with associated burn times. • Total thrust versus time. • Location of engine gimbal point and vehicle hold down points. • Acceleration of gravity. • Reference area of vehicle. • Atmospheric density at sea level. • Several time points which are identified as design points are selected from the GASP outputs with the associated angle of attacks, mach numbers, dynamic pressures, and engine gimbal angles.*
Output Parameters • Engine gimbal angle versus flight time. • Mach number versus flight time. • Lateral acceleration versus flight time. • Angular acceleration versus flight time. • Angle of attack versus flight time. • Dynamic pressure versus flight time.	Output Parameters • Bending moment distribution for each design time. • Axial force distribution for each design time. • Lateral shear distribution for each design time. • Lateral deflection for each design time.

*The gimbal angles from GASP are idealized values and must be increased by a predetermined amount to account for misalignments, actuator error, etc.

Table 1-3

Major Element Summary

GASP		LASS-1	
Rigid body trajectory	Yes	Performs calculations at all time points along the trajectory	No
Elastic body trajectory	No	Performs calculations at preselected time points	Yes
Three degrees of freedom	Yes	Aerodynamic force coefficient distributions are calculated with the program	No
Six degrees of freedom	No	Aerodynamic force coefficient distributions are linearly interpolated from stored tables at fixed mach numbers	Yes
Flat earth	No	Weight distribution at each time of analysis is a required input	No
Round earth	Yes	Weight distribution at each time of analysis is automatically calculated from the stored data	Yes
Minimum drift control system	Yes	Local variations of angle of attack considered	No
Synthetic wind profile with embedded gust - fixed altitude	Yes	Local variations of dynamic pressure considered	No
Synthetic wind profile with embedded gust - variable altitude	No	The analysis uses a static equivalent force approach and the dynamic effects are accounted for by a fixed input factor	Yes
Center of pressure Variable with mach number	Yes	The analysis uses a completely dynamic approach with all vibration and shock effects considered directly	No
Center of gravity Variable with flight time	Yes	Bending moment calculated at all preselected times	Yes
Total weight variable with flight time	Yes	Axial force calculated at all preselected times	Yes
Polar inertia variable with flight time	Yes	Lateral shear calculated at all preselected times	Yes
Thrust variable with atmospheric pressure	Yes	Slope and deflection in lateral direction calculated at all preselected times	Yes
Capability of specifying fixed and gimbaled engines	Yes	Torsional deflections considered	No
Aerodynamic force coefficients are required input	Yes	Space vehicle completely described by E1 distribution	Yes
Aerodynamic force coefficients are calculated within the program	No		

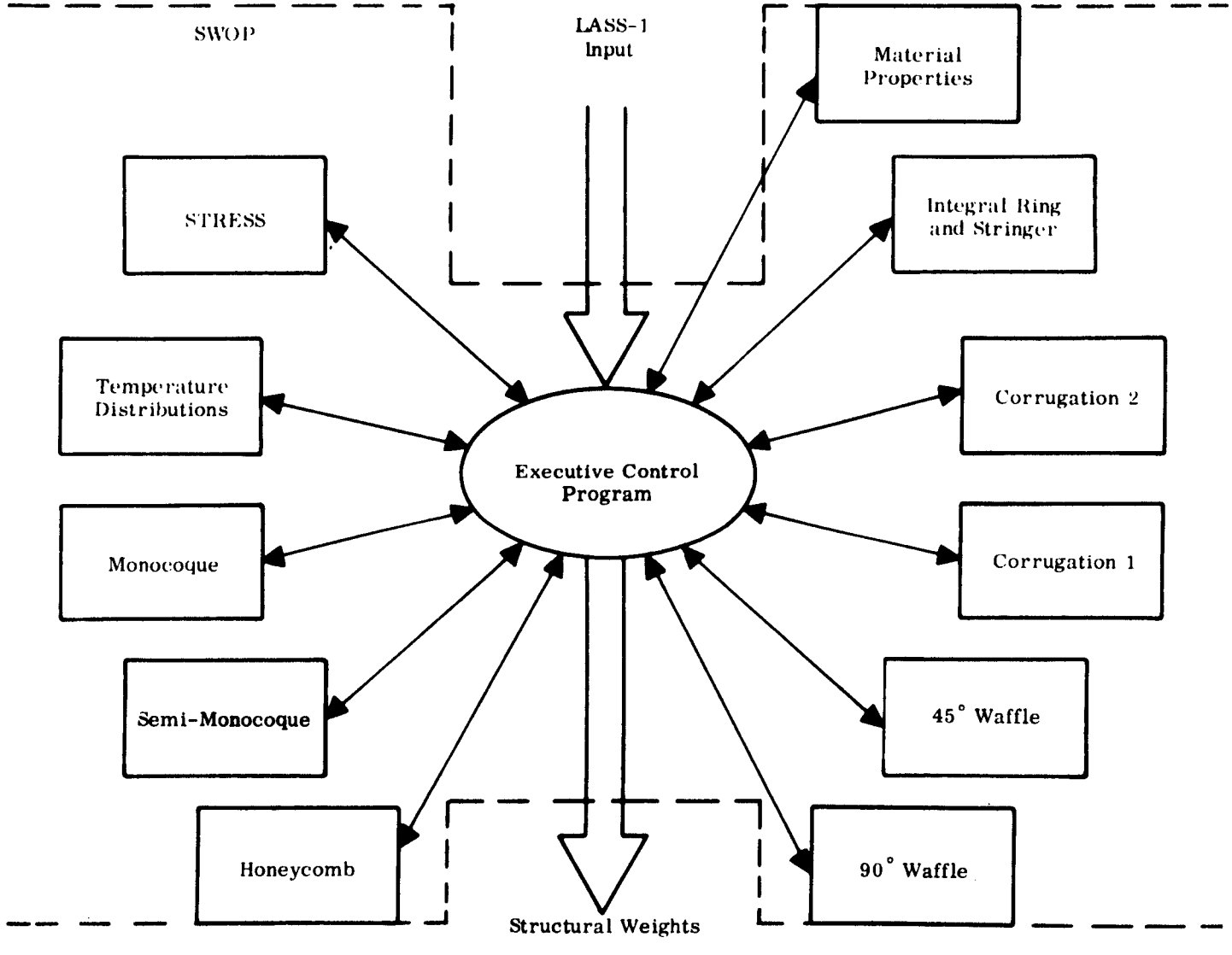

Figure 1-2. Organization of SWOP

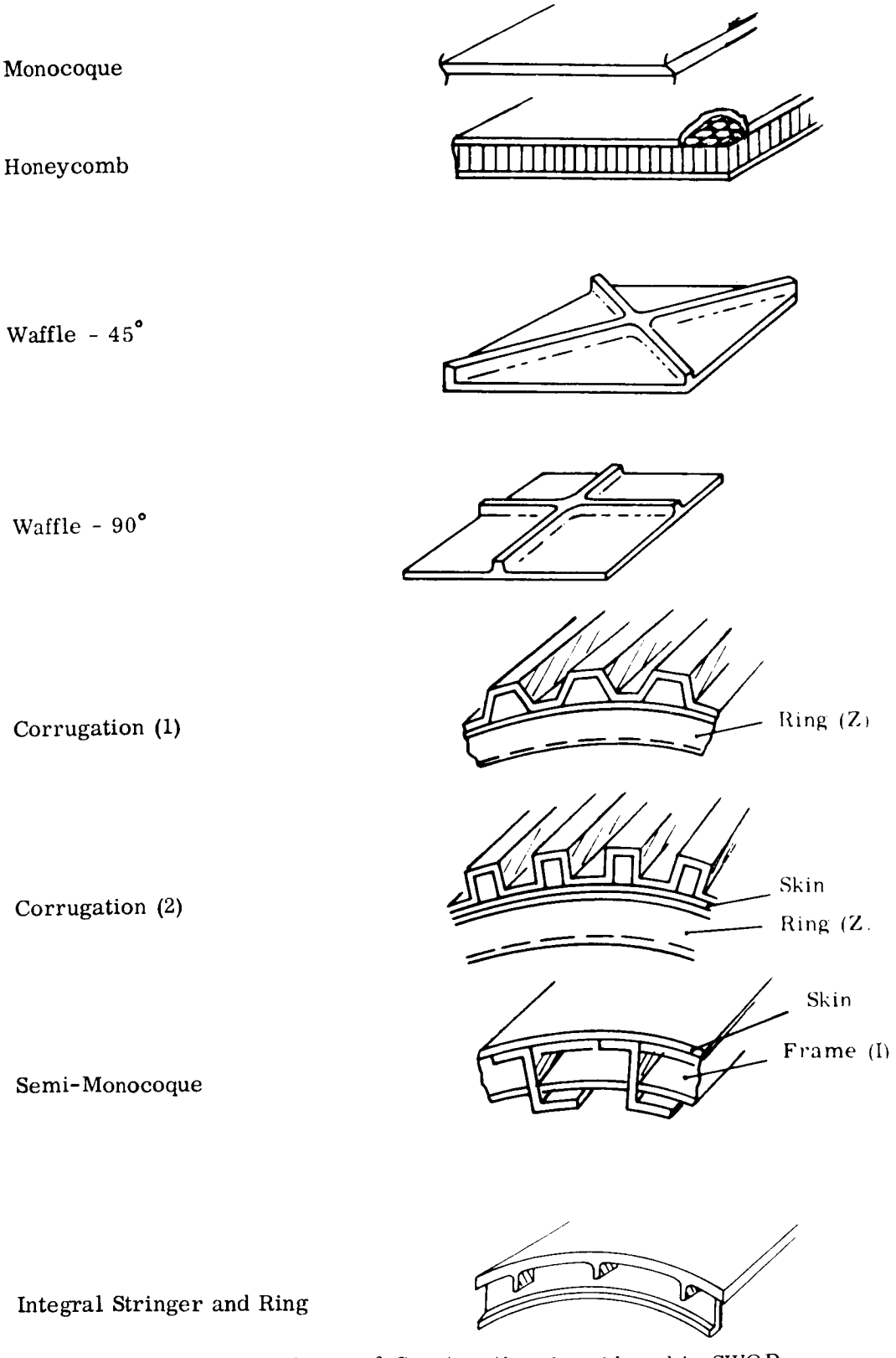

Figure 1-3. Types of Construction Considered in SWOP

design criteria, an off-optimum design is generally inevitable. The "optimum" analysis of each type of construction must be modified to handle these cases. Table 1-4 presents a list of parameters to be considered in this respect.

During the development of this computer program, consideration was given to the types of parameters which would be varied in order to obtain weight sensitivity coefficients. The results are briefly summarized in Table 1-5. At the present time, with the limited experience in running the program, not all of the parameters listed in Table 1-5 have been studied. Some preliminary results are presented in Section 2.

Table 1-4

Off-Optimum Input Options

* Not Applicable **Not Available	Monocoque*	Honeycomb	Waffle - 45°	Waffle - 90°	Corrugation (1)	Corrugation (2)	Semi-Monocoque	Integral Stringer and Ring**
Skin Thickness							X	
Core Thickness		X						
Rib Spacing			X	X				
Total Depth			X	X				
Ring Spacing					X		X	
Corrugation Pitch					X			
Corrugation Height					X	X		
Ring Height					X		X	
Stringer Spacing							X	
Stringer Height							X	
Ring Thickness							X	
Stringer Thickness							X	

Table 1-5

Elements to be Considered in Weight Sensitivity Coefficient Studies

	GASP	LASS-1	STRESS	Monocoque	Sandwich	Semi-Monocoque	Waffle - 45°	Corrugation	Waffle - 90°	Integral Stringer and Ring
Inflight Winds	X									
Ground Winds		X								
Bending Stiffness Distribution		X								
Ullage Pressure			X							
Material Properties				X	X	X	X	X	X	X
Factors of Safety				X	X	X	X	X	X	X
Failure Criteria				X	X	X	X	X	X	X
Geometric Proportions of Walls					X	X	X	X	X	X
Percent Ullage Volume			X							
Propellant Densities			X							
Propellant Flow Rates			X							
Dynamic Multipliers		X								
Fabrication Factors				X	X	X	X	X	X	X
Payload Weight	X									

Table 1-6 presents the scope of the Weight/Performance Constraint Analyses Structural Program. The types of construction which are being considered are largely those being used in the Saturn V launch vehicle. It should be noted that the weight of non-calculable items is being included in the program as indicated in Table 1-6. This weight is accounted for by factors which have been determined from experience in manufacturing the various types of construction.

The structural materials that will be in the program for immediate use by simply specifying the material number are given below.

1.	Aluminum	7075-T6
2.	Aluminum	2024-T4
3.	Aluminum	2014-T6
4.	Aluminum	2219-T87
5.	Magnesium	HK 31A-H24
6.	Beryllium	Y5804, QMV-5
7.	Stainless Steel	15-7
8.	Steel	AISI 4340 Alloy
9.	Titanium	6AL-4V

If another material is desired, the material properties can easily be inserted as input. This flexibility allows a wide range of material to be specified in any analysis.

1.5 CONSTRAINTS

It is obvious that all of the factors which must be considered by a design engineer in designing and manufacturing a structure cannot be included in a program of this type. Many decisions must be made on such things as cost of material, cost of fabrication, in-house capabilities, etc. Consideration of the advantages and disadvantages of these factors requires engineering judgment and this cannot be put into a computer program. Some of the more important manufacturing limitations can and have been incorporated in this program, however. For instance, calculated skin thicknesses are compared to the minimum thicknesses which can be practically manufactured for the type of material considered. The calculated thicknesses are not allowed to become smaller than these minimum thicknesses. A list of parameters which are considered to be subject to practical limitations are given in Table 1-7. Table 1-8 defines these limitations quantitatively.

The monocoque construction consists of a single face thickness so the constraint concerned with here is the minimum sheet thickness which can be practically manufactured. The honeycomb sandwich construction involves the core thickness, core density, and the

Table 1-6

Scope of the Projected Capability of the Weight/Performance Structural Program

Type of Shells		Monocoque	Honeycomb	45° Waffle	90° Waffle	Corrugation	Semi-Monocoque	Integral Stringer and Ring
General Instability	a. Cylindrical	Yes	Yes	Yes	Yes	Yes	Yes	Yes
	b. Conical	Yes	Yes	Yes	Yes	Yes	Yes	Yes
	c. Spherical	Yes	Yes	Yes	Yes	No	No	No
	d. Ellipsoidal	Yes	Yes	Yes	Yes	No	No	No
Local Instability	a. Cylindrical	No	Yes	Yes	Yes	Yes	Yes	Yes
	b. Conical	No	Yes	Yes	Yes	Yes	Yes	Yes
	c. Spherical	No	Yes	Yes	Yes	No	No	No
	d. Ellipsoidal	No	Yes	Yes	Yes	No	No	No
Discontinuity Analysis of Shells		No	No	No	No	No	No	No
Thermal Stress Analysis		No	No	No	No	No	No	No
Failure Criteria		Yes	Yes	Yes	Yes	Yes	Yes	Yes
Hydrostatic Test		Yes	Yes	Yes	Yes	Yes	Yes	Yes
Manufacturing Limitations		Yes	Yes	Yes	Yes	Yes	Yes	Yes
Material Properties versus Temperature		Yes	Yes	Yes	Yes	Yes	Yes	Yes
Min. Weight Comparison Using Various Materials		Yes	Yes	Yes	Yes	Yes	Yes	Yes
Compact Printout Format for Weight Comparison		Yes	Yes	Yes	Yes	Yes	Yes	Yes
Ring Shapes and Proportions		N.A.	N.A.	Yes	Yes	Yes	Yes	Yes
Stringer Spacing		N.A.	N.A.	Yes	Yes	Yes	Yes	Yes
Ring Spacing		N.A.	N.A.	Yes	Yes	Yes	Yes	Yes
Weight of Non-Calculable Items		Yes	Yes	Yes	Yes	Yes	Yes	Yes
Safety Factors		Yes	Yes	Yes	Yes	Yes	Yes	Yes
Inelastic Properties*		No	Yes	No	No	Yes	Yes	No
Stringer Shapes and Proportions		N.A.	N.A.	Yes	Yes	Yes	Yes	Yes

* - Inelastic Properties included only by use of reduced modulus.
N.A. - Not applicable.
Yes - Item considered.
No - Item not considered.

Table 1-7

Parameters which are Subject to Practical Limitations for Various Types of Construction

	Monocoque	Honeycomb	Waffle - 45°	Waffle - 90°	Corrugation	Semi-Monocoque	Integral Stringer and Ring
Core Shear Modulus		X					
Core Cell Diameter		X					
Skin/Face Thickness	X	X	X	X	X	X	X
Core Thickness		X					
Rib/Stringer Spacing			X	X		X	X
Ring/Frame Spacing			X	X	X	X	X
Rib/Stringer Height			X	X		X	X
Stringer Thickness			X	X		X	X
Frame Thickness			X	X	X	X	X
Fillet Radius			X	X			
Corrugation Pitch					X		
Corrugation Height					X		
Rib/Frame Height			X	X		X	
Corrugation Thickness					X		

Table 1-8

Material Parameters for Various Types of Construction

Type Construction	Parameter	Limiting Value (inches)						Fabrication Factor
		Aluminum	Magnesium	Steel	Titanium	Fiber-glass	Beryllium	
Monocoque	Skin Thickness - Minimum	.020	.032	.020	.020	.020	.020	1.05
Honeycomb Sandwich	Face Thickness - Minimum	.012	.016	.005	.005	.030	.012	1.25
	Core Thickness - Minimum	.125	.125	.125	1.25	.125	.125	
	- Maximum	←		Input			→	
	Core Density (Modulus) - Minimum			Input			→	
	- Maximum	←		Input			→	
	Cell Diameter - Minimum	←		Input			→	
Waffle - 45° and 90°	Rib Spacing - Minimum	≥ Cutting Head Diameter + Rib Thickness						
	Rib Thickness - Minimum	.080	.080	.080	.080	-	.080	1.20
	Skin Thickness - Minimum	.080	.080	.080	.080	-	.080	
	Over-All Thickness - Minimum	←		Input			→	
	- Maximum	←		Input			→	
	Rib Spacing - Maximum	←		15 x Overall Height			→	
Corrugation	Skin Thickness - Minimum	.020	.032	.020	.020	.020	.020	1.20
	Corrugation Thickness - Minimum	.020	.032	.020	.020	.020	.020	
	Depth - Minimum	←		Input			→	
	- Maximum	←		Input			→	
	Ring Thickness - Minimum	.020	.032	.020	.020	.020	.020	
Semi-Monocoque	Skin Thickness - Minimum	.020	.032	.020	.020	.020	.020	1.20
	Ring Spacing - Minimum, Maximum	←		Input			→	
	Stringer Spacing - Minimum, Maximum	←		Input			→	
	Ring/Stringer Height - Minimum	←		Input			→	
	- Maximum	←		Input			→	
	Ring/Stringer Thickness - Minimum	←		Input			→	
Integral Ring and Stringer	Skin Thickness - Minimum	.080	.080	.080	.080	-	.080	1.20
	Ring Thickness - Minimum	.080	.080	.080	.080	-	.080	
	Stringer Thickness - Minimum	.080	.080	.080	.080	-	.080	
	Ring/Stringer Height - Minimum	←		Input			→	
	- Maximum	←		Input			→	
All Construction	Sheet Length - Maximum	←		Input			→	

cell diameter of the honeycomb as well as the face thickness which was considered for the monocoque construction. Core thickness and core density are governed from both a minimum and a maximum thickness criteria. Note that the minimum core thickness has been selected as 1/8 inch for all of the materials. The maximum core thickness, minimum and maximum core density, and minimum cell diameter have been left as input so that the program user can select these values according to the type of problem being handled. For the waffle construction, provisions are made for the practical aspects of mechanical milling through the specification of a minimum value for the rib spacing. This minimum spacing must be at least equal to the cutting head diameter plus the rib thickness. Provisions are made also for the input of the maximum and minimum value of the overall thickness of the waffle construction. This flexibility will allow the user to specify a range within which the overall thickness must be. For instance, if the waffle pattern is to be milled from a two-inch-thick sheet of stock material, then this constraint is imposed by inputting both the minimum and maximum values of overall thickness as two inches.

All types of construction have the minimum skin thickness criterion imposed. In addition, certain parameters can be input for the corrugation, semi-monocoque, and integral stringer and ring constructions. The minimum and maximum values of corrugation depth can be input and also the range of stringer and ring heights can be input for the integral stringer and frame and semi-monocoque constructions. Provisions are made also for specifying the minimum ring and stringer spacing in the semi-monocoque subprogram. This allows the user to assure that the calculated spacing will not be so small that it would be impractical to manufacture.

In all of the subprograms for the various types of constructions, a maximum sheet length can be input. It is assumed that a large tank, for instance, would be composed of a number of these sections of maximum sheet length, L. The thickness of each of these lengths is allowed to vary; in other words, each of the sections is designed to withstand the loads imposed within that section.

The calculated weights of the structure necessary to support a set of loads will not reflect the true weight of the structure as built, because the weight of non-calculable items is always present. In this program, an attempt is made to account for these items through a fabrication factor. The fabrication factors shown in Table 1-8, namely 1.05

for monocoque and 1.25 for honeycomb, have been obtained by analyzing re-entry vehicle structural weight data. It was found that the non-calculable items in monocoque construction result in a 10-percent weight increase and in honeycomb sandwich construction a 50-percent weight increase. Due to the greatly increased size of Saturn type structures, these increases were cut in half to 5 percent and 25 percent, respectively. Thus, the corresponding fabrication factors are 1.05 and 1.25. A similar approach is being used for other types of construction and the results are presented in Table 1-8. These fabrication factors can be adjusted as more information about actual Saturn V hardware becomes available.

While the Weight/Performance Constraint Analyses was being developed, decisions were made as to the amount of sophistication that should be included in the program. There are many factors that have an influence on this degree of sophistication. The major questions that must be answered in this respect are, what is the intended application for the program and what is the accuracy required to give the desired results? The answer to the first question is that the main application of this program is intended to be a tool for overall program control; a tool which will provide program management with a means of rapidly assessing the impact on the program of various proposed changes. The accuracy of the results must be consistent with this goal. In this particular application, greater depth in analyses to get more accurate results may not be desirable. For instance, it would hardly be practical to develop a comprehensive stress analysis program, considering such things in detail as thermal stress and discontinuity stresses when these factors normally have localized effects. It has been shown, for example, in the investigation of the effect of such factors on the overall structural weight, that the effect of discontinuity stresses on the structural weight of big booster tanks is negligible. So, in some respects, the failure to include these factors may be considered as limitations; however, they are considered as of little consequence in this application of this program. Other items considered to be of the same order of approximation are the theory used for predicting elliptical shell critical buckling loads and the use of rigid body instead of flexible body analyses in determining the bending moment and axial force distributions on the vehicle. The analyses of the common bulkheads included the consideration of buckling due to the potential compressive load on the convex side of the shells. These shells are ellipsoidal in some stages of the Saturn V vehicle and, since a method for predicting ellipsoidal shell instability was not immediately available, the ellipsoidal heads were treated as equivalent spherical shells.

The conclusion drawn thus far in respect to the rigid body analysis used in this program versus an elastic body analysis is that the additional contribution to the Saturn V vehicle load resulting from elastic body consideration is small. This was indicated by a check case[1] and a comparison of the actual maximum bending moment with the maximum bending moment calculated by the LASS-1 program for the same conditions (maximum $q\alpha$) shows a difference of about 9 percent. The difference in the corresponding maximum axial loads is about 6 percent. All of this difference is not necessarily due to dynamic effects because of the possible error in interpreting values from curves for input to the program.

Even though the dynamic effect appears to be small and would probably be insignificant when calculating weight changes, dynamic correction factors are included in the LASS-1 program for application to the bending moment and axial loads.

The Saturn V has a fairly low L/D value and the dynamic effects will probably be small for smaller L/D vehicles. When considering large L/D vehicles, the dynamic effect could become very significant when exposed to sharp gusts. In this case, the development of a program to consider the elastic body may be necessary, however the need for this is not anticipated at this time.

The stiffness and weight distribution of the vehicle are input in the form of stored tables in the LASS-1 program. During subsequent calculations involving the variation of structural or other parameters, these distributions of weight and stiffness are not corrected to account for these variations. These variations are assumed to have a negligible effect on the original distributions because of the small order of magnitude of the parameter variation.

SECTION 2

RESULTS

2.1 WEIGHT SENSITIVITY COEFFICIENTS STUDY

The primary objective of this program is to provide meaningful information for management planning and control. To be useful, the information transmitted to management must meet certain predetermined requirements. The starting point is, of course, to have a clear definition of what information is wanted. This seems obvious enough until it is recalled that many organizations generate information which is not useful, needed, or wanted.

Assuming a clear-cut need for certain types of information, several questions need to be resolved. For simplicity, these questions can be stated as: What?, When?, How?, Who? Answers to these questions may not be simple. Taking them in order, the first question is: What kind of information is needed or wanted? The answer will come out of the nature of the subject being studied and the depth of information wanted. In some cases, there may be a requirement not only for information about the effect of implementing proposed changes, but also about possible alternate approaches and their consequences. This brief elaboration will serve to illustrate that the answer to what kind of information is wanted deserves careful definition.

Not only does the final decision on this question influence the information requirements to perform the study, it influences the selection of mathematical models and their utilization. The matter of when information is needed usually is resolved by the nature of the problem being studied. This program is designed to give answers on a quick-reaction basis which are based on the most recent technical data available. The limiting factor will probably be the time required to reduce the raw numerical output to a concise and meaningful format.

The question of how the information yielded by this program is to be transmitted refers to the form to be employed rather than the channel to be used. The form requirements are that the information be clear, concise, complete, and undistorted. Clarity is obtained usually by employing graphic devices which convey meaning quickly. They can

employ words, numbers, pictures, symbols, lines, bars, etc., arranged into charts, tables, pictograms, and the like.

The question of who is to receive the information is not a concern about protocol but about the level of refinement and the depth of detail needed in the reports. If, for example, the report is for top management only, the inclusion of details of value only to department managers merely introduces "noise" into the communication system.

The application of these general principals to a specific problem is not an easy task since the raw numerical data for some studies can be extensive. Suppose, for example, that it is required to establish relationships between several launch vehicle parameters and structural weight. The first step would be to specify a reference or nominal vehicle configuration. By making a run through the computer program, the primary structural weight associated with this nominal configuration is determined, and is used as a basis for comparison in subsequent runs.

Once the structural weight of the nominal configuration is established, we can proceed to determine the effect of varying certain parameters of structural weight. For example, if we wish to find how changes in the factor of safety influence the structural weight, we choose several different values of factor of safety which are slightly different than the nominal value and make a run through the computer program for each of them. The results of each computer run will be a complete structural weight breakdown by stages and interstages for each value of factor of safety. This process can then be repeated for other parameters such as thrust-to-weight ratio, ullage pressure, allowable working stress, payload weight, probability of winds, etc.

It is obvious that weight tabulations for a study involving several parameters and variations thereof would be extensive and difficult to comprehend for quick management decisions. Since this violates the intended objective of this program, a method has been devised to present this type of detailed weight data in a concise format which can be assimilated quickly. This method presents the results as a comprehensive matrix of weight sensitivity coefficients. We obtain these coefficients by plotting the structural weights which were calculated for various values of a given design parameter such as ullage pressure or factor of safety as shown in Figure 2-1. If the relationship of the structural weight is reasonably linear for small variations of the design parameters,

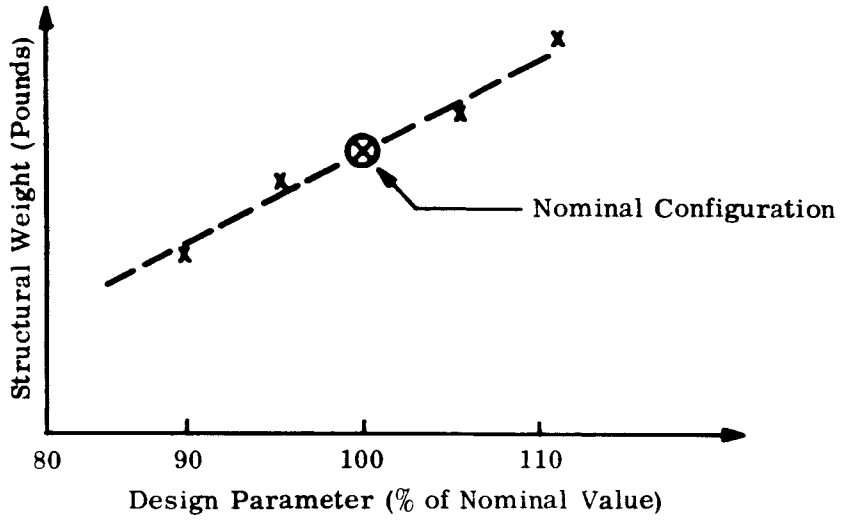

Figure 2-1. Structural Weight versus Design Parameter - Linear

about their nominal values, a straight line can represent these calculated weights with acceptable accuracy. The slope of this straight line, therefore, characterizes the effect of varying a given design parameter on structural weight. This slope is called the weight sensitivity coefficient which has the units "Pounds of Structural Weight per Percent Change of Parameter" or, by dividing this quantity by the appropriate performance tradeoff factor, it could be given in the units "Pounds of Equivalent Payload per Percent Change of Parameter."

It is possible that variation of some parameters which have a strong influence on the trajectory may have nonlinear relationships with structural weight. In those cases, it will be necessary to present the results in the slightly less compact form of a graph as shown in Figure 2-2.

Each stage or interstage structure will therefore have either a weight sensitivity coefficient or a simple graph for each parameter of interest. Data presented in this format will allow management to digest a large amount of data very quickly and permit them to make quick decisions on proposals relating to changes in launch vehicle parameters.

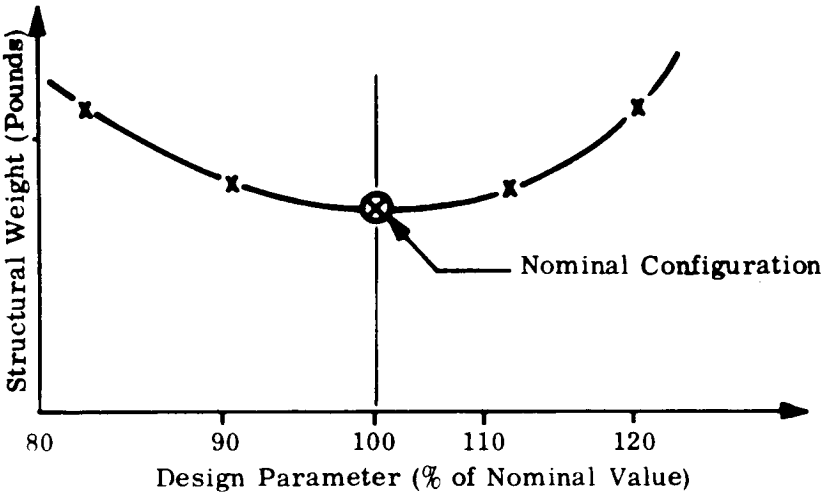

Figure 2-2. Structural Weight versus Design Parameter - Nonlinear

2.2 TYPICAL RESULTS

The true value of a program of this type becomes apparent only through using the program and observing the results of particular studies. In order to demonstrate some of the features of the program, a series of computer runs was made in order to assess the change in structural weight when certain parameters were varied about a defined nominal. The configuration used in this study is shown in Figure 2-3. The aerodynamic, weight, and control data used in the GASP and LASS-1 programs were taken from Reference 1. Otherwise, the nominal configuration was defined to be:

Material	2219-T87 Aluminum
Ultimate factor of safety	1.40
Allowable working stress	44,286 psi
Ullage pressure	36 psi
Thrust-to-weight ratio	1.25
Payload weight	95,000 lbs
Inflight Winds	95% Probability of Occurance

In each computer run, the primary structural weight is calculated subject to the loads imposed at prelaunch, maximum $q\alpha$, and maximum thrust. The computer printout for a typical case is shown in Figure 2-4 and Figure 2-5. These data were used as a basis for calculating structural weight sensitivity coefficients as outlined previously. Consideration was given to six parameters -- Factor of Safety, Allowable Working Stress, Ullage Pressure, Thrust-to-Weight Ratio, Payload, and Inflight Wind Loads. Weight sensitivity

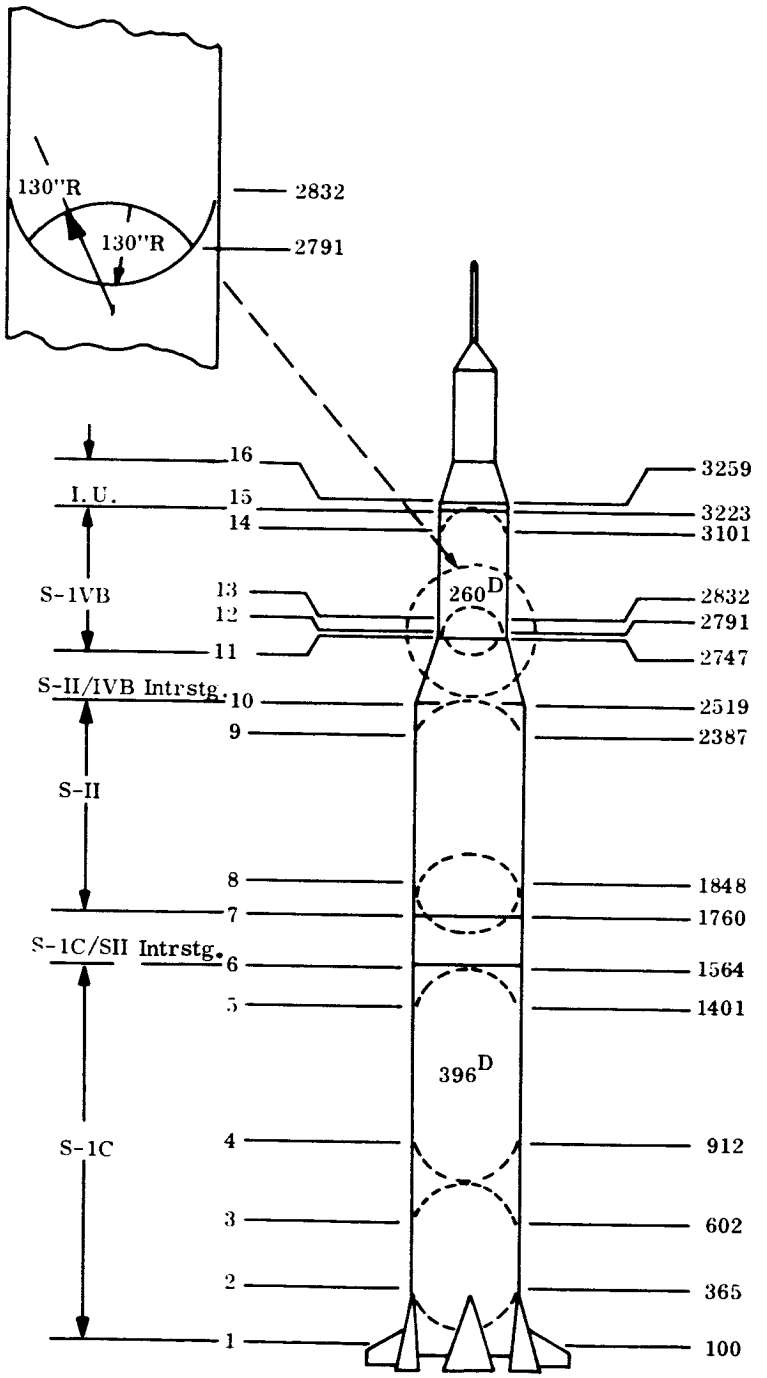

Figure 2-3. Saturn V Launch Vehicle Configuration

MATRIX OF COMPARATIVE WEIGHTS FOR MATERIAL AL 2219-T87

IDENTIFICATION					MONOCOQUE	OPEN FAC COR	CLOSE FAC CR			MINIMUM
1	1	DISC	1	CYL	0.270185E 05	0.860833E 04	0.175461E 05	0.000000E-38	0.000000E-38	0.860833E 04
2	2	DISC	2	BHD	0.387046E 04	0.000000E-38	0.000000E-38	0.000000E-38	0.000000E-38	0.387046E 04
2	1	DISC	2	CYL	0.189894E 05	0.000000E-38	0.156221E 05	0.000000E-38	0.000000E-38	0.156221E 05
3	3	DISC	3	THD	0.262445E 04	0.000000E-38	0.000000E-38	0.000000E-38	0.000000E-38	0.262445E 04
3	1	DISC	3	CYL	0.320478E 05	0.100683E 05	0.208215E 05	0.000000E-38	0.000000E-38	0.100683E 05
4	2	DISC	4	BHD	0.574361E 04	0.000000E-38	0.000000E-38	0.000000E-38	0.000000E-38	0.574361E 04
4	1	DISC	4	CYL	0.319932E 05	0.000000E-38	0.459395E 05	0.000000E-38	0.000000E-38	0.319932E 05
5	3	DISC	5	THD	0.389635E 04	0.000000E-38	0.000000E-38	0.000000E-38	0.000000E-38	0.389635E 04
5	1	DISC	5	CYL	0.145819E 05	0.434788E 04	0.839729E 04	0.000000E-38	0.000000E-38	0.434788E 04
6	1	DISC	6	CYL	0.173976E 05	0.534577E 04	0.100428E 05	0.000000E-38	0.000000E-38	0.534577E 04
7	1	DISC	7	CYL	0.761488E 04	0.208357E 04	0.401830E 04	0.000000E-38	0.000000E-38	0.208357E 04
8	2	DISC	8	BHD	0.584436E 04	0.000000E-38	0.000000E-38	0.000000E-38	0.000000E-38	0.584436E 04
8	3	DISC	8	THD	0.156661E 05	0.000000E-38	0.000000E-38	0.000000E-38	0.000000E-38	0.156661E 05
8	1	DISC	8	CYL	0.153126E 05	0.000000E-38	0.366153E 05	0.000000E-38	0.000000E-38	0.153126E 05
9	3	DISC	9	THD	0.205729E 04	0.000000E-38	0.000000E-38	0.000000E-38	0.000000E-38	0.205729E 04
9	1	DISC	9	CYL	0.841076E 04	0.236437E 04	0.293011E 04	0.000000E-38	0.000000E-38	0.236437E 04
10	1	DISC	10	CYL	0.139762E 05	0.352095E 04	0.730946E 04	0.000000E-38	0.000000E-38	0.352095E 04
11	1	DISC	11	CYL	0.156694E 04	0.375335E 03	0.819467E 03	0.000000E-38	0.000000E-38	0.375335E 03
12	2	DISC	12	BHD	0.753259E 03	0.000000E-38	0.000000E-38	0.000000E-38	0.000000E-38	0.753259E 03
12	3	DISC	12	THD	0.228173E 04	0.000000E-38	0.000000E-38	0.000000E-38	0.000000E-38	0.228173E 04
12	1	DISC	12	CYL	0.791882E 03	0.000000E-38	0.921609E 03	0.000000E-38	0.000000E-38	0.791882E 03
13	2	DISC	13	BHD	0.226042E 03	0.000000E-38	0.000000E-38	0.000000E-38	0.000000E-38	0.226042E 03
13	1	DISC	13	CYL	0.279437E 04	0.000000E-38	0.587268E 04	0.000000E-38	0.000000E-38	0.279437E 04
14	3	DISC	14	THD	0.590822E 03	0.000000E-38	0.000000E-38	0.000000E-38	0.000000E-38	0.590822E 03
14	1	DISC	14	CYL	0.325883E 04	0.917676E 03	0.114316E 04	0.000000E-38	0.000000E-38	0.917676E 03
		TOTALS			0.239329E 06	0.376322E 05	0.177999E 06	0.000000E-38	0.000000E-38	0.147701E 06

Figure 2-4. Typical Output Format for SWOP Program Structural Weight Sensitivity Coefficient Study

MATRIX OF COMPARATIVE WEIGHTS FOR MATERIAL AL 2219-T87

IDENTIFICATION					HONEYCOMB	45DEG WAFFLE	90DEG WAFFLE			MINIMUM
1	1	DISC	1	CYL	0.931004E 04	0.215433E 05	0.233248E 05	0.000000E-38	0.000000E-38	0.931004E 04
2	2	DISC	2	BHD	0.407335E 04	0.387046E 04	0.387046E 04	0.000000E-38	0.000000E-38	0.387046E 04
2	1	DISC	2	CYL	0.879975E 04	0.122777E 05	0.133658E 05	0.000000E-38	0.000000E-38	0.879975E 04
3	3	DISC	3	THD	0.273386E 04	0.262445E 04	0.262445E 04	0.000000E-38	0.000000E-38	0.262445E 04
3	1	DISC	3	CYL	0.112689E 05	0.255074E 05	0.276167E 05	0.000000E-38	0.000000E-38	0.112689E 05
4	2	DISC	4	BHD	0.600834E 04	0.574361E 04	0.574361E 04	0.000000E-38	0.000000E-38	0.574361E 04
4	1	DISC	4	CYL	0.223854E 05	0.304616E 05	0.296595E 05	0.000000E-38	0.000000E-38	0.223854E 05
5	3	DISC	5	THD	0.403503E 04	0.389635E 04	0.389635E 04	0.000000E-38	0.000000E-38	0.389635E 04
5	1	DISC	5	CYL	0.416076E 04	0.105594E 05	0.117125E 05	0.000000E-38	0.000000E-38	0.416076E 04
6	1	DISC	6	CYL	0.490749E 04	0.125954E 05	0.139708E 05	0.000000E-38	0.000000E-38	0.490749E 04
7	1	DISC	7	CYL	0.207264E 04	0.540657E 04	0.604464E 04	0.000000E-38	0.000000E-38	0.207264E 04
8	2	DISC	8	BHD	0.611244E 04	0.584436E 04	0.584436E 04	0.000000E-38	0.000000E-38	0.584436E 04
8	3	DISC	8	THD	0.581161E 04	0.720979E 04	0.720979E 04	0.000000E-38	0.000000E-38	0.581161E 04
8	1	DISC	8	CYL	0.158956E 05	0.221729E 05	0.211209E 05	0.000000E-38	0.000000E-38	0.158956E 05
9	3	DISC	9	THD	0.215404E 04	0.205729E 04	0.205729E 04	0.000000E-38	0.000000E-38	0.205729E 04
9	1	DISC	9	CYL	0.150941E 04	0.534754E 04	0.596954E 04	0.000000E-38	0.000000E-38	0.150941E 04
10	1	DISC	10	CYL	0.274427E 04	0.945007E 04	0.105493E 05	0.000000E-38	0.000000E-38	0.274427E 04
11	1	DISC	11	CYL	0.409671E 03	0.111606E 04	0.123485E 04	0.000000E-38	0.000000E-38	0.409671E 03
12	2	DISC	12	BHD	0.895540E 03	0.753259E 03	0.753259E 03	0.000000E-38	0.000000E-38	0.753259E 03
12	3	DISC	12	THD	0.850293E 03	0.156103E 04	0.156103E 04	0.000000E-38	0.000000E-38	0.850293E 03
12	1	DISC	12	CYL	0.476226E 03	0.561450E 03	0.534812E 03	0.000000E-38	0.000000E-38	0.476226E 03
13	2	DISC	13	BHD	0.271522E 03	0.226042E 03	0.226042E 03	0.000000E-38	0.000000E-38	0.226042E 03
13	1	DISC	13	CYL	0.276792E 04	0.371634E 04	0.338224E 04	0.000000E-38	0.000000E-38	0.276792E 04
14	3	DISC	14	THD	0.690864E 03	0.590822E 03	0.590822E 03	0.000000E-38	0.000000E-38	0.590822E 03
14	1	DISC	14	CYL	0.564869E 03	0.208654E 04	0.227355E 04	0.000000E-38	0.000000E-38	0.564869E 03
		TOTALS			0.120910E 06	0.197200E 06	0.205137E 06	0.000000E-38	0.000000E-38	0.119541E 06

Figure 2-5. Typical Output Format for SWOP Program Structural Weight Sensitivity Coefficient Study

coefficients are tabulated in Table 2-1 through Table 2-6 for the total launch vehicle using Monocoque, Honeycomb, 45°Waffle, 90° Waffle, Semi-Monocoque and Integral Stringer and Ring types of construction. Since the corrugation types of construction are intended to be used in the unpressurized sections of the launch vehicle only; Table 2-7 through 2-14 present weight sensitivity coefficients for eight types of construction in unpressurized sections only. In all of these tables, the nonlinearity of the thrust to weight ratio variations made it necessary to present the data in the form of graphs in Figure 2-6 through Figure 2-19.

In all of the tables, the weight sensitivity coefficients are presented as the pounds of equivalent payload for a one percent increase in the parameter being varied. The numbers in parenthesis represent changes in structural weight. For example if we assume that the factor of safety is increased 1 percent, from Table 2-1 it is seen that, for monocoque construction, the S-IC stage structural weight would increase 644 pounds. Assuming a Performance Trade-Off Factor of 15.0 the payload capability would therefore be decreased 43 pounds.

2.3 DISCUSSION AND INTERPRETATION OF RESULTS

The weight sensitivity coefficient approach has been used because it is a simple and straightforward method of presenting numerical results. This over-simplification sometimes obscures some of the more subtle implications of the analysis, so it will be worthwhile to have an awareness of the more common pitfalls in interpreting the results. In calculating the weight sensitivity coefficients, it has been assumed that the parameters being varied have a linear relationship with structural weight. Most of the parameters which are of interest in these types of studies can be considered linear for small variations about the nominal configuration with only negligible error. In order to discuss the nature of the nonlinearities, it is advisable to talk about two different classes of parameters: those that have an influence on the trajectory, and those that do not have an influence on the trajectory. Examples of the first classification are engine thrust, vehicle mass properties, and propellant loading. Examples of parameters which do not significantly affect the trajectory are ullage pressure, factor of safety, and material properties. Several studies have been made for variation of the parameters ullage pressure and factor of safety and it has been found that, for reasonable changes in these parameters, the increased structural weight will have a negligible influence on the mass characteristics of the launch vehicle in a trajectory analysis. In other words, the output of the SWOP program is not used to modify the input to the GASP program because the changes in weight are very small compared to the total weight of the vehicle and the

Table 2-1

Monocoque Structural Weight Sensitivity Coefficients
(Total Launch Vehicle)

	*P.T.F.	Factor of Safety	Allowable Working Stress	Ullage Pressure	Thrust-to-Weight Ratio	Payload Change	Inflight Wind Loads
S-IC Stage	15.0	- 43 (+644)	+ 41 (-616)	+ 13 (-195)	See Figure 2-6	- 2.1 (+31.3)	- 90 (+1344)
S-IC/S-II Interstage	14.0	-4.8 (+ 67)	+4.6 (- 64)	0 (0)		- 0.3 (+ 3.8)	- 13 (+ 177)
S-II Stage	3.2	-111 (-354)	+106 (-339)	- 23 (+ 72)		- 3.7 (+11.7	- 69 (+ 220)
S-II/S-IVB Interstage	3.2	- 17 (+ 54)	+ 16 (- 52)	0 (0)		- 1.4 (+ 4.4)	- 62 (+ 198)
S-IVB Stage	1.0	- 76 (+ 76)	+ 72 (- 72)	-3.8 (+3.8)		- 4.1 (+ 4.1)	- 65 (+ 65)
I.U.	1.0	-3.7 (+3.7)	+3.6 (-3.6)	0 (0)		- 0.6 (+ 0.6)	- 50 (+ 50)

Table 2-2

Honeycomb Structural Weight Sensitivity Coefficients
(Total Launch Vehicle)

	*P.T.F.	Factor of Safety	Allowable Working Stress	Ullage Pressure	Thrust-to-Weight Ratio	Payload Change	Inflight Wind Loads
S-IC Stage	15.0	- 50 (+743)	+ 47 (-710)	- 16 (+235)	See Figure 2-7	-0.1 (+1.8)	- 20 (+ 297)
S-IC/S-II Interstage	14.0	-3.2 (+ 45)	+3.1 (- 43)	0 (0)		-0.2 (+2.7)	- 8.4 (+ 117)
S-II Stage	3.2	-103 (+330)	+ 98 (-315)	- 51 (+164)		-0.2 (+0.7)	- 32 (+ 101)
S-II/S-IVB Interstage	3.2	-7.8 (+ 25)	+7.5 (- 24)	0 (0)		-0.7 (+2.1)	- 28 (+ 89)
S-IVB Stage	1.0	- 66 (+ 66)	+ 63 (- 63)	- 42 (+ 42)		-2.7 (+2.7)	- 78 (+ 78)
I.U.	1.0	-1.4 (-1.4)	+1.4 (-1.4)	0 (0)		-0.2 (+0.2)	- 20 (+ 20)

*Performance Trade-Off Factor - The ratio of change in stage or module weight to the change in payload capability.

Weight Sensitivity Coefficients are the pounds of equivalent payload for a one percent increase in the parameter being varied. The numbers in parenthesis are the changes in structural weight.

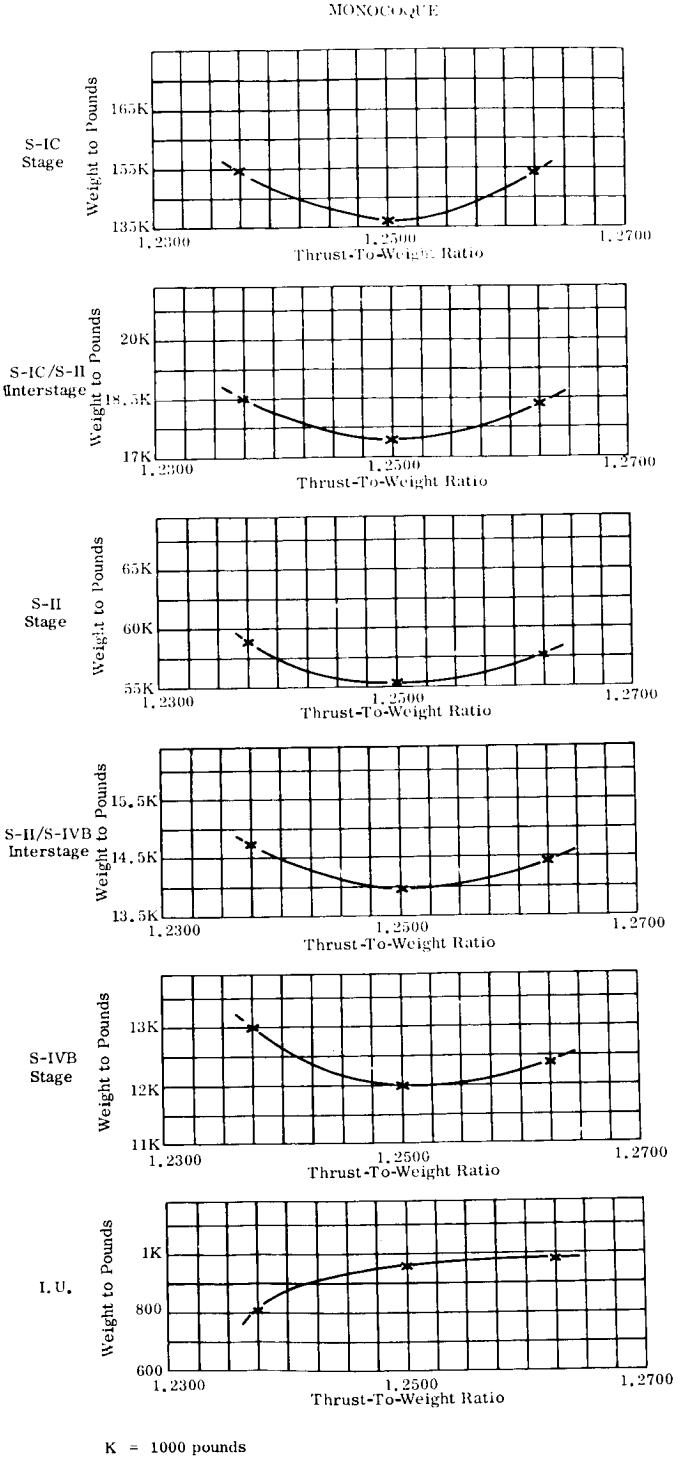

Figure 2-6. Effect of Thrust-to-Weight Ratio Variation on Structural Weight - Monocoque Construction - Total Launch Vehicle

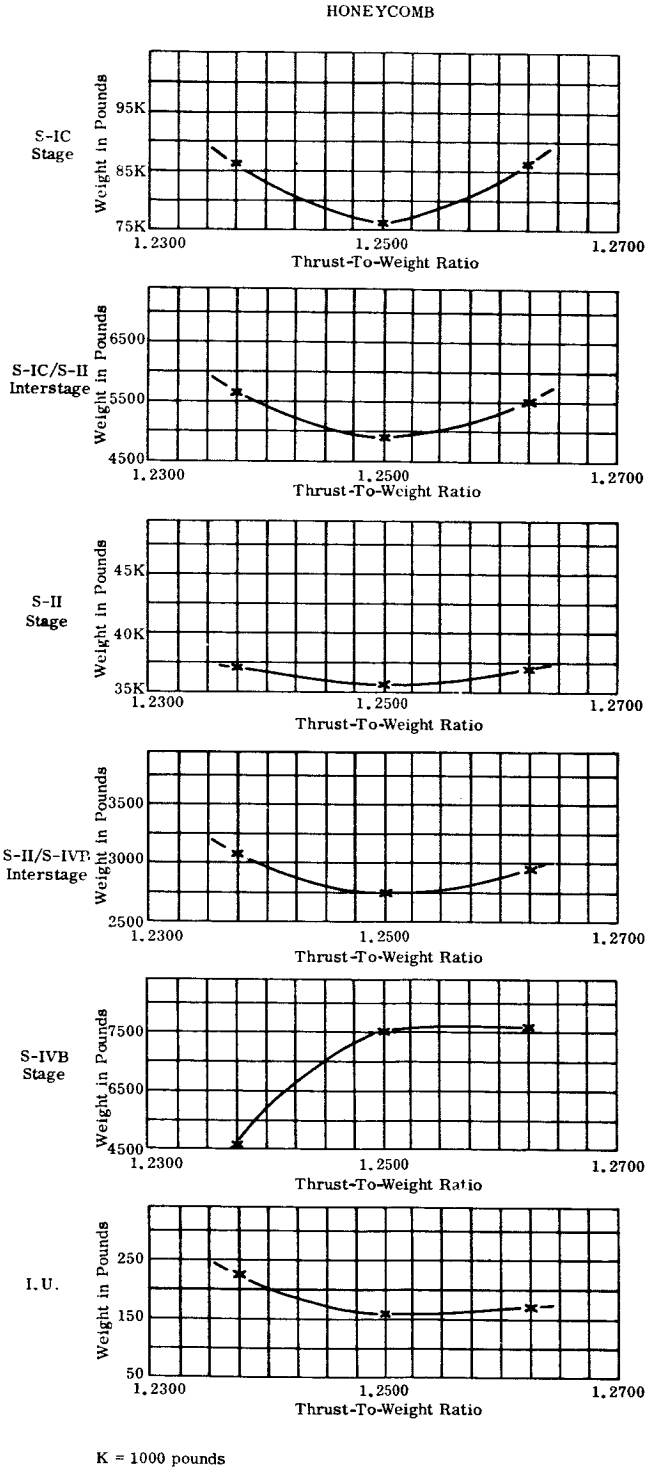

Figure 2-7. Effect of Thrust-to-Weight Ratio Variation on Structural Weight - Honeycomb Construction - Total Launch Vehicle

Table 2-3

45° Waffle Structural Weight Sensitivity Coefficients (Total Launch Vehicle)

	*P.T.F.	Factor of Safety	Allowable Working Stress	Ullage Pressure	Thrust-to-Weight Ratio	Payload Change	Inflight Wind Loads
S-IC Stage	15.0	- 61 (+915)	+ 58 (-875)	- 14 (+207)	See Figure 2-8	-0.5 (+6.8)	- 33 (+496)
S-IC/S-II Interstage	14.0	-4.9 (+ 68)	+4.6 (- 65)	0 (0)		-0.3 (+3.8)	- 14 (+200)
S-II Stage	3.2	-112 (+357)	+107 (-341)	- 40 (+128)		-0.8 (+2.5)	-141 (+452)
S-II/S-IVB Interstage	3.2	-15.3 (+ 49)	+14.7 (- 47)	0 (0)		-1.2 (+3.8)	- 69 (+221)
S-IVB Stage	1.0	- 79 (+ 79)	+ 76 (- 76)	- 29 (+ 29)		-9.7 (+9.7)	- 78 (+ 78)
I.U.	1.0	-4.2 (+4.2)	+4.0 (-4.0)	0 (0)		-0.4 (+0.4)	- 50 (+ 50)

Table 2-4

90° Waffle Structural Weight Sensitivity Coefficients (Total Launch Vehicle)

	*P.T.F.	Factor of Safety	Allowable Working Stress	Ullage Pressure	Thrust-to-Weight Ratio	Payload Change	Inflight Wind Loads
S-IC Stage	15.0	- 63 (+945)	+ 60 (-904)	- 9 (+135)	See Figure 2-9	-0.5 (+7.6)	- 45 (+671)
S-IC/S-II Interstage	14.0	-5.9 (+ 83)	+5.7 (- 80)	0 (0)		-0.3 (+4.1)	- 14 (+202)
S-II Stage	3.2	-133 (+424)	+127 (-405)	- 55 (+177)		-0.9 (+2.8)	- 63 (+203)
S-II/S-IVB Interstage	3.2	- 17 (+ 53)	+ 16 (- 51)	0 (0)		-1.3 (+4.2)	- 66 (+212)
S-IVB Stage	1.0	- 83 (+ 83)	+ 80 (- 80)	- 44 (+ 44)		-1.8 (+1.8)	- 26 (+ 26)
I.U.	1.0	-4.5 (+4.5)	+4.3 (-4.3)	0 (0)		-0.4 (+0.4)	- 51 (+ 51)

*Performance Trade-Off Factor - The ratio of change in stage or module weight to the change in payload capability.

Weight Sensitivity Coefficients are the pounds of equivalent payload for a one percent increase in the parameter being varied. The numbers in parenthesis are the changes in structural weight.

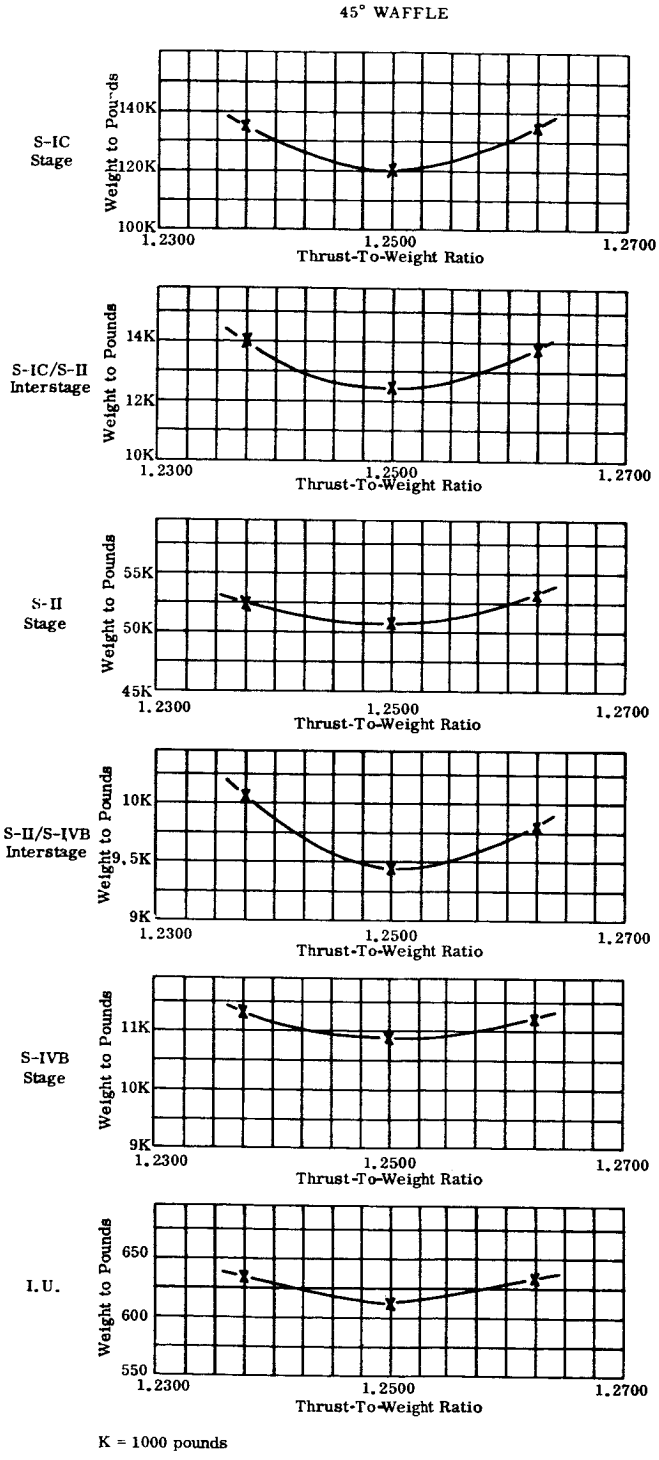

Figure 2-8. Effect of Thrust-to-Weight Ratio Variation on Structural Weight - 45° Waffle Construction - Total Launch Vehicle

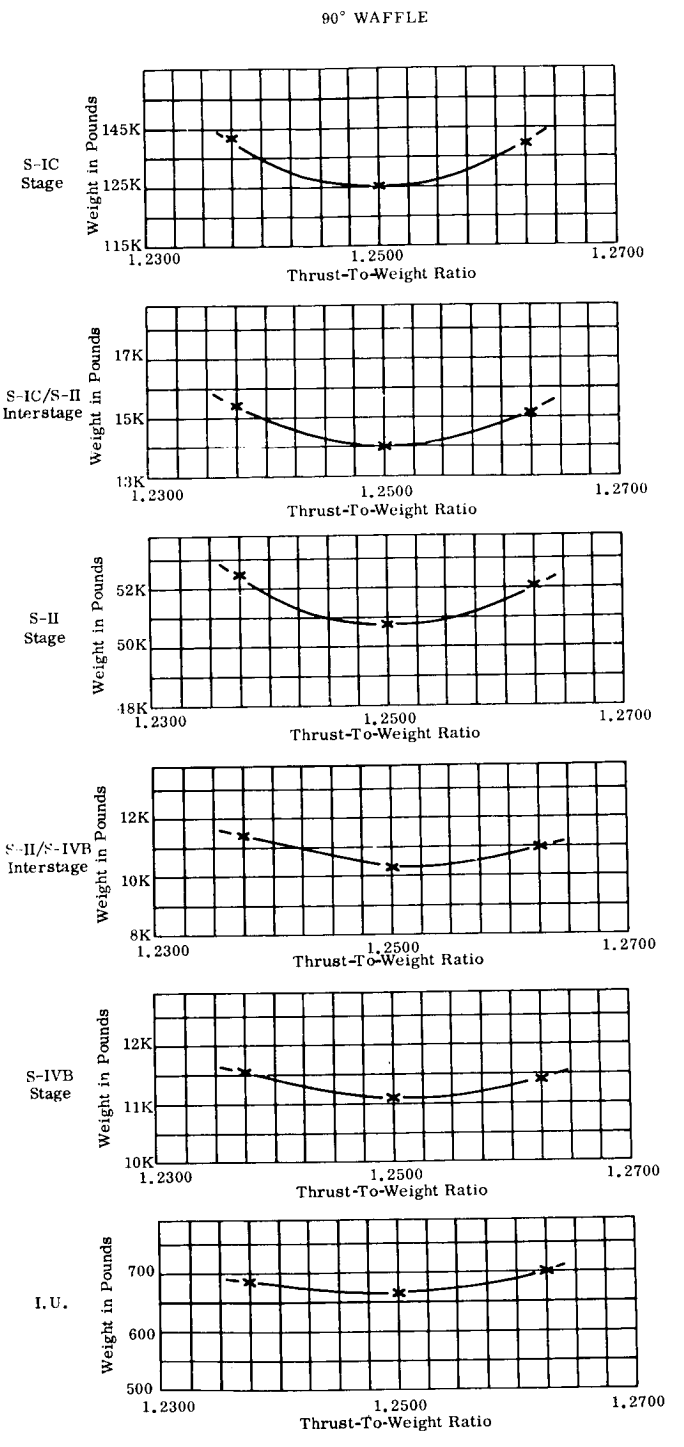

Figure 2-9. Effect of Thrust-to-Weight Ratio Variation on Structural Weight - 90° Waffle Construction - Total Launch Vehicle

Table 2-5

Semi-Monocoque Structural Weight Sensitivity Coefficients
(Total Launch Vehicle)

	*P.T.F.	Factor of Safety	Allowable Working Stress	Ullage Pressure	Thrust-to-Weight Ratio	Payload Change	Inflight Wind Loads
S-IC Stage	15.0	- 51 (+772)	+ 49 (-738)	- 16 (+246)	See Figure 2-10	- 2.7 (+40.5)	- 37 (+ 550)
S-IC/S-II Interstage	14.0	-2.9 (+ 40)	+2.7 (- 38)	0 (0)		- 0.2 (+ 2.3)	- 7.9 (+ 110)
S-II Stage	3.2	-118 (+377)	+113 (-361)	- 29 (+ 92)		- 21 (+ 68)	- 929 (+2974)
S-II/S-IVB Interstage	3.2	-6.9 (+ 22)	+6.6 (- 21)	0 (0)		- 0.5 (+ 1.7)	- 28 (+ 90)
S-IVB Stage	1.0	- 62 (+ 62)	+ 59 (- 59)	(+ 22)		- 5.2 (+ 5.2)	- 332 (+ 332)
I.U.	1.0	-6.1 (+6.1)	+5.8 (-5.8)	0 (0)		- 0.9 (+ 0.9)	- 25 (+ 25)

Table 2-6

Integral Stringer and Ring Structural Weight Sensitivity Coefficients
(Total Launch Vehicle)

	*P.T.F.	Factor of Safety	Allowable Working Stress	Ullage Pressure	Thrust-to-Weight Ratio	Payload Change	Inflight Wind Loads
S-IC Stage	15.0	- 64 (+ 965)	+ 62 (- 923)	+7.4 (-111)	See Figure 2-11	- 0.5 (+ 8.1)	- 5.9 (+ 89)
S-IC/S-II Interstage	14.0	- 3.1 (+ 43)	+ 2.9 (- 41)	0 (0)		- 0.2 (+ 3.4)	- 11 (+ 150)
S-II Stage	3.2	- 311 (+ 994)	+ 297 (- 951)	- 76 (+244)		- 0.6 (+ 1.9)	- 444 (+1422)
S-II/S-IVB Interstage	3.2	-10.6 (+ 34)	+10.3 (- 33)	0 (0)		- 1.0 (+ 3.2)	- 59 (+ 190)
S-IVB Stage	1.0	- 197 (+ 197)	+ 188 (- 188)	-6.5 (+6.5)		- 9.8 (+ 9.8)	- 145 (+ 145)
I.U.	1.0	- 9.8 (+ 9.8)	+ 9.4 (- 9.4)	0 (0)		- 2.6 (+ 2.6)	- 25 (+ 25)

*Performance Trade-Off Factor - The ratio of change in stage or module weight to the change in payload capability.

Weight Sensitivity Coefficients are the pounds of equivalent payload for a one percent increase in the parameter being varied. The numbers in parenthesis are the changes in structural weight.

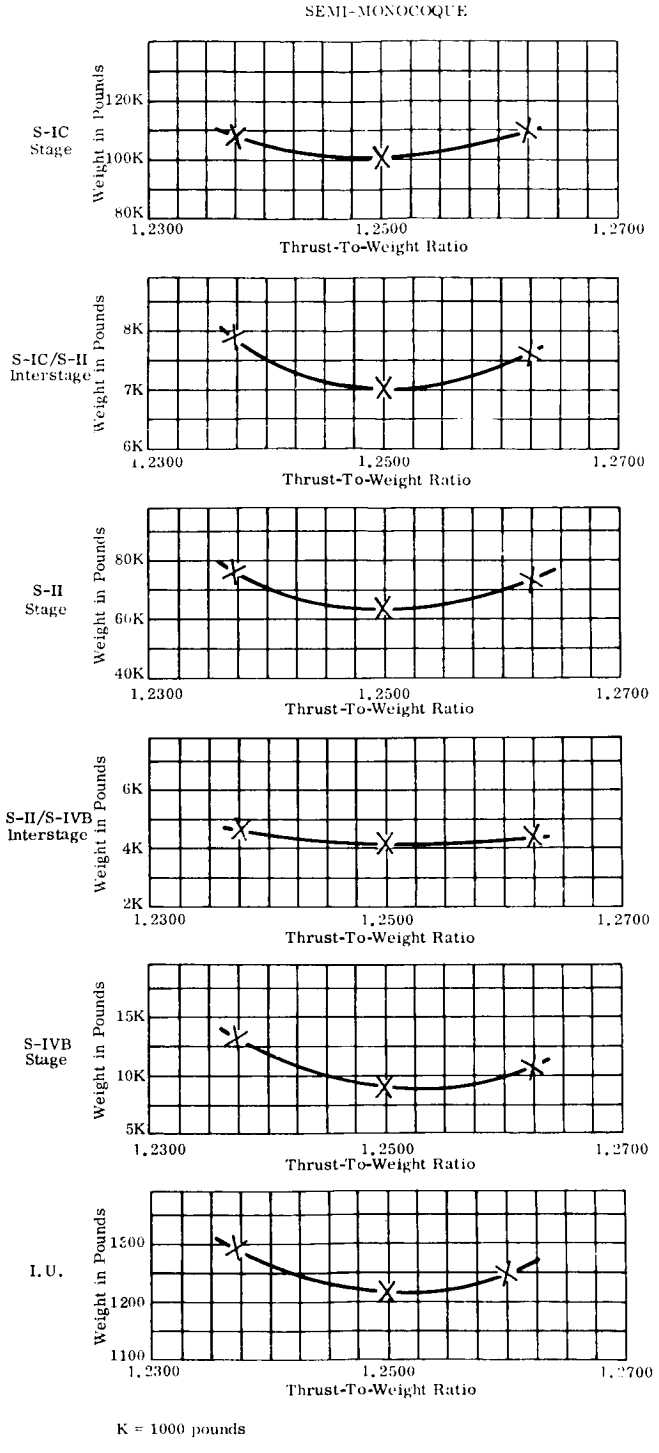

Figure 2-10. Effect of Thrust-to-Weight Ratio Variation on Structural Weight - Semi-Monocoque Construction - Total Launch Vehicle

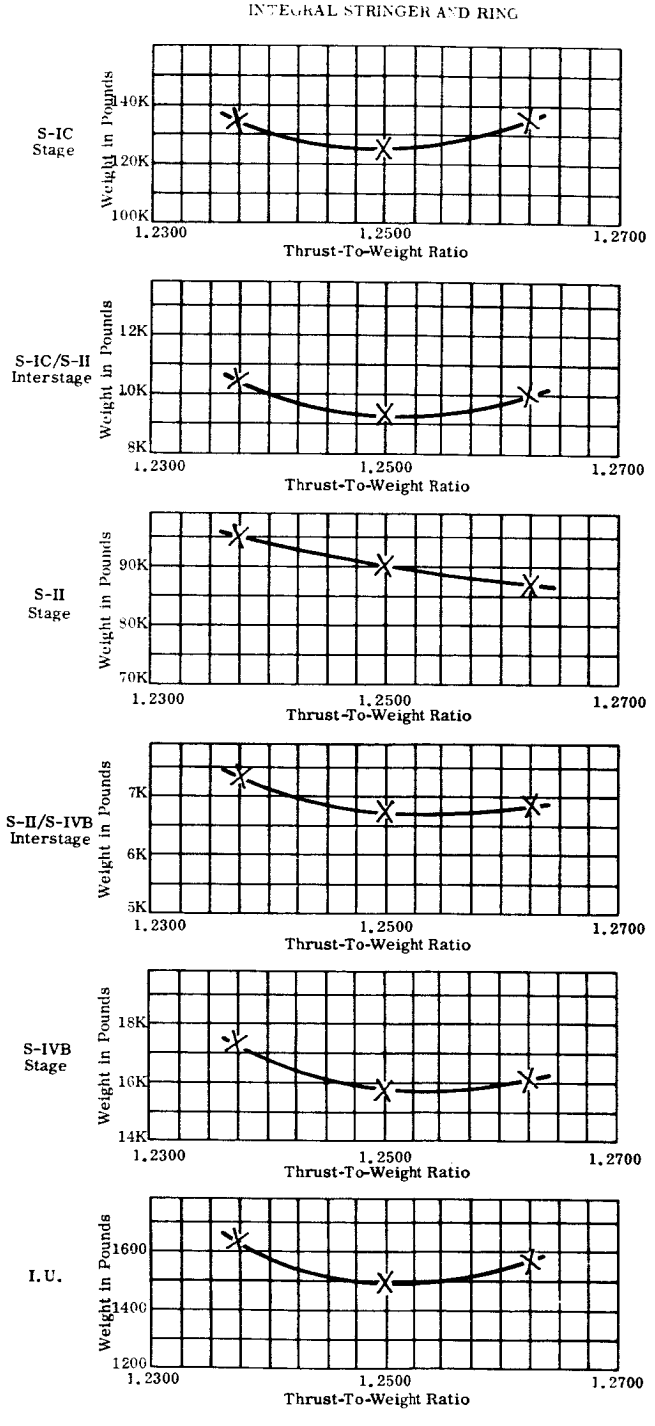

Figure 2-11. Effect of Thrust-to-Weight Ratio Variation on Structural Weight - Integral Stringer and Ring Construction - Total Launch Vehicle

Table 2-7

Monocoque Structural Weight Sensitivity Coefficients
(Unpressurized Sections of Launch Vehicle Only)

	*P.T.F.	Factor of Safety	Allowable Working Stress	Ullage Pressure	Thrust-to-Weight Ratio	Payload Change	Inflight Wind Loads
S-IC Stage	15.0	- 18 (+272)	+ 17 (-259)	0 (0)	See Figure 2-12	-0.6 (+8.7)	- 24 (+ 364)
S-IC/S-II Interstage	14.0	-4.8 (+ 67)	+4.6 (- 64)	0 (0)		-0.3 (+3.8)	- 13 (+ 177)
S-II Stage	3.2	- 21 (+ 68)	+ 20 (- 65)	0 (0)		-1.4 (+4.6)	- 56 (+ 180)
S-II/S-IVB Interstage	3.2	- 17 (+ 54)	+ 16 (- 52)	0 (0)		-1.4 (+4.4)	- 62 (+ 198)
S-IVB Stage	1.0	- 19 (+ 19)	+ 18 (- 18)	0 (0)		-2.2 (+2.2)	- 38 (+ 38)
I.U.	1.0	-3.7 (+3.7)	+3.6 (-3.6)	0 (0)		-0.6 (+0.6)	- 50 (+ 50)

Table 2-8

Honeycomb Structural Weight Sensitivity Coefficients
(Unpressurized Sections of Launch Vehicle Only)

	*P.T.F.	Factor of Safety	Allowable Working Stress	Ullage Pressure	Thrust-to-Weight Ratio	Payload Change	Inflight Wind Loads
S-IC Stage	15.0	- 16 (+233)	+ 15 (-223)	0 (0)	See Figure 2-13	-0.5 (+6.8)	- 20 (+ 295)
S-IC/S-II Interstage	14.0	-3.2 (+ 45)	+3.1 (- 43)	0 (0)		-0.2 (+2.7)	- 8.4 (+ 117)
S-II Stage	3.2	-10.3 (+ 33)	+10.0 (- 32)	0 (0)		-0.8 (+2.4)	- 30 (+ 96)
S-II/S-IVB Interstage	3.2	-7.8 (+ 25)	+7.5 (- 24)	0 (0)		-0.7 (+2.1)	- 28 (+ 89)
S-IVB Stage	1.0	-8.5 (+8.5)	+8.1 (-8.1)	0 (0)		-0.9 (+0.9)	- 13 (+ 13)
I.U.	1.0	-1.4 (+1.4)	+1.4 (-1.4)	0 (0)		-0.2 (+0.2)	-20.0 (+20.0)

*Performance Trade-Off Factor - The ratio of change in stage or module weight to the change in payload capability.

Weight Sensitivity Coefficients are the pounds of equivalent payload for a one percent increase in the parameter being varied. The numbers in parenthesis are the changes in structural weight.

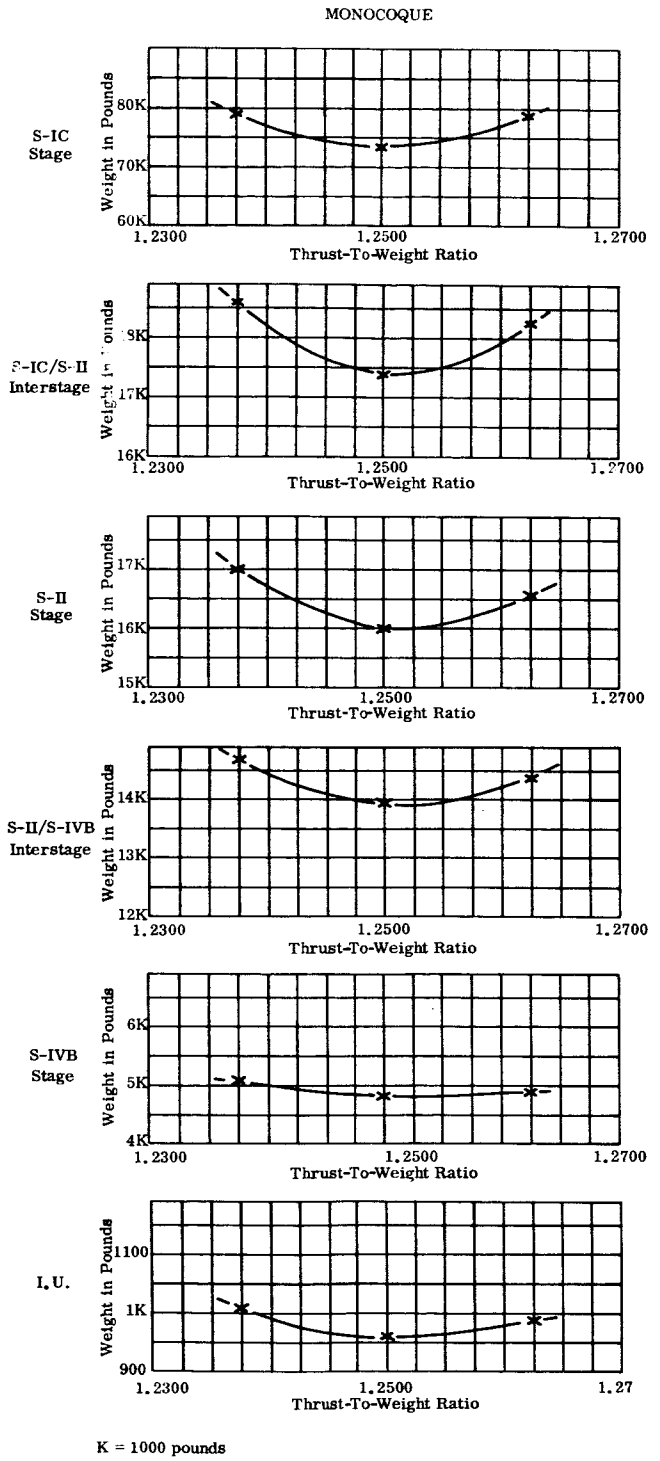

Figure 2-12. Effect of Thrust-to-Weight Ratio Variation on Structural Weight - Monocoque Construction - Unpressurized Sections of Launch Vehicle Only

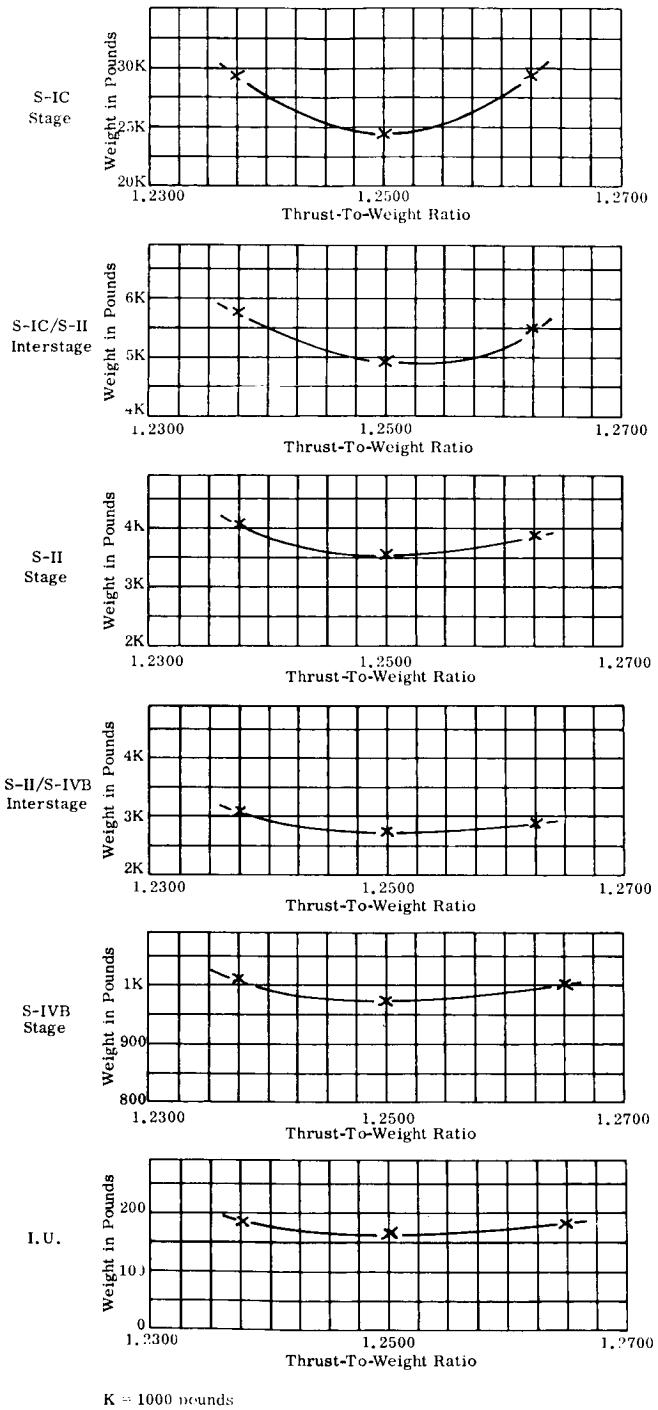

Figure 2-13. Effect of Thrust-to-Weight Ratio Variation on Structural Weight - Honeycomb Construction - Unpressurized Sections of Launch Vehicle Only

Table 2-9

45 Waffle Structural Weight Sensitivity Coefficients
(Unpressurized Sections of Launch Vehicle Only)

	*P.T.F.	Factor of Safety	Allowable Working Stress	Ullage Pressure	Thrust-to-Weight Ratio	Payload Change	Inflight Wind Loads
S-IC Stage	15.0	- 22 (+327)	+ 21 (-312)	0 (0)	See Figure 2-14	-0.6 (+9.4)	- 33 (+496)
S-IC/S-II Interstage	14.0	-4.9 (+ 68)	+4.6 (- 65)	0 (0)		-0.3 (+3.8)	- 14 (+200)
S-II Stage	3.2	- 22 (+ 69)	+ 21 (- 66)	0 (0)		-1.2 (+3.9)	- 64 (+205)
S-II/S-IVB Interstage	3.2	-15.3 (+ 49)	+14.7 (- 47)	0 (0)		-1.2 (+3.8)	- 69 (+221)
S-IVB Stage	1.0	- 21 (+ 21)	+20 (+20)	0 (0)		-1.8 (+1.8)	- 71 (+ 71)
I.U.	1.0	-4.2 (+4.2)	+4.0 (-4.0)	0 (0)		-0.4 (+0.4)	- 50 (+ 50)

Table 2-10

90 Waffle Structural Weight Sensitivity Coefficients
(Unpressurized Sections of Launch Vehicle Only)

	*P.T.F.	Factor of Safety	Allowable Working Stress	Ullage Pressure	Thrust-to-Weight Ratio	Payload Change	Inflight Wind Loads
S-IC Stage	15.0	- 22 (-327)	+ 21 (-312)	0 (0)	See Figure 2-15	-0.7 (+9.9)	- 30 (+455)
S-IC/S-II Interstage	14.0	-5.9 (+ 83)	+5.7 (- 80)	0 (0)		-0.3 (+4.1)	- 14 (+202)
S-II Stage	3.2	- 23 (+ 72)	+ 22 (- 69)	0 (0)		-1.3 (+4.3)	- 63 (+203)
S-II/S-IVB Interstage	3.2	-16.6 (+ 53)	+15.9 (- 51)	0 (0)		-1.3 (+4.2)	- 66 (+212)
S-IVB Stage	1.0	- 21 (+ 21)	+ 20 (- 20)	0 (0)		-1.9 (+1.9)	- 26 (+ 26)
I.U.	1.0	-4.5 (+4.5)	+4.8 (-4.8)	0 (0)		-0.4 (+0.4)	- 51 (+ 51)

*Performance Trade-Off Factor - The ratio of change in stage or module weight to the change in payload capability.

Weight Sensitivity Coefficients are the pounds of equivalent payload for a one percent increase in the parameter being varied. The numbers in parenthesis are the changes in structural weight.

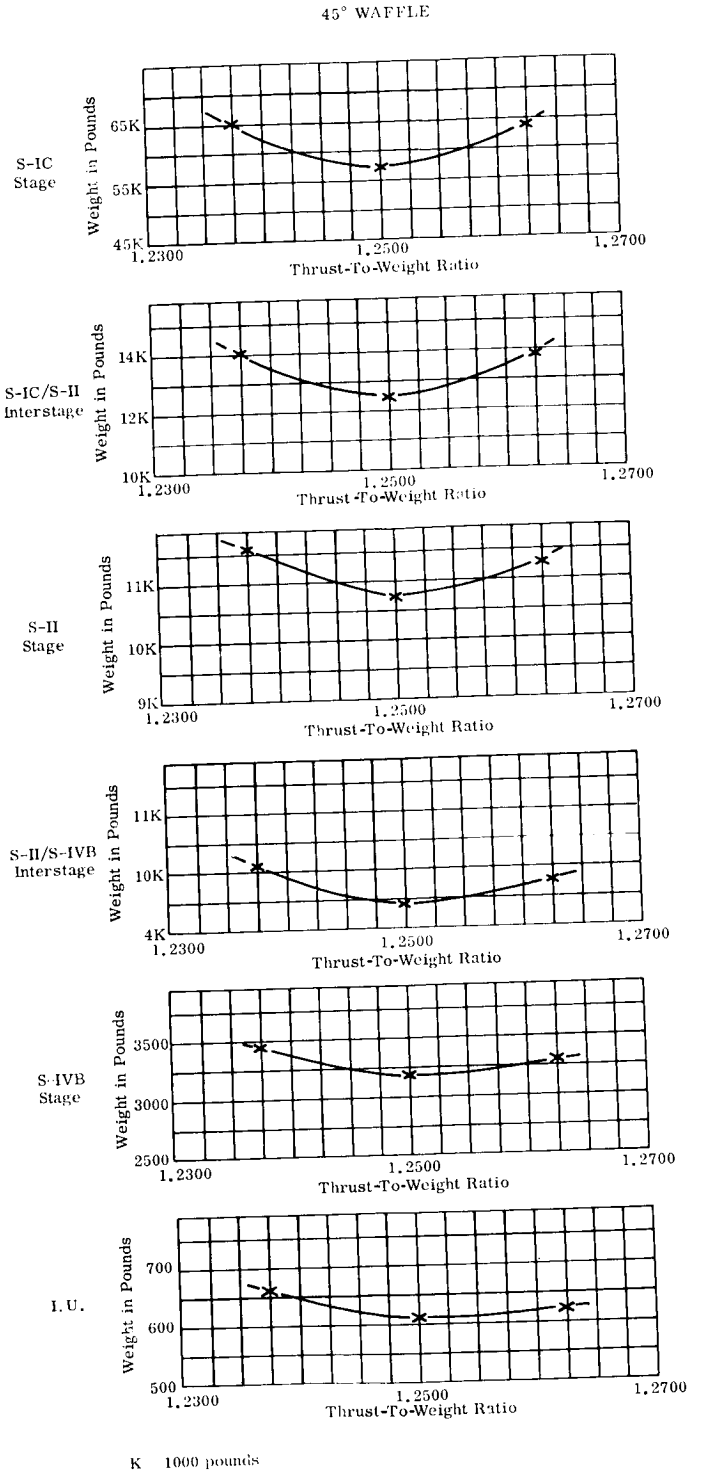

Figure 2-14. Effect of Thrust-to-Weight Ratio Variation on Structural Weight - 45° Waffle Construction - Unpressurized Sections of Launch Vehicle Only

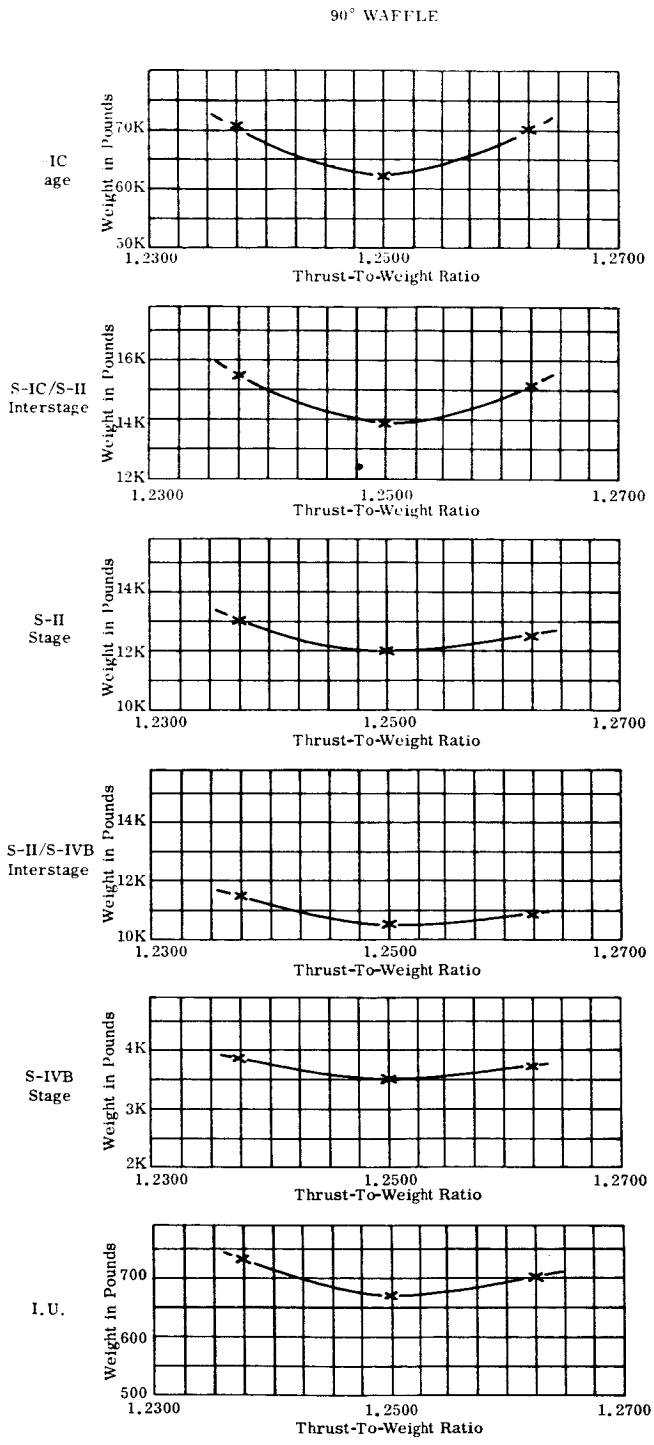

Figure 2-15. Effect of Thrust-to-Weight Ratio Variation on Structural Weight - 90° Waffle Construction - Unpressurized Sections of Launch Vehicle Only

Table 2-11

60 No-Face Corrugation Structural Weight Sensitivity Coefficients
(Unpressurized Sections of Launch Vehicle Only)

	*P.T.F.	Factor of Safety	Allowable Working Stress	Ullage Pressure	Thrust-to-Weight Ratio	Payload Change	Inflight Wind Loads
S-IC Stage	15.0	-7.7 (+116)	+7.4 (-111)	0 (0)	See Figure 2-16	-0.3 (+3.8)	- 11 (+159)
S-IC/S-II Interstage	14.0	-1.9 (+ 27)	+1.8 (- 26)	0 (0)		-0.1 (+1.5)	-4.8 (+ 67)
S-II Stage	3.2	-6.9 (+ 22)	+6.6 (- 21)	0 (0)		-0.5 (+1.7)	- 21 (+ 66)
S-II/S-IVB Interstage	3.2	-5.6 (+ 18)	+5.3 (- 17)	0 (0)		-0.4 (+1.4)	- 21 (+ 66)
S-IVB Stage	1.0	-6.5 (+6.5)	+6.2 (-6.2)	0 (0)		-0.8 (+0.8)	- 68 (+ 68)
I.U	1.0	-1.3 (+1.3)	+1.3 (-1.3)	0 (0)		-0.2 (+0.2)	- 18 (+ 18)

Table 2-12

Single-Face Corrugation Structural Weight Sensitivity Coefficients
(Unpressurized Sections of Launch Vehicle Only)

	*P.T.F.	Factor of Safety	Allowable Working Stress	Ullage Pressure	Thrust-to-Weight Ratio	Payload Change	Inflight Wind Loads
S-IC Stage	15.0	-9.2 (+138)	+8.8 (-132)	0 (0)	See Figure 2-17	-0.5 (+7.8)	- 24 (+366)
S-IC/S-II Interstage	14.0	-6.4 (+ 90)	+6.1 (- 86)	0 (0)		-0.2 (+3.1)	- 11 (+156)
S-II Stage	3.2	- 39 (+125)	+ 37 (-119)	0 (0)		-0.8 (+2.6)	-4.4 (+141)
S-II/S-IVB Interstage	3.2	-11.3 (+ 36)	+10.6 (- 34)	0 (0)		-1.0 (+3.1)	-4.4 (+140)
S-IVB Stage	1.0	-9.3 (+9.3)	+8.9 (-8.9)	0 (0)		-1.2 (+1.2)	-126 (+126)
I.U.	1.0	-1.7 (+1.7)	+1.6 (-1.6)	0 (0)		-0.2 (+0.2)	- 32 (+ 32)

*Performance Trade-Off Factor - The ratio of change in stage or module weight to the change in payload capability.

Weight Sensitivity Coefficients are the pounds of equivalent payload for a one percent increase in the parameter being varied. The numbers in parenthesis are the changes in structural weight.

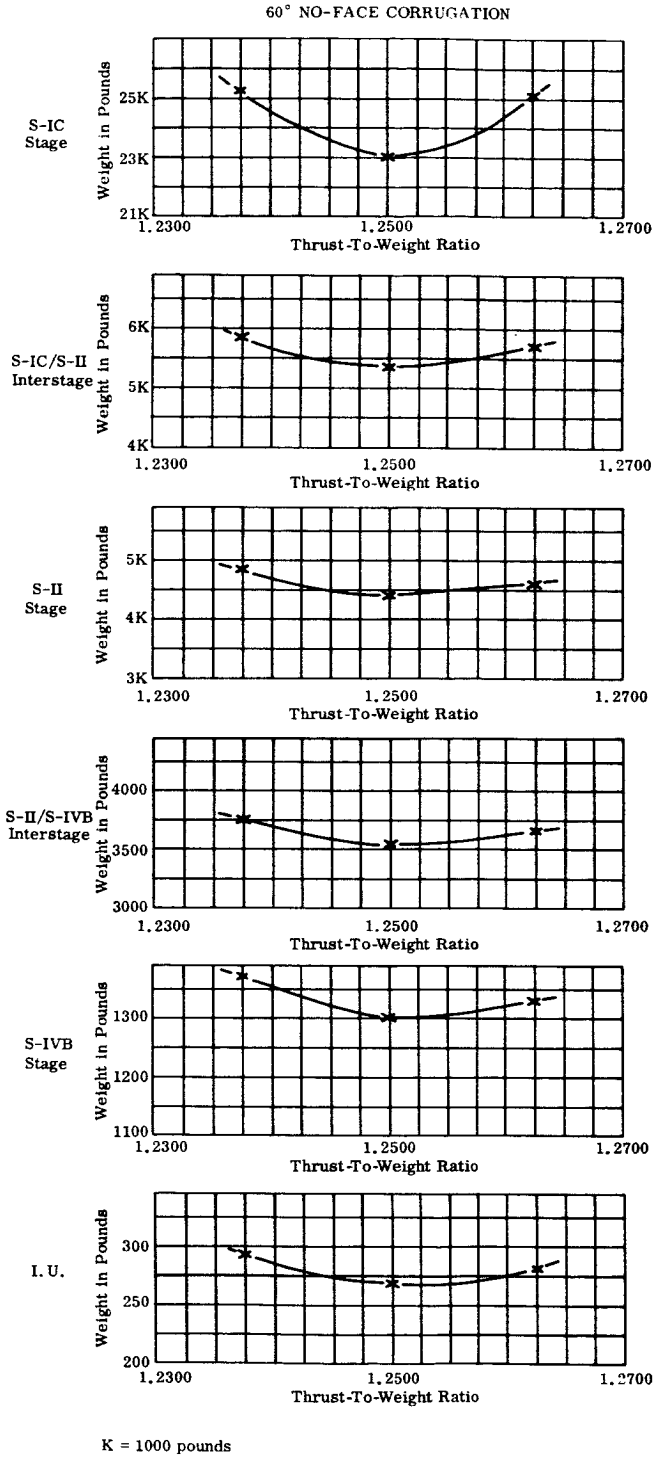

Figure 2-16. Effect of Thrust-to-Weight Ratio Variation on Structural Weight - 60° No-Face Corrugation Construction - Unpressurized Sections of Launch Vehicle Only

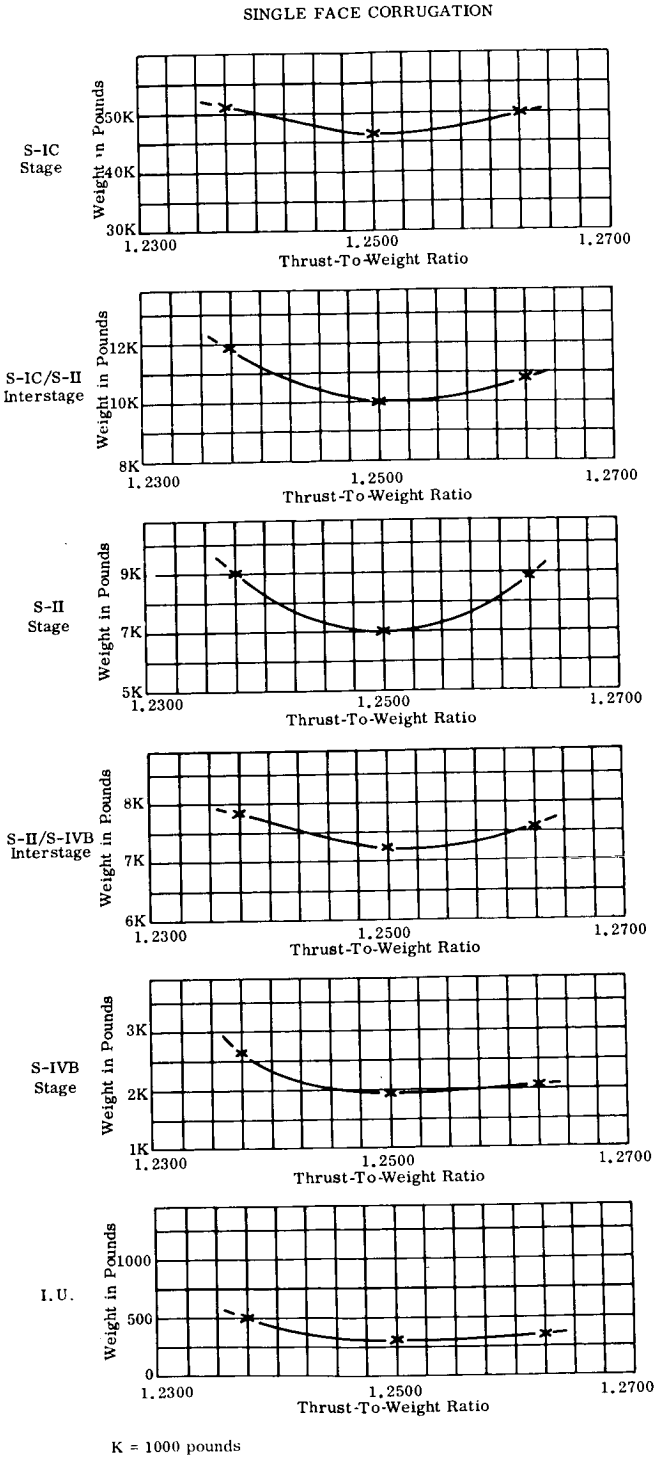

Figure 2-17. Effect of Thrust-to-Weight Ratio Variation on Structural Weight - Single-Face Corrugation Construction - Unpressurized Sections of Launch Vehicle Only

Table 2-13

Semi-Monocoque Structural Weight Sensitivity Coefficients
(Unpressurized Sections of Launch Vehicle Only)

	*P.T.F.	Factor of Safety	Allowable Working Stress	Ullage Pressure	Thrust-to-Weight Ratio	Payload Change	Inflight Wind Loads
S-IC Stage	15.0	- 16 (+ 233)	+ 15 (- 222)	0 (0)	See Figure 2-18	-0.6 (+9.5)	- 21 (+320)
S-IC/S-II Interstage	14.0	- 2.9 (+ 40)	+ 2.7 (- 38)	0 (0)		-0.2 (+2.3)	-7.9 (+110)
S-II Stage	3.2	- 10 (+ 32)	+ 9.7 (- 31)	0 (0)		-0.7 (+2.3)	- 30 (+ 95)
S-II/S-IVB Interstage	3.2	- 6.9 (+ 22)	+ 6.6 (- 21)	0 (0)		-0.5 (+1.7)	- 28 (+ 90)
S-IVB Stage	1.0	- 11 (+ 11)	+ 10 (- 10)	0 (0)		-1.2 (+1.2)	-238 (+238)
I.U.	1.0	- 6.1 (+ 6.1)	+ 5.8 (- 5.8)	0 (0)		-0.9 (+0.9)	- 25 (+ 25)

Table 2-14

Integral Stringer and Ring Structural Weight Sensitivity Coefficients
(Unpressurized Sections of Launch Vehicle Only)

	*P.T.F.	Factor of Safety	Allowable Working Stress	Ullage Pressure	Thrust-to-Weight Ratio	Payload Change	Inflight Wind Loads
S-IC Stage	15.0	- 16 (+ 234)	+ 15 (- 223)	0 (0)	See Figure 2-19	-0.5 (+8.1)	- 23 (+347)
S-IC/S-II Interstage	14.0	- 3.1 (+ 43)	+ 2.9 (- 41)	0 (0)		-0.2 (+3.4)	- 11 (+150)
S-II Stage	3.2	-15.3 (+ 49)	+14.7 (- 47)	0 (0)		-0.4 (+1.2)	- 47 (+151)
S-II/S-IVB Interstage	3.2	-10.6 (+ 34)	+10.3 (- 33)	0 (0)		-0.1 (+3.2)	- 59 (+190)
S-IVB Stage	1.0	- 16 (+ 16)	+ 15 (- 15)	0 (0)		-0.4 (+0.4)	- 98 (+ 98)
I.U.	1.0	- 9.8 (+ 9.8)	+ 9.4 (- 9.4)	0 (0)		-2.6 (+2.6)	- 25 (+ 25)

*Performance Trade-Off Factor - The ratio of change in stage or module weight to the change in payload capability.

Weight Sensitivity Coefficients are the pounds of equivalent payload for a one percent increase in the parameter being varied. The numbers in parenthesis are the changes in structural weight.

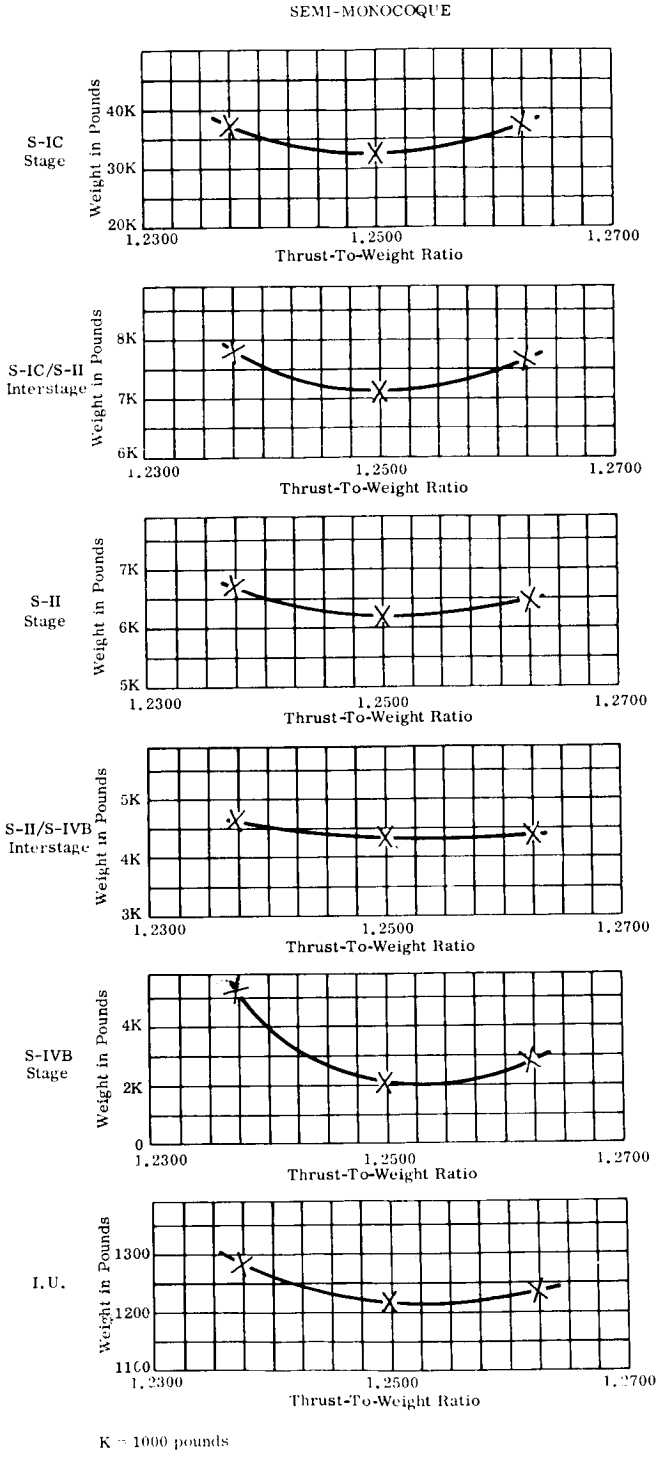

Figure 2-18. Effect of Thrust-to-Weight Ratio Variation on Structural Weight - Semi-Monocoque Construction - Unpressurized Sections of Launch Vehicle Only

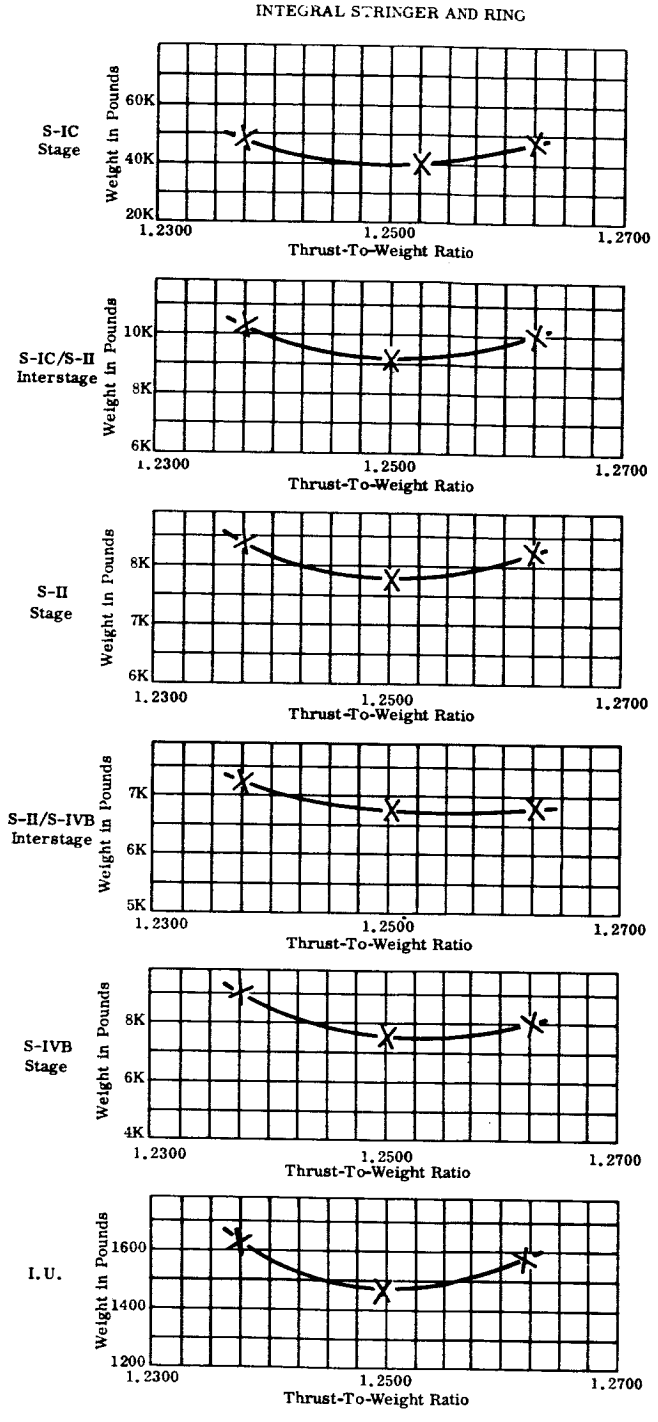

Figure 2-19. Effect of Thrust-to-Weight Ratio Variation on Structural Weight - Integral Stringer and Ring Construction - Unpressurized Sections of Launch Vehicle Only

influence on the trajectory from a structural loads standpoint is negligible. This argument does not hold if there are large variations in parameters such as propellant loading. The changes in propellant weight could be a significant part of the total launch vehicle weight and its effect on the trajectory would have to be evaluated.

To further illustrate the dependence of the trajectory on certain parameters, let us consider an analysis for thrust-to-weight ratio variations. It is first necessary to establish whether the change thrust-to-weight ratio involves a change in the thrust or a change in the weight. If the weight has changed, it is necessary to establish how the weight change is distributed along the vehicle axis and how the other mass characteristics such as mass moment of inertia are affected. It is possible, therefore, to get many different values of weight sensitivity coefficients for the thrust-to-weight ratio variations depending upon how the changes in thrust and weight are established. For simplicity, the analyses which have been performed to date considered thrust-to-weight ratio variations through changes in thrust only. Even with this simplification, there are still some questions to be answered before a unique solution can be specified. In order to gain an understanding of this problem, it will be necessary to discuss the definitions of guidance, control, and trajectory as they are used in this discussion.

The position of the launch vehicle at any particular flight time may be described by the components of the position vector related to an XYZ coordinate system with its origin at the center of the earth. The trajectory, therefore, is the locus of the position of the vehicle which is a function of flight time as well as the XYZ coordinates. By this definition, a path described within the spacial frame is not a trajectory until the position of the vehicle along this path as a function of flight time is also specified.

This leads us into a discussion of the guidance system. The guidance system, in general, specifies a trajectory to be followed by the vehicle for ideal conditions - that is, for no disturbing forces such as winds and no inaccuracies in any of the functional systems. We see that for a given vehicle configuration there are infinitely many trajectories that could be specified by the guidance system; but only one of these trajectories will accomplish the mission with a minimum expenditure of energy. Such a trajectory is called the "optimum trajectory" subject to the other constraints which are imposed. This definition of optimum depends on the reference which has been established; that is, precisely what parameters have been fixed and what parameters have been allowed to vary in

searching for the minimum energy trajectories. The first-stage flight will normally be governed by a gravity turn. Then, for a fixed configuration (i.e., for specified vehicle mass, aerodynamic, thrust, and control configurations), the minimum energy trajectory can be determined. This is not an easy problem, however, as is witnessed by the many trajectory optimization studies which have been (and still are) in progress throughout the technical world. The complexity of a "Trajectory Optimizer" weighed heavily in the decision to exclude it from the scope of this program. The trajectory is, therefore, a required input for the GASP program. For a fixed vehicle configuration, a given trajectory can be specified by a pitch rate profile (i.e., pitch rate as a function of flight time). Since the pitch rate is an important parameter in the control system equations, the input format of GASP requires that the trajectory be specified by a pitch rate profile. The important thing to remember here is that the pitch rate profile specifies a given trajectory for a fixed vehicle configuration, so that any changes in the vehicle characteristics such as thrust or mass properties will also result in a different trajectory which will not necessarily be the optimum one. As long as we are concerned with the idealized condition of the trajectory analysis with no disturbing winds, small changes in the trajectory will have very little effect on the structural loads imposed on the vehicle. Since a gravity turn is specified for the atmospheric flight, the only loads on the vehicle are drag and thrust. Both of these forces are functions of local atmospheric properties and, since the atmospheric properties are functions of altitude, changes in trajectory will be reflected in changes in the drag and thrust loads. For reasonable variations in the trajectories, however, these effects on the loads will be negligible.

Once a trajectory is selected, the next step in the analysis is to determine the response of the aerodynamically unstable vehicle to inflight disturbances such as winds and gusts. This part of the analysis is performed by the GASP program. An accurate model of inflight winds and gusts is not easily formulated, but a synthetic wind profile with an embedded gust was selected as a suitable description for this program. The vehicle is represented by a rigid body where the mass properties vary with flight time to account for the effects of expended propellants. As the rigid body vehicle flies along the prescribed trajectory, the wind loads that have been introduced will cause the vehicle to deviate from the intended course unless a control system is introduced for the vehicle. Thus we see the difference between a control system and a guidance system. The guidance system provides the vehicle with an idealized optimum trajectory, while the control system tries to keep the vehicle as near as possible to the prescribed trajectory when it

is subjected to disturbances such as wind gusts. The largest loads imposed on the structure may well be due to these transients as the vehicle responds to disturbing forces with the aid of the control system. The control system which is used for the rigid body study is given by the simple equation

$$\beta = a_o\phi + a_1\dot{\phi} + b_o\alpha$$

where

β = engine gimbal angle.

ϕ = pitch error.

$\dot{\phi}$ = pitch rate error.

α = angle of attack.

a_o, a_1, b_o = gains of the control system.

The control gains vary with flight time and are chosen so that the vehicle has the proper stability characteristics and minimizes the drift away from the intended trajectory. Just as the optimum trajectory analysis is a study within itself, so is the analysis to determine the control characteristics. For this reason, a control analysis is considered to be outside the scope of this program and the control system gains as a function of flight time are required inputs for the GASP program. Even so, it is informative to investigate briefly the nature of the equations which are used to determine the control gains. The gain, a_1, is used to introduce the proper amount of damping in the system. The magnitudes of the gains a_o and b_o establish the frequency of the control system. In a loads analysis, the frequency of the control system and the amount of damping are of lesser importance. Of greater concern are the relative magnitudes of the gains a_o and b_o. For the drift minimum principle of control, the relative magnitudes of the gains a_o and b_o must be chosen to satisfy the simplified equation

$$\frac{b_o + \left[\dfrac{Aq\ C_{z_\alpha}\ (C_g - C_p)}{F\ C_g}\right]}{a_o} = \frac{Aq\ C_{z_\alpha}\left(\dfrac{C_p}{C_g}\right)}{F - Aq\ C_d}$$

where

a_o, b_o = control system gains.

A = reference area of vehicle.

C_{z_α} = gradient of normal aerodynamic force coefficient.

F = magnitude of thrust vector.

C_g = distance between gimbal point and center of gravity.

C_p = distance between gimbal point and center of pressure.

q = dynamic pressure.

C_d = axial aerodynamic force coefficient.

The input requirements of GASP assume a knowledge of the trajectory, the mass characteristics, the control system gains, the aerodynamic coefficients, and the atmospheric properties. Usually, these data will be available from other more specialized studies, but they will not all be functions of the same independent variable. The control gains, the trajectory, and the mass characteristics will be functions of flight time; the aerodynamic coefficients will be functions of mach number; and the atmospheric properties will be functions of altitude. For a fixed configuration, a functional relationship is established between the three independent variables: mach number, flight time, and altitude. If we then change any of the parameters which affect the GASP analysis, we also will change the functional relationship of these independent variables.

In order to illustrate the significance of the above discussion, let us examine a specific example. First, suppose that a nominal or reference configuration is established and the optimum trajectory and the proper control gains have been determined. It will be possible then to carry the analysis of the nominal configuration through the GASP, LASS-1, and SWOP programs and establish the minimum structural weight subject to the constraints imposed. Now, suppose we would like to determine how much the structural weight changes when the thrust-to-weight ratio changes. In view of our earlier discussion it will be assumed that the thrust will change and the weight of the vehicle will remain unaltered. Then, except for the thrust of the vehicle, all other input data to the GASP program will be the same as for the nominal configuration. We can now trace the progression of events as the flight of the vehicle is simulated in the GASP program. At some arbitrary time after launch, the vehicle will be at a different altitude than the nominal configuration at the same flight time. This is partially due to the change in trajectory (since the trajectory is described by a pitch rate/flight time relationship) and partially due to the increased thrust. We also notice that the velocity at this arbitrary time point is different, so the mach number is different due to the change in veloc-

ity and the difference in atmospheric properties at the new altitude. Thus we see that the relationship between mach number, altitude, and flight time is completely different. From our earlier discussion of the control system, we see that the control system gains will no longer satisfy the requirements of a drift minimum principle. Also, since the synthetic wind profile is at a fixed altitude, the mass characteristics of the vehicle will be different when maximum wind loads occur.

After a little reflection on these events, it is not surprising that changes in certain parameters (such as thrust) have nonlinear relationships with changes in structural weight. It is difficult to make generalizations about the magnitudes of these nonlinearities and, in some cases, even the direction of change in structural weight is difficult to predict for a given change in a parameter. The primary purpose of this discussion is to provide the program user with a means of interpreting the numerical results of an analysis. This is not an easy task and all aspects of the analysis will have to be given careful consideration if the results are to satisfy a useful end.

SECTION 3
RECOMMENDATIONS

In the course of developing this computer program, an awareness of several improvements or extensions to this work have evolved which would provide valuable addition to the present capabilities. Further consideration of these additional features should yield gainful contributions to the utility of this program. These recommendations are described briefly below.

Preliminary results indicate that, in some instances, the honeycomb analysis will select "optimum" designs which are slightly heavier than some "off-optimum" designs. This is due to constraints imposed on the shear modulus of the honeycomb core and its complex interrelation with the buckling criteria. Further study is needed in this area to insure that the minimum weight design will be selected in every case.

Aft bulkheads which are partially filled with liquid can, under certain conditions, have compressive hoop stresses which are of sufficient magnitude to cause local buckling of the bulkhead skin. At the present time, this program does not include an analysis which considers this mode of failure. Additional examinations of this mode of failure are warranted to see if the magnitude of structural weight involved is significant enough to require that another mode of failure be included in the analysis.

Recent studies of eccentrically stiffened orthotropic shells have shown that the eccentricity of the stiffeners can have significant effects on the buckling strength of shells even if the radii of the shells are very large. Techniques which account for the eccentricity of stiffeners are presently included in the analysis of single-face corrugation and integral stringer and ring configurations. These techniques should be extended to the other types of construction that use eccentric stiffeners.

Experience with the results of runs for 45° and 90° waffle configurations indicate that the optimization techniques could be improved by rearrangement of some of the computational operations in the computer program. These improvements will reduce the running time of the computer and will give improved results. The computational procedures

of the STRESS program should also be reviewed and re-aligned to obtain shorter running times on the computer.

In many cases, the rings at joints and kick frames contribute significantly to the total structural weight of a vehicle. At the present time, the consideration of these weights is included in the fabrication factor which modifies all calculated weights. More sophisticated procedures should be devised for calculating the weight of these structural elements to improve the overall effectiveness of the program.

The buckling analyses used in this program are correlated to experimental data with buckling correction factors. Since these factors have a direct bearing on the structural weight, it is important to have buckling correction factors which reflect the most recent experimental data available. Also, the fabrication factors, which were mentioned earlier, must be constantly updated as more data becomes available on actual hardware weight so the non-calculable structural weights can be included as accurately as possible in structural weight calculations.

It would be desirable to perform a series of computer runs which could be used as a basis for generating minimum weight charts. These charts could be used to quickly determine optimum designs. There are at least two types of these charts that would be useful. The first one might be a plot of a weight ratio versus the structural load index for a given material as shown in Figure 3-1.

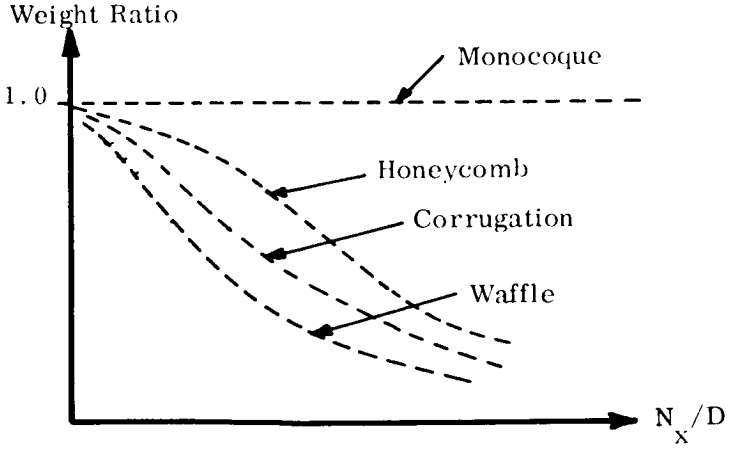

Figure 3-1. Minimum Weight Chart for a Given Material

The weight ratio would be defined as

$$\text{Weight Ratio} = \frac{\text{Weight of Particular Construction}}{\text{Weight of Monocoque Construction}}$$

This type of plot could be developed for cylinders as well as for ellipsoidal and spherical heads.

The other minimum weight chart that would be useful would be a plot of weight ratio versus structural loading index for honeycomb construction made with several different materials as shown in Figure 3-2.

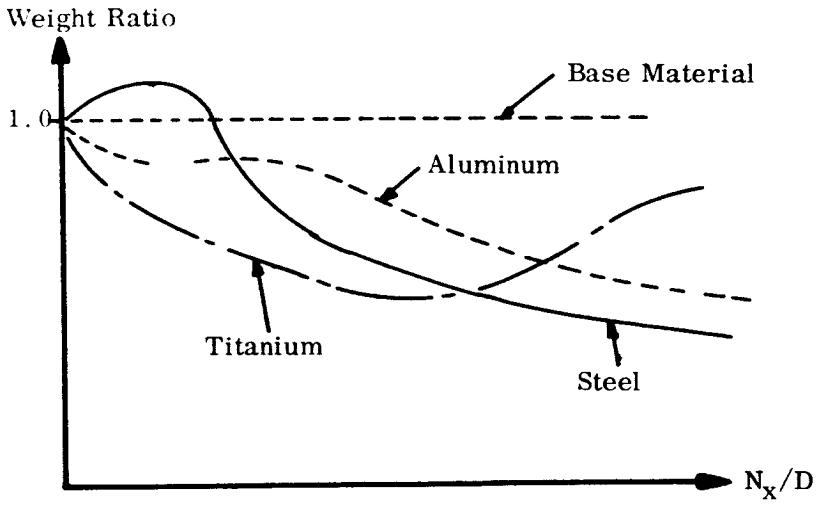

Figure 3-2. Minimum Weight Chart for Honeycomb Construction

The weight ratio in this case is

$$\text{Weight Ratio} = \frac{\text{Weight of Base Material}}{\text{Weight of Particular Material}}$$

Again, this type of plot can be developed for bulkheads as well as for cylinders. The buckling efficiency is dependent upon the modulus of elasticity to density ratio, which is nearly constant for conventional materials operating in the elastic range. Since the honeycomb construction will probably be the only type of construction to have optimum

designs in the elastic-plastic range, this type of minimum weight chart will only be necessary for honeycomb construction.

These charts could be used to compare differences in materials and types of construction very quickly. It should be noted that any differences in weight ratios at low load levels may be attributed to different minimum gages for the various materials.

Presently, the computer program confines itself to the analysis of technical problems which are likely to be given to a program manager for resolution. It is important to realize that these decisions cannot be made solely on the basis of technical evidence. The program manager must also be aware of the impact of his decisions on schedules and monetary resources. The importance of cost is evident when comparisons are made between various stages, modules, and functional systems of space vehicles. The cost of some systems is significantly higher than for others. In a weight reduction program, it is necessary to determine which modules or subsystems are the least expensive to change and how these changes will effect the schedules. Schedule slips can also reduce the effectiveness of the program and delay other related development programs. It is, therefore, advantageous to have executive decisions based upon the facts relating to costs and schedules as well as the technical requirements. This can be accomplished in an efficient manner by extending the scope of this computer program to include schedule and cost considerations. Techniques have been and are being developed which will help to integrate cost effectiveness and schedule predictions, and these techniques could be employed very effectively as additions to this computer program.

SECTION 4

EXECUTIVE CONTROL PROGRAM DESCRIPTION AND PHILOSOPHY

4.1 INTRODUCTION

The current and future trend in digital computer program technology is to ever larger and more complex programs. Quite often, however, these programs tend to be rigid in their formation, inflexible in their input/output, difficult to modify, and programer dependent. It was with these constraints in mind that the executive control program logic was developed.

The design of the program is modular in concept. This means that changes to any one section of the coding will generally not affect any other section. It also means that any number of programers can work on the various modules at one time, since the basic interface logic between modules is always under executive control.

The input/output subroutines of the executive program provide the user with a flexible control that allows selection of run options and output formats at executive time. The input data is checked by a control program subroutine and errors in input format will cause the run to terminate before costly machine time is wasted. A restart capability is also included.

The following paragraphs detail the overall functions, options, and methods of operation of the executive control program developed for the Structural Weight Optimization Program.

4.2 ADVANTAGES

The advantages of executive control program design for the Structural Weight Optimization Program include:

a. Minimal data manipulation by subroutine.

b. Flexibility:

   (1) Wide range of run-time options.

   (2) Executive program guides flow of control through only the modules needed by user-defined job.

c. Convenient output:
   (1) User picks the output matrices desired.
   (2) Optional intermediate output.
   (3) Facility to subtotal weights.
   (4) Matrices scan for and print out minimum weights.

d. Convenient input:
   (1) ID word on READH format cards simplifies input organization.
   (2) Data not frequently changed is prestored, cutting run-time input to minimum.
   (3) Any desired run-time changes of stored data can be made easily.

e. Compatible with different facilities:
   (1) Tape selection is made by user to fit system configuration at his location.
   (2) Modular design allows easy overlay adaptation for each location.
   (3) Nearly all of program is coded in FORTRAN IV.

f. Savings of running time:
   (1) Executive control program bypasses modules not needed by user-defined job.
   (2) Centralization of material property handling, input, output, sheet dividing, and other functions saves time and core locations.

g. Future expansion:
   (1) Provides for addition of more construction subprogram modules.
   (2) Provides space for adding more built-in materials.
   (3) Modular construction simplifies changes (only module being changed needs recompilation).

4.3 STRUCTURAL WEIGHT OPTIMIZATION PROGRAM (EXECUTIVE CONTROL)

4.3.1 CURRENT CAPABILITIES

The current design capabilities of the program are:

a. Construction types (limited to 10; program presently uses 8):
   (1) Monocoque shell.
   (2) Honeycomb sandwich.
   (3) Waffle 45°.

(4) Waffle 90°.

(5) No-face corrugation.

(6) Single-face corrugation.

(7) Semi-monocoque.

(8) Integral ring and stringer stiffened.

(9), (10) Blank for future expansion.

b. Materials (up to 12; program now uses 9):

(1) Aluminum 2014-T6.

(2) Aluminum 7075-T6.

(3) Aluminum 2024-T4.

(4) Aluminum 2219-T87.

(5) Titanium 6A1-4V.

(6) Steel AISI-4340.

(7) Magnesium HK31A-H24.

(8) Stainless Steel PH15-17Mo.

(9) Beryllium Y5804-QMV5.

(10), (11), (12) Blank for future expansion.

c. Design parameters, such as:

(1) Safety factors.

(2) Fuel densities.

(3) Fuel flow rates.

(4) Ullage pressures above fuel (includes time dependence).

(5) Hydrostatic test fluid density.

(6) Dynamic multipliers for moments from LASS-1 program.

(7) Dynamic multipliers for axial forces from LASS-1 program.

(8) Fuel temperatures.

(9) Fabrication factors.

d. Construction subprogram options:

(1) Setting limits on construction parameters (manufacturing limitations or desirable ranges).

(2) Specifying fixed values of construction parameters usually optimized (generally resulting in somewhat off-optimum designs since only the remaining non-fixed parameters are then optimized):

(a) Fixed core thicknesses (honeycomb sandwich).

(b) Fixed rib spacing (45° waffle and 90° waffle).

(c) Fixed total depth (45° waffle and 90° waffle).

(d) Fixed corrugation depth (no-face and single-face corrugation).

(e) Fixed ring spacing (no-face corrugation).

(f) Fixed corrugation thickness (no-face corrugation).

(g) Fixed frame spacing (semi-monocoque).

(h) Fixed frame thickness (semi-monocoque).

(i) Fixed frame height (semi-monocoque).

(j) Fixed skin thickness (semi-monocoque).

(k) Fixed stringer thickness (semi-monocoque).

(l) Fixed stringer pitch (semi-monocoque).

(m) Fixed stringer height (semi-monocoque).

The wide variety of optional operations indicated above required the development of a highly efficient input method to allow maximum run-time flexibility with a minimum volume of simple input. Results are clearly presented in final output matrices, and the option of easily obtainable detailed intermediate output is also available. The final program is compatible with the IBM 7094, IBM 7044, and GE 625/635 computers, and is easily adapted to the system in use at any particular location. The most efficient way to fulfill these program requirements has been to design the program according to the executive control program concept.

4.3.2 METHOD

The executive control program consists of a controlling main program and modules designed to do a particular task. The main program guides the flow of control through the necessary modules as it determines which sequences are required to satisfy the preselected job options.

The following modules are used:

a. XQTIVE - the executive control program - a FORTRAN IV main program handles control cards that the customer uses to define his job, then calls the input handling module, STRESS tape generating module, the LOOP module, and the output matrix module. It stacks jobs in one run and has a job timing feature available for use on computers with an interval timer.

b. Input module handles run-time input for each job.

c. LOOP subprogram - performs sequencing and looping for vehicle sections. construction subprograms, and materials. As each suboptimization returns its resultant weights, they are stored in the proper summary matrix. LOOP also performs sheet divisions and determines maximum loads in each sheet before it calls a construction subprogram.

   The DIVIDE subroutine prints out details of sheet divisions and maximum loads when specified.

   The INTERP subroutine interpolates on stored material properties to find properties at temperature of station under consideration.

d. MATRIX subprogram prints out comparative matrices including minimums and totals.

   The CRUNCH subroutine is used by MATRIX in computing subtotals for matrices of comparative subtotal weights.

e. STRESS and its subroutines take moments and axial forces from the LASS-1 program, then resolve all forces into stress resultants which include effects of liquid levels, flow rates, ullage pressures, and hydrostatic tests. The maximum values (over the time points under consideration) of the stress resultants are saved on the restart tape for the LOOP routine's sequence of structural subprograms or for future runs.

f. MONMAS and its subprograms perform computation of monocoque shell construction parameters. They will print intermediate output if requested and can handle both cylinders and heads.

g. HONMAS and its subprograms perform optimization and option computations for honeycomb sandwich structures, and print out intermediate output if requested. They can handle both heads and cylinders.

h. W45MAS and its subroutines perform optimization and option computations for 45° waffle constructions, printing out intermediate output if specified. Both cylinders and heads may be computed.

i. W90MAS and its subroutines perform optimization and option computations for 90° waffle constructions, printing out intermediate output if specified. Both cylinders and heads may be computed.

j. CR1MAS and its subroutines perform optimization and option computations for no-face corrugation sections, printing out intermediate output if requested. Applicable only to cylinders.

k. CR2MAS and its subroutines perform optimization and option computations for single-face corrugation sections, printing out intermediate output if specified. Applicable only to cylinders.

l. SEMMAS and its subroutines perform optimization and option computations for semi-monocoque constructions, printing out intermediate output if specified. Applicable only to cylinders.

m. INTMAS and its subroutines perform optimization computations for integral ring and stringer constructions, printing out intermediate output if specified. Applicable only to cylinders.

Data needed by more than one subprogram is handled through "common" blocks accessible to the right routines. The resolved loop and meridional stresses, however, are stored on tapes which may be saved for later runs. This results in a minimum of data manipulation, as well as permitting computations to restart from the stresses tape.

Because of the large size of the Structural Weight Optimization Program, all of it can not fit into core at the same time. Modular construction allows for easy division of the program into sections small enough to fit into the computer. The main control routine and the common blocks used to keep data accessible to all routines are kept in core at all times, but other modules and common blocks needed by only a few routines are read into core only as needed.

To keep the program compatible with the IBM 7044, IBM 7094, and GE 625/635 computers, FORTRAN IV coding is used whenever possible. Only one major routine, READH, is written in machine language. It exists in versions for both IBM machines

presently, and an additional version will be written for the GE625/635 in the near future. To aid compatibility between locations, physical tape and logical unit selections are variable.

4.3.3 INPUT OUTLINE

The executive control program input is designed to reduce data volume to the minimum required to define the given job.

As previously discussed, the program maintains the capability to alter at run time any data which changes infrequently and therefore is prestored.

Prestored data is kept in the block data program. It includes:

a. Tape selections.
b. Stored material properties.
c. Temperature profile.
d. Fabrication factors.
e. Ullage pressure time variations.
f. Names for use in matrix labeling.

All prestored data except tape selections can be changed or added to at run time. This permits the user to avoid tedious inputting of large amounts of data, but maintain the ability to change stored data with run-time input when desired.

Tape selections for a given facility are generally not flexible and most users have little, if any, knowledge of the logical tape units available to them. It was thus decided to prestore the tape designations for each facility. The routine in which tape selection is made is easily recompiled in the unlikely event that a facility changes its tape designations.

All run-time input is handled through the READH routine which reads cards with a six-letter ID name and free-field format for both integer and floating point numbers.

The ID word on all READH input cards labels all input, thus permitting the user the flexibility of a random input arrangement except for the initial control cards which must be in a sequential order.

The READH routine is independent of system I/O which facilitates usage at the various sites.

4.3.4 OUTPUT OUTLINE

All output can be selected or supressed at run time, as the user sees fit. Whenever a type of output is supressed, any computations which can therefore be omitted are by-passed to save computer time. There are three levels of output as follows:

a. Detailed output of each optimization procedure:
   (1) Sheet divisions and maximum loads per sheet - computed once for each construction subprogram specified for a structural section to be divided up into sheets.
   (2) Construction details of the best solution - computed for each material specified for the "construction subprogram - structural section" combination under consideration.

b. Comparative matrices - these show the weights of each structural section specified in a matrix that compares different structural subprograms, materials, design parameters, or program options.

c. Comparative subtotal matrices - which show the structural section weights added up into subtotals specified at run time and put into comparative matrices. The subtotal feature is valuable in examining total weights of stages, interstages, tanks, etc.

Sample output sheets are included with this user's manual under the detailed input/output instructions section.

4.3.5 MATRIX FORMATS

4.3.5.1 General

There are five main types of comparative weight matrices. The subtotal and individual section matrices of the same type are similar, except that one contains subtotal weights while the other contains weights for each individual structural component.

Note that computer printer size limits the number of construction types, material, options, or design parameter values that may be compared in a single matrix. This hardware limitation may be bypassed by dividing the total job desired into matrices

that are small enough for the printer, and then using the stacked jobs feature of this program to run the smaller matrices as stacked jobs in the same computer run.

A job of type 2, 3, or 4 may produce its output in more than one matrix type. These three job types may output via any or all three of matrix types 2, 3, or 4. Jobs of type 1 or 5 may output only their respective matrix.

Stacked jobs are separate jobs computed in the same computer run. This feature means that many jobs may be run at one loading of the computer, thus saving computer time. The "JOBS" input card specifies how many jobs are to be stacked in this run, and the separate data packages for each job follow.

4.3.5.2 Format One

Comparative Weight Matrix for Stress Program Parameters for Construction _____ and Material _____.

Section or Subtotal Identification	Param. Value ID (1)		Param. Value ID (6)	Minimum
TANK 1 BHD.	W_{11}	W_{12}	W_{16}	$W_{min}(1)$
TANK 1 CYL.	W_{21}			$W_{min}(2)$
ETC.				
	Weights Printed Here			
Totals	$W_{total}(1)$			W_{min} total

A job of type 1 performs parameter studies requiring recomputations of the stress tape, such as parameter studies on ullage pressure or fuel flow rates. The weights are printed in matrix form and the minimum weight for each structural section is put in the minimum column. The columns are then totaled. If the construction is not applicable to a particular section, the space contains a zero.

4.3.5.3 Format Two

Comparative Weight Matrix for Different Construction Types for Material _____.

Identification of Section or Subtotal	Construction One	Construction Two	Construction Five	Minimum
TANK 1 BHD.	W_{11}	W_{12}	W_{15}	$W_m(1)$
TANK 1 CYL.	W_{21}			
ETC.	Weights Printed Here			
Totals	$W_{total}(1)$			W_{min} total

A job of type 2 investigates the effect of changing construction types for a given material. The weights are printed in matrix form, with the minimum weight for each section put in the minimum column. The columns are then totaled. Construction and material combinations not applicable to a section are filled with zeros.

4.3.5.4 Format Three

Comparative Weight Matrix for Different Materials for Construction Type _____.

Identification of Section or Subtotal	Material One	Material Two	Material Six	Minimum
TANK 1 BHD.	W_{11}	W_{12}	W_{16}	$W_m(1)$
TANK 1 CYL.	W_{21}			
ETC.	Weights Printed Here			
Totals	$W_{total}(1)$			W_{min} total

A job of type 3 investigates the effect of changing materials for a given construction type. The weights are printed in matrix form with the minimum weight for each section in m, the minimum column. Each column is then totaled. Construction and material combinations not applicable to a section are filled with zeros.

4.3.5.5 Format Four

Comparative Weight Matrix for Section or Subtotal _____.

Material	Material One	Material Two	Material Six
Subprogram			
Construction One	W_{11}	W_{12}	W_{16}
Construction Two	Weights Printed Here		
Construction Three			
Construction Five	W_{51}		W_{56}

The minimum weight occurs for subprogram _____, and material _____.

A job of type 4 compares weights of different construction and material combinations for a given structural section or subtotal. The weights appear in matrix form, and the minimum weight configuration is specified below the matrix. Particular combinations of construction and material which are inapplicable to the section or weren't specified by the user are filled with blanks.

4.3.5.6 Format Five

Matrix of Comparative Weights for Different Option Settings for Construction _____ and Material _____.

Section or Subtotal Identification	Option One	Option Two	Option Six	Minimum
TANK 1 BHD.	W_{11}	W_{12}	W_{16}	$W_{min}(1)$
TANK 1 CYL.	W_{21}			
TANK 1 THD.	W_{31}			
ETC.	Weights Printed Here			
Totals	$W_{total}(1)$			W_{min}total

A job of type 5 compares weights for different option settings for a particular construction and material combination. The weights are printed in matrix form and the minimum weight for each section or subtotal is placed in the minimum column. The columns are then totaled. If the construction is not applicable to a particular section, the space contains a zero.

4.3.6 FLOW CHART

An overall flow chart is given in Appendix D.

SECTION 5

PROGRAM DESCRIPTION

5.1 GASP-RIGID BODY LAUNCH SIMULATION

5.1.1 GENERAL DESCRIPTION OF PROGRAM

The Generalized Aerospace Program (GASP) is used as the first step in the analysis of the loads imposed on a space vehicle. The general function of this analysis is to determine the response of the space vehicle to aerodynamic and control loads which are present during atmospheric flight. The mathematical description of the true physical problem has been the subject of many technical studies in recent years. While these studies have resulted in many analyses of varying sophistication, none can be described as "exact" solutions of the general problem. In any study the mathematical model must be chosen so that the application of this analysis is not seriously constrained by the simplifying assumptions. At the same time, the mathematical model must not be overly rigorous so that the analysis becomes unduly complicated.

It is these general guidelines which helped to establish the mathematical model to be used in this particular analysis. The space vehicle is described as a rigid body whose mass properties (weight, center of gravity, polar moment of inertia) are variable with flight time. The motion of the space vehicle is described by three coordinates, two in translation and one in rotation. Thus, the motion of the vehicle is constrained to a single trajectory plane. The forces which are imposed are aerodynamic forces, and control forces. The aerodynamic forces are considered as functions of mach number, angle of attack, and dynamic pressure. The center of pressure location is expressed as a function of mach number and atmospheric properties are given by the ARDC Model Atmosphere of 1959.

The space vehicle can, in general, be treated as an aerodynamically unstable vehicle which is artificially stabilized with gimbaled engines. The general form of the control equation is

$$\beta = a_o \phi + a_1 \dot{\phi} + b_o \alpha$$

where

a_0, a_1, b_0 are control gains.

ϕ is the position error.

$\dot{\phi}$ is the position rate error.

α is the angle of attack.

The control gains are considered to be functions of flight time and are determined to satisfy some control principle such as minimum acceleration, minimum drift, etc. All calculations which have been performed to date with this analysis have used the drift minimum principle (DMP), since the control gains have been readily available from Reference 1.

The mathematical model just described is used to determine the rigid body motions of the space vehicle. This implies the assumption that the forces on the space vehicle in this part of the analysis are independent of the elasticity of the space vehicle. In general, this is not true since the applied forces will cause deformations which result in local variations of angle of attack and dynamic pressure which, in turn, affect the magnitude of the applied forces. The general study of these effects comes under the heading of aeroelastic analysis. While for very flexible aerodynamic bodies the aeroelastic effects may be of great importance, for most space vehicles which are of major importance today the aeroelastic effects may be excluded with negligible error.

All of the equations used in describing the mathematical model are presented in detail in Appendix B. These equations compose a program called simply the Wind Stress Launch Program - 27B. This program is included under the GASP system which is a general approach to the problem of developing flight simulation error analysis programs. A library of programs and program parts (modules) is maintained, and any of these may be incorporated into a new simulation effort without further testing. The GASP concept allows large programs to be subdivided into smaller, independent pieces so that maximum use can be made of existing programs (see Figure 5-1).

A wide range of operation is possible using GASP. A given program may consist of one or several machine loads, depending upon the particular needs of the user. Parts of a large simulation and analysis program may be executed at different times and the results saved on magnetic tape, allowing complete analysis of a given section before moving on

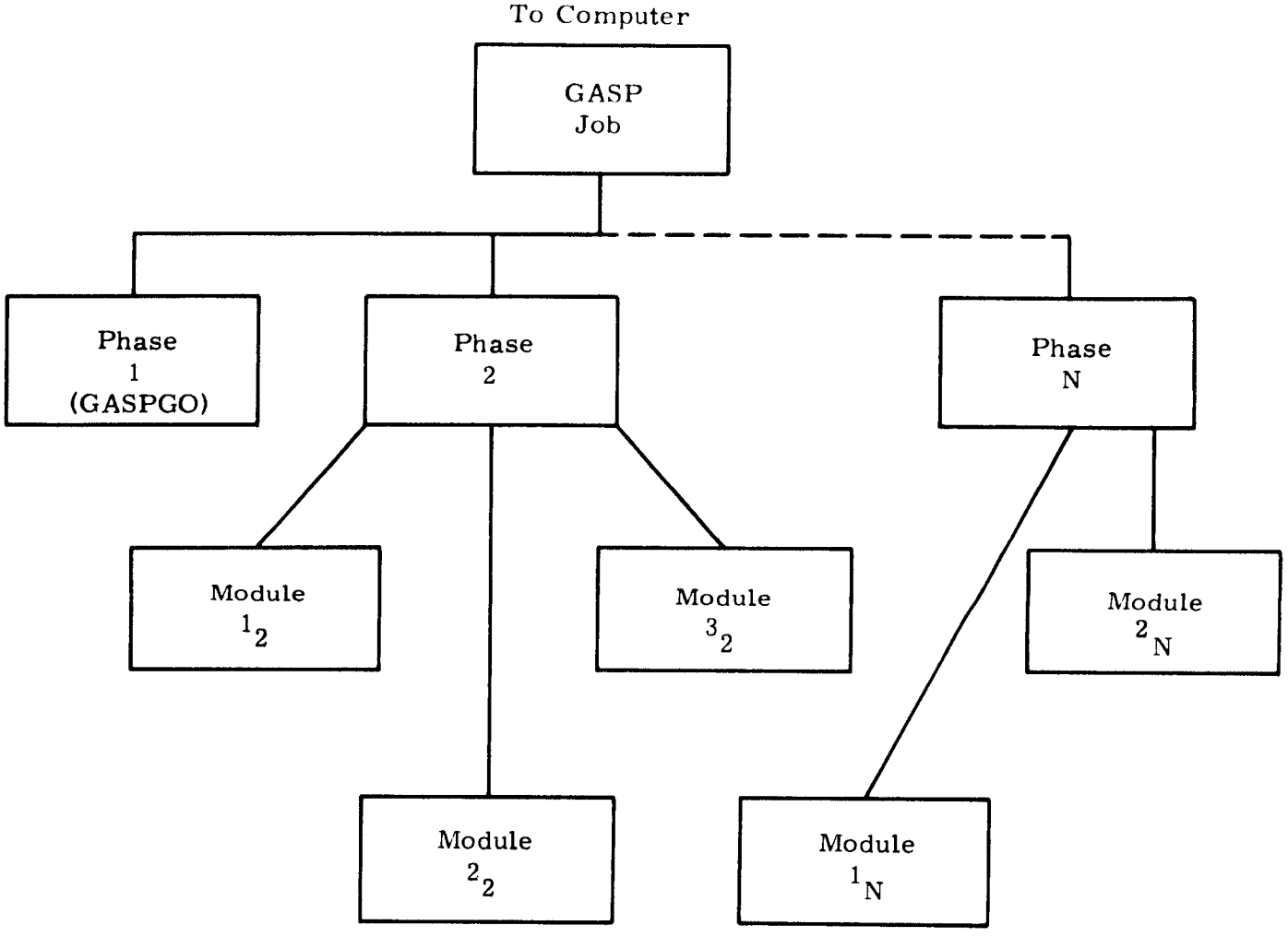

Figure 5-1. GASP Structure

to the next part. Since the generation and analysis of data can be separate operations, one simulation may well suffice for a number of post-flight analyses. The GASP system is also a valuable tool for program development. A particular computation or decision function may be accomplished in a number of ways, and the comparative benefits of each method may be analyzed by inserting them one at a time into the program. Only the module containing the operation of interests needs to be replaced.

In addition, the following advantages of GASP should be of specific interest to the user:

a. Short lead time - Simulation or analysis problems generally include a number of standard operations such as numerical integration, interpolation, and coordinate transformations. As the GASP library becomes more complete, most of these standard operations will be available in finished form. The programer determines the manner in which these operations are related in the particular problem and programs any special-purpose operations not currently available. The resultant reduction in programing and program testing is passed along to the user as a decrease in program development time.

b. Increased program reliability - Preprogramed components of the GASP system have been thoroughly tested; hence, testing of a new program can be mostly devoted to testing new modules and overall program accuracy. Since more extensive tests can be conducted for a given amount of machine time, overall program reliability is improved.

c. Internal compatibility - All of the GASP programs share a block of data (COMMON) which is dimensioned for double precision. This feature allows a computation to be upgraded in accuracy by merely rewriting it in double precision. The added advantage of such capability is that sensitive operations such as coordinate transformations can be accomplished in double precision while the rest of the program can be a single precision.

d. External compatibility - GASP programs make extensive use of magnetic tape. Since data is saved for an entire simulation, communication with other programs is easily achieved. For example, the output of a GASP simulation can be converted to an appropriate form for immediate processing by error analysis routines.

The Wind Stress Launch Simulation Program is a subset of the GASP system of programs. Since the GASP program handles the basic programing problems of trajectory

design work (input, program control, integration, and output), the programing problems involved in the development of the Wind Stress Launch Simulation Program were reduced to the writing of the appropriate derivative list and the desirable output formats. The following simplified flow chart, Figure 5-2, illustrates the functions of GASP in this application.

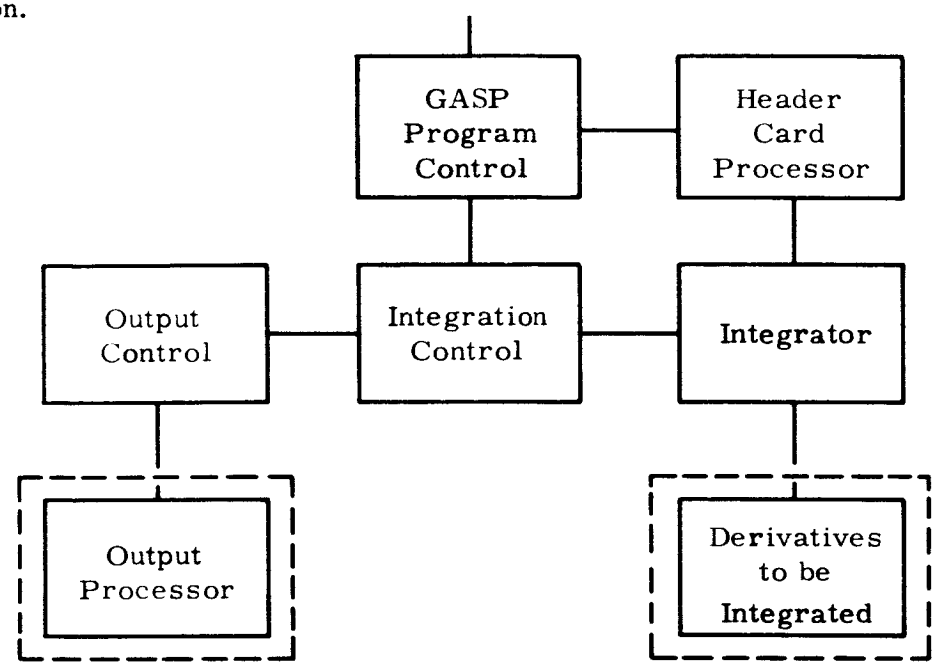

Figure 5-2. Block Diagram of GASP System

The addition of the blocks enclosed by dotted lines represent the additions necessary to include the Wind Stress Launch Simulation Program under the GASP system.

A more detailed consideration of the actual computations performed in the GASP program is contained in Appendix B.

5.1.2 INPUT AND OUTPUT - USE OF PROGRAM

The general input and output parameters which are of interest in the GASP program are listed in Table 1-1 in Section 1. The input to the program is furnished by header cards which are described in the following pages. A listing of a typical set of header cards is presented in Figure 5-3. The output format is indicated by Figure 5-4.

```
1PHASE  1                    G A S P   P R O G R A M          10/13/65          PAGE  1

          INPUT HEADER CARDS TO THIS PHASE

          CONTRL  6   3   10  INDEPE   GO     MAX     *
          CONSTS  (2.09030000000.7  (1.40752E+16  (0.0  (32.17  (2.09030000000.7
                  (0.0  (0.0  (0.0  *
          PHASE  TIME      150.0   1.    -1.    *
          LAUNCH GEO  DP  (0.00 (0.0  (0.0  (0.0  (90.0  (180.0  *
          TIMES   (.1  (0.0  (0.0  *
          VEHICL  6.005.6  33.  855.298  *
          STEER   90. 0. 0. 0. 0. 0. 0. 0. 0. GNIDE *
          EXTRAS  POWER  1727001.96  15446.6928  0.  0.  5690.872  1. 5. 4.  1. *
          TABLE MACHNO   PRINT  *
          MACHNOU. .11 .30 .35 .40 .45 .50 .60 .70 .90 .95 1.0 1.05 1.10 1.15 1.25
                1.50 1.70 1.90 2.10 2.3 2.55 3.1 3.5 4. 4.75 6.0 6.5 7.0 8.0 *
          TABLE DRAGCO   PRINT *     DRAG COEFFICIENTS
          DRAGCO
          AXIAL   1.150   1.150  .530  .42  .37  .35  .335  .335  .38  .63
          AXAIL    .69  .73  .78  .809  .81  .79  .65  .592  .543  .51  .481
          AXIAL  .453  .4  .37  .33  .28  .218  .195  .175  .14
          NORM1  4.6  4.61  4.68  4.7  4.71  4.74  4.78  4.85  5.  5.7  5.73
          NORM2     5.74  5.73  5.68  5.6  5.43  4.85  4.5  4.35  4.3  4.29
          NORM3   4.28  4.2  4.12  4.02  3.9  4.2  4.4  4.57  4.6  *
          TABLE WEIGHT  *
          TABLE MINERT  *
          TABLE POWWT  *
          TABLE POWCG  *
          TABLE POWMN  *
          TABLE POWCP  *
          TABLE GT2 *
          TABLE PR2 *
          TABLE GT1  *
          TABLE GC1  *
          C         *   95 PERCENT MAXIMUM WIND WITH .09 SHEAR   *
          TABLE ALTAB PRINT *
          ALTAB -100.   0. 18514. 22267. 24267. 26267. 28267. 30267. 31634. 32293.
          ALTAN232949. 33605. 34262. 34590. 34918. 35000. 35820. 35902. 45931.
          ALTAB3  65617. 98425. 196850. 262467.  *
          TABLE   WINTAB  PRINT  *
          WINTAB
          WNTB1 0. 0.   44.3  53.1  60.7  71.5  87.3 109.9 130.2 142.1 156.2 173.9
              2  200.1 216.5 246.1 271.2 271.2 246.1 246.1  82.0  82.0 459.3 459.3
```

Figure 5-3. Typical GASP Header Card Listing

****** GENERALIZED AEROSPACE SIMULATION PROGRAM ******

* INITIAL CONDITIONS *

TIME AT START OF PHASE- 0.00 SEC

INERTIAL			RELATIVE	
X=	20902999.808 FT	*	ALTITUDE=	0.000 FEET
Y=	-0.000 FT	POSITION	LATITUDE=	0.000 DEGREES(POS NORTH)
Z=	0.000 FT	*	LONGITUDE=	180.000 DEGREES(POS EAST)
		*		
XDOT=	0.000 FT/SEC	*	SPEED=	0.000 FT/SEC
YDOT=	-0.000 FT/SEC	VELOCITY	PATH ANGLE=	1.000 DEGREES(POS UP)
ZDOT=	0.000 FT/SEC	*	PATH AZIMUTH=	0.000 DEGREES(POS EAST)

* VEHICLE CHARACTERISTICS *

MASS= 186664.6 SLUGS WEIGHT= 6004999.9 LBS
DIAMETER= 33.00 FEET SURFACE AREA= 855. SQ FT.

* VEHICLE IS IN FREE FLIGHT *

* EARTH MODEL *

EARTH IS ASSUMED NON-SPHERICAL
SEMIMAJOR AXIS= 20902999.808 FT SEMIMINOR AXIS= 20902999.808 FT
ANGULAR VELOCITY= 0.
GO= 32.1700 FT/SEC2 GM= 1.4075280E 16 FT3/SEC2
HARMONICS- J= 0.0000000 E-39 D= 0.0000000 E-39 H= 0.0000000 E-39

Figure 5-4. Output Format - GASP

TIME(SEC)	X(FT)	Y(FT)	Z(FT)	XDOT(FT/SEC)	YDOT(FT/SEC)	ZDOT(FT/SEC)
ALTITUDE(FT)	RANGE ANGLE(DEG)	ATTITUDE(DEG)	XDOTA(FT/SEC)	YDOTA(FT/SEC)	ZDOTA(FT/SEC)	
ATTITUDE ERR(DEG)	RATE ERROR(DPS)	ANGLE OF ATTACK(DEG)	GIMBAL ANGLE(DEG)	DYN PRS(LB/FT2)	Q.ALPHA(LB/FT2)	
THRUST(LBS)	WEIGHT(LB)	CG(FT)	CP(FT)	MACH NO	RADIAL ACC	
144.00	21078599.680	0.000	-235089.172	2835.959	0.000	-6452.415
176910.74	-0.638992		24.710887	2518.404	0.000	-6666.295
0.024791	-0.001240		-4.015188	0.013452	33.707	*2.362
1726878.5	1907572.2	136.460	168.300	6.469	0.000	
145.00	21081450.240	0.000	-241687.874	2865.336	0.000	-6585.363
179834.87	-0.656620		24.469413	2538.415	0.000	-6805.404
0.023316	-0.000573		-4.013844	0.012639	31.898	*2.235
1726891.1	1879117.8	137.882	168.300	6.639	0.000	
146.00	21084330.496	0.000	-248260.666	2895.084	0.000	-6720.605
182792.14	-0.674607		24.227984	2558.688	0.000	-6946.870
0.021887	-0.000872		-4.008043	0.011287	30.114	*2.107
1726902.6	1850663.4	139.304	168.300	6.816	0.000	
147.00	21087240.448	0.000	-255049.872	2925.213	0.000	-6858.209
185783.07	-0.692958		23.986271	2579.229	0.000	-7090.763
0.020174	-0.001042		-3.997612	0.009832	28.357	*1.979
1726913.3	1822209.1	140.727	168.300	6.998	0.000	
148.00	21090180.864	0.000	-261977.896	2955.733	0.000	-6998.248
188808.21	-0.711680		23.744464	2600.046	0.000	-7237.154
0.018367	-0.001133		-3.982890	0.008459	26.630	*1.851
1726923.0	1793754.7	142.149	168.300	7.187	0.000	
149.00	21093152.000	0.000	-269047.200	2986.653	0.000	-7140.795
191868.12	-0.730779		23.502575	2621.148	0.000	-7386.119
0.016479	-0.001188		-3.964025	0.007151	24.940	*1.726
1726931.8	1765300.4	143.571	168.300	7.382	0.000	

Figure 5-4. Output Format - GASP (Cont.)

```
1PHASE  1                          G A S P   P R O G R A M          10/13/65

TIME(SEC)        X(FT)              Y(FT)              Z(FT)          XDOT(FT/SEC)     YDOT(FT/SEC)     ZDOT(FT/SEC)
     ALTITUDE(FT)     RANGE ANGLE(DEG)     ATTITUDE(DEG)      XDOTA(FT/SEC)    YDOTA(FT/SEC)    ZDOTA(FT/SEC)
ATTITUDE ERR(DEG)     RATE ERROR(DPS)   ANGLE OF ATTACK(DEG)   GIMBAL ANGLE(DEG)   DYN PRS(LB/FT2)   Q.ALPHA(LB/FT2)
     THRUST(LBS)          WEIGHT(LB)         CG(FT)             CP(FT)          MACH NO          RADIAL ACC

                                        THE MAXIMUM   Q    CONDITIONS.

   72.58      20938716.416                  0.000          -13174.377          1163.334            0.000          -821.825
          35720.73              -0.036050              53.488559                1014.093            0.000          -1048.268
       =3.089767                -0.613731              -9.437798                1.195598              762.954          -125.674
        1675297.2                3942058.9          95.575          123.886          1.504              0.002

                                        THE MAXIMUM QALPHA CONDITIONS.

   71.90      20938022.144                  0.000          -12688.075          1150.989            0.000          -799.324
          35026.12              -0.034720              54.265088                1003.094            0.000          -1026.649
       =2.731525                -0.499658              -9.930584                1.875324              759.872          -131.702
        1673494.3                3959131.5          95.465          122.106          1.475             -0.011

                                        THE MAXIMUM ALPHA  CONDITIONS.

   71.90      20938022.144                  0.000          -12688.075          1150.989            0.000          -799.324
          35026.12              -0.034720              54.265088                1003.094            0.000          -1026.649
       =2.731525                -0.499658              -9.930584                1.875324              759.872          -131.702
        1673494.3                3959131.5          95.465          122.106          1.475             -0.011
```

Figure 5-4. Output Format - GASP (Cont.)

5.1.3 GASP HEADER CARD DESCRIPTION

5.1.3.1 General

The GASP I system has a flexible input format that enables the user to specify only those parameters necessary to execute a particular simulation. Required cards are kept to a minimum.

In general, header cards are interpreted using columns 1-6. These locations contain a TITLE. Information contained in columns 7-72 may consist of alphanumeric SPECIFICATIONS and numerical DATA. All information must be in standard READH format. Each titled header card may consist of several physical cards (up to 20 words total), but an asterisk must follow the final entry. Only the first six letters of a specification are ever interpreted, so words may often be abbreviated. Data may be entered in either octal or single precision floating point, and critical variables may usually be entered in double precision if desired.

The following description discusses the header card inputs presently available. Any term in brackets may be omitted. If a preset choice is available, this is indicated by an underscore.

5.1.3.2 Job Control Card

5.1.3.2.1 GASPGO Card

The first physical header card in every GASP I deck must be a GASPGO card. On this card, tape assignments and program linkages are defined. The subroutine description concerning program GASPGO describes the format of the card in greater detail. For a single link run, only the run number needs to be specified.

5.1.3.2.2 ENDG Card

Following the last simulation phase must be an ENDG card. This card signals the end of computation and initiates the output processing activities. Two specifications are allowed on the ENDG card, REWIND or UNLOAD. In any case, an asterisk is required to follow the last data word.

Only the first word in the data field is scanned. Thus, all the following examples result in the binary output tape being rewound:

```
ENDG    REWIND *
ENDG    REWIND OUTPUT TAPE *
ENDG    REWIND AND TAKE A BREAK *
```

In like manner, the word UNLOAD in place of REWIND will result in the binary output tape being rewound and unloaded.

5.1.3.3 Phase Control Card

Each discrete phase requires both a GASP card at the beginning of the header cards for the phase and an ENDCSE card following the last header card for that phase.

5.1.3.3.1 GASP Card

Each phase is headed by a GASP card which specifies the type of action to be taken between phases. One of three specifications are required as the first item:

BASIC - If the phase is the first (or only) element of the simulation.

PERTURB - If the phase requires reinitialization, the PERTURB option is used. This is the case when running multiple cases.

CONTINUE - The CONTINUE card signals a temporary interruption in the simulation. This option is used for staging and other related operations.

The remaining space on the GASP card may be used for identification. This data will be used as a title by the output processor. Asterisks may be used on either side of the identification as illustrated below:

```
GASP    BASIC       ***SAMPLE OUTPUT***
GASP    CONTINUE     *LUNAR TRAJECTORY
```

5.1.3.3.2 ENDCSE Card

The last card of each phase must be an ENDCSE card. The appearance of this card signals the end of the input processing for the phase, and several transformations may be selected at this time.

Two specifications may appear on the ENDCSE card, ORIENT and TRANSFORM. Specification ORIENT produces a standard earth launch orientation for a rigid body. The roll axis of the vehicle is assumed to be normal to the surface of the earth, and the yaw axis points in the opposite direction from the azimuth. The pitch axis completes the right-hand set. (See subroutine PRAXIS for further details.) Specification TRANSFORM computes inertial cartesian coordinates of position and velocity from altitude, latitude, longitude, relative speed, path angle, and path azimuth. (See subroutines DLNCH1 and DLNCH2 for further details.)

5.1.3.3.3 PHASE Card

The PHASE card allows the integration procedure to be interrupted. The basic format is given below. Quantities in brackets may be omitted if desired. Underlined quantities will be assumed by the input processor if no explicit values are given:

$$\text{PHASE} \quad \text{VAR}\,[\,,\,\text{NP}] \quad \underline{\text{ACT.}} \quad \text{TOL.} \quad \underline{\begin{matrix}+1\\-1\end{matrix}} \quad \underline{\begin{matrix}0.\\\text{INCR.}\end{matrix}} \quad \underline{\begin{matrix}\text{ACT.}\\\text{CUT.}\end{matrix}} \quad *$$

On the PHASE card, VAR is the decimal location in COMMON of the variable to be monitored. If this variable is to apply over an entire run, NP should be zero. Otherwise, NP should be the phase number preceded by a comma. If a variable with NP = 0 is exceeded, the run is terminated immediately. Thus, the format can be used to specify operating limits and error conditions. A variable paired with a non-zero NP causes program operation to be interrupted when the action value (ACT) is exceeded. At this time, all variables with non-zero NP are removed from the monitor table.

As indicated above, ACT is the value of the associated variable at which the program is to interrupt computation. ACT should be specified as a single precision floating point number.

The next number on the card should be the desired iteration tolerance; that is, the allowable discrepancy between the computed value of VAR and ACT. A maximum of 10 iterations will be performed in an effort to achieve the desired accuracy (see subroutine ITERAT). Experience indicates that one or two iterations are usually sufficient.

The next number on the card is a flag word to indicate the direction from which the variable approaches ACT. If VAR is decreasing toward ACT, a + 1. should be used. If VAR is increasing toward ACT, a - 1. must be inserted.

Provision has been made for systematically incrementing the action value to some pre-specified cutoff value. The increment is supplied as INCR and the cutoff value as CUT. These may be omitted if desired.

5.1.3.3.4 CONTROL Card

The CONTROL card provides miscellaneous control information to the GASP system. The card format is:

CONTROL	NEQN.	MEQN.	NFREQ.	DUMP EXIT GASPXT INDEPENDENT	*

NEQN is the number of equations of motion integrated (e.g., 6 for point mass, 12 or 15 for a rigid body depending on whether two or three body axes are integrated).

MEQN is the number of extra equations to be integrated (present maximum is 10).

NFREQ is the number of integration steps per output print.

The fourth word on the card may specify an error option. If an error occurs and control is transferred to TERMN, the standard error routine, this word is checked. If the contents correspond to one of the options indicated above, the appropriate action follows:

If word is	Transfer is to
DUMP	DUMP Routine
EXIT	EXIT Routine
GASPXT	GASPXT Routine
INDEPENDENT	XEQLEE Routine
(None of the above)	Routine appropriate to error code

Subroutine XEQLEE may be incorporated into a module execution list to allow multiple independent cases to be processed. If no such routine is included, the library routine

XEQLEE is loaded which, if called, will transfer control to EXIT. Most of the internal options result in a call to EXIT also.

5.1.3.3.5 TIMES Card

The TIMES card may contain as many as three floating point, double precision numbers. These are:

```
TIMES    (DT.    (T.    (HAGZ.    *
```

In the above example, DT is the desired integration step size in seconds, T is the starting time for the phase in seconds, and HAGZ is an hour angle through which the position and velocity vectors are rotated in order to accommodate special coordinate sets. For example, in order to obtain output in a Vernal Equinox Inertial Set, HAGZ should contain the hour angle between Aries and the Prime Meridian at the time of launch. If T is unspecified, the time is left unchanged. If HAGZ is unspecified, it is assumed to be zero.

5.1.3.3.6 LAUNCH Card

The LAUNCH card provides input position and velocity data. Three forms are allowable: (1) Single precision inertial cartesian, (2) double precision inertial cartesian, and (3) single precision spherical. The forms of each of these are illustrated below:

```
LAUNCH   CART   X.   Y.   Z.   X.   Y.   Z.   *
LAUNCH   CART   (X.  (Y.  (Z.  (X.  (Y.  (Z.  *
LAUNCH   GEOG   H.   FLAT.  FLONG.  BETA.  GAMMA.  AZL. *
```

In the last example:

H is the altitude in feet.

FLAT is the geographic latitude in degrees.

FLONG is the geographic longitude in degrees.

BETA is the relative velocity magnitude.

GAMMA is the path angle of the relative velocity vector measured from the local horizon, positive up.

AZL is the path aximuth measured from the north pole, positive eastward, to the projection of the relative velocity vector.

All data is in floating point and follows the standard READH format. The word following LAUNCH is the specification and determines the manner in which the following data is to be interpreted. Only the first three letters of the specification are examined, so the word may be of any length. For example, GEO, GEOG, GEOGRAPHIC, GEODETIC, and GEOCENTRIC are all acceptable.

5.1.3.3.7 ORIENT Card

This card allows data concerning the orientation of a rigid body to be inserted in the simulation. All data must be supplied in double precision floating point form. The first three numbers are the direction cosines of the roll axis in inertial cartesian coordinates. The second three values are the direction cosines of the yaw axis, and the last three are the direction cosines of the pitch axis. The pitch axis components may be omitted, in which case they are computed from the roll and yaw axes.

NOTE

> These values are not affected by the insertion of an hour angle on the TIMES card. Hence caution must be observed in setting up the simulation to avoid introducing two inertial sets, one for the orientation axes and one for the position and velocity measurements.

This card may be omitted completely for point mass simulations or cases in which the standard launch configuration is desired. For a standard launch, supply altitude, latitude, and longitude of the launch site, using a LAUNCH card with GEOX specification. Beta should be set to 0., GAMMA to 90°, and AZL to the downrange direction. See subroutines DLNCH1, DLNCH2, and PRAXIS for pertinent computations.

5.1.3.3.8 CONSTS Card

The CONSTS card allows the physical constants within the system to be redefined. All data must be supplied in double precision. The number of constants to be redefined may be any length, but the sequence must be maintained. Thus, in order to change the gravitation parameter GM, it is also necessary to redefine GO, A, B, and W(Ω). The following values are automatically set to the indicated double precision values:

GO	=	32.146472 ft/sec^2	Gravitational acceleration.
A	=	2.0925696E+7 ft	Semimajor axis or radius.

B	=	2.0855546E+7 ft	Semiminor axis.
W(Ω)	=	7.292115E-5 rad/sec	Angular velocity of rotation.
GM	=	1.407645E+16 ft^3/sec^2	Gravitational parameter.
J	=	0.0	First harmonic.
D	=	0.0	Second harmonic.
H	=	0.0	Prolateness factor.

If a spherical earth is to be simulated, set A = Re and B = 0.

5.1.3.3.9 VEHICL Card

This card is used to read various values concerning the vehicle being simulated. The following example indicates the data to be entered on this card.

VEHICL WT. D. S. [CA.] *

in which:

WT is the weight of the vehicle at the start of the phase, in pounds.
D is the diameter of the vehicle in feet.
S is the aerodynamic reference area in square feet.
CA is the axial drag coefficient.

The drag coefficient need not be entered if drag tables are being used.

5.1.3.3.10 STEER Card

The STEER card allows various data for the guidance module. The actual data format depends on the particular guidance module in use. Up to 18 single precision guidance values may be read, and these are stored in consecutive locations in the STEER block in COMMON memory.

5.1.3.3.11 EXTRAS Card

It is impossible to anticipate the data which may be required for any simulation. In order to provide built-in escape, the EXTRAS option is included. When such a card is encountered, subroutine PROCES is called. This subroutine may be easily modified to process any type of data, yet the basic header card processor remains unaffected. The current standard version of PROCES recognizes four specifications, POWER, HEAT,

MAXG, and CHANGE:

a. The POWER specification allows thrust models to be introduced.

```
EXTRAS    POWER  F.  AC.  FW1.  FW2.  DWT.  FL1.
PEXTRA(1)  (2)  (3)  *
```

in which:

F is the nominal (vacuum) thrust per engine (lbs).

AC is the exhaust area (square inches).

FW1 and FW2 are fuel flow coefficients.

DWT is the weight flow rate for the stage (lb/sec).

FL1 is the distance of the gimbal, from station 0 in the vehicle (feet).

PEXTRA(1) is the total number of engines in stage.

PEXTRA(2) is the number of movable engines in stage.

PEXTRA(3) is the number of fixed engines in stage.

Particular thrust modules may make different use of the format, and the specific module writeup should be consulted for proper data preparation.

b. The HEAT specification performs computations in connection with the heating rate modules:

```
EXTRAS    HEAT    NCR.    *
```

in which NCR is the nose cone radius (feet). The square root of NCR is computed and stored for use during the integration.

c. The MAXG specification causes a zero to be stored in STEER (19) for use in computing maximum instantaneous g-force during a flight. No other data is required on this card.

d. The CHANGE specification causes an immediate transfer of control to subroutine GASPXT.

5.1.3.3.12 * Card

This card allows extra comments and identifying information to be inserted in the input deck and printed as a part of the input data summary. For greatest efficiency, an asterisk should also appear before the actual comment.

5.1.3.3.13 TABLE Card

The TABLE card permits tabular data to be read by the program. The form for entering a table is:

```
TABLE   TABDAT   *                    card n
        5.0   7.0   13.52 . . . . .* card n+1, *
```

If it is desired to have this data appear in the input summary, the word PRINT should appear following the table name on the TABLE card. Otherwise, only the TABLE card itself will appear.

It is also possible to reserve a block for a table at execution time. This is done by adding a table count following the name. This results in a table of specified size being reserved in unused upper core.

To erase the internal table of table names insert a TABLE card in the deck with zeros in place of the table name.

All tabular values are processed by subroutines DESIG and TABLES. For a more detailed discussion of the actual procedure, refer to the module descriptions for these routines. The maximum number of separate tables that can be accommodated is 25.

5.1.3.4 Output Control Cards

The SCAN card is used by the SCAN program (Program 1000). It contains three integer constants required to properly process a binary output tape. The format is:

```
SCAN    O, N1    O, N2    O, N3    *
```

in which:

N1 is the output frequency.
N2 is 0 if no end-of-phase output is requested.
N2 is 1 if end-of-phase output is requested.
N3 is the number of lines per printout.

It should be noted that N1 is the ratio of binary tape records to output prints. Thus, if both N1 and NFREQ is large, hardly any printout will occur at all. The first time point and the last time point of a phase will always be written, regardless of the value of N1.

Integer N2 signals whether or not a dump of COMMON following the final printout of a phase is desired. If N2 is nonzero, COMMON will be dumped in both octal and decimal providing a useful guide to the actual condition of all variables at the end of a phase. This dump can be eliminated by setting N2 equal to 0.

N3 specifies the number of lines of output produced by the output routine if called. This provides the SCAN program with information necessary to properly restore the page and print title information.

5.1.4 WIND STRESS LAUNCH SIMULATION PROGRAM INPUT DESCRIPTION

All input to the Wind Shear Launch Simulation program will conform to the GASP header card descriptions, restrictions, and requirements. In addition to the header cards needed to describe the initial conditions of the launch, the following tabular information must be supplied to the program by means of the GASP table header card option:

a. Mach Number versus Drag

1. Table Name: MACHNO
   Type: Independent
   Variable: Mach number
2. Table Name: DRAGCO
   Type: Dependent on table MACHNO
   Variable: Axial drag force (first table)
   Normal drag force (second table)

b. Weight versus Moment of Inertia

3. Table Name: WEIGHT
   Type: Independent
   Variable: Weight
4. Table Name: MINERT
   Type: Dependent on table WEIGHT
   Variable: Moment of inertia

c. Weight versus Center of Gravity

5. Table Name: DOWNT
   Type: Independent
   Variable: Weight
6. Table Name: POWCG
   Type: Dependent on table DOWNT
   Variable: Center of gravity of the vehicle

d. Mach Number versus Center of Pressure

7. Table Name: POWMN
   Type: Independent
   Variable: Mach numbers
8. Table Name: POWCP
   Type: Dependent on table POWMN
   Variable: Center of pressure of the vehicle

e. Time versus Commanded Pitch Rate

9. Table Name: GT2
   Type: Independent
   Variable: Time
10. Table Name: PR2
    Type: Dependent on table GT2
    Variable: Commanded pitch rate

f. Time versus Time Varying Guidance Constants

11. Table Name: GT1
    Type: Independent
    Variable: Time
12. Table Name: GC1
    Type: Dependent on table GC1
    Variable: First guidance constant (first table)
    Second guidance constant (second table)
    Third guidance constant (third table)

The following rules apply to the use of all tables:

1. The independent tables will always have algebraically increasing numbers.
2. No more than one thousand words of total tabular information are allowed.
3. For each independent table, there may be more than one dependent table under one table name (i.e., if table ABC is dependent, and contains three actual tables, and is dependent on table XYZ which has N entries, then table ABC will have 3N entries of which the first N entries are the first table, the second N entries are the second table, and the third N entries are the third table).

5.1.5 ROUTINES USED IN THE WIND STRESS LAUNCH SIMULATION

a. GASP Control Routines

1. START 1 - Dummy main program used as an entry point to the GASP program.
2. START - Controls basic logic flow of the GASP program.
3. STZ - Zeros out all of common except the constants block.
4. XEQ - Secondary control routine.

b. GASP Input Routines

5. SETUP - Header card reading control routine.
6. ICCHG - Sets up the terminal flight conditions from the PHASE header cards.
7. PROCES - Stores information which is read in from the EXTRAS header cards.
8. DESIG - Stores tabular information.
9. LAUNCH - Converts geographic coordinates into inertial cartesian coordinates.
10. PRAXIS - Dummy routine (not used by BMP).
11. MZETA - Dummy routine (not used by BMP).

c. GASP Integration Routines

12. TRJGEN - General integration control routine.
13. TERROR - Checks integration errors when a variable-step integration mode is chosen.

14. ICCKER - (Secondary entry point to subroutine ICCHG). Checks for terminal conditions and controls the iteration to the terminal conditions.

15. INTGRT - Fourth-order Runge-Kutta integrator.

d. GASP Output Control Routines

16. CKOUT - Print frequency control routine.

e. General GASP Routines Which are Used in the Wind Stress Launch Simulation

17. ARDC59 - Finds as a function of altitude:
    1. Local speed of sound.
    2. Air density.
    3. Temperature.
    4. Atmospheric pressure.

18. TABLES - Finds appropriate tables which will be used in a specific subroutine.

19. GLINT - Performs linear interpolation from the tables.

20. PGHD - Prints page headings.

f. Routines Used in the Derivative List for the Wind Stress Launch Simulation Program

1. DERIV - Execution list of routines which will calculate the derivatives for BMP.

2. GUIDE - Contains the guidance equations.

3. DYNAMO - Controls routine for the calculation of atmospheric forces and powered flight.

4. GRAV - Computes inertial gravitational forces.

5. ALT - Computes altitude, longitude, and latitude.

6. MACH - Computes the mach number, relative velocity, and angle of attack.

7. DRAG - Computes the drag coefficients.

8. POWER - Computes inertial thrust forces.

9. AERF - Resolves the aerodynamic forces into inertial forces.

10. TORQUE - States the torque equations.

11. STATE - States the equations of motion.

g. Output Routines for the Wind Stress Launch Simulation Program

1. FTITLE - Writes title page.
2. OUTPUT - Converts and sets up output to be printed.
3. WRITE - Writes out output.

5.2 LASS-1 - DETERMINATION OF STRUCTURAL LOADS

5.2.1 GENERAL DESCRIPTION OF PROGRAM

The next step in the analysis of the loads on the space vehicle structure is to determine the axial force distributions and the bending moment distributions along its axis. For the analysis, the space vehicle is represented by a non-uniform beam with lateral and axial load distributions. The load distributions can be classified as aerodynamic, control, and resultant loads. Since the dynamic aspects of these loads are considered in the Wind Stress Launch Simulation of GASP, it is possible to treat all applied forces in this part of the analysis as static or static equivalent forces for a specific instant of time.

In the rigid body analysis, it is sufficient to describe the aerodynamic and mass characteristics of the space vehicle as overall quantities which act at the center of pressure and the center of gravity respectively. In this analysis, the nature of the distribution of aerodynamic and inertia forces along the vehicle axis is required for each instant of time where an analysis is to be performed. It will be possible to select several "design points" from the output of the Wind Stress Launch Simulation to be studied further in the analysis programed in LASS-1. That is, while the rigid body simulation does repeated calculations over small time intervals to accurately define the motion of the space vehicle, we can select several points in time from the rigid body solution which will completely specify the "worst case" loads in the LASS-1 analysis. Some examples of these design points would be maximum axial acceleration and maximum $q\alpha$ product.

The total force distributions which exist for each "design point" are integrated numerically to find bending moment distributions, axial force distributions, and deflections of the space vehicle relative to the selected coordinate system. The bending moment distribution and the axial force distribution for each design point are written on a binary tape which can be scanned in subsequent analyses such as the analysis within the program SWOP. The SWOP program is discussed in another section of this report.

The required input and output parameters are listed in Table 1-1 of the Introduction. One of the most important features of the LASS-1 program is the capability to store within the program a large block of input data associated with a particular space vehicle configuration. Examples are axial and normal aerodynamic force coefficient distributions stored for several specific mach numbers. When a "design point" requests an analysis for some arbitrary mach number, an automatic linear interpolation developes the aerodynamic coefficient distributions for the design point. An automatic linear interpolator also selects the proper mass distribution for any "design point." The studies performed to date with this analysis have used data presented in Reference 1. The input format and the equations in the analysis, in general, conform to the manner in which the aerodynamic and mass data is presented in this reference.

The detailed equations of the analysis are presented in more detail in Appendix C.

5.2.2 INPUT AND OUTPUT - USE OF PROGRAM

The input sheets for LASS-1 are shown in Figures 5-5 and 5-6. This rather simple input format is easily understood with the aid of the User's Manual which is presented in the following pages. The output format is represented by typical printout sheets in Figures 5-7 through 5-14.

5.2.3 PROGRAM DOCUMENT FOR LASSMP AND LASS-1 (PART 1)

1. Program Number - 29I
   Program Name - LASSMP - Loads Analysis of Saturn Structures
   Date of Issue - 28 May 1965
2. Program Obsolesced - None.
3. General Description - This program is designed to set up conditions for entering LASS-1, the subroutine which performs the actual loads analysis. It will read the stored table data, referred to in the report by the requester, either from cards or from binary tape if those data have been previously stored there by this program.
4. Usage and Restrictions - The program was written in FORTRAN IV for running under GG-IBSYS; READH input format is used.
5. Particular Description - Since this program performs no computations required for the loads analysis, but serves only to set up conditions for calling the computational subroutine, Figure 5-15 gives a nearly adequate

LASS - 1 - DATA FORM

Page _____ of _____

NAME _____ PAY # _____ CHARGE # _____ EXT. _____

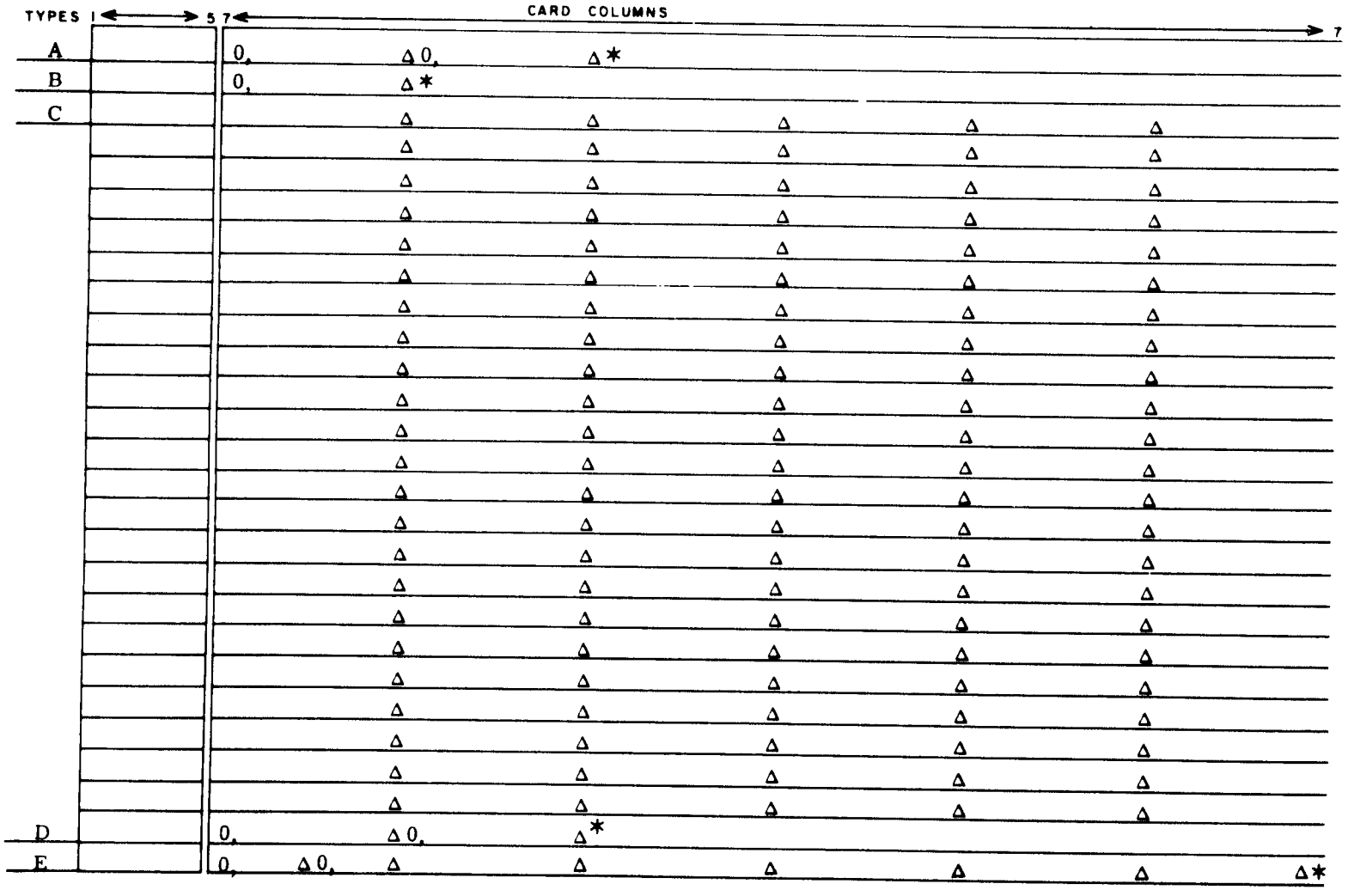

Figure 5-5. Input Format - LASS-1 (Front)

DATA PREPARATION FOR LASS1

Each line on the opposite side represents a card to be punched. Cross out all lines not to be punched.

Pages 2 and 3 of Part 1, Page 1 of Part 2 and the revised flowchart from the program document will be helpful in preparing data.

CARD TYPE A

The number in the first field, (K1), on this card determines the source of the stored tables. The number in the second field, (K2), determines whether any changes to the tables are to be made before execution.

CARD TYPE B

The number in the only field, (K1), on this card determines which physical quantities are to be read from the following Type C cards.

CARD TYPE C

The numbers in the six fields on each of these cards describe the vehicle or its environs. There may not be more than 250 quantities (42 cards) supplied and there must be an asterisk (*) punched after the last quantity in the set.

CARD TYPE D

After the last set of B-C type cards, the first field on this card must contain 18 or 19 and the second field must contain 1 or 2 depending on whether a tape record or a printed record of the stored table is desired.

CARD TYPE E

The number in the first field, (K1), on this card determines the mode of analysis. The number in the second field, (K2), determines whether or not printout will be made. The numbers in the next five fields must conform to the sample data below and are described in part two of the program document.

SAMPLE DATA FOR TYPE C AND E CARDS

ENGINEERING NOTATION	KEYPUNCH FORM
3.7×10^{-2}	0.0037 or 3.7-3
-7.695×10^{6}	-7695000. or -7.695+6
2.0×10^{-12}	2.-12 only *

*No more than eight significant figures may be expressed.

No quantity may be continued from one card to the next.

A decimal point must be expressed. A + or - sign must be expressed to separate the mantissa from the characteristic.

All other input (K1 and K2) must be expressed as 1 or 2 digit numbers without decimal points.

Figure 5-6. Input Format - LASS-1 (Rear)

FLIGHT TIME = 71.CCO SECONDS

MACH NUMBER = 1.350C

ANGLE OF ATTACK = 8.550CC DEGREES

DYNAMIC PRESSURE = C.5CCOOOE 01 POUNDS PER SQUARE INCH

ENGINE CONTROL ANGLE = 2.3CCOC DEGREES

TOTAL VEHICLE WEIGHT = C.3818881E 07 POUNDS

TOTAL THRUST = C.834315E C7 POUNDS

GIMBAL STATION = 1CC.OCO

TOTAL NORMAL AERODYNAMIC FORCE = C.543325E 06 POUNDS

CENTER OF PRESSURE STATION = 1585.C2C

PITCH MOMENT OF INERTIA = 0.681853E 10 INCH-POUND-SECONDS SQUARED

CENTER OF GRAVITY STATION = 1251.800

LATERAL RIGID BODY ACCELERATION = 0.819935E C2 INCHES PER SECOND SQUARED

ANGULAR RIGID BODY ACCELERATION = -0.186953E-C1 RADIANS PER SECOND SQUARED

MAXIMUM BENDING MOMENT = 0.253284E 09 INCH-POUNDS

STATION OF MAXIMUM BENDING MOMENT = 1C30.000

Figure 5-7. Output Format - LASS-1 Lateral Inflight Analysis Summary

STATION (IN.)	SHEAR (LBS.)	BENDING MOMENT (IN.-LBS.)	RELATIVE SLOPE (RAD.)	RELATIVE DEFLECTION (IN.)
-110.000	-0.709882E 03	-0.141774E 05	-0.271342E-08	-0.542685E-07
-90.000	-0.152005E 04	-0.445784E 05	-0.112452E-07	-0.279173E-06
-70.000	-0.239016E 04	-0.923819E 05	-0.289259E-07	-0.857691E-06
-50.000	-0.343488E 04	-0.161079E 06	-0.597545E-07	-0.205278E-05
-30.000	-0.463889E 04	-0.253857E 06	-0.108340E-06	-0.421957E-05
-10.000	-0.599867E 04	-0.373831E 06	-0.179886E-06	-0.781730E-05
10.000	-0.758463E 04	-0.525527E 06	-0.280465E-06	-0.134266E-04
30.000	-0.944052E 04	-0.714334E 06	-0.417179E-06	-0.217702E-04
50.000	0.394740E 03	-0.706439E 06	-0.552383E-06	-0.328178E-04
70.000	0.827148E 04	-0.541009E 06	-0.655925E-06	-0.459363E-04
90.000	0.105255E 05	-0.435754E 06	-0.697624E-06	-0.529126E-04
100.000	0.278386E 06	0.234810E 07	-0.472925E-06	-0.576418E-04
110.000	0.280158E 06	0.795125E 07	0.104885E-05	-0.366649E-04
130.000	0.286241E 06	0.136761E 08	0.366628E-05	0.366606E-04
150.000	0.290510E 06	0.194863E 08	0.739570E-05	0.184575E-03
170.000	0.295213E 06	0.253905E 08	0.122551E-04	0.429677E-03
190.000	0.299586E 06	0.313823E 08	0.182613E-04	0.794903E-03
210.000	0.303319E 06	0.374486E 08	0.254285E-04	0.130347E-02
230.000	0.305055E 06	0.435497E 08	0.337634E-04	0.197874E-02
250.000	0.301859E 06	0.495867E 08	0.432537E-04	0.284381E-02
270.000	0.294093E 06	0.515577E 08	0.456966E-04	0.307230E-02
275.000	0.434735E 06	0.575784E 08	0.565605E-04	0.392070E-02
290.000	0.423806E 06	0.660545E 08	0.731779E-04	0.538426E-02
310.000	0.409683E 06	0.742491E 08	0.918567E-04	0.722140E-02
330.000	0.393299E 06	0.821141E 08	0.112514E-03	0.947168E-02
350.000	0.376203E 06	0.896387E 08	0.135065E-03	0.121730E-01
370.000	0.358083E 06	0.967990E 08	0.163123E-03	0.154354E-01
390.000	0.339754E 06	0.103595E 09	0.193150E-03	0.192984E-01
410.000	0.321492E 06	0.110025E 09	0.225042E-03	0.237993E-01
430.000	0.303296E 06	0.116091E 09	0.259695E-03	0.289932E-01
450.000	0.287551E 06	0.121843E 09	0.296066E-03	0.349145E-01
470.000	0.287310E 06	0.127580E 09	0.296447E-03	0.408434E-01
490.000	0.287163E 06	0.133331E 09	0.336247E-03	0.475684E-01
510.000	0.287001E 06	0.139071E 09	0.379707E-03	0.551625E-01
530.000	0.286797E 06	0.144807E 09	0.424559E-03	0.636617E-01
550.000	0.286571E 06	0.150539E 09	0.479700E-03	0.732557E-01
570.000	0.286350E 06	0.156268E 09	0.536524E-03	0.839862E-01
590.000	0.286139E 06	0.161998E 09	0.595429E-03	0.958948E-01
610.000	0.285983E 06	0.167699E 09	0.661193E-03	0.109119E-00
630.000	0.284983E 06	0.173397E 09	0.729192E-03	0.123702E-00

Figure 5-8. Output Format - LASS-1 Lateral Inflight Analysis Tabulation

```
FLIGHT TIME =  71.CCC SECCNDS

MACH NUMBER =  1.35CC

ANGLE OF ATTACK =  8.55CCC DEGREES

DYNAMIC PRESSURE =  C.5CCOCOE C1 PCLNDS PER SQUARE INCH

ENGINE CONTROL ANGLE =  2.3CCCC DEGREES

TOTAL VEHICLE WEIGHT =  C.3818C1E C7 PCUNDS

TOTAL THRUST =  0.834315E C7 PCUNDS

GIMBAL STATION =  1CC.CCO

TOTAL DRAG =  0.36174CE C6 PCUNDS

AXIAL ACCELERATION =  C.PC62C6E C3 INCHES PER SECCND SQUARED
```

Figure 5-9. Output Format - LASS-1 Axial Inflight Analysis Summary

STATION (IN.)	AXIAL FORCE DISTRIBUTION (LBS.)
-110.000	-0.537761E 04
-90.000	-0.106963E 05
-70.000	-0.168036E 05
-50.000	-0.233777E 05
-30.000	-0.305218E 05
-10.000	-0.383811E 05
10.000	-0.473122E 05
30.000	-0.578088E 05
50.000	-0.701235E 05
70.000	-0.850074E 05
90.000	-0.123859E 06
100.000	-0.189014E 06
110.000	0.800889E 07
130.000	0.800626E 07
150.000	0.800393E 07
170.000	0.800828E 07
190.000	0.798954E 07
210.000	0.797055E 07
230.000	0.795093E 07
250.000	0.793765E 07
270.000	0.792436E 07
275.000	0.792218E 07
290.000	0.791471E 07
310.000	0.790644E 07
330.000	0.789838E 07
350.000	0.788878E 07
370.000	0.643755E 07
390.000	0.643435E 07
410.000	0.643119E 07
430.000	0.642759E 07
450.000	0.642472E 07
470.000	0.642128E 07
490.000	0.641861E 07
510.000	0.641581E 07
530.000	0.641256E 07
550.000	0.640928E 07
570.000	0.640554E 07
590.000	0.640268E 07
610.000	0.639559E 07
630.000	0.638981E 07
650.000	0.638626E 07

Figure 5-10. Output Format - LASS-1 Axial Inflight Analysis Tabulation

FLIGHT TIME = 0. SECONDS

MACH NUMBER = 0.

TOTAL VEHICLE WEIGHT = 0.599C63E 07 POUNDS

MAXIMUM BENDING MOMENT = 0.21513CE 09 INCH-POUNDS

STATION OF MAXIMUM BENDING MOMENT = 100.000

Figure 5-11. Output Format - LASS-1 Lateral Prelaunch Analysis Summary

STATION (IN.)	BENDING MOMENT (IN. LBS.)	SLOPE (RAD.)	DEFLECTION (IN.)
-110.000	0.	0.	0.
-90.000	0.	0.	0.
-70.000	0.	0.	0.
-50.000	0.	0.	0.
-30.000	0.	0.	0.
-10.000	0.	0.	0.
10.000	0.	0.	0.
30.000	0.	0.	0.
50.000	0.	0.	0.
70.000	0.	0.	0.
90.000	0.	0.	0.
100.000	0.215130E 09	0.	0.
110.000	0.214857E 09	0.411210E-04	0.822419E-03
130.000	0.214306E 09	0.821364E-04	0.246515E-02
150.000	0.213742E 09	0.123044E-03	0.492603E-02
170.000	0.213166E 09	0.163841E-03	0.820286E-02
190.000	0.212578E 09	0.204526E-03	0.122934E-01
210.000	0.211976E 09	0.245096E-03	0.171953E-01
230.000	0.211362E 09	0.285548E-03	0.229063E-01
250.000	0.210735E 09	0.325880E-03	0.294239E-01
270.000	0.210095E 09	0.365932E-03	0.311035E-01
275.000	0.209960E 09	0.375548E-03	0.367367E-01
290.000	0.209440E 09	0.428237E-03	0.453015E-01
310.000	0.208772E 09	0.480758E-03	0.549166E-01
330.000	0.208098E 09	0.533108E-03	0.655788E-01
350.000	0.207392E 09	0.585282E-03	0.772844E-01
370.000	0.206717E 09	0.636200E-03	0.901884E-01
390.000	0.206071E 09	0.704930E-03	0.104287E-00
410.000	0.205415E 09	0.764471E-03	0.119576E-00
430.000	0.204751E 09	0.825551E-03	0.136088E-00
450.000	0.204077E 09	0.886509E-03	0.153818E-00
470.000	0.203395E 09	0.887116E-03	0.171561E-00
490.000	0.202703E 09	0.947625E-03	0.190513E-00
510.000	0.202002E 09	0.101075E-02	0.210728E-00
530.000	0.201292E 09	0.107365E-02	0.232201E-00
550.000	0.200572E 09	0.114659E-02	0.255133E-00
570.000	0.199842E 09	0.121926E-02	0.279518E-00
590.000	0.199103E 09	0.129166E-02	0.305352E-00
610.000	0.198353E 09	0.136945E-02	0.332740E-00

Figure 5-12. Output Format - LASS-1 Lateral Prelaunch Analysis Tabulation

FLIGHT TIME = C. SECONDS

MACH NUMBER = C.

TOTAL VEHICLE WEIGHT = C.599C64E C7 POUNDS

Figure 5-13. Output Format - LASS-1 Axial Prelaunch Analysis Summary

STATION (IN.)	AXIAL FORCE DISTRIBUTION (LBS.)
-110.000	0.225433E-00
-90.000	-0.254627E 04
-70.000	-0.547037E 04
-50.000	-0.861797E 04
-30.000	-0.124105E 05
-10.000	-0.167967E 05
10.000	-0.217679E 05
30.000	-0.275966E 05
50.000	-0.344199E 05
70.000	-0.441022E 05
90.000	-0.588667E 05
100.000	-0.915319E 05
110.000	0.586737E 07
130.000	0.585478E 07
150.000	0.583826E 07
170.000	0.582592E 07
190.000	0.581543E 07
210.000	0.580508E 07
230.000	0.579005E 07
250.000	0.575924E 07
270.000	0.571338E 07
275.000	0.571338E 07
290.000	0.565816E 07
310.000	0.559338E 07
330.000	0.552224E 07
350.000	0.545110E 07
370.000	0.537838E 07
390.000	0.530565E 07
410.000	0.523291E 07
430.000	0.516014E 07
450.000	0.508734E 07
470.000	0.501445E 07
490.000	0.494193E 07
510.000	0.486934E 07
530.000	0.479653E 07
550.000	0.472370E 07
570.000	0.465084E 07
590.000	0.457801E 07
610.000	0.450396E 07
630.000	0.443352E 07

Figure 5-14. Output Format - LASS-1 Axial Prelaunch Analysis Tabulation

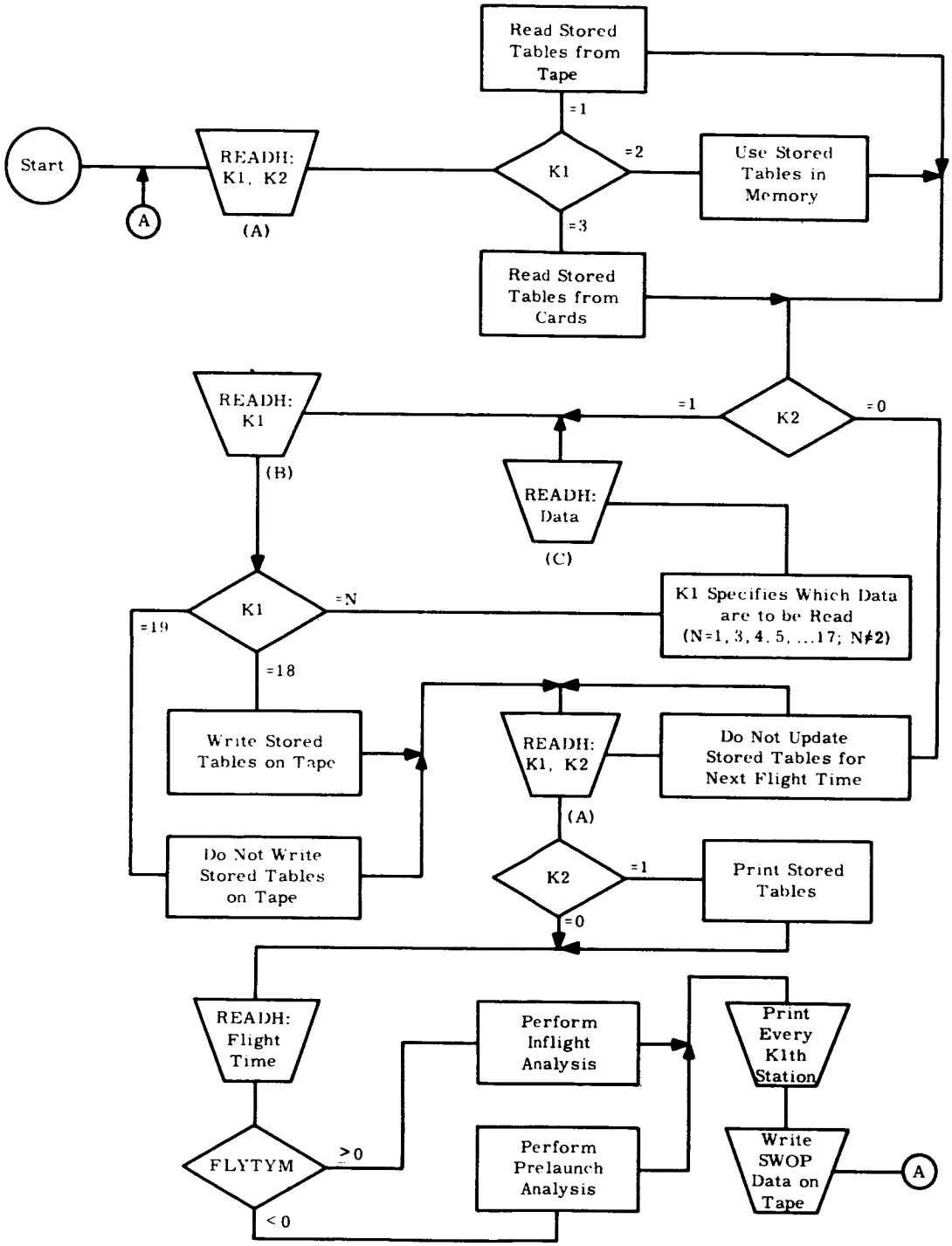

Figure 5-15. LASS-1 Flow Chart

description. It remains only to define the input data. All of the input data are stored in common arrays except for three sets of common singles. Each array and each set of common singles are loaded by reading in an appropriate value for a constant, K1, and then reading in the data. The array name, the appropriate value of K1, its definition, and dimensions follow. Unless otherwise stated, the maximum size of each array is 250 locations.

6. Description of Input - The first items read in are K1 and K2. Figure 5-15 indicates their functions:

Name	K1 =	Definition	Dimension
AP(I)	1	Longitudinal distance along the vehicle from some arbitrary station.	inches
AQ(I)	*	AP(I+1)-AP(I). These are computed and need not be read in. AQ(L) = 0.0.	inches
AR(I)	3	Dry weight of the vehicle at Station 1.	pounds
AS(I)	4	Propellant weight stored at Station 1.	pounds
AT(I)	5	The time after launch at which the propellant at Station 1 has been expended.	seconds
AU(I)	6	Bending stiffness at Station 1.	$inches^2$-lbs
AV(I)	7	Wind velocity at Station 1.	inches/sec
AW(I)	8	Angle of attack multiplier at Station 1.	-
AX(I)	9	Dynamic pressure multiplier at Station 1.	-
AY(I)	10	Cross flow coefficient for ground winds at Station 1. Note that there may be up to 250 stations along the longitudinal axis and that L (read in later) must be equal to the number of these stations.	-
CZMACH(I)	11	Mach number. Linear interpolation is performed on CZA, CZB, and CZC (defined below) using respectively, the first 10, the second 10, and the third 10 of the words in this array. Therefore, CZMACH(I) must be less than CZMACH(I+1) within each of the above three subsets of values of this array. Maximum array size is 30 words.	-

Name	K1 =	Definition	Dimension
CZA(I)	12	Normal linear aero force coefficient.	per degree
CZB(I)	13	Normal nonlinear aero force coefficient.	
CZC(I)	14	Drag coefficient. (In storing CZA, CZB, and CZC, note that if there are L stations and more than one value for mach number, the values of CZA, CZB, and CZC are each stored in the first L words, the second L words, etc. Do not reserve 250 locations for values of CZA, for example, unless there are 250 stations along the longitudinal axis of the vehicle. Maximum array size is 2500 words.)	
THRVFT(I)	15	Alternating values of time and thrust as a function of time. Maximum array size is 500 words.	seconds

The first set of common singles are defined below:

K1 is read in as 16

G	Acceleration of gravity at earth's surface	ft/sec^2
S	Reference area of vehicle	$inches^2$
RHO	Atmospheric density at sea level	$slug/inch^3$
CT1	0.2	
CT2	0.8	

The second set of common singles are defined below. K1 is read in as 17.

These values of I refer to the array AP and identify the station:

ICO	Engine gimbal point.
IHO	Vehicle hold-down point.
IHB	Vehicle weight support point.
IHTL	Lower propellant tank support point.
ITT	Point between propellant tanks. Note that AS(ITT+1) and AT(ITT) must be 0.0 and that AT(I) must be a decreasing sequence. (AT(I) > AT(I+1) except AT I=ITT.)
IHTU	Upper propellant tank support point.
L	Uppermost point of vehicle. (= the number of stations.)

The control constants K1 and K2 serve various functions which are most clearly seen by reading Figure 5-15. Included is a provision for writing the stored tables onto binary tape 934 and for reading the tables from that tape if long-term storage is desired.

The third set of common singles are read in within the subroutine LASS-1 and are described in Part 2 of this document.

As indicated in Figure 5-15, the stored tables may be read from binary tape 934 if they have been previously stored there.

7. Description of Output - The entire stored tables may be stored on binary tape 934 if desired. Note that the term "stored tables" refers to all the arrays and the common singles defined on the previous pages. The option of printing the stored tables exists.

8. Internal Checks and Programed Stops - There are no internal checks on the data, but the following must be observed:
   a. The arrays AP, AR, AU, AV, AW, AX, and AY must all contain the same number of entries, and L must be read in with this value.
   b. Any zero values of AU will be treated as ones since they appear as divisors.
   c. Whatever value between 1 and N-1 is read in for ITT, AT(ITT) must be zero.
   d. AT(I) to AT(ITT) and AT(ITT+1) to AT(250) must both be monotonically decreasing sequences, each of which must contain at least one value greater than FLYTYM and one or more values equal to zero and no negative values.
   e. Each of the 3 ten-word subsets of CZMACH must be a monotonically increasing sequence containing at least one value greater than ZMACH and no negative values.
   f. If any of the 3 subsets of CZMACH contain more than one value for mach number, and there are L stations, the corresponding array CZA, CZB, or CZC will contain KL values read into the first KL locations, where K is the number of values of mach number, and L is the number of stations.
   g. The first, third, fifth, ..., etc., values read in for THRVFT must be a monotonically increasing sequence, the first of which is less than or equal to FLYTYM and the last greater than FLYTYM.

9. Library/System Subroutines - READH, (TSB), (SLI), (RLR), (RWT), (STB), (SLO), (WLR), (STH), (FIL), EXIT.
10. Independent Subroutines - LASS-1
11. Completion Date - 23 June 1964.

5.2.4 PROGRAM DOCUMENT FOR LASSMP AND LASS-1 (PART 2)

1. Program Number - 29I
   Program Name - LASS-1
   Date of Issue - 28 May 1964
2. Programs Obsolesced - None.
3. General Description - This subroutine carries out the actual loads analysis in any one of four modes:
   a. Lateral inflight analysis.
   b. Axial inflight analysis.
   c. Lateral prelaunch analysis.
   d. Axial prelaunch analysis.

   The program needs loading only once to carry out any number of analyses in any combination.
4. Usage and Restrictions - The subroutine was written in FORTRAN IV for running under GG-IBSYS; READH input format is used.
5. Particular Description - The equations, definitions, and units of variables are attached. The subroutine is divided into five major functional segments, one for each of the four modes of analysis, and one for output.
6. Description of Input - The inputs to this subroutine consist of the common data described in part one and the following:

K1	Specifies mode of analysis:
	= 1 Lateral inflight.
	= 2 Axial inflight.
	= 3 Lateral prelaunch.
	= 4 Axial prelaunch.
K2	Specifies print option:
	= 0 No printout.
	0 Printout. For lateral modes, every "K2"-th station will be printed.

FLYTYM	Time after launch.	sec
ZMACH	Mach number.	-
ALFA	Angle of attack.	deg
Q	Dynamic pressure.	lbs/in^2
BETA	Engine gimbal angle.	deg

7. Description of Output - The output consists of two parts; preliminary - those items used in later computations, and final - the results of the analysis. The outputs are listed below and the applicable modes indicated:

	Mode			
Preliminary	1	2	3	4
Singles:				
Flight time	X	X		
Mach number	X	X		
Angle of attack	X	X		
Dynamic pressure	X	X		
Engine gimbal angle	X	X		
Arrays:				
Station	X	X	X	X
Lateral weight distribution	X		X	
Bending stiffness	X		X	
Normal linear aero force coefficient	X			
Normal nonlinear aero force coefficient	X			
Angle of attack multiplier	X			
Dynamic pressure multiplier	X			
Axial weight distribution		X		X
Drag coefficient		X		
Ground wind cross-flow coefficient			X	
Ground wind velocity			X	
Final				
Singles:				
Flight time	X	X	X	X
Mach number	X	X	X	X
Angle of attack	X	X		
Dynamic pressure	X	X		
Engine control angle	X	X		
Total vehicle weight	X	X	X	X
Total thrust	X	X		
Gimbal station	X	X		
Total normal aero force	X			
Center of pressure	X			
Pitch moment of inertia	X			
Center of gravity	X			
Lateral rigid body acceleration	X			
Angular rigid body acceleration	X			
Maximum bending moment	X		X	

	Mode			
	1	2	3	4
Final				
Singles:				
Maximum bending moment station	X		X	
Total drag		X		
Axial acceleration		X		
Arrays:				
Station	X	X	X	X
Shear	X			
Bending moment	X		X	
Relative slope	X		X	
Relative deflection	X		X	
Axial force distribution		X		X

8. Internal Checks and Programed Stops - See paragraph 8 of Part 1 of this document.
9. Library/System Subroutines - READH, (STH), (FIL), SIN, COS.
10. Independent Subroutines - None.
11. Completion Date - 23 June 1964.

5.3 SWOP - STRUCTURAL WEIGHT OPTIMIZATION PROGRAM UNDER EXECUTIVE CONTROL

5.3.1 INTRODUCTION

The main computational modules of the executive program are the STRESS subprogram and the various construction suboptimization subprograms.

The STRESS subprogram interface with the various construction subprograms is a convenient break in the computations at which to divide the program for restart capability. At this point, the resultant stresses are stored on a tape from which any number of construction suboptimization runs can later be made. This allows a wide variety of construction options to be run from the restart point.

Thus, an executive run can consist of a complete run, a STRESS tape generation only, or a construction suboptimization run only from a previously generated restart tape.

The STRESS tape-generating subprogram and each construction suboptimization subprogram are self contained modules and can be replaced by dummy routines when not needed

for a particular run. This saves computer time in the loading phase of the computer operation. Furthermore, the STRESS subprogram input is input in one block, and can be completely omitted when starting from a previously generated loads tape.

5.3.2 DESCRIPTION

Input cards fall into five classes:

a. Control Cards - individual cards used to define number and type of job. A knowledge of the input flow chart is needed in setting up the correct sequence of these few cards.

b. PROCES Cards - these are handled by the routine PROCES for the STRESS subprogram. They are an independent group needed only for the runs where new STRESS tapes are generated and are input together in one group. They are described in more detail in paragraph 5.3.3.

c. CASEIN Cards - these are handled by the routine CASEIN and set up the construction and material loops, and the construction subprogram options.

d. Block Data Changing Cards - used to alter at run time stored data blocks that contain fabrication factors, material properties, and similar data.

NOTE

Only those cards needed for a particular job need be input (the others are to be omitted). However, only complete jobs must be input. All input is wiped out between stacked jobs to reduce errors, making input on only complete jobs necessary—not just the data changed from the last stacked job.

There are two cases, however, where cases are stacked within a job. Whenever running a STRESS parameter study or a job that requires computating a STRESS tape, the input for each stacked case of STRESS needs only to contain the data changes from the case just preceding it. This procedure saves rewinding and recomputing of tapes on a STRESS parameter study, and makes stacking STRESS cases on one tape more convenient.

The other instance when cases are stacked within a job occurs when an option compression matrix (job type 5) is being computed. When comparing options, each set of CASEIN handled data cards needs to contain only the data changed from the previous option compare case. Refer to the flow chart for illustration.

5.3.3 EXECUTIVE PROGRAM INPUT INSTRUCTIONS

5.3.3.1 General

5.3.3.1.1 Format

All header cards for this program are read by READHP which permits the user to enter data between columns 7 to 72 of each data card. Each data entry must be separated by at least one blank. Data may be entered on more than one card and each read is terminated by an asterisk in the data field.

In addition to the above requirements, an identification word must be entered, starting in column 1, on the first card to be read by each individual read. Each read is identified by checking the IDentification word in control dictionary within the program.

The input header cards will be described in the following manner:

Sample Header Card

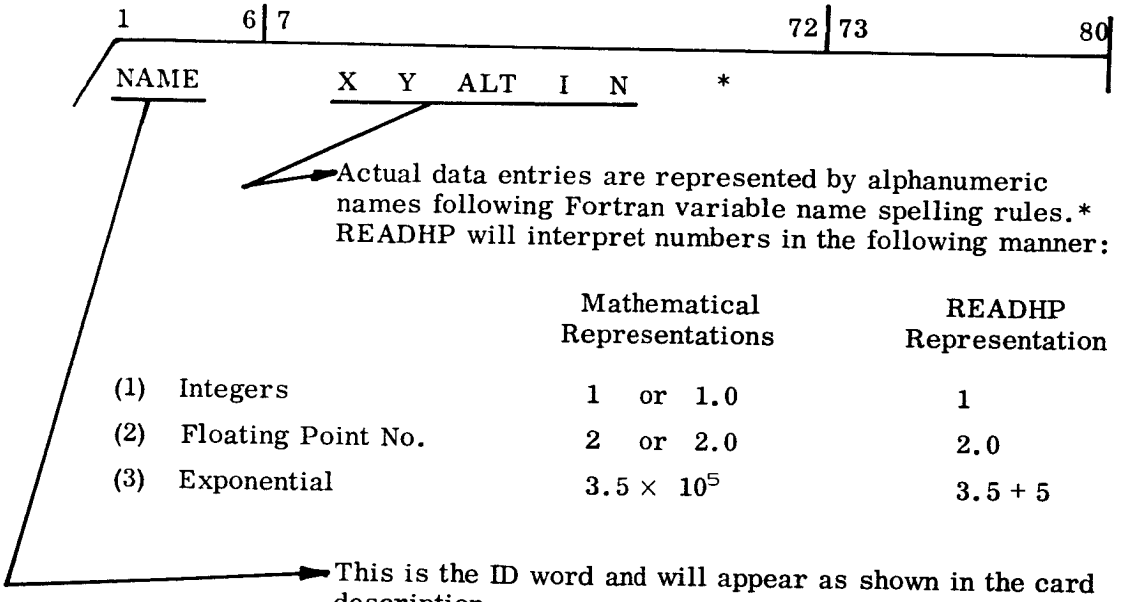

*All variable names beginning with I, J, K, L, M, or N are integers and will have NO decimal point. All other names are considered floating point numbers and will need a decimal point.

If this sample header card were to be used, an actual data card may appear as follows:

NAME	8.0	9.5 + 8	16.0	8	10	*

or

NAME	8.0	950000000.0	16.0	8	10	*

5.3.3.1.2 Sequence of Input

The sequence of input is as shown in the flow chart, Figure 5-16.

5.3.3.1.3 Jobs Card

The format of the jobs card is as shown:

JOBS	NOJOBS	*

NOJOBS = Number of stacked jobs in this run, occupies NC(1) in NC/CN array.

*All variable names beginning with I, J, K, L, M, or N are integers and will have NO decimal point. All other names are considered floating point numbers and will need a decimal point.

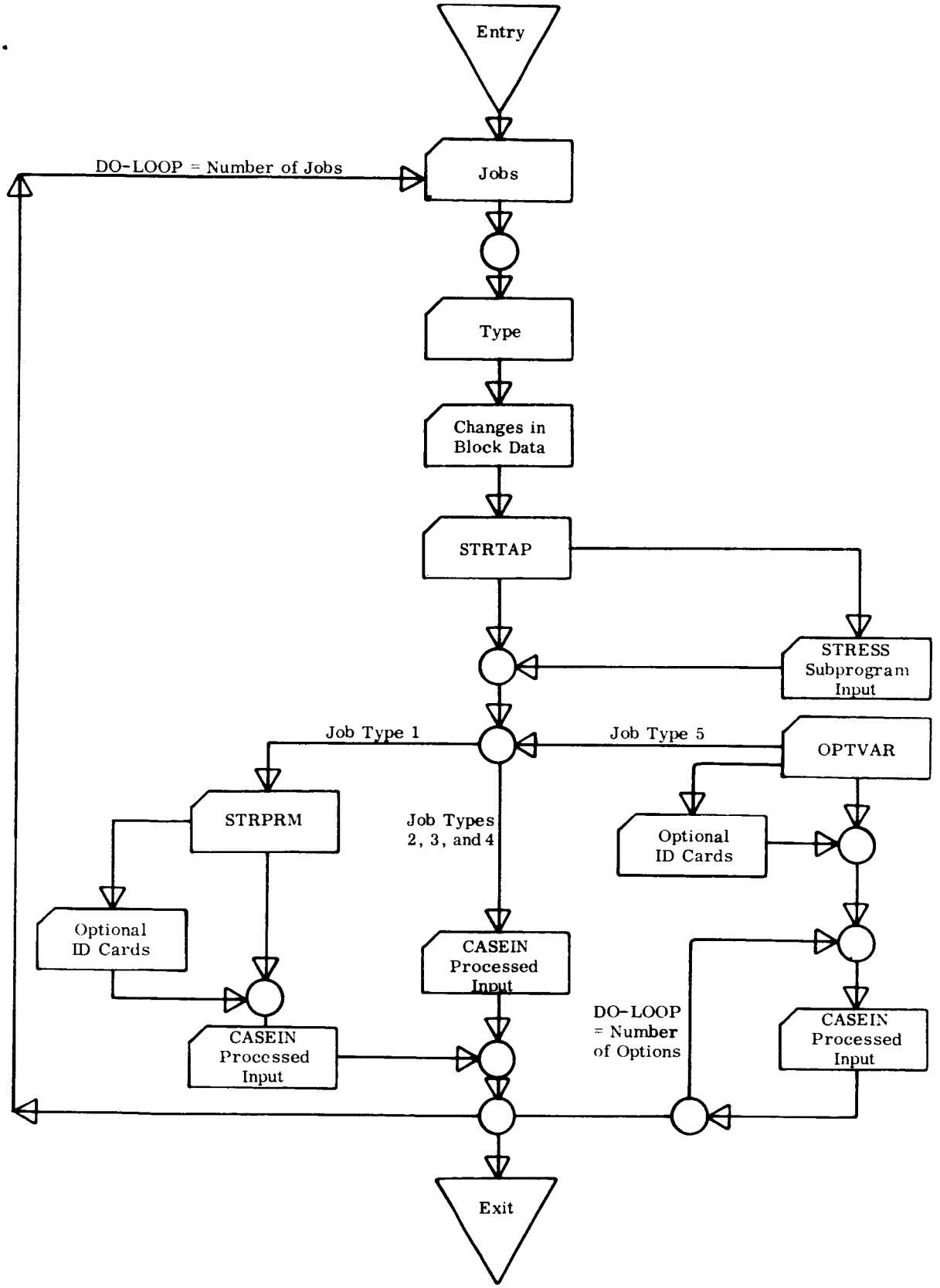

Figure 5-16. Flow Chart for Input Organization

TYPE IJBTYP N1 N2 N3 N4 N5 N6 *

IJBTYP = Signal for type of job, occupies NC(2) in NC/CN array.

= 1 ⇒ Compare different values of STRESS parameters for a given construction and material.

= 2 ⇒ Compare different construction types for a material.

= 3 ⇒ Compare different materials for a given construction.

= 4 ⇒ Compare different material/construction combinations for a structural section.

= 5 ⇒ Compare different executive options, or compare different construction subprogram options for a given construction and material.

N1 = Signal for subtotal matrix, occupies NC(150).

= 0 ⇒ Don't print subtotals matrix.

= 1 ⇒ Print subtotals matrix.

N2 = Signal for sections matrix, occupies NC(151).

= 0 ⇒ Don't print sections matrix.

= 1 ⇒ Print sections matrix.

N3 = Signal for details of construction printout, occupies NC(152).

= 0 ⇒ Don't print detailed printout.

= 1 ⇒ Print detailed printout.

*All variable names beginning with I, J, K, L, M, or N are integers and will have NO decimal point. All other names are considered floating point numbers and will need a decimal point.

N4 = Signal for additional matrices, occupies NC(153).

NOTE

Matrices 2, 3, and 4 are only different, 2-dimensional slices of a 3-dimensional array showing weights for sections versus constructions versus materials.

N4 = 0 ⇒ No additional matrices wanted.

= 1 ⇒ One additional matrix type will be specified.

= 2 ⇒ Two additional matrix types will be specified.

N5 ⇒ Signal for first additional matrix, stored in NC(154).

N6 ⇒ Signal for second additional matrix, stored in NC(155).

N5 and N6, when used, may equal 2, 3, or 4, as is desired.

Block Data Changing Cards

NEWMAT	IMAT	PROP(ITMAT, 1-12)	*

IMAT = Index of material to be added or to receive new properties (1-12).

PROP(ITMAT, 1-12) = The ten non-temperature dependent properties stored for each material as follows:

PROP(ITMAT, 1) = Density of material.

2 = Poisson's ratio.

3 = Monocoque minimum skin thickness.

4 = Honeycomb minimum face thickness.

5 = W45 and W90 minimum rib thickness.

6 = W45 and W90 skin thickness.

7 = Corrugation minimum skin thickness.

*All variable names beginning with I, J, K, L, M, or N are integers and will have NO decimal point. All other names are considered floating point numbers and will need a decimal point.

PROP(ITMAT, 8) = Corrugation minimum corrugation thickness.
(Cont.)

9 = Corrugation minimum ring thickness.

10 = Semi-monocoque minimum skin thickness.

11 = Integral stiffened minimum skin thickness.

PROP(ITMAT, 12) = Integral stiffened minimum stringer thickness.

PROP(ITMAT, 13-16) = Are 4 spaces saved for expansion, and may be used if needed later.

This card must be followed by a card with a 12-letter name in columns 1-12. This name is used in matrix printout titles.

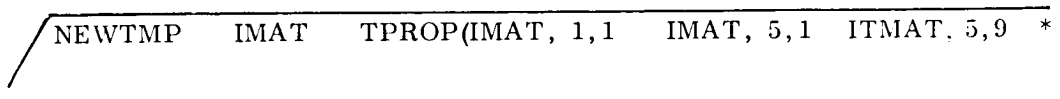

IMAT = Index of material to be added or to receive new properties (1-12).

TPROP(IMAT, 1, 1 ITMAT, 5, 9) = 45° temperature dependent material properties. Give E_c, σ yield, σ_{ult}, $\sigma_{\square}$, $\sigma_{\square}$ for each of 9 temperatures presently used (100° - 300° in 50° increments).

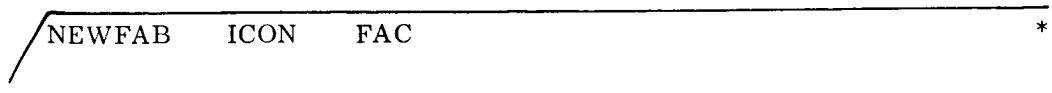

IFAB = Index of construction subprogram to receive new fabrication factor.

FAC = Value of the factor.

*All variable names beginning with I, J, K, L, M, or N are integers and will have NO decimal point. All other names are considered floating point numbers and will need a decimal point.

```
/NEWTLE      NDISC      NTYP                                    *
```

NDISC = Discontinuity number of section to receive new name for matrices.

NTYP = Type code of section to receive new name for matrices.

This card must be followed by a card which contains the 12 letter name to be given to the specified section in columns 1 through 12.

```
/SECTION NAME
```

```
/NONEW                                                         *
```

This card signals that all block data changes are complete for this job, and that flow of control is to leave the block data changing section. The block data changing cards may be in any order as long as the name cards follow the correct header (READH format) card, and as long as the NONEW card is the last card in the block data changes. When no stored data is to be changed, use the NONEW card to bypass the data changing section of the program.

```
/STRTAP              N1     NR     NP                          *
```

N1 = Signal for status of STRESS program tape.

= 1 ⇒ We have an already computed STRESS tape on NTAPE 4.

= 2 ⇒ We will compute a STRESS tape and then perform structural suboptimizations.

= 3 ⇒ We will compute a STRESS tape, but will not perform structural suboptimizations, saving the tape for future runs.

*All variable names beginning with I, J, K, L, M, or N are integers and will have NO decimal point. All other names are considered floating point numbers and will need a decimal point.

When N1 = 2 or 3, a LASS 1 output tape must be mounted on NTAPE 1, a save tape for the STRESS program must be mounted on NTAPE 4, and scratch tapes must be mounted on NTAPE 2 and NTAPE 3.

NR = Run number to pick off the STRESS or LASS 1 tape.

NP = Phase number to pick off the STRESS tape.

The LASS 1 tape has stacked runs on it.

The STRESS program numbers phases (or stacked cases) for each LASS 1 run it uses. For jobs of type 1, NR and NP indicate run and phase at which to start parameter study from the STRESS tape.

/STRPRM NOPRM NAMPRS *

NOPRM = Numbers of parameter values to run (paper size limits use to a maximum of 6, use stacked runs for more).

NAMPRS = 0 ⇒ No names follow.

= 1 ⇒ Name cards (format 2A6) follow for matrix column headers (one name card for each parameter case). This card used only for jobs of type 1.

/OPTVAR NOPTS NAMOS *

NOPTS = Number of option setting to run.

NAMOS = 0 ⇒ No names follow.

= 1 ⇒ Name cards (format 2A6) follow for matrix column headers (one name card for each option setting). This card used only for jobs of type 5.

*All variable names beginning with I, J, K, L, M, or N are integers and will have NO decimal point. All other names are considered floating point numbers and will need a decimal point.

CASEIN Processed Input

The routine CASEIN processes general input for the executive control program. It sets up material and program loops and sets all options.

All input is wiped out between jobs to decrease mistakes. Jobs of type 1, 2, 3, or 4 require one package of CASEIN input.

A special case is the job of type 5, which compares weights for different executive or subprogram options. In this case "NOPTS" number of CASEIN input packages must be stacked in one job, since we are comparing NOPTS number of option settings. These CASEIN input packages only need include the input changes from the immediately preceding option setting (because they are part of the same job).

/SAFFAC SFY SFU *

SFY = Safety factor for yield stress, stored in CN(7) of NC/CN array.

SFU = Safety factor for ultimate stress, stores in CN(8).

/SCTION NS NE *

NS = Discontinuity number at which to start weight computations, stored in NC(5).

NE = Discontinuity number at which to end weight computations, stored in NC(6).

*All variable names beginning with I, J, K, L, M, or N are integers and will have NO decimal point. All other names are considered floating point numbers and will need a decimal point.

LOADSM	INDLM	FLM	*

INDLM = An index to be set to one if a loads multiplier is to be used, stored in NC(9).

FLM = Actual factor to multiply stresses by if INDLM = 1.

Omit this card if no loads multiplier is to be used.

SUBUSE	NSP	NS1 - - - up to - - - NS5	*

NSP = The total number of construction subprograms (up to 5) that user wishes to enter into a single page of matrix output.

NS1 to NS5 = The NSP number of indices of the actual programs to be run (see reference table of indices).

MATUSE	NMAT	NM1 - - - to - - - NM6	*

NMAT = The total number of materials (up to 6) that user wishes to enter into a page of matrix output.

NM1 to NM6 = The NMAT number of actual material indices to be used (see reference table of indices).

The limits of 5 subprograms and 6 materials were set by limitations on paper size of computer output. To run more construction subprograms and materials used stacked jobs.

*All variable names beginning with I, J, K, L, M, or N are integers and will have NO decimal point. All other names are considered floating point numbers and will need a decimal point.

Material Indices

1.	Aluminum	2014 - T6
2.	Aluminum	7075 - T6
3.	Aluminum	2024 - T4
4.	Aluminum	2219 - T87
5.	Titanium	6A1 - 4V
6.	Steel	AISI - 4340
7.	Magnesium	HK 31A - H24
8.	Stainless Steel	PH 15 - 17 Mo
9.	Berylium	Y5804 - QMV5
10.		
11.	Blanks for future expansion	
12.		

Construction Subprogram Indices

1. Monocoque
2. Honeycomb Sandwich
3. Waffle 45°
4. Waffle 90°
5. No-face corrugation
6. Single face corrugation
7. Semi-monocoque
8. Integrally stiffened
9. Blanks for future expansion
10.

For the "NEWFAB" card the following additional indices are used.

11. Monocoque Heads
12. Honeycomb Sandwich Heads
13. Waffle Heads

SUBNAM	NM	M1 - - - up to - - -M6	*

SUBNAM = 6 letter subprogram name according to the following code:

MONOCQ - Monocoque

HONCOM - Honeycomb Sandwich

WAF45D - Waffle 45°

WAF90D - Waffle 90°

CORUG1 - No-face corrugation

CORUG2 - Single-face corrugation

SEMIMQ - Semi-monocoque

INTSTF - Integrally stiffened

There are 2 blank names reserved for future expansion.

NM = Total number of materials to be run with this subprogram (up to 6).

M1 . . to . . M6 = The actual material indices as indicated in the index code.

NOTE

The MATUSE and SUBUSE cards set up the matrix and these subprogram cards set up the individual loops - thus avoiding the need to run all subprograms with all materials. Unused combinations in the matrix are filled with zeroes.

SPROPT	X(I)	I - - - up to - - -22	*

SPROPT = 6-letter code name to indicate which subprograms run time options are being input on this card. The following code applies.

*All variable names beginning with I, J, K, L, M, or N are integers and will have NO decimal point. All other names are considered floating point numbers and will need a decimal point.

MONOPT - Monocoque

HONOPT - Honeycomb Sandwich

W45OPT - Waffle 45°

W90OPT - Waffle 90°

CR1OPT - No-face corrugation

CR2OPT - Single-face corrugation

SEMOPT - Semi-monocoque

INTOPT - Integrally stiffened

X(I) = The run-time inputs (options, limits, constants, etc.). I up to 22.

The X(I) are described in the input descriptions of each construction subprogram.

In the run-time input and options cards, 2 card names are set aside as blanks for insertion of future expansions.

STOTAL	NST	NS	NE	NSB	NST	NEB	NET	*

NST = Number of this subtotal (up to 10 are provided for in the storage arrays).

NS = Discontinuity at which to start adding up this subtotal.

NE = Discontinuity at which to finish adding up this subtotal.

NSB = Signal for including bottom head at NS.

NST = Signal for including top head at NS.

NEB = Signal for including bottom head at NE.

NET = Signal for including top head at NE.

*All variable names beginning with I, J, K, L, M, or N are integers and will have NO decimal point. All other names are considered floating point numbers and will need a decimal point.

Heads inclusion signals are to be set equal to 1 if the head is to be included. Signal is to be set to 0 if the head is not to be included in this subtotal, or if the signal is inapplicable to this discontinuity.

NOTE

A 72-letter description card (format 12A6) must follow each STOTAL card.

CASEND *

This card signals that all input for this case is finished and that control is to be returned to the executive control program from the input cataloging routine CASEIN.

*All variable names beginning with I, J, K, L, M, or N are integers and will have NO decimal point. All other names are considered floating point numbers and will need a decimal point.

5.3.3.1.14 Output Matrix Formats

a. Format 1 - Type Construction/Material

Section	X_1	X_2	X_3	X_4	X_5	→
1-2 2-3 3-4 ↓	Weights will be printed here.					
Total						

A job of type No. 1 is used for parameter studies requiring recomputation of the loads tape.

b. Format 2 - Material

Section	Monocoque	Honeycomb	Corrugation	Waffle	→
1-2 2-3 3-4 ↓	Weights will be printed here.				
Total					

A job of type No. 2 investigates the effect of changing construction types for a given material.

c. Format 3 - Section

Construction	Al.	Be	Ti	St	→	
Monocoque Waffle Honeycomb ↓	Weights will be printed here.					

A job of type No. 3 shows weights for different structural concepts for each section investigated.

d. Format 4 - Construction Type

Section	Al.	Be	Ti	St	→
1-2 2-3 3-4 ↓	Weights will be printed here.				
Total					

Output matrix of a job of type No. 4 shows weights of different materials for a given construction.

e. Format 5 - Type Construction/Material

Section	Y_1	Y_2	Y_3	Y_4	Y_5	→
1-2 2-3 3-4 ↓	Weights will be printed here.					
Total						

Jobs of type No. 5 compare weights for different settings of subroutine options or different values of subroutine parameters.

5.3.3.2 STRESS Subprogram (Input and Output)

5.3.3.2.1 General

The first two computer programs discussed in this user's manual are concerned with finding the magnitudes of the aerodynamic and control loads and determining how these external loads are reacted through the structure of the space vehicle. In the STRESS subprogram described here, the pressure loads are analyzed and all external forces are resolved in orthogonal stress resultants in the plane of the structural system. These resultants are then stored on the restart tape for use by the construction subprograms. A flow chart is illustrated in Figure 5-17.

The structural system in this analysis is assumed to be formed of elliptical and conical shells. It is noted that spherical and cylindrical shells are special cases of these two general classes of shells. The structure and the loading is assumed to be axisymmetric and the shell parameters are identified at several hundred fixed points along the shells in the meridional direction. The envelope dimensions of the structure are described by specifying radii of curvature, cone angle, or other identifying geometric parameters.

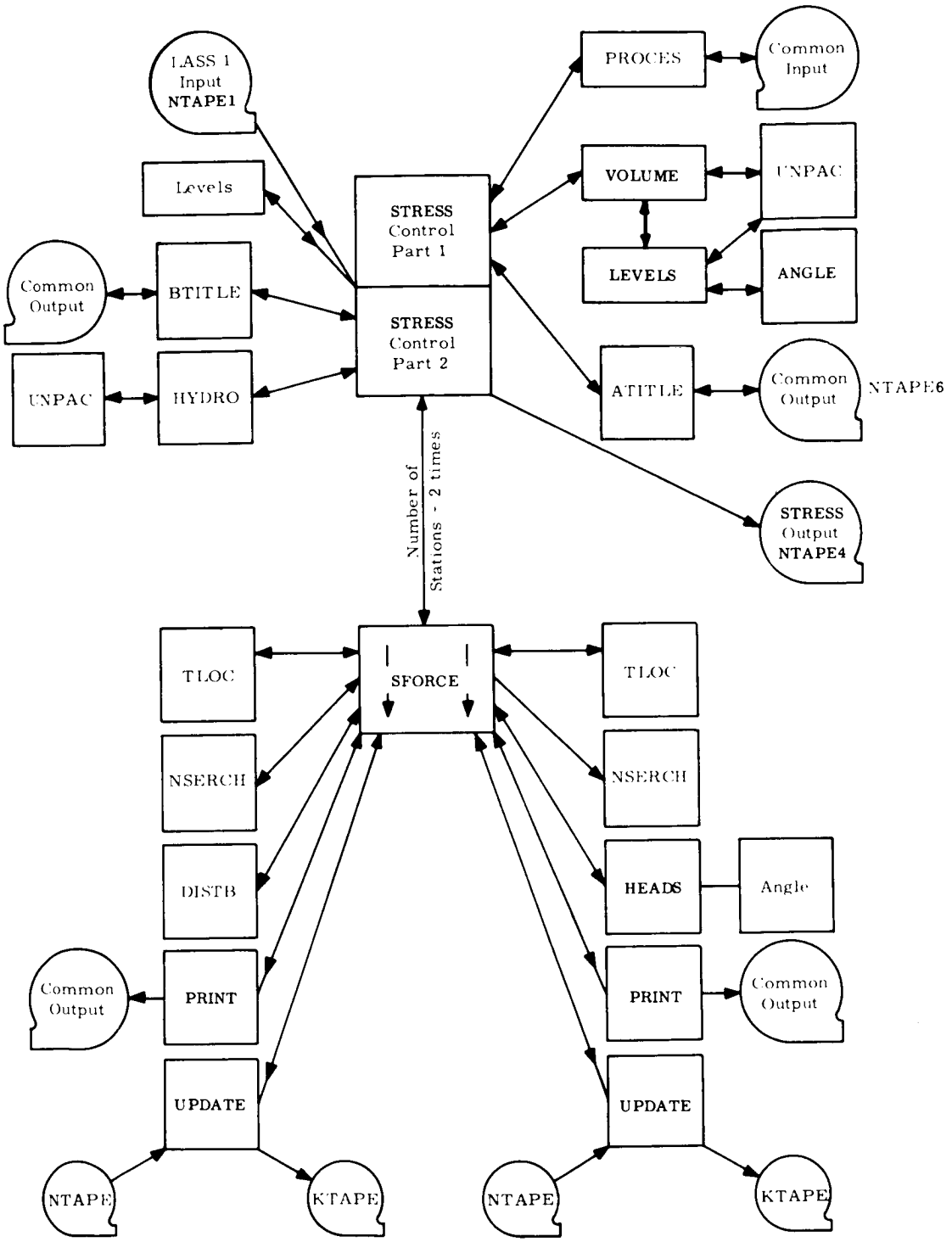

Figure 5-17. STRESS Flow Chart

The loads applied to the shells are continuously varying with time, but it is possible to describe this variation by performing analyses at several discrete time points during a mission. The total pressure at every point along the shells must be determined at each of these discrete time points. Since the total pressure is the sum of the hydrodynamic pressure of the propellants and the ullage pressure in the tanks, it is necessary to analyze the time variations of these pressures. The "Ullage Pressure/Time" relationship is a required input parameter. The hydrodynamic pressure is a function of axial acceleration, propellant density, and level of propellant. Axial acceleration is found from GASP, and the propellant density is a required input. Only the level of the propellant must be calculated.

The initial loading of the tank is specified by giving the percent of total volume which is ullage space as an input parameter. Knowledge of the envelope dimensions of the tank permit a calculation of the total volume with the equations presented in Part 1 of Appendix E. Once the initial propellant level is calculated, the level at any other flight time can be found by subtracting the volume of propellant burned. This obviously requires a knowledge of the propellant flow rate. The equation for the total pressure at a point "d" units below the propellant level of the propellant is then given by

$$P_{total} = P_{ullage} + \beta \gamma d$$

where

P_{total} = total pressure.

P_{ullage} = ullage pressure.

β = axial acceleration in g's.

γ = propellant density.

d = distance below propellant level.

Once the total pressure has been found for every station at each time point, then the pressure forces can be combined with the other external loads found in LASS-1. The loads are combined by resolving all forces into stress resultants in the plane of the shells. The stress resultant for the meridional and circumferential directions of a general shell section are given by the equations in Part 2 of Appendix E.

Using the equation of Appendix E, a complete catalogue of stress resultants, N_x and N_e are developed for each station at each flight time to be considered. It is important to note that these stress resultants depend only on the envelope dimensions of the shells and are independent of the type of wall construction. Thus, this catalogue of stress resultants are used to analyze all sections of the launch vehicle whether they may be monocoque, waffle, integral stiffened skin, or any other type of construction.

There is, however, another load condition that must be considered other than the pre-launch and inflight, and this is the hydrostatic test condition for the tanks. After a tank which has been designed for a certain internal pressure loading is manufactured, it is common procedure to subject the tank to a pressure test. This test will subject the tank to, at least, the maximum pressure environment which the tank will experience during actual flight conditions. This test is commonly called the hydrostatic test. It will be accounted for in this program by hypothetically filling the tank with liquid and then pressurizing the tank until the pressure envelope matches or exceeds by a specified amount the pressure experienced during flight at the most critical point.

For instance, at liftoff, each fuel or LOX tank will have a pressure distribution which is a combination of gas pressure and liquid pressure as depicted in Figure 5-18. During the flight, the gas pressure may vary with time and the axial acceleration will vary as will the liquid level. An envelope of maximum pressures at each station of the tank is generated as a result of this variation with time and the general envelope is illustrated in Figure 5-19. The hydrostatic test envelope is that represented by the dashed curve in Figure 5-19.

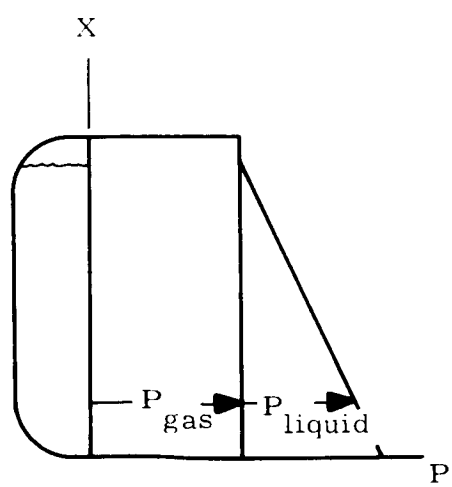

Figure 5-18. Initial Pressure Distribution

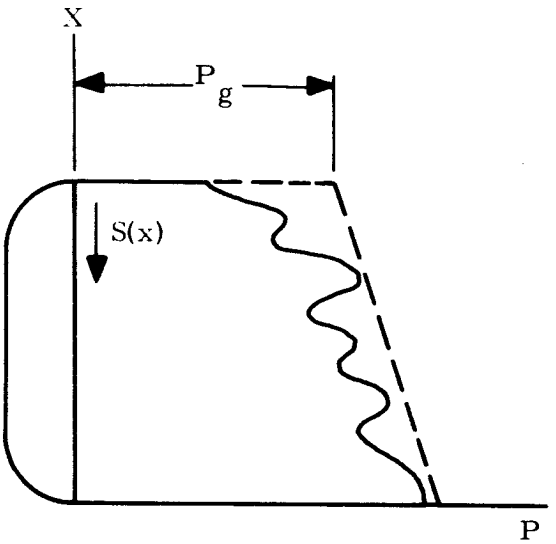

Figure 5-19. Envelope of Maximum Pressures

This envelope has the mathematical form

$$P_s(x) = P_G \gamma_t S(x)$$

which is a linear function with the slope depending upon the specific weight of the test fluid. The pressure, P_G, is determined such that the flight envelope of maximum pressures is enclosed.

When the pressure, P_G, is known, the test pressure envelope is then multiplied by a factor which may be equal to or greater than unity. That is, the final hydrostatic test envelope can be represented as

$$P_F(x) = mP_s(x), \ (m \geq 1)$$

Using this pressure distribution, a membrane analysis is performed with all other loads absent and a hydrostatic test stress resultant distribution is calculated. If the strength criteria selected is independent of the type of construction, then the time variable can be eliminated by choosing the worst combination of stress resultants at each station for all the time points considered. This distribution is then compared with that resulting from the hydrostatic test calculation and the worst combination is chosen. The structure must be designed to withstand this load environment. A summary of these loads is printed on the optional output sheets of the stress subprogram as shown in Figure 5-20. Note also, that the maximum compressive load is chosen for use in buckling design.

```
TANK     1     1111.0       140.00714      237.00000     140.00714
       198.0     198.0        198.0        140.00714       198.0
       140.00714        0.0          0.0            224.99287       0.0  *
TANK   2     1121.0     140.00714      489.00      140.00714       198.0
        198.0       198.0       140.00714     198.0      140.00714
          0.0           0.0         771.99287      0.0       *
TANK    3    1121.0      140.00714      0.0      140.00714       198.0
        198.0       198.0      140.00714      198.0      140.00714
        0.0           0.0         1707.99287          0.0       *
TANK     4       2131.0      140.00714      398.99286       140.00714
        198.0       198.0       198.0     140.00714      198.0
         140.00714      198.00       0.0          1848.000        0.0    *
TANK    5  1121.0  89.0   0.0   89.0  123.365   123.365
                    130.0       130.0       130.0        130.0
          0.0          0.0                          2701.0          0.0    *
TANK      6     3131.0     130.0      269.0      130.0      130.0
        130.0       130.0      130.0       130.0      130.0       -41.0
          0.0             2701.00          0.0           *
STAGE   100.0        198.000         0          1
        365.0000     198.000       23           1
        602.0000     198.000       13           1
        912.0000     198.000       23           1
        1401.000     196.000       13           1
         1564.00      198.0000      2     1
        1760.000     198.000        2           1
       1848.000     198.000     34              1
       2387.000     198.000     13              1
       2519.000     198.000     2               1
       2747.000     130.000     2               1
       2791.000       130.000       35          1
         2832.000      130.000     24      1
          3101.000     130.00      13     1
          3223.000      130.00       2     1
          3259.00     130.000     2     1              *
OPTION    MEMBRN      *
RUN NO    1    DYNAM  1.09    1.06     *
TIMES    -1.0    155.0    1    16    4.0          0.0    0.0   *
FUEL    1  8358.00   .029225    70.0     70.0      *
FUEL    2  19843.333   .041088 -290.0   -200.0     *
FUEL    3  8358.00   .0025463   -402.00   -300.0      *
TABLE    1    -10.0    0.0   40.0    80.0    120.0    155.0
FUEL 1       31.0    32.0    33.0     34.0     35.0    36.0
FUEL 2     37.0    38.0    39.0      40.0     41.0    42.0
FUEL 3     40.0    38.0    36.0     34.0     32.0     30.0    *
TABLE     2     100.0    365.0    602.0    612.0    1401.0    1564.0
        1760.0    1818.0     2387.0    2219.0    2747.0    2791.0
          2832.0    3101.0    3223.0    3269.0
TEMP       60.0    61.0    62.0     63.0    64.0    65.0    66.0     67.0    68.0
      70.0    65.0    71.0    72.0    73.0    74.0     75.0          *
ENDCSE    *
```

Figure 5-20. Output Format - STRESS Monocoque Analysis (Input Header Cards)

****** STRUCTURAL WEIGHT OPTIMIZATION PROGRAM ******

RUN 1
PHASE 1

** INITIAL CONDITIONS **

TOTAL NUMBER OF STRUCTURAL DISCONTINUITIES= 16
TOTAL NUMBER OF TANKS= 6
HEIGHT OF ANALYSIS INTERVAL= 4.0000 INCHS
ANALYSIS WILL BE PERFORMED BETWEEN DISCONTINUITY 1 AND 16
THE DYNAMIC MULTIPLIER FOR THE FORCES = 1.0600000
THE DYNAMIC MULTIPLIER FOR THE MOMENTS = 1.0900000

* VEHICLE CHARACTERISTICS *

STATION	HEIGHT	RADIUS	TYPE
1	100.00000	198.000000	0
2	365.00000	198.000000	23
3	602.00000	198.000000	13
4	912.00000	198.000000	23
5	1401.00000	198.000000	13
6	1564.00000	198.000000	2
7	1760.00000	198.000000	2
8	1848.00000	198.000000	34
9	2387.00000	198.000000	13
10	2519.00000	198.000000	2
11	2747.00000	130.000000	2
12	2791.00000	130.000000	35
13	2832.00000	130.000000	24
14	3101.00000	130.000000	13
15	3223.00000	130.000000	2
16	3259.00000	130.000000	2

Figure 5-20. Output Format - STRESS Monocoque Analysis (Cont.)

* TANK CHARACTERISTICS *

TANK	VOLUME	ULLAGE	LIQUID LEVEL	V-TOP	V-MIDDLE	V-BOTTOM	FUEL
1	0.52181228E 08	0.00000000E-38	0.51701427E 03	0.11495799E 08	0.29189630E 08	0.11495799E 08	1
2	0.85218303E 08	0.00000000E-38	0.76901427E 03	0.11495799E 08	0.60226705E 08	0.11495799E 08	2
3	0.22991598E 08	0.00000000E-38	0.28001428E 03	0.11495799E 08	0.00000000E-38	0.11495799E 08	2
4	0.66384854E 08	0.00000000E-38	0.67900713E 03	0.11495799E 08	0.49141156E 08	0.57478997E 07	3
5	0.49935007E 07	0.00000000E-38	0.17800000E 03	0.24967503E 07	0.00000000E-38	0.24967503E 07	2
6	0.18491265E 08	0.00000000E-38	0.44000000E 03	0.46013859E 07	0.14281994E 08	0.46013859E 07	3

* FUEL CHARACTERISTICS *

FUEL	BURN RATE	SPECIFIC WEIGHT	TEMPERATURE OF FUEL	TEMPERATURE OVER FUEL
1	0.83580000E 04	0.29225000E-01	0.70000000E 02	0.70000000E 02
2	0.19843333E 05	0.41088000E-01	-0.29000000E 03	-0.20000000E 03
3	0.83580000E 04	0.25463000E-02	-0.40200000E 03	-0.30000000E 03

Figure 5-20. Output Format - STRESS Monocoque Analysis (Cont.)

```
** ANALYSIS FOR A FLIGHT TIME OF  -1.00000 SEC **

AXIAL ACCELERATION= 0.00000000E-38
ACCELERATION IN G'S =   1.000000
TANK CHARACTERISTICS
     TANK  1
          LIQUID LEVEL.....=  517.01427
          ULLAGE VOLUME....=  0.00000000E-38
          ULLAGE PRESSURE...=  31.90000
     TANK  2
          LIQUID LEVEL.....=  769.01427
          ULLAGE VOLUME....=  0.00000000E-38
          ULLAGE PRESSURE...=  31.90000
     TANK  3
          LIQUID LEVEL.....=  280.01428
          ULLAGE VOLUME....=  0.00000000E-38
          ULLAGE PRESSURE...=  31.90000
     TANK  4
          LIQUID LEVEL.....=  679.00713
          ULLAGE VOLUME....=  0.00000000E-38
          ULLAGE PRESSURE...=  31.90000
     TANK  5
          LIQUID LEVEL.....=  178.00000
          ULLAGE VOLUME....=  0.00000000E-38
          ULLAGE PRESSURE...=  31.90000
     TANK  6
          LIQUID LEVEL.....=  440.00000
          ULLAGE VOLUME....=  0.00000000E-38
          ULLAGE PRESSURE...=  31.90000
```

Figure 5-20. Output Format - STRESS Monocoque Analysis (Cont.)

```
                    ** ANALYSIS FOR A FLIGHT TIME OF  72.90000 SEC **

AXIAL ACCELERATION= 0.10187350E 04
ACCELERATION IN G'S =   3.638608
TANK CHARACTERISTICS
      TANK  1
            LIQUID LEVEL.....=  298.74730
            ULLAGE VOLUME....=  0.21134515E 08
            ULLAGE PRESSURE...=  33.82250
      TANK  2
            LIQUID LEVEL.....=  432.56829
            ULLAGE VOLUME....=  0.35689795E 08
            ULLAGE PRESSURE...=  33.82250
      TANK  3
            LIQUID LEVEL.....=  280.01428
            ULLAGE VOLUME....=  0.00000000E-38
            ULLAGE PRESSURE...=  33.82250
      TANK  4
            LIQUID LEVEL.....=  679.00713
            ULLAGE VOLUME....=  0.00000000E-38
            ULLAGE PRESSURE...=  33.82250
      TANK  5
            LIQUID LEVEL.....=  178.00000
            ULLAGE VOLUME....=  0.00000000E-38
            ULLAGE PRESSURE...=  33.82250
      TANK  6
            LIQUID LEVEL.....=  440.00000
            ULLAGE VOLUME....=  0.00000000E-38
            ULLAGE PRESSURE...=  33.82250
```

Figure 5-20. Output Format - STRESS Monocoque Analysis (Cont.)

```
                    ** ANALYSIS FOR A FLIGHT TIME OF 149.00000 SEC **

AXIAL ACCELERATION= 0.18893269E 04
ACCELERATION IN G'S =   5.893514
TANK CHARACTERISTICS
     TANK  1
          LIQUID LEVEL.....=  121.94064
          ULLAGE VOLUME....=  0.42898203E 08
          ULLAGE PRESSURE...=  35.82857
     TANK  2
          LIQUID LEVEL.....=  134.16132
          ULLAGE VOLUME....=  0.72442074E 08
          ULLAGE PRESSURE...=  35.82857
     TANK  3
          LIQUID LEVEL.....=  280.01428
          ULLAGE VOLUME....=  0.00000000E-38
          ULLAGE PRESSURE...=  35.82857
     TANK  4
          LIQUID LEVEL.....=  679.00713
          ULLAGE VOLUME....=  0.00000000E-38
          ULLAGE PRESSURE...=  35.82857
     TANK  5
          LIQUID LEVEL.....=  178.00000
          ULLAGE VOLUME....=  0.00000000E-38
          ULLAGE PRESSURE...=  35.82857
     TANK  6
          LIQUID LEVEL.....=  440.00000
          ULLAGE VOLUME....=  0.00000000E-38
          ULLAGE PRESSURE...=  35.82857


THE LAST TIME POINT ON THE LASS1 TAPE IS  149.00000 FOR RUN  1 ,PHASE  1
```


Figure 5-20. Output Format - STRESS Monocoque Analysis (Cont.)

If the strength criteria is not independent of the type of construction, time cannot be eliminated and the shell thickness calculations must be made for each time point plus the hydrostatic test case, and the thicknesses are then compared to determine the larger for each station or section whatever the case may be. This does not affect the choosing of the buckling design load, however.

5.3.3.2.2 User's Manual for the STRESS Program

5.3.3.2.2.1 General

All header cards for this program are read by READHP which permits the user to enter data between columns 7 to 72 of each data card. Each data entry must be separated by at least one blank. Data may be entered on more than one card and each read is terminated by an asterisk in the data field.

In addition to the above requirements, an identification mark must be entered, starting in column 1, on the first card to be read by each individual read. Each read is identified by checking the identification word in the control dictionary within the program. The following control words are now recognized by this program.

a. TIMES
b. FUEL
c. TABLE
d. TANK
e. STAGE
f. OPTION
g. ENDCSE
h. FINISH
i. RUN NO

Each individual read need not be in any special order since the read is identified by the control dictionary (by means of the ID word) within the program.

5.3.3.2.2.2 Specific Header Card Requirements

The input header cards will be described as illustrated in the following sample card:

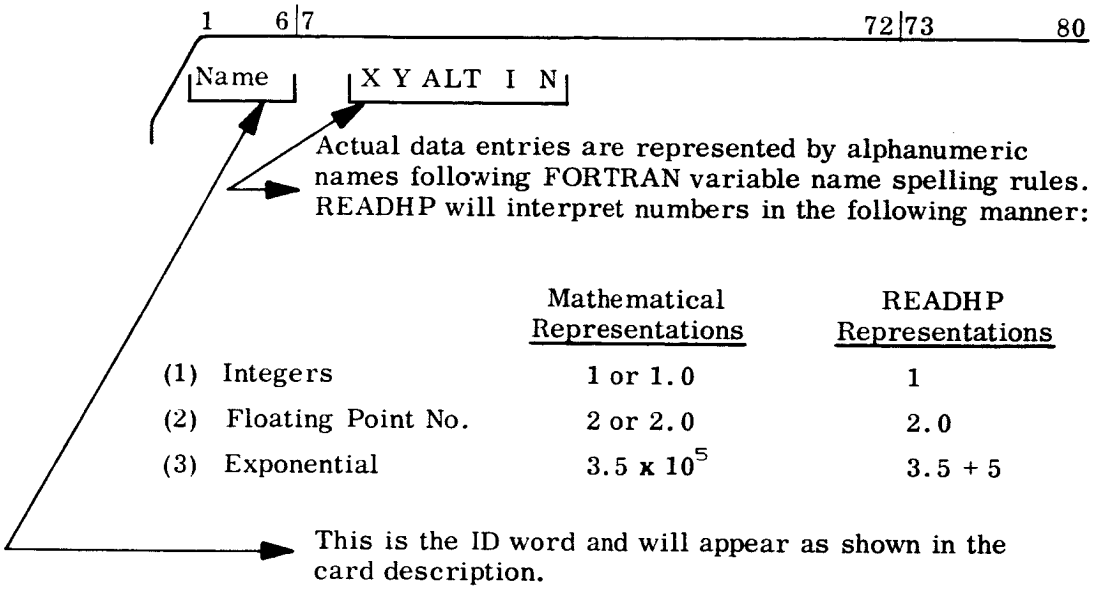

	Mathematical Representations	READHP Representations
(1) Integers	1 or 1.0	1
(2) Floating Point No.	2 or 2.0	2.0
(3) Exponential	3.5×10^5	3.5 + 5

If this sample header card were to be used, an actual data card might appear as follows

```
NAME    8.0    9.5 + 8    16.0    8    10    *
                    or
Name    8.0    950000000.0    16.0    8    10    *
```

5.3.3.2.2.3 Data Card Requirements

1.
```
TIMES   STIME   ETIME   IST   LST   DH   PSTART   PEND   *
```

where:

STIME = the time of flight where the analysis will be started (sec).

ETIME = the time of flight where the analysis will be terminated (sec).

*All variable names beginning with I, J, K, L, M, or N are integers and will have NO decimal point. All other names are considered floating point numbers and will need a decimal point.

IST = discontinuity number where analysis is to be started (see description of STAGE card for discontinutiy number description).

LST = discontinuity number where analysis is to be stopped.

DH = the height interval increment at which the analysis is to be performed (inches).

PSTART = the time of flight in seconds when the printing is to start.

PEND = the time of flight in seconds when the printing is to end.

2.

FUEL N BR GAM T_1 T_2 *

where:

N = the fuel ID number (1, 2, 3, 4, or 5).

BR = burn rate (lbs/sec).

GAM = specific weight of fuel (lbs/in^3).

P = pressure above fuel (lbs/in^2).

T_1 = Temperature of the fuel (degrees fahrenheit).

T_2 = Temperature of the gas above the fuel (degrees fahrenheit).

3.

Card 2

AT BT RBB RTT HLOC PULL *

Card 1

TANK N TYPE HB HM HT RB RT AB BB

where:

N = the tank number (number the tanks consecutively starting with 1). The tank number has to be with respect to height of the tank, i.e., tank 3 is higher than tank 2 and tank 2 is higher than tank 1. Only 10 tanks are allowed.

TYPE = a code number which describes the tank. This code number will always have 4 digits to the left of the decimal point and none to the right.

The thousandth's digit is used to describe the top head:

1 = convex

2 = concave

The hundredth's digit is used to describe the bottom head:

1 = convex

2 = concave

3 = convex - complex

The tenth's digit agrees with the fuel number of the fuel used in the tank.

The one's digit agrees with the metal number of the metal that the tank is constructed of (see Figure 5-21).

HB = the distance from the lowest point on the tank to the highest point of bottom head (inches).

HM = the distance from the highest point of the bottom head to the lowest point of the top head (inches).

HT = the distance from the lowest point of the top head to the highest point on the tank (inches).

RB = the radius of the tank at the height HB (inches).

RT = the radius of the tank at the height HB + HM (inches).

AB = semimajor axis of the bottom head (inches).

BB = semiminor axis of the bottom head (inches).

AT = semimajor axis of the top head (inches).

BT = semiminor axis of the top head (inches).

RBB = the radius of the tank at its lowest point (inches).

RTT = the radius of the tank at its highest point (inches).

HLOC = the distance from the structure's reference point (0.0 height) to the lowest point on the tank (inches).

PULL = percent ullage in the tank at the start of the flight.

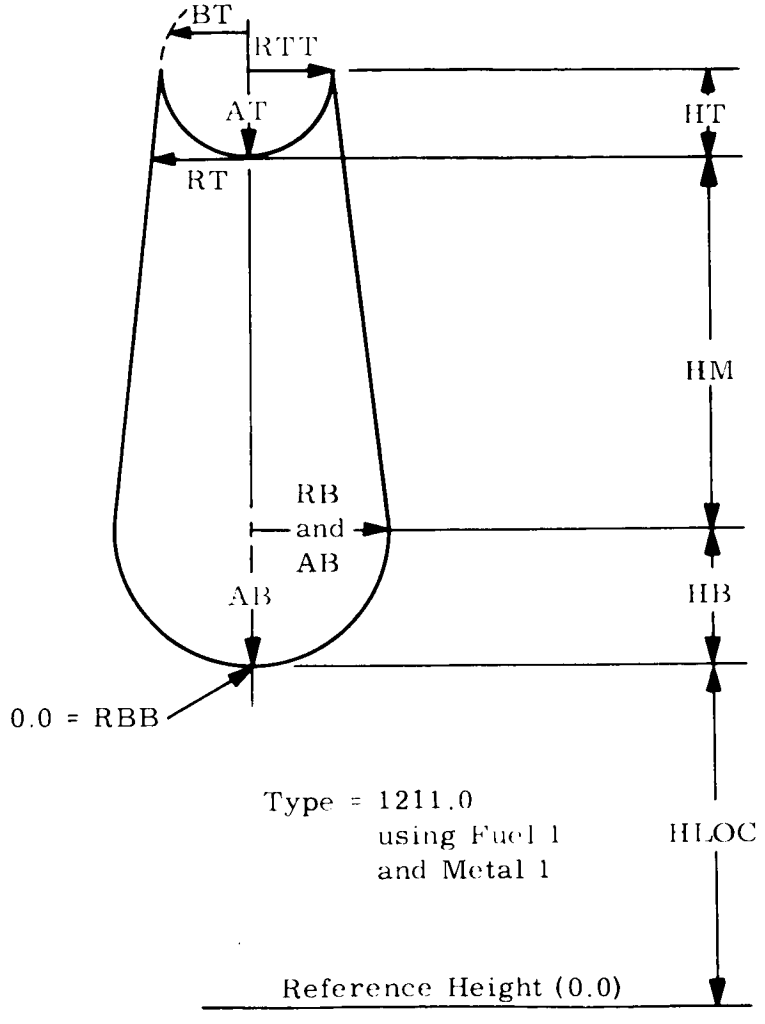

Figure 5-21. Tank Diagram

4.

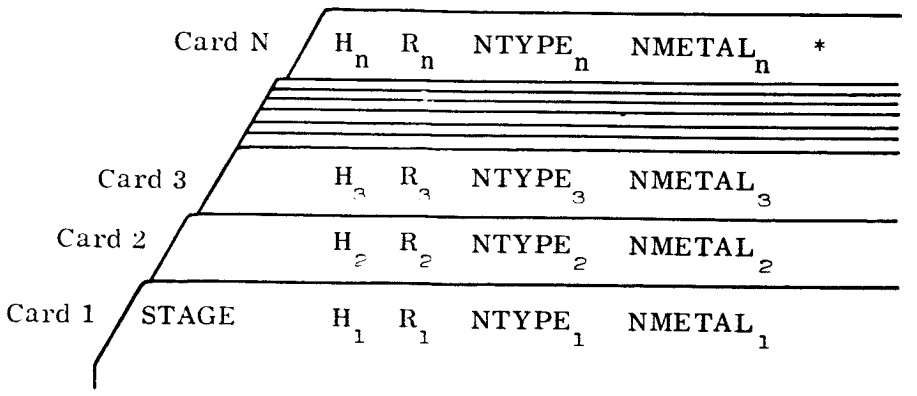

This input is used to mathematically describe the shape of the structure by stations (see Figure 5-22). In order to describe a station, the program must know three values (height, radius, and type). As noted above (card example), the information about all of the stations is read with one read (please note that there is only an asterisk on the last card). The stations must be ordered with respect to increasing height. The program will number the stations consecutively starting with 1 (i.e., card 1 represents station 1); Station 1 must be the lowest point on the structure to be analyzed.

H = the height of the station from a zero reference on the vehicle* (inches).

R = the radius at H (inches).

NTYPE = a code number which describes the station. The following code numbers are now recognized by the program.

- 0 = no discontinuities and no tanks.
- 2 = two discontinuities and no tanks.
- 13 = three discontinuities (two shells and a top head of a tank).
- 23 = three discontinuities (two shells and a bottom head of a tank).
- 24 = three discontinuities (two shells and a partial bottom head).
- 33 = three discontinuities (two shells and a compound** top head).
- 34 = four discontinuities (two shells, a bottom head, and a compound top head).

* This reference must conform to the reference point used in the LASS-1 program (see Tape Descriptions).

**A compound head, in this use, refers to a head which acts as a common head for two tanks.

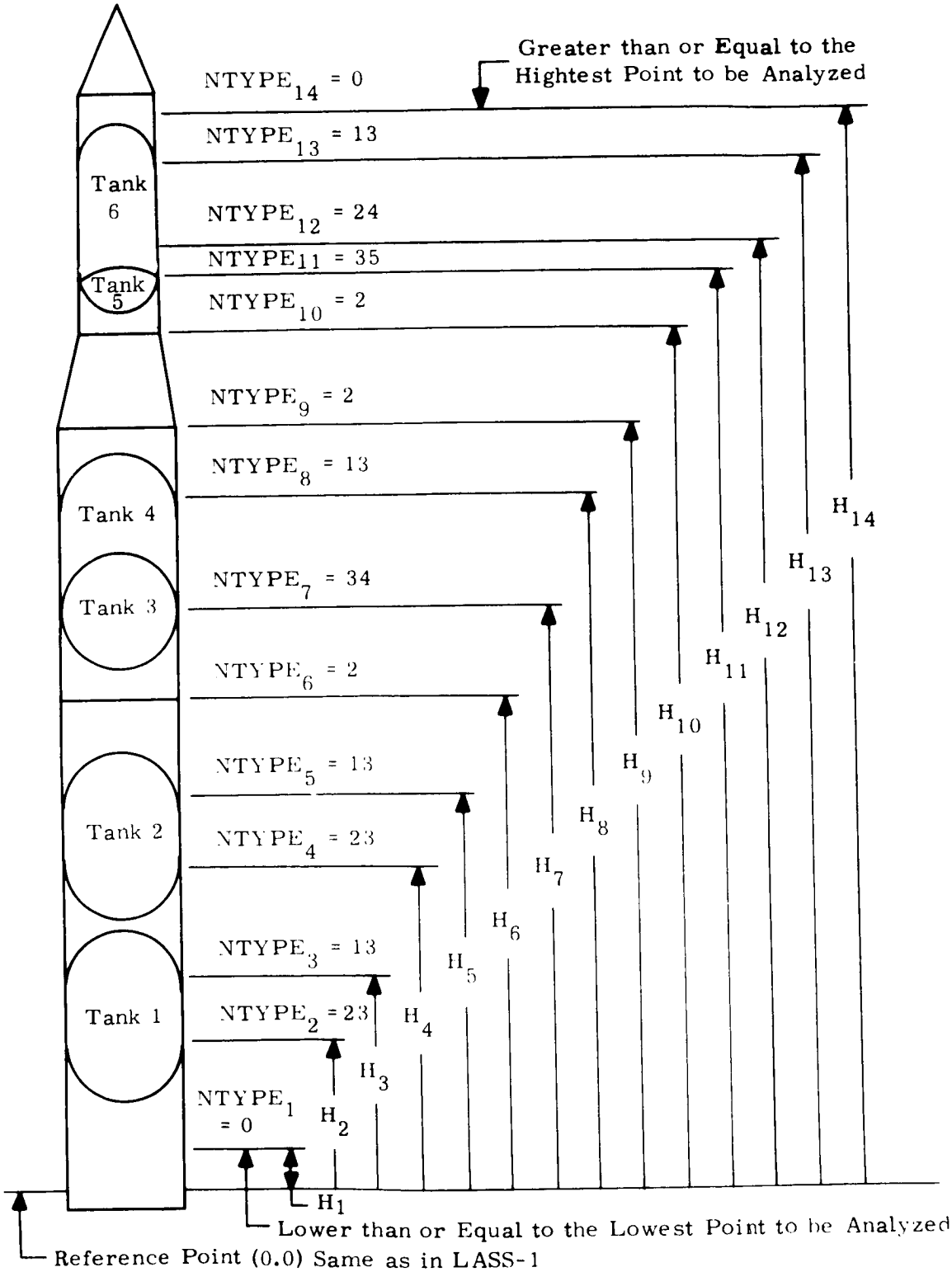

Figure 5-22. Structure to be Analysed

35 = three discontinuities (bottom head, top head, and partial bottom head).

NMETAL = a metal ID number. This number will agree with a metal ID number of the metal that is to be used for the skin area above this station, but below the next higher station.

5.

```
OPTION   Word 1   Word 2   GAMT   HYMX   *
```

where:

Word 1 = the word MEMBRN or NO. If MEMBRN is specified, the membrane solution will be performed; otherwise, this solution will be ignored.

Word 2 = the word HYDRO or NO. If HYDRO is specified, a hydrostatic test analysis will be performed.

GAMT = the specific weight of the liquid to be used in the hydrostatic test (lbs/in^3). If GAMT is set to (0.0), the actual fuel specific weights will be used.

HYMX = the hydrostatic multiplier.

Two examples of the above card are as follows:

```
OPTION   MEMBRN   HYDRO   .03611   1.0   *
```

```
OPTION   MEMBRN   *
```

6.

```
RUN NO   N   Word 1   XMM   FM   *
```

where:

N = an integer which agrees with a run on the LASS-1 input tape to SWOP.

Word 1 = DYNAM. If this word is omitted or misspelled, the rest of this data field will be omitted. If the DYNAM option is specified, the next two floating point numbers will contain dynamic multipliers.

XMM = dynamic multiplier for moments inputted by LASS-1.

FM = dynamic multiplier for the forces inputted by LASS-1.

7.

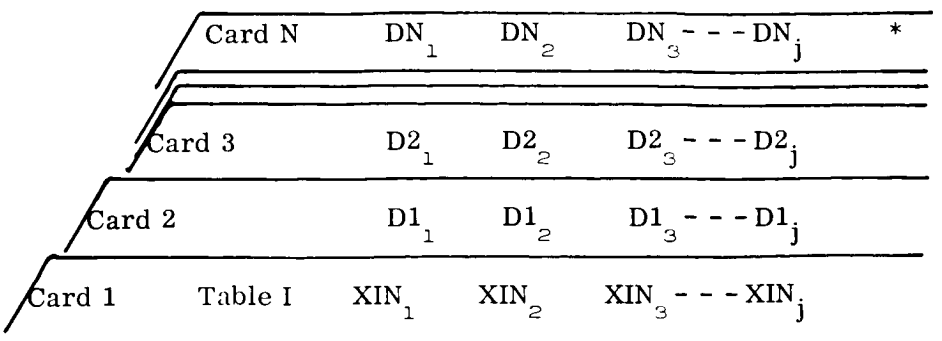

where:

I = The Table Number.

XIN = Independent Table.

.

.

.

DN = The Dependent Tables.

The STRESS program has two tables, which may be read in by means of Table cards.

Table 1 is the time versus Ullage Pressure Table and the table entries are as follows:

I = 1.

XIN = Time Table in ascending order with 6 entries (seconds).

D1 = Ullage Pressure Table for Fuel 1 (6 entries).

D2 = Ullage Pressure Table (LBS/IN^2) for Fuel 2 (6 entries).

D3 = Ullage Pressure Table (LBS/IN^2) for Fuel 3 (6 entries).

D4 = Ullage Pressure Table (LBS/IN^2) for Fuel 4 (6 entries).

D5 = Ullage Pressure Table (LBS/IN^2) for Fuel 5 (6 entries).

Table 2 is the Height versus Temperature Table and the table entries are as follows:

I = 2.

XIN = Height Table in ascending order with 16 entries (inches).

D1 = Temperature Table (16 entries) (Degrees Fahrenheit).

*All variable names beginning with I, J, K, L, M, or N are integers and will have NO decimal point. All other names are considered floating point numbers and will need a decimal point.

8. ENDCSE *

This card tells the program that there are no more cards to be processed for this case and consequently the program will start to perform the analysis on the desired structure. When multiple cases are run, only cards identified by 1 read (all information between card ID name and an asterisk) that need to be changed must be re-entered.

9. FINISH *

This card tells the program that there are no more cases to be processed.

Much time can be saved and many errors can be avoided if the input is written on FORTRAN coding sheets. If this advice is followed, the FORTRAN coding sheets can be directly keypunched by a keypunch operator since the information is now in a 1 to 1 ratio with the cards to be punched. On the following pages is a sample input for this program in the forms ready to be keypunched (see Figures 5-23 and 5-24).

5.3.3.2.2.4 Tape Requirements

This program requires four tapes, 2 scratch, one input, and one output. The two scratch tapes can be and should be utility tapes and are addressed indirectly. The scratch will be addressed in the program as either NTAPE2 or NTAPE3.

In addition, the program will expect on NTAPE1, a LASS-1 binary input tape. The LASS-1 tape will contain a time history of force-moment-height profile of the vehicle. As mentioned before, the reference height (0.0) of the card input of SWOP must agree with the reference height of the LASS-1 input.

Whenever the program is run, it will always write a summarized time history of stress on NTAPE4.

FORTRAN CODING FORM

PAY No 0007
CHARGE No 007-007
Program SWOP
Programmer C. BROWN
Date
Punching Instructions
Graphic
Punch
Card Form #
Page of
Identification

C FOR COMMENT

STATEMENT NUMBER	CONTINUATION	FORTRAN STATEMENT
TIMES		64.0, 74.0, 2, 12, 4, 0, 64.0, 74.0, *
FUEL		1, 8358.0, .029225, 36.0, *
FUEL		2, 19843.3, .041088, 36.0, *
TANK		1, 1111.0, 140.007, 237.0001, 140.007, 178.0
		198., 198., 140.007, 198.0, 140.007, 0.0, 0.0
		224.99, 10.0, *
TANK		2, 1121.0, 140.007, 48.9, 140.007, 198.0
		198.0, 198.0, 140.007, 198., 140.007, 0.0, 0.0
		7171.992, 20.0, *
TANK		3, 1111.0, 140.007, 0.0, 140.007, 198.0
		198., 198., 140.007, 198., 140.007, 0.0, 0.0
		1707.98, 6.0, *
TANK		4, 8121.0, 140.007, 398.996, 140.007, 198.0, 198.0, 198.0
		140.007, 198.0, 140.007, 0.0, 198.0, 184.00, 4.5, *
TANK		5, 1111., 130.0, 41.0, 130.0, 130.0, 130.0, 130.0, 130.0, 130.0, 130.0
		0.0, 0.0, 2619., 1.0, *
TANK		6, 2120.0, 130.0, 177.0, 130.0, 130.0, 130.0, 130.0, 130.0, 130.0
		130.0, 130.0, 0.0, 130.0, 2790.0, 0.0, *
OPTION		MEMBRN, *
RUN NO		1, *

ASD 656

Figure 5-23. FORTRAN Coding Form (First Sheet)

FORTRAN CODING FORM

		Punching Instructions	Page of
Program		Graphic	Card Form #	Identification
Programmer	Date	Punch		73 80

C FOR COMMENT

STATEMENT NUMBER 1 5	Cont 6	FORTRAN STATEMENT 7 10 15 20 25 30 35 40 45 50 55 60 65 70 72
STAGE		0.0 198.0 0 1
		365.0 198.0 23 1
		602.0 198.0 13 1
		912.0 198.0 23 1
		1401.0 198.0 13 1
		1848.0 198.0 34 1
		2387.0 198.0 13 1
		2519.0 198.0 2 1
		2746.0 130.0 2 1
		2749.0 130.0 23 1
		2790.0 130.0 33 1
		3097.0 130.0 13 1
		3255.0 130.0 2 1 *
ENDCSE		*
OPTION		MEMBRN HYDRO .03611 1.0 *
FINISH		*
$IBSYS		

ASD 656

Figure 5-24. FORTRAN Coding Form (Second Sheet)

The block data subroutine assigns numerical values to NTAPE1 through NTAPE12 (there is room for assignment of LGU numbers to 12 tapes, allowing for future expansion). These numerical values are the FORTRAN logical unit addresses of these tapes. NTAPE5 is to be assigned the system input tape LGU, and NTAPE6 is to be the output tape.

5.3.3.2.2.5 Routines Used in STRESS

a. Control Sections

1. STRESS - Controls starting, processing of input, and general logic flow of the program.
2. SFORCE- Control routine for membrane calculations.

b. Calculation Routines

1. ANGLE - Finds cone angles in radians.
2. DISTB - Performs membrane calculations at desired intervals on the skin of the vehicle. This routine also does hydrostatic test check when desired.
3. HYDRO - Finds hydrostatic test conditions.
4. HEADS - Performs membrane calculations at desired intervals on all desired heads.
5. LEVELS - Finds liquid levels and cone angles at liquid levels for all desired tanks.
6. NSERCH - Performs a binary search of LASS-1 input for desired values.
7. ROOT - Finds roots of first- to fourth-degree equations.
8. TERMN - Error exit routine.
9. TLOC - Determines specific information about area to be analyzed.
10. UNPAC - Deciphers control words.
11. UPDATE - Writes and edits a summary tape.
12. VOLUME- Finds partial and total volumes of vehicle tanks.
13. GLINT - Generalized linear interpolater.

c. Output Routines

1. ATITLE - Prints basic case information.

2. BTITLE - Prints specific case information.
3. PRINT - Prints specific structural information.

d. Input Routines

1. PROCES- Reads header cards.

5.3.3.2.2.6 Program Description

The STRESS program has been written completely in FORTRAN IV and is compatible with the IBM 7090, IBM 7040, and the GE 600 series computers. The program uses an in-house input routine (READHP) which is written in both 7044 and 7094 MAP. This special input routine will have to be re-written for GE 600.

The program was written in a highly modular fashion in order to ease debugging problems and costs, simplify the modification of the program, and to simplify the understanding of the program. A large common package is used for the communication link between the programs subroutines. Figure 5-25 describes the basic programs organization.

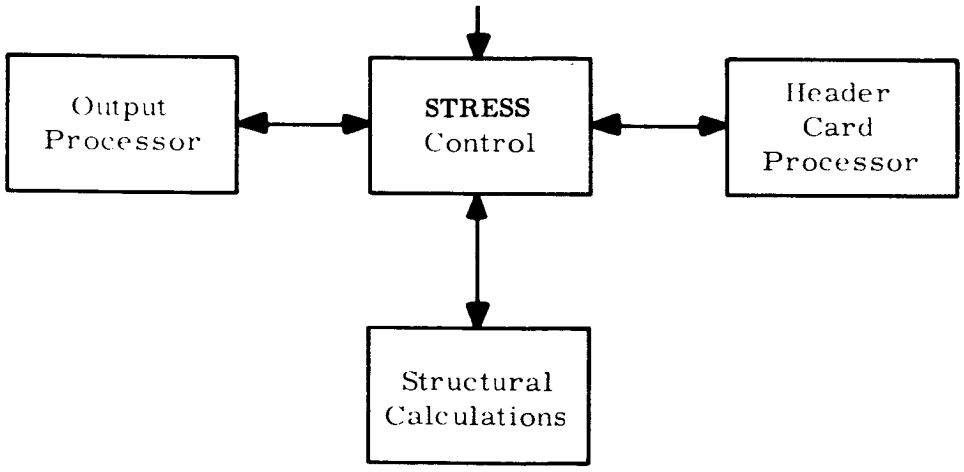

Figure 5-25. Simplified STRESS Flow Chart

The program is completely in single precision and the English unit system is used throughout the program.

5.3.3.3 Monocoque Subprogram

When the monocoque program is specified to be run by the control program, the following card is used to input the specifics of the construction:

MONOPT	SHEETL	NSMH	NBUCK	*

where:

"MONOPT" = the required identification word for this subprogram input. This must be in columns 1 through 6.

SHEET L = floating point - maximum sheet length to use in designing cylindrical sections.

NSMH = integer - number of sheets in which to divide heads.

NBUCK = integer - buckling, analysis signal:

0 => perform membrane solution only (ignore buckling).

1 => perform buckling analysis only, and design to governing condition.

Figure 5-26 is a sample printout of the monocoque subprogram output.

5.3.3.4 Honeycomb Sandwich Subprogram

5.3.3.4.1 Honeycomb Sandwich Cylinders

The function of the honeycomb subroutine is to design an optimum cylindrical structure with strength and buckling as the governing criteria. The program will determine the required face and core thicknesses and the core shear modulus.

The various K-sections (tanks and interstages) are divided into equal lengths, dependent upon the maximum sheet length that is commercially available. The option to specify this length is available in the form of an input. Each of these lengths are designed for the critical loading condition (buckling or strength) that exists during any time of the flight. Various limitations have been built into the program such as minimum allowable face thickness, maximum and minimum allowable core thickness, maximum and minimum available values of core shear moduli, and maximum allowable core cell diameter. The resulting design will consist of stepped face thicknesses, constant core thickness, and variable shear core modulus (see Figure 5-27). The weight of the optimized structure is then calculated.

MONOCOQUE SUBPROGRAM SHEET DIVISIONS FOR DISC # TYPE 3, THE DISC # IS

SHEET NO.	STATION LOCATION BEG	END	WEIGHT BEG	END	RADIUS BEG	END	MAX COMP. NX	HOOP LOADING NY	MAX (NX2-NXNY+NY2)**.5	MAX (NX+NY)
			IN		IN		LB/IN	LB/IN	LB/IN	LB/IN
1	1	41	1949.2	1988.0	138.2	0.2	-3018.38	-2431.27	2771.86	-2288.66

MONOCOQUE SHELL CONSTRUCTION ANALYSIS FOR MATERIAL AL 7075-T6

SHEET NUMBER	YIELD STRENGTH	DESIGNED SKIN THICKNESSES IN INCHES ULT. STRENGTH	BUCKLING	FINAL (MAXIMUM)	SHEET WEIGHT LBS.
1	0.4331225535E-01	0.5037938923E-01	0.7427353111E 00	0.7427353111E 00	0.1574468638E 05

TOTAL WEIGHT OF THIS SECTION IS 0.1574468638E 05

MONOCOQUE SHELL CONSTRUCTION ANALYSIS FOR MATERIAL AL 2024-T4

SHEET NUMBER	YIELD STRENGTH	DESIGNED SKIN THICKNESSES IN INCHES ULT. STRENGTH	BUCKLING	FINAL (MAXIMUM)	SHEET WEIGHT LBS.
1	0.4630457898E-01	0.6153698285E-01	0.7357611215E 00	0.7357611215E 00	0.1544489938E 05

TOTAL WEIGHT OF THIS SECTION IS 0.1544489938E 05

Figure 5-26. Sample Monocoque Subprogram Printout

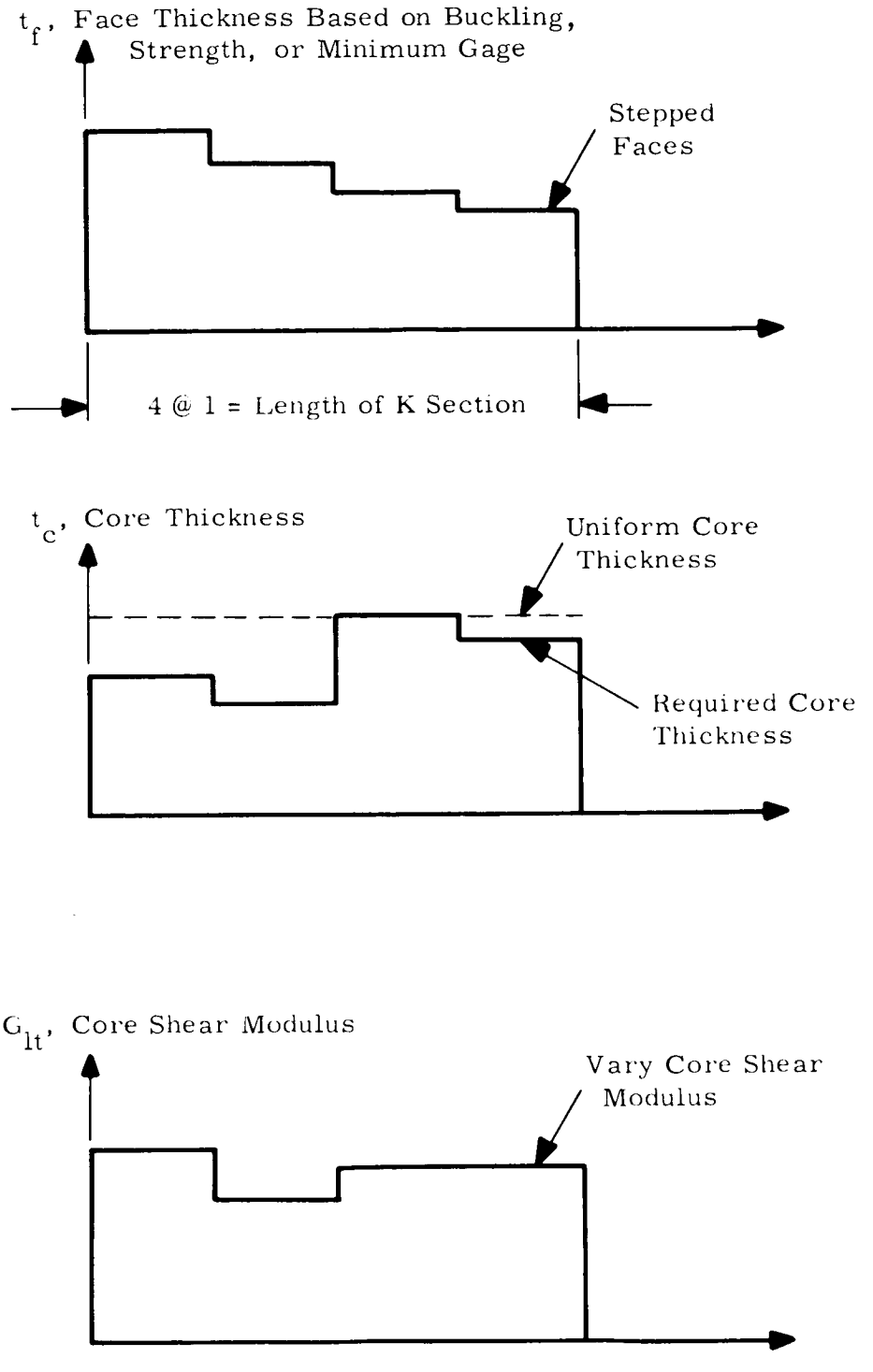

Figure 5-27. Face and Core Parameters

The following is an outline of the honeycomb subroutine:

a. Divide each K-section into equal lengths as follows:
   1. Let L equal the length of the K-section (defined as a single tank or interstage).
   2. Let L_{input} equal the input of maximum allowable sheet length.
   3. Divide L/L_{input} and round off to the next highest whole number, n, e.g., if $L/L_{input} = 5.25$, use $n = 6$.
   4. Equal lengths, $l = L/n$.

b. From the SWOP program, determine the maximum strength loading condition and maximum compressive buckling load for each of the l-sections.

c. Based on the maximum compressive load for each l-section, design the shell for buckling.
   1. Multiply the compressive load by the ultimate safety factor.
   2. Determine the maximum core shear modulus based on yield stress from one of the following limitations:
      (a) Face wrinkling.
      (b) Shear instability.
      (c) Minimum value that is commercially available.
   3. Determine the core thickness required based on the above determined core shear modulus and yield stress.
   4. Calculate correction factor, K_1, and determine optimum face working stress.
   5. Check to insure that the optimum face working stress satisfies both the ultimate and limit load criteria.
   6. Determine required core thickness based on the optimum face working stress.
   7. Determine the maximum allowable core cell diameter based on monocell buckling.
   8. Increase the initial value of core shear modulus by a finite amount and perform steps 3 through 7. Continue this until the maximum allowable value of core shear modulus is reached.

9. Eliminate any combination of core thickness and shear modulus that complies with the following:
   (a) Calculated maximum allowable cell diameter is less than the minimum available core cell diameter corresponding to the core shear modulus.
   (b) Calculate core thickness is greater than the maximum allowable.
   (c) Calculate core thickness is less than the minimum allowable.
10. Choose the combination of core shear modulus and core thickness that results in the minimum weight.

d. Based on maximum strength loading condition design the sheet for strength. Check to insure that the design satisfies both the ultimate and limit load criteria.

e. Choose the maximum required face thickness per 1-section based on one of the following:
   1. Buckling.
   2. Strength.
   3. Minimum gage.

f. If the face thickness of any 1-section is governed by strength or minimum gage, the core thickness can be reduced (due to the fact that the buckling stress level has been reduced) by using the maximum compressive load in the 1-section and the increased face thickness to calculate the reduced core that is required for stability using the previously determined optimum core shear modulus.

g. Choose the maximum required core thickness within a K-section and use a core of constant thickness.

h. If a 1-section is governed by buckling and the uniform core thickness is greater than the required core thickness, the face thickness is reduced until the core thickness required approaches the uniform core or until the face thickness approaches the thickness based on strength or minimum gage.

i. Calculate the resulting weight of the K-section.

The honeycomb subroutine is also provided with the option of specifying the core thickness. The various sections (tanks and interstages) are divided into equal lengths (as

has been previously described) and designed for the critical loading condition (buckling and strength) that exists. Even though the core thickness is specified, the program will optimize the required core shear modulus. The resulting design will consist of stepped face thicknesses, specified core thickness, and variable core shear modulus.

5.3.3.4.2 Honeycomb Ellipsoidal Heads

The function of the honeycomb ellipsoidal heads subroutine is to design an optimum ellipsoidal shell subjected to a uniform external pressure loading. The program will determine the optimum face thickness, core thickness, and core shear modulus based upon strength or buckling, whichever is the governing criteria.

The ellipsoidal head is subdivided into equal heights depending upon the number of stepped faces that are desired (see Figure 5-28). The option to specify the number of equal heights is available in form of an input. Each of the equal heights is designed for the critical loading condition that occurs during any time of flight. Various practical limitations have been built into the program such as minimum allowable face thickness, maximum and minimum allowable core thicknesses, maximum and minimum available values of core shear modulii, and maximum allowable core cell diameter. The resulting optimum design will consist of stepped face thickness, constant core thickness, and variable core shear modulus. The weight of the optimized structure is then calculated.

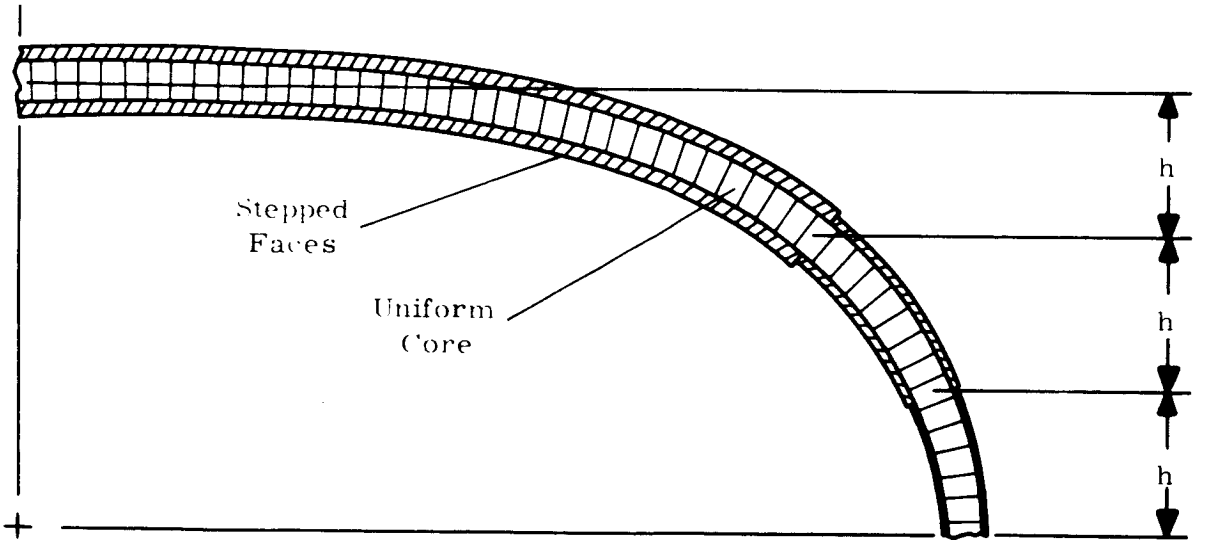

Figure 5-28. Honeycomb Ellipsoidal Head

The following is an outline of the ellipsoidal shell subroutine:

a. Divide the height of the shell up into equal heights:
   1. Let H = the height of the shell.
   2. Let m = the input number of stepped faces desired.
   3. Equal heights, h = H/m.
b. From the SWOP program, determine the maximum strength and minimum meridional compressive load for each equal height.
c. Based on the maximum compressive load for each h-section, design the shell for buckling.
d. Based on maximum strength loading condition, design each h-section for strength. Check to insure that the design satisfies both the ultimate and limit load criteria.
e. Choose the maximum required face thickness per h-section based on the maximum of the following:
   1. Buckling.
   2. Strength.
   3. Minimum gage.
f. If the face thickness in any given h-section is governed by strength or minimum gage, the core thickness can be reduced since the buckling stress level has been decreased. Using the maximum compressive load in the h-section and the increased face thickness, calculate the core thickness required for stability using the previously determined optimum core shear modulus.
g. Choose the maximum required core thickness with each equal height section and use a core of constant thickness.
h. If an equal height section is governed by buckling and the uniform core thickness is greater than the required core thickness, the face thickness is reduced until the core thickness required approaches the uniform core or until the face thickness approaches the thickness based on strength or minimum gage.
i. Calculate the resulting weight of the ellipsoidal head.

The honeycomb ellipsoidal heads subroutine is also provided with the option of specifying the core thickness. The various equal heights are designed for the critical loading condition (buckling or strength) that exists. Even though the core thickness is specified,

the subroutine will choose the optimum core shear modulus. The resulting design will consist of stepped face thicknesses, specified uniform core thickness, and a variable core shear modulus.

5.3.3.4.3 Input Description

The input format for the honeycomb sandwich suboptimization subprogram of SWOP follows exactly the general format for SWOP input (see description of general SWOP input).

Data is entered in columns 7 through 72 of each data card, with each data entry separated by at least one blank. The identification word HONOPT must be entered in columns 1 through 6 of the first card. The data may be entered on as many cards as needed, but an asterisk must follow the last entry to terminate the reading in of data for the honeycomb subprogram.

The honeycomb input may be placed anywhere in the input deck and is processed by the CASEIN routine. For example:

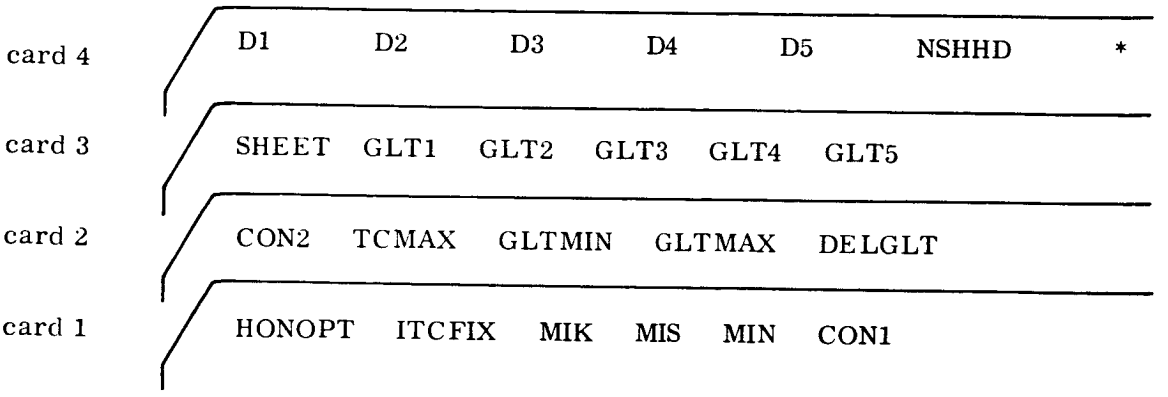

The numbers ITCFIX, MIK, MIS, MIN, and NSHHD are integers, the rest are floating point. The word HONOPT is the required name in columns 1 through 6, the other entries must have numbers inserted as follows:

MIS = Maximum number of iterations allowed for T_{core} iteration procedure in subroutine STEPTO.

MIN = Maximum number of iterations allowed for σ_{opt} iterations in subroutine STPSIX.

ITCFIX = A signal to distinguish an option built into the program:

0 => find optimum core thicknesses.

1 => design optimum under constraint of a fixed input core thickness input in space for TCMAX.

MIK = Maximum number of iterations allowed for K_1 optimization procedure in subroutine TONINE.

CON1 = C_1, the specific shear modulus of the core material (psi/lbs/ft^3).

CON2 = C_2, the specific modulus of elasticity of the core material (psi/lbs/ft^3).

TCMAX = T_{cmax}, the maximum core thickness allowed (inches).

NOTE

TCMAX is to the input giving the required core thickness when the ITCFIX = 1 option is later added!

GLTMIN = G_{ltmin}, the core shear modulus at which to begin investigation (psi).

GLTMAX = G_{ltmax}, the core shear modulus at which to terminate investigation (psi).

DELGT = ΔG_{lt}, the interval at which to investigate core shear moduli (psi).

(Example: G_{ltmin} = 15000, G_{ltmax} = 75000, G_{lt} = 20000, means investigate 15000 to 75000 in steps of 20000).

SHEET = The maximum sheet length allowed (used in stepping both honeycomb and monocoque constructions).

FLT1, FLT2, FLT3, GLT4, GLT5 are values of core shear modulus at which there is a change in minimum available core cell diameter; these must have 5 values, the 5th value slightly greater than GLTMAX. D1, D2, D3, D4, D5 are minimum available core cell diameters corresponding to GLT1, GLT2, etc. The input value covers the range of GLT that is less than the corresponding values of GLT1, GLT2, etc.

NSHHD is the number of sheets in which to divide the heads construction of honeycomb sandwich.

NOTE

For the maximum number of iterations, use the following:

MIK = 10
MIS = 50
MIN = 10

The heads iterative procedures use the same values of MIK, MIS, and MIN as the analogous cylinder procedure.

An explanation of the input relation between allowable core cell diameters and core shear moduli is as follows. When selecting the optimum core shear modulus, the cell diameter must not be greater than the maximum allowable required to preclude monocell buckling. If this value equals 1.0, it means that we have no axial compressive load on this section. For example, Figure 5-29 shows the availability of core shear modulus versus core cell diameter for an aluminum hexagonal core.

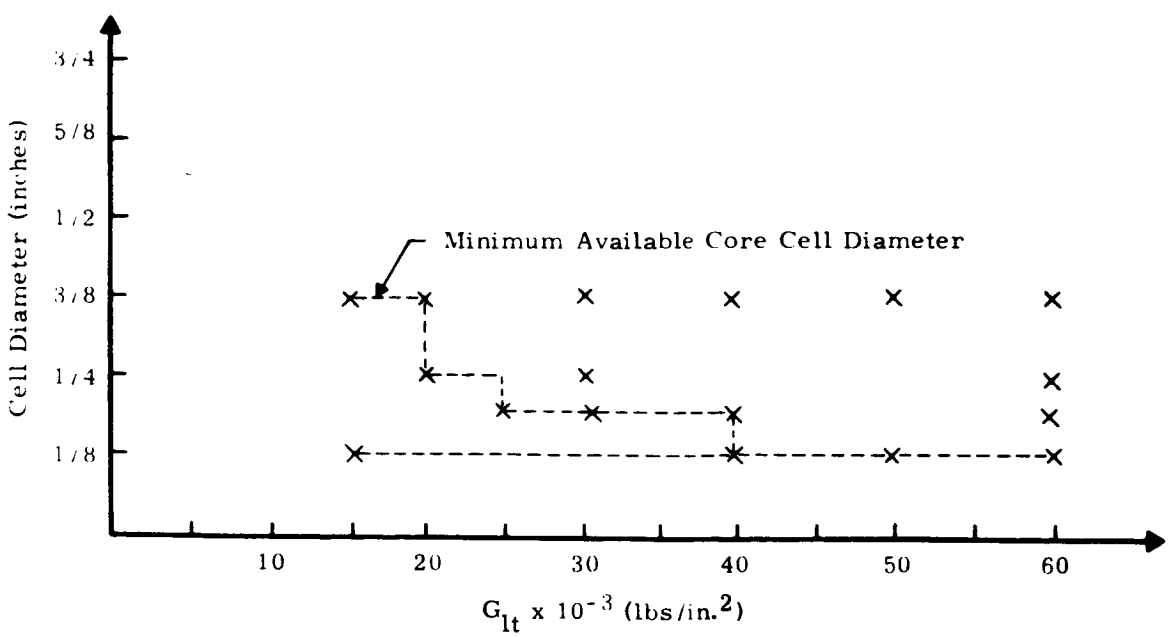

Figure 5-29. Availability of Core Shear Modulus versus Core Cell Diameter for an Aluminum Hexagonal Core

The input in this case would appear as follows:

card 6	.375	.25	.1875	.125	.125	NSHHD
card 5	20,000	25,000	40,000	60,000	60,000	

5.3.3.4.4 Output Description

The output (see Figure 5-30) is provided for each section (tank or interstage) under the following headings:

a. Sheet number - designated number for equal length sheets within a section. The numbers begin at the aft end of the section.
b. Strength face thickness - required face thicknesses based on the strength criteria (inches).
c. Buckling thicknesses - required core and face thicknesses based on the buckling criteria (inches).
d. Non-uniform thicknesses - required core thickness based on buckling and the maximum face thickness based on buckling, strength, or minimum gage (inches).
e. Final face thickness and uniform core - uniform core thickness based on the required maximum within the K-section and the final face thicknesses based on the uniform core (inches).
f. Core shear modulus - optimum core shear modulus to be used (psi).
g. Weights using non-uniform core - weight of the face plus the core based on the non-uniform thicknesses (pounds).
h. Weights using uniform core - weight of the face plus the core based on the uniform thicknesses (pounds).

5.3.3.5 45° Waffle Stiffened Subprogram

5.3.3.5.1 General

The function of the waffle stiffened subprogram is to design an optimum cylindrical or conical structure with strength and buckling as the governing criteria. Conical sections are analyzed by treating them as a cylinder of equivalent length and radius. The program will determine the following optimum design parameters: skin thickness, rib thickness, rib spacing, and the overall depth.

HONEYCOMB SUBPROGRAM SHEET DIVISIONS FOR DISC 3 TYPE 1, THE DISC 3 CYL

SHEET NO.	STATION LOCATION BEG	END	HEIGHT BEG	END	RADIUS BEG	END	MAX COMP. NX	HOOP LOADING NY	MAX (NX2-NXNY+NY2)**.5	MAX (NX+NY)
			IN		IN		LB/IN	LB/IN	LB/IN	LB/IN
1	1	26	602.0	702.0	198.0	198.0	-7223.73	0.00	7223.73	-0.00
2	26	51	702.0	802.0	198.0	198.0	-7447.44	0.00	7447.44	-0.00
3	51	79	802.0	912.0	198.0	198.0	-7598.61	0.00	7598.61	-0.00

HONEYCOMB STRUCTURAL ANALYSIS FOR MATERIAL AL 7075-T6

SHEET NO.	STRENGTH FACE THICK	BUCKLING THICKNESS FACE	CORE	NON-UNIFORM THICKNESS FACE	CORE	THICKNESS FINAL FACE	UNIF. CORE	CORE SHEAR MOD.	MAX ALLOWABLE CORE CELL DIAM
	INCH	INCH		INCH		INCH		PSI	INCH
1	0.0657	0.0699	5.6040	0.0699	5.6040	0.0693	5.8623	15000.00	1.2901
2	0.0677	0.0718	5.7578	0.0718	5.7578	0.0715	5.8623	15000.00	1.3326
3	0.0691	0.0731	5.8623	0.0731	5.8623	0.0731	5.8623	15000.00	1.3678

****WEIGHTS USING NON-UNIFORM CORE THICKNESS****

****THE WEIGHT OF SHEET 1IS 0.27320338E 04LBS.****
****THE WEIGHT OF SHEET 2IS 0.28058536E 04LBS.****
****THE WEIGHT OF SHEET 3IS 0.31412384E 04LBS.****

****THE WEIGHT OF THE ABOVE SECTION IS 0.86791257E 04LBS.****

****WEIGHTS USING UNIFORM CORE THICKNESS****

****THE WEIGHT OF SHEET 1IS 0.27379248E 04LBS.****
****THE WEIGHT OF SHEET 2IS 0.28064429E 04LBS.****
****THE WEIGHT OF SHEET 3IS 0.31412384E 04LBS.****

****THE WEIGHT OF THE ABOVE SECTION IS 0.86856061E 04LBS.****

Figure 5-30. Sample Honeycomb Sandwich Subprogram Printout

Based upon the maximum sheet lengths that are commercially available, the various K-sections (tank and interstages) are divided into equal lengths. The option to specify this length is available in the form of an input. Each of these lengths is designed for the critical loading condition (buckling or strength) that exists during any time of the flight. The optimum design parameters are restricted to the following manufacturing limitations: minimum rib spacing, minimum rib and skin thicknesses, and maximum and minimum overall depth.

The following is an outline of the waffle subprogram:

a. Divide each K-section into equal lengths as follows:
   1. Let L equal the length of the K-section (defined as a single tank or interstage).
   2. Let L_{input} equal the input of maximum allowable sheet length.
   3. Divide L/L_{input} and round off to the next highest whole number, n, e.g., if L/L_{input} equals 5.25, use n equals 6.

b. From the SWOP program, determine the following loading conditions that exist for each 1-section:
   1. Maximum strength loading.
   2. Maximum compressive loading.
   3. Maximum algebraic sum of the compressive loading and the corresponding hoop loading.

c. Design an optimum structure based on buckling or strength:
   1. Optimum proportions, as a function of overall depth, are determined based on the compressive loading.
   2. If there is no compressive loading a small value (unity) is assigned to determine the optimum proportions.
   3. Maintaining the optimum proportions, the strength condition is investigated (ultimate and limit criteria).
   4. If strength governs, the parameters are increased proportionally to develop the necessary strength.
   5. The various manufacturing limitations are checked. If any of the design parameters are increased due to violation of minimum gage, the other parameters are adjusted such that the same load carrying capacity exists (buckling or strength depending on the governing condition).

d. Calculate the weight of the resulting K-section.

The 45° waffle subprogram is also provided with the option to specify the overall waffle depth or the rib spacing. Given one of these options, the other three design parameters are chosen such that an optimum design results. Basically, the same procedure is used as has been previously described with the exception that the optimization is performed with three parameters rather than four.

5.3.3.5.2 Waffle Stiffened Ellipsoidal Shells

The function of the waffle stiffened heads subprogram is to design an optimum shell subjected to external collapsing pressure. Only shells with meridional compressive loading are considered. If there is no compressive loading, the shell is strength governed and there is no need for a shell of waffle stiffened construction since a monocoque based on strength would require the same amount of material. Therefore, if there is no compressive loading, the program will automatically design a monocoque shell. Since this subroutine does not have a stepped construction ability, the strength governed cases will result with a uniformly thick monocoque shell. If it is desired to step the uniform thickness, it is simply a matter of using the monocoque subroutine which has the capability of stepping the faces.

For buckling governed cases, the following optimum design parameters are determined: overall waffle depth, skin thickness, rib thickness, and rib spacing. These design parameters are restricted to minimum thickness requirements for the skin and ribs. If the optimum design violates the minimum gage, the thicknesses are increased to satisfy these requirements. Due to the increase in these parameters, the remaining ones are altered such that the same load carrying capacity exists. This would result in a so-called off optimum design due to the manufacturing limitations.

The following is an outline of the ellipsoidal shell subroutine:

a. From the SWOP program, determine the following loading conditions:
   1. Maximum compressive meridional loading.
   2. Maximum von Mises loading.
b. Design an optimum structure based on buckling. If there is no compressive loading, a monocoque shell is designed based on strength.
c. Investigate minimum gage requirements. If any of the design parameters are increased to satisfy minimum gage, the other parameters are altered such that the same load carrying capacity exists.

d. Check strength based maximum von Mises loading:
   1. If strength is violated, increase the skin thickness.
   2. The other design parameters are not altered.

e. Calculate the weight of the resulting design.

A description of the input-output is as follows:

W45OPT	C4	C5	HMAX	HMIN	TSHEET	VIP4

where:

C4 - ratio of fillet radius to overall depth.

C5 - ratio of cutting head radius to overall depth.

HMAX - maximum allowable depth.

HMIN - minimum allowable depth.

TSHEET - manufacturer's sheet length.

VIP4 - indicator for options:

1. VIP4 = .1 for H-option, the input value of H will be read in location of HMAX.
2. VIP4 > .1 for rib spacing option, input the actual value of rib spacing in VIP4 location.

All header cards for this program are read by READHP which permits the user to enter data between columns 7 through 72 of each data card. Each data entry must be separated by at least one blank. Data may be entered on more than one card and each read is terminated by an asterisk in the data field.

In addition to above requirements, an identification word must be entered in column 1 on the first card to be read by each individual read. Each read is identified by checking the identification word in control.

Subroutine WHAT prints waffle structural analysis information as follows:

a.	Sheet number	N
b.	Weight of each sheet	W
c.	Skin thickness	TS
d.	Web thickness	TWS
e.	Rib spacing	BS

f.	Overall depth	H
g.	Fillet radius	RWS
h.	Cutting head radius	RN

Data needed for STRESS program to run the waffle subprogram is as follows:

a.	Compressive N_x	UPD(400, 7)
b.	$\sqrt{N_x^2 - N_x N_y + N_y^2}$	UPD(400, 5)
c.	Length of section	UPD(400, 1)
d.	Radius	UPD(400, 4)
e.	Algebraic quantity $N_x + N_y$	UPD(400, 13)
f.	$-N_x + N_y$	-UPD(400, 11) + UPD(400, 12)

Figure 5-31 shows a sample printout from the 45° waffle stiffened subprogram.

The nomenclature required from the executive control program for the 45° waffle subprogram is as follows:

Name	Definition	ECP Name
MUE	Poisson's ratio	PROP (ITMAT, 2)
E	Modulus of elasticity (psi)	TPROP(II, 1, KK)
DEN	Material density (lbs/ft^3)	PROP(ITMAT, 1)
SIGY	σ_{yield} of material (psi)	TPROP (II, 2, KK)
SIGULT	$\sigma_{ultimate}$ of material (psi)	TROP (II, 3, KK)
SFULT	Safety factor, ultimate	CN(8)
SFYLD	Safety factor, yield	CN(T)
SHEET	Manufacturer's sheet length	SHEET
TMIN	Minimum gage thickness (inches)	PROP (ITMAT, 6)
TRIB	Minimum rib thickness (inches)	PROP (ITMAT, 5)
FABX(3)	Fabrication factor	FABX(3)

5.3.3.5.3 Waffle Stiffened Heads

Subroutine WHEAD has been designed to analyze waffle stiffened heads. It is called into use by subroutines W45MAS and W90MAS when needed. There is no direct input to this routine; the necessary information is shared with other routines.

45DEG WAFFLE SUBPROGRAM SHEET DIVISIONS FOR DISC 3 TYPE 1, THE DISC 3 CYL

SHEET NO.	STATION LOCATION REG	END	WEIGHT REG	END	RADIUS REG	END	MAX COMP. NX	HOOP LOADING NY	MAX (NX2-NXNY+NY2)**.5	MAX (NX+NY)
			IN		IN		LB/IN	LB/IN	LB/IN	LB/IN
1	1	79	602.0	912.0	138.0	198.0	-7598.61	0.00	7598.61	-7598.61

WAFFLE STRUCTURAL ANALYSIS

SHEET NO.	WEIGHT	THICKNESS SKIN	RIB	RIB SPACING	OVERALL DEPTH	FILLET	CUTTING
	LBS	IN	IN	IN	IN	IN	IN
1	32756.09	0.5306	0.5633	18.5719	2.6531	0.6633	0.4633

THE TOTAL WEIGHT, OF THIS SECTION IS 32756.09 LBS.

Figure 5-31. Sample 45° Waffle Stiffened Subprogram Printout

The analysis includes the calculation and testing of design parameters until an optimum set has been reached. Once minimum gage requirements and strength requirements are satisfied, the weight is calculated and output with the optimum design parameters, as follows:

a. Skin thickness (inches).
b. Rib thickness (inches).
c. Rib spacing (inches).
d. Rib depth (inches).
e. Fillet radius between ribs (inches).
f. Fillet radius between skin and ribs (inches).
g. Height of head (inches).
h. Semi-axes (a &b) (inches).
i. Total weight (lbs).

5.3.3.6 90° Waffle Stiffened Subprogram

5.3.3.6.1 General

The description of the 90° waffle stiffened subprogram is identifical to that of the 45° waffle stiffened subprogram (see paragraph 5.3.3.5).

5.3.3.6.2 Input

W900PT SEA4 SEA5 HMAX9 AMIN9 SHEET VIP

where:

SEA4 - ratio of fillet radius to overall depth.
SEA5 - ratio of cutting head radius to overall depth.
HMAX9 - maximum allowable depth.
HMIN9 - minimum allowable depth.
SHEET - manufacturer's sheet length.
VIP - indicator for options:

1. VIP = .1 for H option, the input value of H will be read in location of HMAX.
2. VIP > .1 for rib spacing option, input the actual value of rib spacing in VIP location.

5.3.3.6.3 Output

Subroutine WHAT prints waffle structural analysis information as follows:

a.	Sheet number	N
b.	Weight of each sheet	W
c.	Skin thickness	TS
d.	Web thickness	TWS
e.	Rib spacing	BS
f.	Overall depth	H
g.	Fillet radius	RWS
h.	Cutting head radius	RN

Data needed from STRESS program to run waffle routine is as follows:

a.	Compressive N_x	UPD(400, 7)
b.	$\sqrt{N_x^2 - N_x N_y + N_y^2}$	UPD(400, 5)
c.	Length of section	UPD(400, 1)
d.	Radius	UPD(400, 4)
e.	Algebraic quantity $N_x + N_y$	UPD(400, 13)
f.	$-N_x + N_y$	-UPD(400, 11) + UPD(400, 12)

For a sample 90° waffle stiffened output, see Figure 5-32.

5.3.3.6.4 Nomenclature

The nomenclature needed from the executive control program for the 90° waffle program is as follows:

Name	Description	ECP Name
MUE	Poisson's ratio	PROP (ITMAT, 2)
E	Modulus of elasticity (psi)	TPROP (II, 1, KK)
DEN	Material density (lbs/ft^3)	PROP (ITMAT, 1)
SY	σ_{yield} of material (psi)	TPROP (II, 2, KK)
SU	$\sigma_{ultimate}$ of material (psi)	TPROP (II, 3, KK)
CN(8)	Safety factor, ultimate	CN(9)
CN(7)	Safety factor, yield	CN(7)

****
90DEG WAFFLE SUBPROGRAM SHEET DIVISIONS
* FOR DISC 3 TYPE 1, THE DISC 3 CYL *
****

SHEET NO,	STATION LOCATION BEG	END	HEIGHT BEG	END	RADIUS BEG	END	MAX COMP. NX	HOOP LOADING NY	MAX (NX2-NXNY+NY2)**.5	MAX (NX+NY)
			IN		IN		LB/IN	LB/IN	LB/IN	LB/IN
1	1	79	602.0	912.0	198.0	198.0	-9587.63	-0.00	9587.63	-9587.63

****
90 DEGREE WAFFLE STRUCTURAL ANALYSIS
* FOR MATERIAL AL 2014-T6 *
****

SHEET NO.	WEIGHT	THICKNESS SKIN	RIB	RIB SPACING	OVERALL DEPTH	HEAD RADIUS FILLET	CUTTING
	LBS	IN	IN	IN	IN	IN	IN
1	33946.84	0.3459	0.5064	11.5290	3.8430	0.9607	0.9607

THE TOTAL WEIGHT OF THIS SECTION IS 33946.84 LBS.

Figure 5-32. Sample 90° Waffle Stiffened Subprogram Printout

Name	Description	ECP Name
SHEET	Manufacturer's sheet length	SHEET
TMIN	Minimum gage thickness (inches)	PROP (ITMAT, 6)
TRIB	Minimum rib thickness (inches)	PROP (ITMAT, 5)
FABX(4)	Fabrication factor	FABX(3)

5.3.3.7 No-Face 60-Degree Corrugation Subprogram

5.3.3.7.1 General

For the general optimization procedure, the design parameters are calculated first for zero number of rings. The parameters for zero rings are retained and used as a base for future calculations. Each time the weight is found for a particular number of rings it is compared to the previous calculation consisting of one less ring. This is continued until an optimum number of rings has been found.

The program is provided with an input value which represents the maximum sheet shock length that is available. The maximum loading is chosen for each of these equal length sheets and designed independently of the others. Each separately designed equal length sheet, when combined together, will form the cylinder length as shown in Figure 5-33.

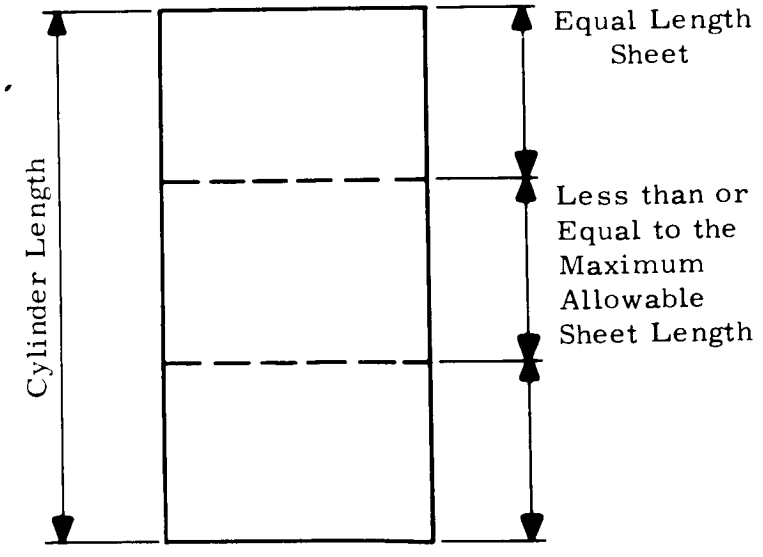

Figure 5-33. Input Parameters

However, it has been learned after many trial cases that specifying the maximum sheet length interferes with the optimization of the number of rings. Consequently, it is advised to input a value of the maximum allowable sheet length that is much larger than the cylinder length. In this manner, a constant corrugation design will result for the entire cylinder length plus the optimum number of rings will not be interfered with. It should be pointed out that regardless of the number used, the program will still operate smoothly; but to insure an optimum design, a large sheet length number should be used.

Due to the fact that this type of construction is not practical for internal pressures, only axially loaded cylinders are considered. If an internal pressure loading is encountered, the program will be automatically bypassed and a zero weight will be printed out for that case.

This program is provided with the option of specifying the corrugation depth, corrugation skin thickness, and the number of rings. In each case, only one parameter can be specified at a time.

5.3.3.7.2 Input

The following are descriptions for necessary input parameters:

INOPT	0: no option. 1: number of rings input. 2: thickness of corrugation input. 3: depth of corrugation input.
MINIMUM DEPTH	Minimum allowable depth of corrugation.
MAXIMUM DEPTH	Maximum allowable depth of corrugation.
SHEET	Sheet length to be used. For corrugated, it is found that a section of one sheet length produces a more optimum design.
IMRING	Material of the ring - an integer from 1 to 12 (1 to 9 presently) to represent the material.
COROPT	For INOPT 1, 2, 3, the value to be input is stored in COROPT, i.e., if INOPT 2, COROPT to the input thickness of corrugation

The input card format is:

CR1ϕPT	INϕPT	MIN DEPTH	MAX DEPTH	SHEET	IMRING	CORϕPT	*
CR1ϕPT	2	.5	10.	350.	6	.13768	*

(If INOPT = 2, thickness is input as .13768.)

where:

CR1OPT is the name of the card.

No commas are necessary between data items, but there must be one intervening blank.

5.3.3.7.3 Output

The following items (see Figure 5-34) are output for the analysis:

a. Number of sheets.
b. Section identification: discontinuity and type.
c. Section properties: height, radius, maximums.
d. Material of analysis.
e. Number of rings: number of rings giving the smallest sheet weight.
f. Total ring weight: the weight of all rings on this sheet.
g. Total weight: the weight of shell and rings.
h. Thickness: thickness of corrugation.
i. Pitch: length of one corrugation.
j. Depth: perpendicular depth of corrugation.
k. Weight of ring between sheets n and n + 1.
l. Total weight of section.

5.3.3.8 Single-Face Corrugation Subprogram

5.3.3.8.1 General

Given a section divided into equal length sheets, this subroutine will calculate the strength/weight ratios as function of C_1, C_2, and C_3 (predefined parameters, examples of which are shown below) and store the ratios in descending order. Choosing the largest S/W ratio, the corresponding C_1, C_2, and C_3 will be assumed optimum for testing purposes. If local buckling, panel buckling, or maximum corrugation height is violated, the next largest value of S/W ratio is chosen and testing is repeated until no test is violated.

OPEN FAC COR SUBPROGRAM SHEET DIVISIONS FOR DISC 3 TYPE 1, THE DISC 3 CYL

SHEET NO.	STATION LOCATION BEG	END	HEIGHT BEG	END	RADIUS BEG	END	MAX COMP. NX	HOOP LOADING NY	MAX (NX2-NXNY+NY2)**.5	MAX (NX+NY)
			IN		IN		LB/IN	LB/IN	LB/IN	LB/IN
1	1	79	602.0	912.0	198.0	198.0	-7598.61	0.00	7598.61	-7598.61

OPEN FACE CORRUGATION STRUCTURAL ANALYSIS FOR MATERIAL AL 7075-T6

SHEET NUMBER	NUMBER OF RINGS	TOTAL RING WEIGHT(LBS)	TOTAL WEIGHT LBS	THICKNESS INCHES	PITCH INCHES	DEPTH INCHES
1	3	1051.0215	9924.3168	0.1390	10.7722	3.1097

******** THE TOTAL WEIGHT OF THIS SECTION IS 9924.3168 ********

OPEN FACE CORRUGATION STRUCTURAL ANALYSIS FOR MATERIAL AL 2024-T4

SHEET NUMBER	NUMBER OF RINGS	TOTAL RING WEIGHT(LBS)	TOTAL WEIGHT LBS	THICKNESS INCHES	PITCH INCHES	DEPTH INCHES
1	3	1060.9840	9771.3221	0.1377	10.7215	3.0953

******** THE TOTAL WEIGHT OF THIS SECTION IS 9771.3221 ********

Figure 5-34. Sample Output for No-Face 60-Degree Corrugation

C_1	20	25	30	35	40
C_2	20	25	30	35	40
C_3	500	1200	1900	2600	3300

The strength is then checked and new design parameters calculated. If strength governs, a new corrugation thickness will be calculated and new design parameters are selected to satisfy strength requirements before further testing. In either case, i.e., strength governing or buckling governing, minimum gage is checked and, if satisfied, weight is then calculated and output immediately with the corresponding geometry information. If minimum gage is violated, it must be satisfied and ring spacing increased prior to calculation of weight and output.

5.3.3.8.2 Input

The following are descriptions for necessary input parameters:

L_{INPUT} Maximum sheet length commercially available (inches).

dc_{max} Maximum allowable corrugation depth (inches).

dc_{min} Minimum allowable corrugation depth (inches).

ψ_S Index which indicates location of the stringer:

= +1, stringer is on the outside.

= 0, indicates symmetry.

= -1, stringer is on the inside.

ψ_R Index which indicates location of ring:

= +1, ring is on the outside.

= 0, indicates symmetry.

= -1, ring is on the inside.

The following options are available:

Option Control	Corresponding
0	No entry
1	Overall corrugation depth (inches) (d_c)
2	Specify ring spacing (inches)
3	Specify ring depth (inches)(d_r)

The input card format is:

CR2OPT	L_{INPUT}	$d_{c_{max}}$	$d_{c_{min}}$	S	R	OPTION	VALUE	*

where columns 1 through 6 are CR2OPT and columns 7 through 72 are input values. There must be at least one space between values, and the last value must be followed by an asterisk.

5.3.3.8.3 Output

The following is output for each sheet:

a. Corrugation depth, d_c (inches).
b. Corrugation skin thickness, t_s (inches).
c. Skin thickness, t_s (inches).
d. Ring spacing (inches).
e. Ring depth, d_r (inches).
f. Ring flange width (inches).
g. Weight (lbs).

For the entire section:

Total weight (lbs).

A sample printout is shown in Figure 5-35.

5.3.3.9 Integral Stringer and Ring Stiffened Subprogram

5.3.3.9.1 Input

The following input is required at run time for the integral stringer and ring stiffened construction subprogram. The input card may be placed anywhere in the input package to be handled by the CASEIN input processing routine of the executive control program. Note that the card conforms to the READH format.

INTOPT	BWMAX	BWMIN	ψ_S	ψ_R	SHEETL	*

where

INTOPT = The required name in columns 1 through 6 of the input card. This is used to identify the card in input processing.

```
**************************************************************************
* SUBPROGRAM FOR THE OPTIMIZATION OF SINGLE FACE CORRUGATION WITH RINGS *
*                DETAILS OF ANALYSIS FOR MATERIAL
```

SHEET NO.	CORRUGATION DEPTH INCH	CORRUGATION THICKNESS	SKIN THICKNESS INCH	NUMBER OF RINGS	RING SPACING INCH	RING DEPTH INCH	RING FLANGE WIDTH INCH	SHEET WEIGHT LBS
1	6.0000	0.1632	0.3265	6	69.8571	3.2649	1.6325	48623.7100

```
**** THE TOTAL WEIGHT OF THE ABOVE SECTION IS  0.48623710E 05 LBS. ****
```

Figure 5-35. Sample Output Format for Single-Face Corrugation

Data appears in columns 7 through 72 in READH format in the following sequence:

BWMAX = Maximum allowable stringer depth (inches).

BWMIN = Minimum allowable stringer depth (inches).

e_S = Eccentricity factor which indicates the location of the stringer as follows:

S = +1. => stringer is on the outside of the skin.

S = -1. => stringer is on the inside of the skin.

S = 0. => indicates stringer is symmetrically positioned.

e_R = Eccentricity factor which indicates the location of the ring:

R = +1. => ring is on the outside of the skin.

R = -1. => ring is on the inside of the skin.

R = 0. => ring is synmetrically positioned.

SHEETL = Maximum sheet length commercially available for this construction type. Ring spacing will be optimized for sections of this length. It sometimes proves advantageous to indicate sheet length greater than any section length to allow the ring spacing to be optimized for the whole structural unit, and then checking to see that no ring spacing is greater than the sheet length. This prevents a short sheet length from interfering with the ring-spacing optimization for a whole structural unit.

5.3.3.9.2 Output (Figure 5-36)

When specified at run-time, the following input is printed out for each sheet used in the construction of a structural unit:

t_s = the skin thickness.

t_w = the stringer thickness.

b_s = stringer spacing.

b_w = stringer depth (also equals ring flange width).

b_R = ring spacing.

b_r = ring depth.

t_w = ring thickness (web and flange).

W = weight of equal-length sheet.

W_t, the total weight, can be printed out with the detailed output and/or entered into the section-by-section (and/or the subtotals) matrix.

```
*******************************************
*INTEG STIFND SUBPROGRAM SHEET DIVISIONS*
* FOR DISC  3 TYPE 1, THE DISC  3  CYL  *
*******************************************
```

SHEET NO.	STATION BEG	LOCATION END	HEIGHT BEG (IN)	HEIGHT END (IN)	RADIUS BEG (IN)	RADIUS END (IN)	MAX COMP. NX LB/IN	HOOP LOADING NY LB/IN	MAX (NX2-NXNY/NY2)**.5 LB/IN	
1	1	79	602.0	912.0	198.0	198.0	-7598.61	0.00	7598.71	-0.00

```
*********************************************
*   INTEGRAL  STRINGER  AND  RING  STIFFENED  *
*STRUCTURAL ANALYSIS FOR MATERIAL AL  2014-T6 *
*********************************************
```

SHEET	WEIGHT LBS.	SKIN THICKNESS INCH	STRINGER THICKNESS INCH	STRINGER SPACING INCH	STRINGER DEPTH INCH	RING SPACING INCH	RING DEPTH INCH	RING FLANGE WIDTH INCH	RING THICKNESS INCH
1	17959.88	0.225	0.250	7.499	2.500	34.444	6.249	2.500	0.250

****THE WEIGHT OF THE ABOVE SECTION IS 0.17959877E 05LBS.****

Figure 5-36. Sample Output Format for Integral Stringer and Ring Stiffened Subprogram

5.3.3.10 Semi-Monocoque Subprogram

5.3.3.10.1 General

Each section to be analyzed is broken into equal lengths not larger than the maximum allowable sheet length, which is an input parameter. The maximum loading is chosen for each of the equal-length sheets and each sheet is designed independently; combining the sheets gives the section design. The program allows the specification of certain dimensions, and also allows maximum and minimum values to be assigned to all length dimensions and minimum values to be assigned to thickness dimensions. This option can be used to assure a practical design.

If no panel dimensions are input, calculations begin by making an optimum design for buckling for a sheet length. A check is made to see if this design is adequate for direct stress considerations. If the design is not sufficient, an iteration procedure determines the necessary skin thickness and other dimensions which are sufficient for both strength and buckling. The parameters are then checked to see if they are in the allowable input range. If a parameter is not in the allowable range, it is set equal to the closer limit value and the necessary adjustments are made to the calculation procedure. Following the weight calculation, the next sheet is then considered.

If a panel dimension is specified by the input, the optimum buckling design is determined based upon this restraint, and then the same procedure is followed as discussed above.

5.3.3.10.2 Descriptions of Necessary Input Parameters

The following are necessary input parameters:

L_{up}	Maximum frame spacing.
L_{low}	Minimum frame spacing.
$t_{f_{low}}$	Minimum frame thickness.
$t_{s_{low}}$	Minimum stringer thickness.
$t_{m_{low}}$	Minimum gage thickness for skin.

b_{up} Maximum stringer pitch.

b_{low} Minimum stringer pitch.

$b_{s_{up}}$ Maximum stringer height.

$b_{s_{low}}$ Minimum stringer height.

SHEET Sheet length.

Descriptions of the option input parameters are:

INA = Indicator for frame options:

0: No frame options.

1: L - frame spacing is input.

2: t_f - frame thickness is input.

3: b_f - frame height is input.

The value of L, t_f, or b_f is input on the card directly behind INA. If INA = 0, the next item input is INB.

INB = Indicator for skin and stringer options:

0: No skin and stringer options.

1: t - skin thickness is input.

2: t_s - stringer thickness is input.

3: b - stringer pitch is input.

4: b_s - stringer height is input.

The value of t, t_s, b, or b_s is input on the card directly behind INB. If INB = 0, end of card signal is entered after INB.

5.3.3.10.3 Input Format

Input cards are as follows:

The second card starts in Column 7.

second card	$b_{s_{low}}$	SHEET	INA	VALUE OF OPTION IF ANY	INB	VALUE OF OPTION IF ANY	*			
first card	SEMOPT	L_{up}	L_{low}	$t_{f_{low}}$	$t_{s_{low}}$	$t_{m_{low}}$	b_{up}	b_{low}	$b_{s_{up}}$	

where

SEMOPT is the name of the cards and is always the first item.

No commas are necessary between data items, but there must be one intervening blank.

The entries are ended by an * following the last item.

A sample input is:

INA = 0

INB = 1, thickness (t) input, t = 0.1378

Column 7

```
.036    120.    0    1    .1378    *

SEMOPT  8.22  1.87  .038  .001  0.0  6.97  2.33  2.33
```

5.3.3.10.4 Output (Figure 5-37)

The following items are output for the analysis:

a. Number of sheets.
b. Section identification, discontinuity and type.
c. Section properties, height, radius, maximums.
d. Material of analysis.
e. Skin thickness.
f. Weight of sheet.
g. Frame properties, spacing, flange length, height, thickness.
h. Stringer properties, pitch, flange length, height, thickness.
i. Total weight of section.

Also output throughout the program are any error conditions such as parameters out of bounds, calculations diverging, and possibly a no solution condition. Any restraint conditions are also output such as minimum thickness being larger than required for buckling and strength.

```
**************************************
* SEMI-MONOCOQUE STRUCTURAL ANALYSIS *
*      FOR MATERIAL AL  2219-T87     *
**************************************
```

SHEET	SKIN THICKNESS	WEIGHT	FRAME SPACING	FRAME FLANGE LEN	FRAME HEIGHT	FRAME THICKNESS	STRINGER PITCH	STRINGER FLANGE LEN	STRINGER HEIGHT	STRINGER THICKNESS
1	0.3309	0.0000	42.5080	3.3969	5.2260	0.1303	10.0000	1.1190	3.7299	0.0508

******** THE TOTAL WEIGHT OF THIS SECTION IS 0.0000 ********

Figure 5-37. Sample Output Format for Semi-Monocoque Subprogram

APPENDIX A

MATERIAL PROPERTIES

A.1 GENERAL

The following room temperature properties of each material are required: E_c, ρ, μ, σ_{yield}, σ_{ult}, σ_o, and $\sigma_{o.85}$. The first five properties are self-explanatory, however σ_o and $\sigma_{o.85}$ need further explanation. These properties are required to describe the elastic-plastic portion of the stress-strain curve, namely E_{tan} and E_{sec}. In order to describe the stress-strain curve in mathematical terms, the Ramberg-Osgood[2] equation is used as follows

$$\frac{\epsilon}{\epsilon_o} = \frac{\sigma}{\sigma_o} + \frac{3}{7}\left(\frac{\sigma}{\sigma_o}\right)^n$$

where

$$n = 1 + \frac{(0.3851)}{\left(\log \frac{\sigma_o}{\sigma_{o.85}}\right)}$$

log is to the base 10.

The above is graphically depicted in Figure A-1.

Re-arranging terms, the following relationships can be obtained

$$\frac{E_{sec}}{E_c} = \eta_i = \frac{\sigma}{\sigma + \frac{3}{7}\,\sigma_o\left(\frac{\sigma}{\sigma_o}\right)^n}$$

$$\sqrt{\frac{E_t}{E_c}} = \eta_w = \sqrt{\frac{1}{1 + \frac{3}{7}\,n\left(\frac{\sigma}{\sigma_o}\right)^{n-1}}}$$

$$\frac{\sqrt{E_t E_{sec}}}{E_c} = \eta = \sqrt{\frac{\sigma}{\left[1 + \frac{3}{7} n \left(\frac{\sigma}{\sigma_o}\right)^{n-1}\right]\left[\sigma + \frac{3}{7}\sigma_o \left(\frac{\sigma}{\sigma_o}\right)^{n}\right]}}$$

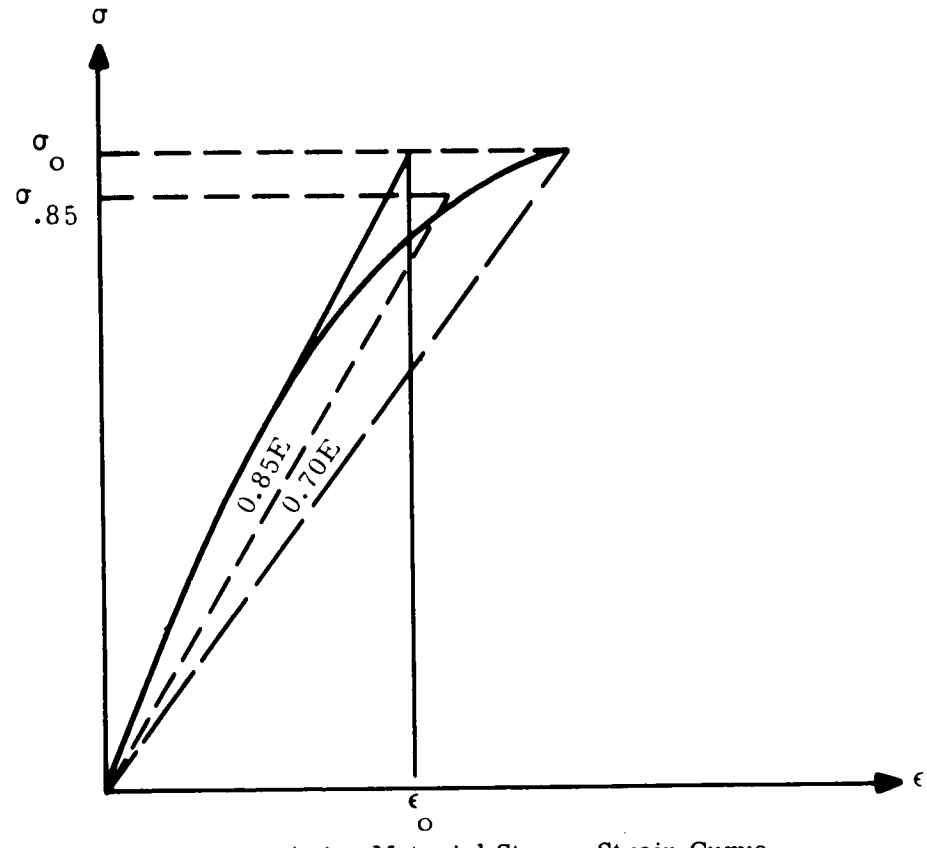

Figure A-1. Material Stress-Strain Curve

The material properties include the following at various temperature levels: E_c, σ_{yield}, σ_{ult}, σ_o, and $\sigma_{o.85}$.

A.2 MATERIAL PROPERTIES TABLES

The following tables show material properties versus temperature for various materials.

Table A-1

Material Properties versus Temperature for 2014-T6 Aluminum Clad[3,4]

Temp (°F)	Percent σ_y at Room Temp	Percent σ_{ult} at Room Temp	σ_y ($\times 10^3$ psi)	σ_{ult} ($\times 10^3$ psi)	σ_o* ($\times 10^3$ psi)	$\sigma_{0.85}$* ($\times 10^3$ psi)	Percent E_c at Room Temp	E_c ($\times 10^6$ psi)	ρ (lbs/ft^3)	μ
Room	100	100	56	64	63	58	100	10.7	174	0.30
0	101.5	102.5	57	65.5	64.5	59	101	10.8	174	0.30
- 50	103	105	58	67	66	60	102	10.9	174	0.30
-100	107	109	60	70	68.6	62	103	11.0	174	0.30
-150	109	111	61	71	70	63.3	103.5	11.1	174	0.30
-200	110	112.5	62	72	71	64	104	11.15	174	0.30
-250	113	123.5	63.5	79	77.9	65.5	105	11.25	174	0.30
-300	116	128	65	82	80.7	67.2	106	11.35	174	0.30

*The properties from -50° to -300°F have been obtained by using the same percent increase as for yield.

Table A-2

Material Properties versus Temperature for 7075-T6 Aluminum[3,4]

Temp (°F)	Percent σ_y at Room Temp	Percent σ_{ult} at Room Temp	σ_y ($\times 10^3$ psi)	σ_{ult} ($\times 10^3$ psi)	σ_o** ($\times 10^3$ psi)	$\sigma_{0.85}$* ($\times 10^3$ psi)	Percent E_c at Room Temp	E_c ($\times 10^6$ psi)	ρ (lbs/ft^3)	μ
Room	100	100	64	77	70	63	100	10.5	174.5	0.30
0	107	103.5	68.5	79.5	73.75	67.5	100.75	10.575	174.5	0.30
- 50	114	107	73	82	77.5	72	101.5	10.65	174.5	0.30
-100	117	110	75	85	79.5	73.5	102	10.7	174.5	0.30
-150	120	113	77	87	81.5	75.5	102.5	10.75	174.5	0.30
-200	125	116	80	89	84.5	78.5	103	10.85	174.5	0.30
-250	127	117	81	90	85.5	80	104	10.9	174.5	0.30
-300	130	121	83	93	88	82	106	11	174.5	0.30

* These properties from -50° to -300°F have been obtained by using the same percent increase as for the yield since the room temperature properties are almost identical.

**These properties from -50°F to -300°F have been obtained by using the average percent increase between that used for yield and ultimate.

Table A-3

Material Properties versus Temperature for 2024-T4 Aluminum[3,5]

Temp (°F)	Percent σ_y at Room Temp	Percent σ_{ult} at Room Temp	σ_y ($x10^3$psi)	σ_{ult} ($x10^3$psi)	σ_o* ($x10^3$psi)	$\sigma_{0.85}$* ($x10^3$psi)	Percent E_c at Room Temp	E_c ($x10^6$psi)	ρ (lbs/ft^3)	μ
Room	100	100	42	63	46	43	100	10.7	172.8	0.3
0	100.5	100	42.25	63	46.25	43.25	102	10.9	172.8	0.3
- 50	101	100	42.5	63	46.5	43.5	104	11.1	172.8	0.3
-100	101	100	42.5	63	46.5	43.5	106	11.3	172.8	0.3
-150	102	101.5	43	64	47	44	107	11.45	172.8	0.3
-200	107	106	45	67	49	46	108	11.60	172.8	0.3
-250	113	108	47.5	68	52	48.5	110	11.8	172.8	0.3
-300	124	111	52	70	57	53.2	112	12.0	172.8	0.3

*These properties from -50° to -300°F have been obtained by using the same percent increases as for yield since the room temperature properties are approximately equal.

Table A-4

Material Properties versus Temperature for 2219-T87 Aluminum[5,6]

Temp (°F)	Percent σ_y at Room Temp	Percent σ_{ult} at Room Temp	σ_y ($x10^3$psi)	σ_{ult} ($x10^3$psi)	σ_o ($x10^3$psi)	$\sigma_{0.85}$ ($x10^3$psi)	Percent E_c at Room Temp	E_c ($x10^6$psi)	ρ (lbs/ft^3)	μ
Room	100	100	50	62	52	50	100	10.4	172.8	0.30
0	102	102	51	63.25	52.25	51	100.5	10.45	172.8	0.30
- 50	104	104	52	64.5	52.5	52	101	10.5	172.8	0.30
-100	105	106	52.5	65.6	53	52.5	102	10.6	172.8	0.30
-150	107	107	53.5	66.3	55	53.5	103	10.7	172.8	0.30
-200	110	110	55	68.1	57	55	104	10.8	172.8	0.30
-250	113	114	56.5	70.6	59	56.5	106	11.0	172.8	0.30
-300	117	120	58.5	74.4	62	58.5	107	11.1	172.8	0.30

Table A-5

Material Properties versus Temperature for 6A1-4V Titanium[3]

Temp (°F)	Percent σ_y at Room Temp	Percent σ_{ult} at Room Temp	σ_y ($x10^3$psi)	σ_{ult} ($x10^3$psi)	$\sigma_{0.7}$* ($x10^3$psi)	$\sigma_{0.85}$* ($x10^3$psi)	Percent E_c at Room Temp	E_c ($x10^6$psi)	ρ (lbs/ft^3)	μ
Room	100	100	126	130	128	124	100	16	276	0.3
0	106	106	133.5	137.5	135.5	128	101	16.15	276	0.3
- 50	112	112	141	145	143.5	132.5	102	16.3	276	0.3
-100	117	118	148	154	151	146	103	16.5	276	0.3
-150	123	123	155	160	157.5	152.5	103.5	16.6	276	0.3
-200	128	128	162	166	164	158.5	104	16.65	276	0.3
-250	135	135	170	175	173	167.5	105	16.8	276	0.3
-300	144	144	182	187	184.5	178.5	107.5	17.2	276	0.3

*The same percent increases that were used for yield and ultimate were used for the secant yield stresses at 70 percent and 85 percent.

Table A-6

Material Properties versus Temperature for AISI 4340 Alloy Steel[3, 4]

Temp (°F)	Percent σ_y at Room Temp	Percent σ_{ult} at Room Temp	σ_y ($x10^3$psi)	σ_{ult} ($x10^3$psi)	$\sigma_{0.7}$* ($x10^3$psi)	$\sigma_{0.85}$** ($x10^3$psi)	Percent E_c at Room Temp	E_c ($x10^6$psi)	ρ (lbs/ft^3)	μ
Room	100	100	242	260	255	225	100	29	483	0.3
0	100.5	101	243.5	262.5	257.5	222.5	101.7	29.5	483	0.3
- 50	101	102	245	265	260	227	103.5	30	483	0.3
-100	103	104	250	270	266	234	103.5	30	483	0.3
-150	107	106	260	275	270	238	103.5	30	483	0.3
-200	109.5	109.5	265	285	279	246	103.5	30	483	0.3
-250	115	111.5	280	290	284	251	105	30.5	483	0.3
-300	120	115	290	300	293	259	105	30.5	483	0.3

* The same percent increases that are used for ultimate are used for the secant yield of 70 percent E.
**The same percent increases that are used for yield are used for the secant yield at 85 percent E.

Table A-7

Material Properties versus Temperature for HK 31A-H24 Magnesium[3,7]

Temp (°F)	Percent σ_y at Room Temp	Percent σ_{ult} at Room Temp	σ_y ($x10^3$psi)	σ_{ult} ($x10^3$psi)	σ_o* ($x10^3$psi)	$\sigma_{o.85}$* ($x10^3$psi)	Percent E_c at Room Temp	E_c ($x10^6$psi)	ρ (lbs/ft^3)	μ
Room	100	100	25	35	25	23.5	100	6.5	112	0.30
0	101.5	104	25.4	36.5	25.8	23.85	100	6.5	112	0.30
- 50	103	108	25.8	38	25.8	24.2	100	6.5	112	0.30
-100	106	117	26.5	41	26.5	24.9	101.5	6.6	112	0.30
-150	109	124	27.2	43.7	27.2	25.6	103	6.7	112	0.30
-200	112	131	28	46	28	26.3	104.5	6.8	112	0.30
-250	114	136.5	28.5	47.7	28.5	26.8	106	6.9	112	0.30
-300	116	142	29	50	29	27.2	108	7.0	112	0.30

*These properties from -50° to -300°F have been obtained by using the same percent increase as for the yield since the room temperature properties are approximately equal.

Table A-8

Material Properties versus Temperature for PH15-7Mo, RH 950 Condition[3,8]

Temp (°F)	Percent σ_y at Room Temp	Percent σ_{ult} at Room Temp	σ_y ($x10^3$psi)	σ_{ult} ($x10^3$psi)	σ_o*** ($x10^3$psi)	$\sigma_{o.85}$** ($x10^3$psi)	Percent E_c* at Room Temp	E_c ($x10^6$psi)	ρ (lbs/ft^3)	μ
Room	100	100	210	225	215	200	100	30	478	0.30
0	101.25	101.75	212.5	229	219	202	101.75	30.5	478	0.30
- 50	102.5	103.5	215.5	233.5	223	205	103.5	31	478	0.30
-100	106	107.5	222	242	232	212	103.5	31	478	0.30
-150	110	110	231	248.5	237	220	103.5	31	478	0.30
-200	114	113	240	255	244	228	103.5	31	478	0.30
-250	114	113	240	255	244	228	103.5	31	478	0.30
-300	114	113	240	255	244	228	103.5	31	478	0.30

* Assume same increases as AISI 4340, Table A-6.

** The same percent increases that are used for yield are used for the secant yield at 85 percent E.

***The same percent increases that are used for ultimate are used for the secant yield at 70 percent E.

Table A-9

Material Properties versus Temperature for Y5804, QMV-5 Beryllium*

Temp (°F)	Percent σ_y at Room Temp	Percent σ_{ult} at Room Temp	σ_y ($x10^3$psi)	σ_{ult} ($x10^3$psi)	σ_o ($x10^3$psi)	$\sigma_{o.85}$ ($x10^3$psi)	Percent E_c at Room Temp	E_c ($x10^6$psi)	ρ (lbs/ft^3)	μ
Room	100	100	64.5	75	54	43.5	100	42	115	
- 50									↓	
-100										
-150										
-200										
-250										
-300										

*Use room temperatures properties of beryllium from -50° to -300°F since applicable data is not available at this time.

A.3 NOMENCLATURE

E_c Compressive modulus of elasticity (psi).

E_{sec} Compressive secant modulus (psi).

E_{tan} Compressive tangent modulus (psi).

η Tangent - secant modulus reduction factor.

η_w Tangent modulus reduction factor.

η_i Secant modulus reduction factor.

ρ Density of material (lbs/ft^3).

σ_{yield} Yield stress (psi).

σ_{ult} Ultimate stress (psi).

σ_o Secant yield stress at 0.70 E (psi).

$\sigma_{o.85}$ Secant yield stress at 0.85 E (psi).

μ Poisson's ratio.

APPENDIX B

GASP

B.1 INTRODUCTION

This appendix is presented in three parts. Part 1 presents the equations which are used in the Wind Stress Launch Program - 27B, Part 2 is a general description of the philosophy of GASP, and Part 3 is devoted to the operation of the program.

B.2 PART 1 - WIND STRESS LAUNCH SIMULATION PROGRAM

B.2.1 GENERAL

The Wind Stress Launch Simulation Program is a two-dimensional (X-Z plane), three-degree-of-freedom earth launch trajectory generator which is a subset of the GASP programs.

The 1959 ARDC atmospheric model, which is used in this program, determines for a specific altitude the local speed of sound, temperature, atmospheric pressure, and density of the air from stored tabular data. The mach number, which is determined by dividing the wind velocity by the local speed of sound, is used as an independent variable in an input table to find the axial and normal drag forces.

In addition to the relative winds (the wind force caused by vehicle movement through a still atmosphere), the program is capable of imposing local winds by means of tabular input. This wind, at any time, is considered to be a vector quantity acting at the center of pressure.

In order to mathematically describe the pitching movements of the vehicle, the following tabular information is used by the program:

a. Center of gravity versus weight.
b. Center of pressure versus mach number.
c. Polar moment of inertia versus weight.

From the moment of inertia, the angular acceleration can be determined and this is integrated to find angular velocity which, in turn, is integrated to find angular distance (pitch). The vehicle position and velocity are determined by the integration of the equations of motion given below.

The control system aligns the thrust vector of the gimbaled engines so that there is minimum drift from the commanded trajectory. The commanded pitch profile is integrated from the rate profile which is a required input. The control equation is of the form

$$\beta = a_o\phi + a_1\dot{\phi} + b_o\alpha$$

where

β = engine gimbal angle.

ϕ = pitch error.

$\dot{\phi}$ = pitch rate error.

α = angle of attack.

a_o, a_1, b_o are gains of the control system which vary with flight time. These are required inputs which must be determined to satisfy a predetermined control scheme such as minimum drift.

B.2.2 EQUATIONS

The following equations are used in the Wind Stress Launch Simulation Program. Refer to Figure B-1 for relation of various quantities.

B.2.2.1 Equations of Motion

$$\ddot{X} = \frac{(F_{ax} + F_x)}{m} + g_x$$

$$\ddot{Z} = \frac{(F_{az} + F_z)}{m} + g_z$$

$$\dot{\omega}_p = \ddot{\theta}_a = \frac{T_{tot}}{I_p}$$

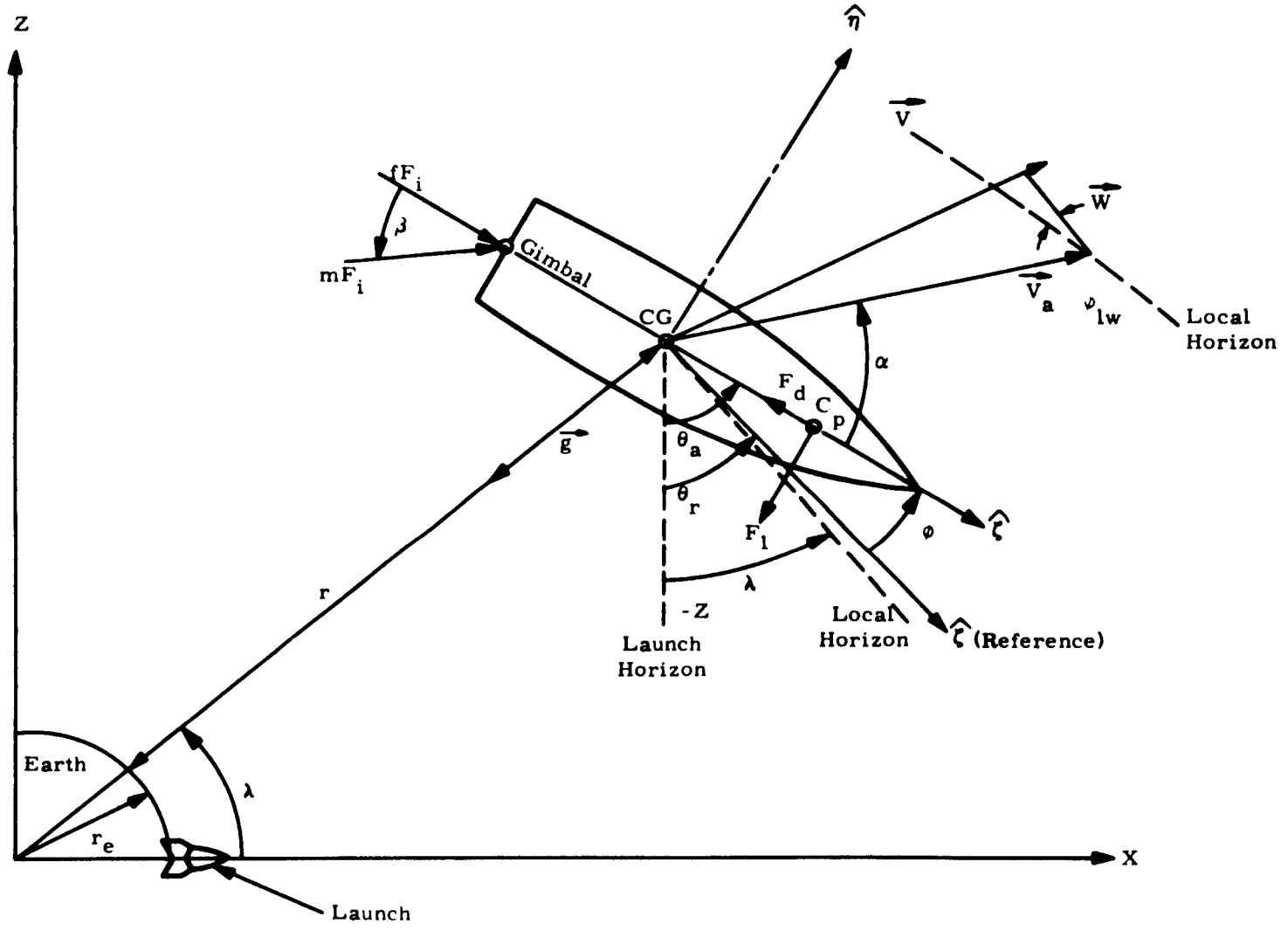

Figure B-1. Reference Coordinates for Wind Stress Launch Simulation Analysis

where

F_{ax} and F_{az}	are the components of axial drag referred to inertial coordinates.
F_x and F_z	are the components of the thrust referred to inertial coordinates.
g_x and g_z	are the components of the acceleration of gravity referred to inertial coordinates.
T_{tot}	is the total moment about the pitch axis.
I_p	is the polar moment of inertia about the pitch axis.
m	is the mass of the vehicle.

B.2.2.2 Force Model

B.2.2.2.1 Gravity

$r = (X^2 + Z^2)^{\frac{1}{2}}$ = radius from origin to vehicle.

$h = r - r_e$ = altitude.

$\lambda = \tan^{-1} \frac{Z}{X}$ = latitude (range angle).

where $-\pi \leq \lambda \leq \pi$

$$g_x = \frac{-GmX}{r^3}$$

$$g_z = \frac{-GmZ}{r^3}$$

where G is the universal gravitational constant.

B.2.2.2.2 Drag Model

The terms ρ, P, and c are computed as functions of altitude using the 1959 ARDC model atmosphere, where ρ, P, and c are density, pressure, and the speed of sound, respectively.

Given local winds as function of altitude

V_{lw} = magnitude.

ϕ_{lw} = angle of wind with respect to local horizon.

then

$$W_x = V_{lw}\left(\frac{X}{r}\sin\phi_{lw} - \frac{Z}{r}\cos\phi_{lw}\right)$$

$$W_z = V_{lw}\left(\frac{X}{r}\cos\phi_{lw} + \frac{Z}{r}\sin\phi_{lw}\right)$$

The components of relative velocity are

$$\dot{X}_a = \dot{X} - W_x$$

$$\dot{Z}_a = \dot{Z} - W_z$$

The magnitude of the relative velocity is

$$|V_a| = \left(\dot{X}_a^2 + \dot{Z}_a^2\right)^{\frac{1}{2}}$$

The dynamic pressure is

$$Q = \tfrac{1}{2}\rho|V_a|^2$$

The angle of attack is

$$\alpha = \tan^{-1}\left(\frac{\vec{V}_a\ \hat{\eta}}{V_a\ \hat{\xi}}\right)$$

where $-\pi \leq \alpha \leq \pi$ and the mach number is

$$M = \frac{|V_a|}{c} \quad \text{mach number}$$

Drag coefficients $C_a C_{z\alpha}$ are obtained from tables as a function of mach number, then the axial drag is

$$\vec{F}_d = (-C_a SQ)\,\hat{\xi}$$

and the lift is

$$\vec{F}_l = (C_{z\alpha} SQ\alpha)\,\hat{\eta}$$

and the inertial components of axial drag are

$$F_{ax} = F_d \cdot \xi_x + F_l \frac{\left(\xi_x \cos\alpha - \frac{\dot{X}_a}{|V_a|}\right)}{\sin\alpha}$$

and

$$F_{az} = F_d \cdot \xi_z + F_l \frac{\left(\xi_z \cos\alpha - \frac{\dot{Z}_a}{|V_a|}\right)}{\sin\alpha}$$

Let

cg → distance from gimbal to center of gravity.

cp → distance from gimbal to center of pressure.

Both of these are obtained from table lookup. The weight is

$$W_T = W_{to} - W_t$$

the mass is

$$m = \frac{W_T}{g}$$

and, by table lookup

$$cg = f(W_T)$$

$$cp = f(m)$$

Torque due to lift is

$$T_l \hat{\xi} = (-F_l)\,\hat{\eta} \times (cp - cg)\,\hat{\xi}$$

and the magnitude is

$$|T_l| = \left[-F_l(cp - cg)\right]$$

B.2.2.2.3 Thrust Model

The thrust per engine is

$$F_i = F_{nom} - pAe$$

If we have m movable engines and f fixed engines, the axial thrust is

$$F_{t\xi}\hat{\xi} = (fF_i + m \cos\beta F_i)\,\hat{\xi}$$

and the normal thrust is

$$F_{t\eta}\hat{\eta} = (m \sin\beta F_i)\,\hat{\eta}$$

then the inertial components of thrust are

$$F_x = F_{t\xi} \cdot \xi_x + F_{t\eta} \cdot \vec{\eta}_x$$

and

$$F_z = F_{t\xi} \cdot \xi_z + F_{t\eta} \cdot \eta_z$$

Torque due to thrust is

$$T_t \hat{\xi} = F_{t\eta}\hat{\eta} \times (-cg)\,\hat{\xi}$$

or the magnitude of the thrust torque is

$$|T_t| = -F_{t\eta} cg$$

The total moment is

$$\hat{\xi}\,|T_{tot}| = (T_t + T_l)\,\hat{\xi}$$

$$|T_{tot}| = F_{t\eta}(-cg) + (-F_l)(cp - cg)$$

$$= -F_{t\eta} cg - F_l(cp - cg)$$

The pitch axis moment of inertia is obtained by table lookup

$$I_p = f(W_t)$$

B.2.2.3 Guidance

a. Attitude error is

$$\phi = \theta_a - \theta_r$$

b. Pitch rate error is

$$\dot{\phi} = \dot{\theta}_a - \dot{\theta}_r$$

c. Gimbal angle is

$$\beta = a_o\phi + a_1\dot{\phi} + (-b_o)\,\alpha$$

B.3 PART 2 - PHILOSOPHY OF GASP

B.3.1 STRUCTURE

A GASP simulation consists of a collection of programs, modules, and subroutines which are available as standard units, together with such special-purpose operations as may be required to achieve the desired simulation. Three levels of program structure may be defined: the job, the phase, and the module or subphase.

A job is the program or programs that are all executed during a given continuous period of machine operation. A job ordinarily consists of several separate and related programs (a CHAIN job), or a single program. The term program is used to designate one machine load of instructions and data. Thus, a "job" is a tenuous entity, and the composition of a job is more a matter of convenience than of the actual computations being performed.

The basic component of a job is a phase. A phase occupies the status of a usual program in that it is executed as an entity by the FORTRAN monitor system. The phase is constrained to operate with the same collection of instructions as were loaded at execution time. This restriction prevents a phase from redefining the computations performed during execution. Thus, in the case of a simulation, the force model is defined once for the phase and cannot be replaced or augmented during execution. It is clear that the phase is the basic operational unit of GASP. Since the GASP system

routines do not actively monitor the execution of a phase, there is no limitation concerning when input or output is processed, whether there are special operations performed, or whether more phases follow. Any presently existing program can be executed as a phase under the GASP system, but effective communication with other phases is restricted by compatibility considerations.

A phase may be further subdivided into modules in order to take full advantage of preprogramed routines. A module is defined as a set of subroutines that perform some function independent of any other computations. For example, a guidance module may generate control commands based on quite complex computations. The guidance module would consist of all the computations necessary for determining the control commands together with any required logic functions. Each module is so constructed that it can be incorporated into a phase in place of another module of the same type (e.g., one guidance module for another) without changing the rest of the phase. In some cases, one subroutine can function as a module; however, several subroutines are usually required.

The ultimate decision as to the extent of modularization is determined by both the problem requirements and the stock of available modules. It is usually best to make maximum use of preprogramed modules in order to utilize all the power of the GASP system. However, for smaller jobs, the use of modules could reduce efficiency by incorporating unneeded complexity.

Finally, each module may select special-purpose subroutines from those contained in the GASP subroutine library. Various potential models, coordinate transformations, interpolation routines, and so on, are available in final form. Most of the library subroutines expect the standard GASP COMMON block, and calling sequences are generally not employed.

B.3.2 PROGRAM CONTROL AND SEQUENCING

Control of programs executed under the GASP system is based on the FORTRAN CHAIN concept. Each phase to be executed as part of a job is stored on tape as a machine load. The sequence of programs to be executed is obtained from cards.

All preliminary operations are handled by a small program called GASPGO. This program is the first program to be executed in a GASP job. Data tapes are assigned and the phase execution list is constructed. Upon completion of these operations, the next chain link (phase) is loaded into core and control is transferred to it for execution.

When a given link has been completed, control is passed to subroutine GASPXT which calls the next link into core for execution. GASPXT may also cause a job to be terminated if some error is discovered at any stage of execution.

B.3.3 INPUT/OUTPUT

The basic consideration in the design of input/output procedures was to keep communication as flexible and as straightforward as possible. To this end, a standard binary tape-writing routine was developed. The routine automatically determines the start and extent of the upper memory data block, and writes the entire block on tape at every output time. This operation requires less time than writing a smaller amount of data which may be scattered throughout the core. The resultant binary tape may be scanned as often as required, and all of the data is available at each time point. For smaller programs, it is probably simpler to write output directly as it is generated, and this option is provided.

Input data may be processed either by standard header-card-reading routines, or the user may employ his own processing routines. Every effort has been made to limit the number of header cards to a manageable number. In cases where commonly used quantities are required, such as the radius of the earth or gravitational parameter standard values (for earth), these are automatically used and the user has the option of overriding them. As each header card is read, its contents are printed out, giving the user a permanent record of his problem statement. Since the binary output data may be processed as a separate job, it is possible to check the header-card printouts before processing the output tape and the data processing procedure may be skipped if an error is discovered in the input.

B.3.4 COMPATIBILITY

The structure of the GASP system reduces the amount of extra programing required to modify present programs for use within GASP. In particular, a series of error

programs/analysis programs is easily incorporated into a GASP simulation. The only requirement is a binary output routine to take data from a GASP simulation and write it on tape in the proper format. This results in an extremely powerful analysis tool.

Other programs may be converted to operate under GASP by making minor revisions to the program structure. However, more extensive revisions would be required before these programs could communicate with other programs in the system.

B.3.5 COMPUTATIONAL MODULES

B.3.5.1 Introduction

The basic philosophy of computational modules has not been fully realized. The equations of motion are integrated in a planetocentric inertial set rather than a noninertial vehicle set. Also, the complete set of dynamic modules has not as yet been programed. The present simulation capability is summarized in paragraph B.4. The following section will consider the present conventions that have been evolved for GASP I.

B.3.5.2 Reference Coordinates and Transformations

The primary coordinate set is a quasi-inertial cartesian set with the origin at the center of the reference planet. If the reference planet is the earth, the following orientation is defined: The positive Z axis is collinear with the axis of rotation in the direction of the north pole. The X, Y plane lies in the plane of the equator, and the X axis points in the direction of the prime meridian at time t = 0. If the earth is assumed to rotate, a second earth-centered cartesian set is defined, coincident with the inertial set at time t = 0 and rotating with the earth.

For input and output purposes, a pseudo-spherical coordinate set is defined using altitude, latitude, and longitude to measure position, and a similar set (speed, path angle, path azimuth) to measure velocity. This set may be defined as follows: Altitude is measured along a line through the vehicle normal to the earth's surface. The angle that this line makes with the equatorial plane is the latitude, and the angular displacement of the equatorial projection from the inertial X axis is the longitude. Longitude is measured positive east. The orientation of the velocity vector is measured with respect to a local horizontal plane. The angle between the velocity vector and the local horizontal

is defined as the path angle and is measured positive upward. The angle between the projection of the velocity on the local horizontal and the plane containing the position vector and the inertial Z axis defines the path azimuth, measured positive east from north.

All transformations are in double precision except those which may be incorporated into guidance modules for the purpose of generating control data.

B.3.5.3 Dynamic Modules

The present dynamic modules can handle simulations up to and including quasi-6 degrees of freedom. Modules have been programed which incorporate the torque equations of two-dimensional flight. The following equations are integrated:

a. Position

$$\frac{dx}{dt} = V_x$$

$$\frac{dy}{dt} = V_y$$

$$\frac{dz}{dt} = V_z$$

b. Velocity

$$\frac{dV_x}{dt} = \frac{F_{ax} + F_{tx}}{m} + g_x$$

$$\frac{dV_y}{dt} = \frac{F_{ay} + F_{tv}}{m} + g_y$$

$$\frac{dV_z}{dt} = \frac{F_{az} + F_{tz}}{m} + g_z$$

c. Roll axis

$$\frac{d\hat{\xi}_x}{dt} = \eta_x \omega_p - \zeta_x \omega_y$$

$$\frac{d\hat{\xi}_y}{dt} = \eta_y \omega_p - \zeta_y \omega_y$$

$$\frac{d\hat{\xi}_z}{dt} = \eta_z \omega_p - \zeta_z \omega_y$$

d. Yaw axis

$$\frac{d\eta_x}{dt} = \zeta_x \omega_r - \xi_x \omega_p$$

$$\frac{d\eta_y}{dt} = \zeta_y \omega_r - \xi_y \omega_p$$

$$\frac{d\eta_z}{dt} = \zeta_z \omega_r - \xi_z \omega_p$$

e. The remaining axis (pitch) may be computed in one of two ways:

1. Since the vehicle axes are orthogonal

$$\vec{\zeta} = \hat{\eta} \times \hat{\xi}$$

2. Alternatively, the pitch axis may be integrated using

$$\frac{d\zeta_x}{dt} = \xi_x \omega_y - \eta_x \omega_r$$

$$\frac{d\zeta_y}{dt} = \xi_y \omega_y - \eta_y \omega_r$$

$$\frac{d\zeta_z}{dt} = \xi_z \omega_y - \eta_z \omega_r$$

The values in the differential equations for velocity are as follows:

a. (F_{ax}, F_{ay}, F_{az}) are the inertial components of aerodynamic drag.

b. (F_{tx}, F_{ty}, F_{tz}) are the inertial components of thrust.

c. $(\omega_r, \omega_p, \omega_y)$ are the angular velocity components about the roll, pitch, and yaw axes.

d. (g_x, g_y, g_z) are the inertial components of gravity.

e. m is the mass of the vehicle.

B.3.5.4 Environment Modules

Modules are currently available which will compute gravitational acceleration components on a vehicle with respect to either a spherical or ellipsoidal earth. The ellipsoidal earth model allows the effects of three harmonies (J, D, and H terms) to be simulated. Since the actual physical constants can be controlled by the user, gravitational acceleration in the vicinity of other planets may be simulated.

Aerodynamic drag is simulated by considering the orientation of the vehicle with respect to a relative-wind-oriented coordinate set. Density is computed as a function of altitude using the 1959 ARDC model atmosphere. Both spherical and ellipsoidal earth models are available. Either a constant drag coefficient or variable drag coefficients in tabular form are acceptable input.

Several thrust modules have been programed. One routine, suitable for a mass point only, computes the inertial components of thrust using the equation for thrust force utilized in Program 2368 (two-dimensional satellite insertion program). This relation is

$$|T| = P_c A_t \left(C_{fvac} - \epsilon \frac{P_c}{P_a} \right)$$

in which

P_c is the chamber pressure.

A_t is the throat area.

C_{fvac} is the vacuum thrust coefficient.

ϵ is the nozzle expansion ratio.

P_a is the local atmospheric pressure.

T is the thrust magnitude.

The thrust angles must be computed by a guidance routine.

The second thrust module computes the thrust, center of gravity, and center of pressure of a rigid body. The center-of-mass and center-of-pressure computations may be skipped for a point mass.

The center-of-gravity and center-of-pressure computations require tabular data relating the center of mass to the remaining mass, and giving the center of pressure as a function of the machine number.

B.3.5.5 Guidance and Support Systems

Three guidance modules have been developed to check various configurations.

No capability has presently been incorporated into the GASP system for radar trackers or other support systems. These may be incorporated into the system in either of two ways. The first method is simply to add the required transformation package to the module execution list within a phase. The alternative method requires a separate phase which would accept the standard GASP binary output tape, would perform required transformations, and would write the results on another tape for further processing. This second tape could then become input for an error analysis procedure, after the manner of the PAT system.

The same alternatives are available as applied to the generation of partial derivatives. For complex programs, the two-phase concept is probably the most economical alternative since the user has the option of terminating a run at any time in the event of error, thus saving excess computation. This subject is discussed at greater length in the following section.

B.4 PART 3 - PROGRAM OPERATIONS

B.4.1 EXECUTION LISTS

The unifying element of each phase of a GASP simulation is the control module execution list. Since each module is an independent entity, the only requirement for an execution list is that it directs control through each module in the proper sequence. The execution list is a closed loop routine on the order of a rotary stepping switch as shown in Figure B-2.

As each of the various modules is called, the appropriate operations are performed and control returns to the execution list. Each cycle through the execution list results in one integration step. The normal exit from the list is through the integration control module. However, any module can halt the integration by calling subroutine TERMN. Each module has a distinctive error code so that a certain amount of corrective action is possible. Ordinarily, every call to TERMN causes the job to be terminated.

The standard integration module is a fourth-order Runge-Kutta routine which requires four evaluations of each differential equation for every integration step. In order to accommodate various sets of differential equations, a smaller version of the execution

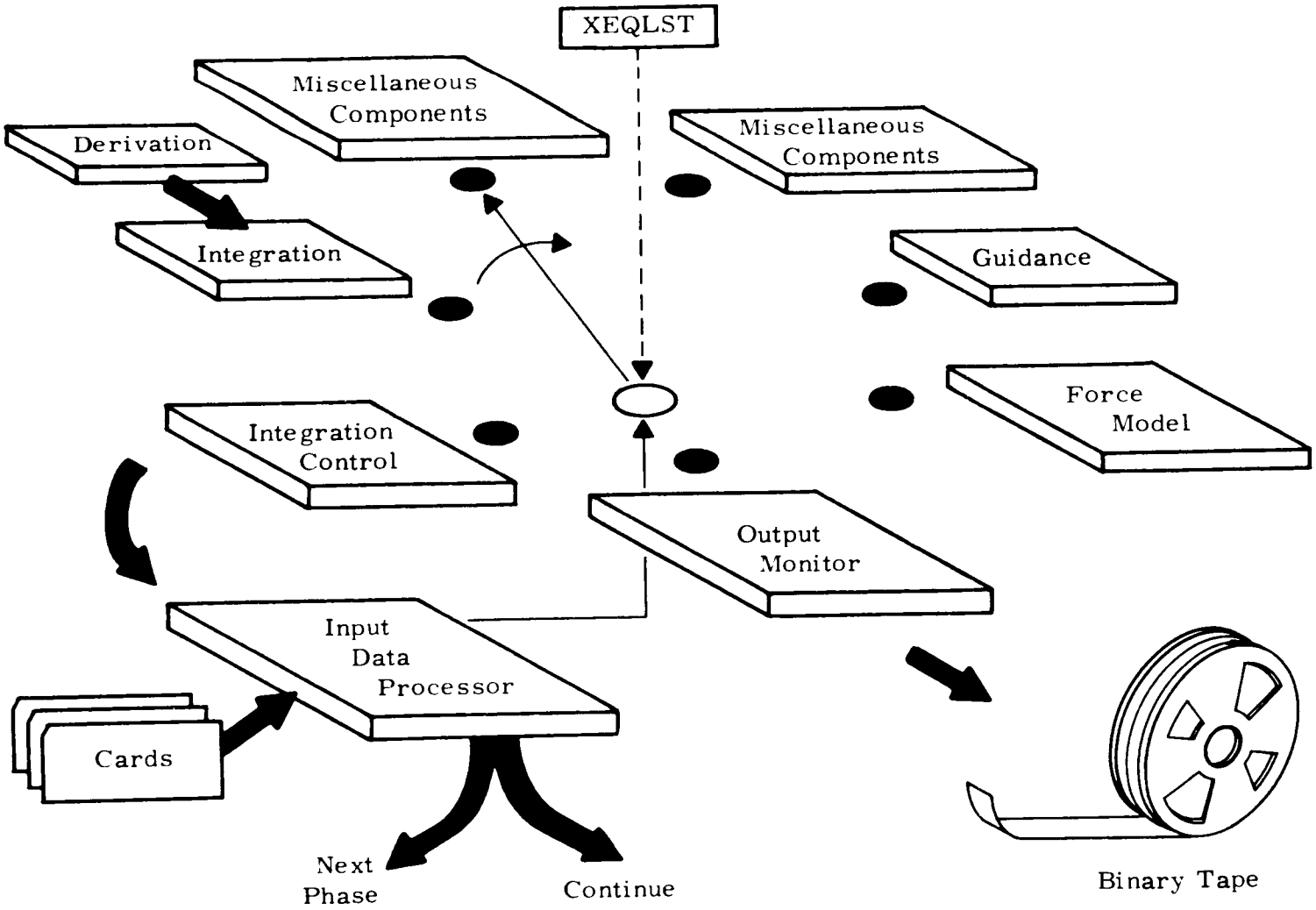

Figure B-2. Execution List

list is employed. At each time to evaluate the system of equations being integrated, control is cycled through the derivative sequence and all derivatives are computed.

Since the derivative execution list is executed four times for each cycle of the control module list, accuracy of the integration can be increased by executing the guidance and force modules as a part of the derivative execution list instead of as a part of the control module execution list. It is clear that the increase in accuracy is coupled with an increase in running time and it is worthwhile to determine whether this is required. If a variable step-size integrator is employed, the guidance and force models could probably be safely left in the control module execution list.

B.4.2 ERROR CONTROLS

There are three basic sources of errors in any computer program: communication, analysis, and computation. Communication errors are those resulting from mistakes in input format, mispunched cards, and incomplete data. The input data processing routines perform a number of consistency checks which are designed to uncover as many of these errors as possible. As each card is read, it is printed out so that a permanent record of all input data is preserved. If an error is discovered, the job is terminated immediately.

Analytical errors may result from conceptual errors or a lack of background concerning the particular case being considered. Examples of these errors are excessive altitude, negative altitude, excessive flight time, excessive burning time, and so on. Several error checks are built into the module, such as testing for negative altitude. Other error conditions, peculiar to the given simulation, may be checked by specifying cutoff conditions at execution time. Any variable in upper memory may be so monitored.

Computational errors include those due to truncation integration, rounding errors, and errors in interpolation procedures. All position, velocity, and orientation variables are dimensioned in double precision so that entire modules can be upgraded in precision should the need arise. In addition, all matrix operations, such as coordinate transformations and the final summation in the Runge-Kutta integration, are always performed in double precision.

B.4.3 MULTIPLE-PHASE JOBS

There are many situations that can be conveniently broken into separate pieces and executed. One example, mentioned above, is to convert and process output from a series of computations as a separate operation. This procedure is most advantageous when much data is generated and it is desired to examine various parts of the data. For example, a translunar trajectory stored on binary tape could be scanned at wide intervals to obtain an estimate of the general character of the trajectory. Successive scans could process partial derivative data or other variables of interest. The taped data would always be available and could be reprocessed as often as needed.

Another application of the multi-phase concept occurs when it is desired to pass information from one program to another. The present PAT system is an example of the flexibility that can be obtained by passing data from program to program automatically. A taped launch sequence could be processed through many separate programs as suggested by Figure B-3. The important point to keep in mind, however, is the fact that this procedure is optional.

The flow chart shown in Figure B-4 represents the flow of information in the Wind Stress Launch Simulation Program under the GASP system.

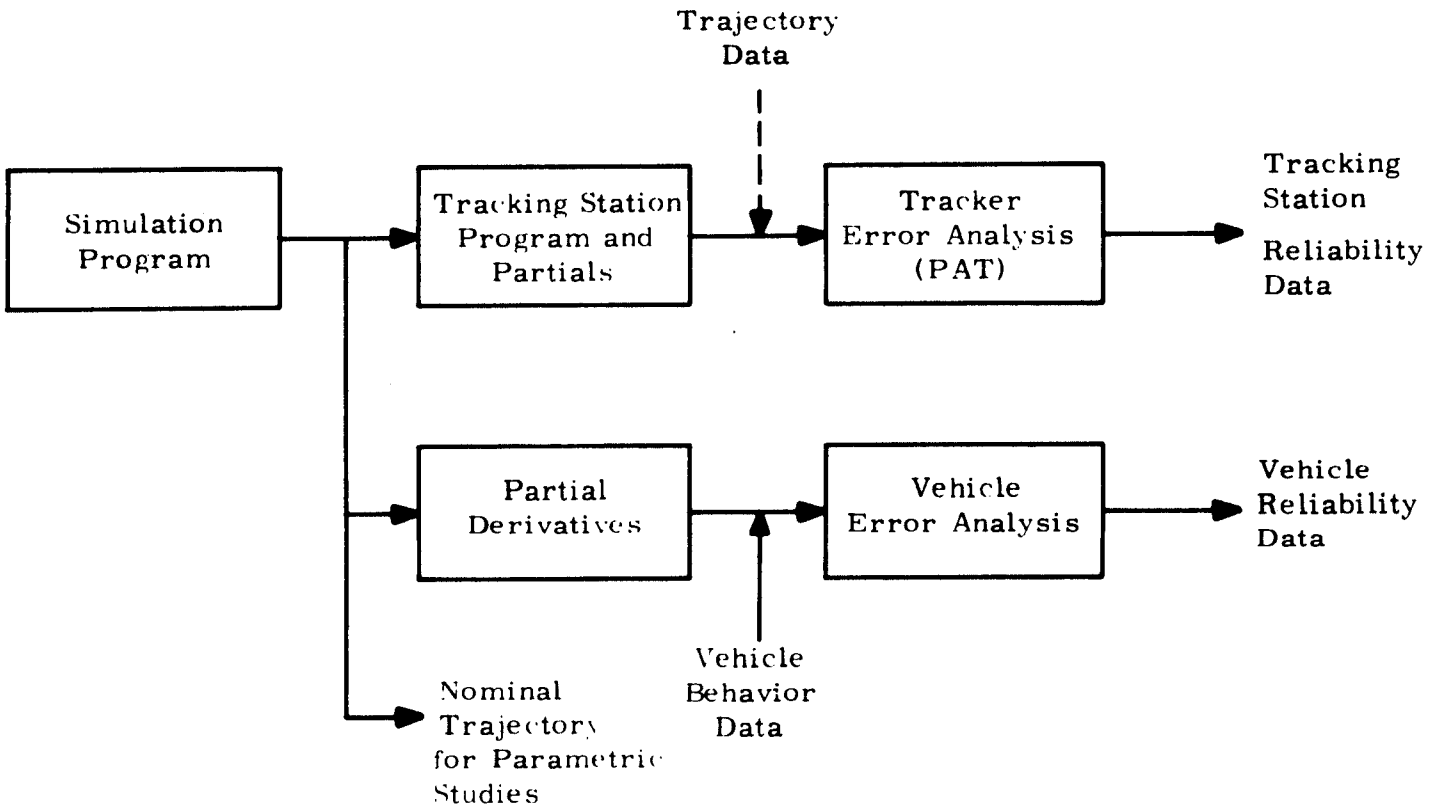

Figure B-3. Taped Launch Sequence

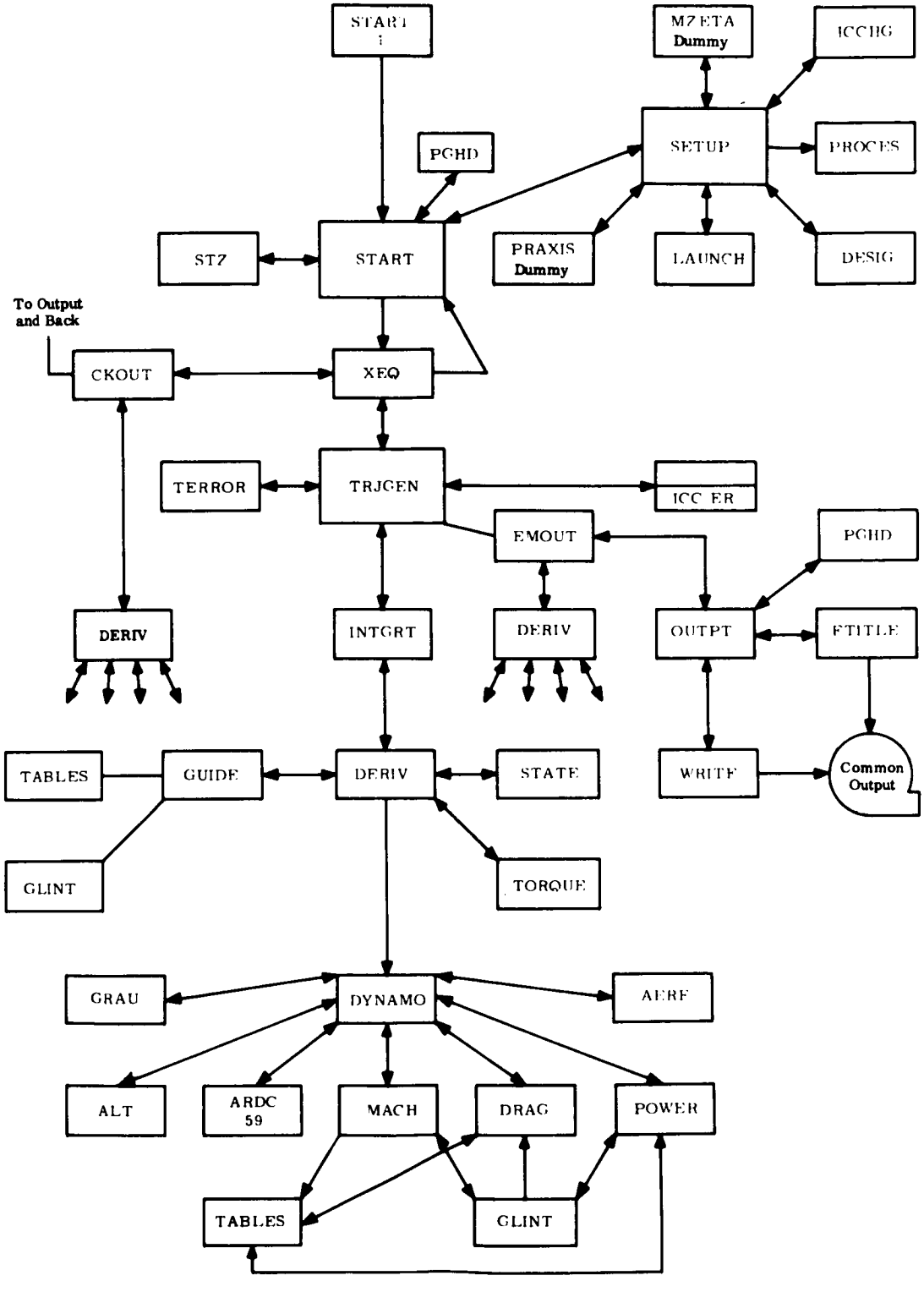

Figure B-4. Wind Stress Launch Simulation Program in the GASP System

APPENDIX C

LASS-1

C.1 INTRODUCTION

The detail equations for the LASS-1 program are presented in the following pages. The flow diagram (Figure C-1) of the analysis is included, as is the configuration detail drawing (Figure C-2), to aid the reader in understanding the analysis. The nomenclature used is sometimes peculiar to this appendix, therefore reference should be made to paragraph C.6, Nomenclature.

C.2 LATERAL - INFLIGHT

C.2.1 PREPARE I

a. Select and store lateral weight distribution, w_i.

b. Select and store linear normal force coefficient, $C_{z_{\alpha_i}}$.

c. Select and store nonlinear normal force coefficient $C_{z_{cf_i}}$

d. Calculate and store angle-of-attack distribution, α_i.

e. Select and store thrust, T.

f. Calculate and store $\sin^3\alpha_i$.

g. Calculate and store dynamic pressure distribution, q_i.

C.2.2 MASS I

a. Calculate total weight

$$W = \sum_i w_i$$

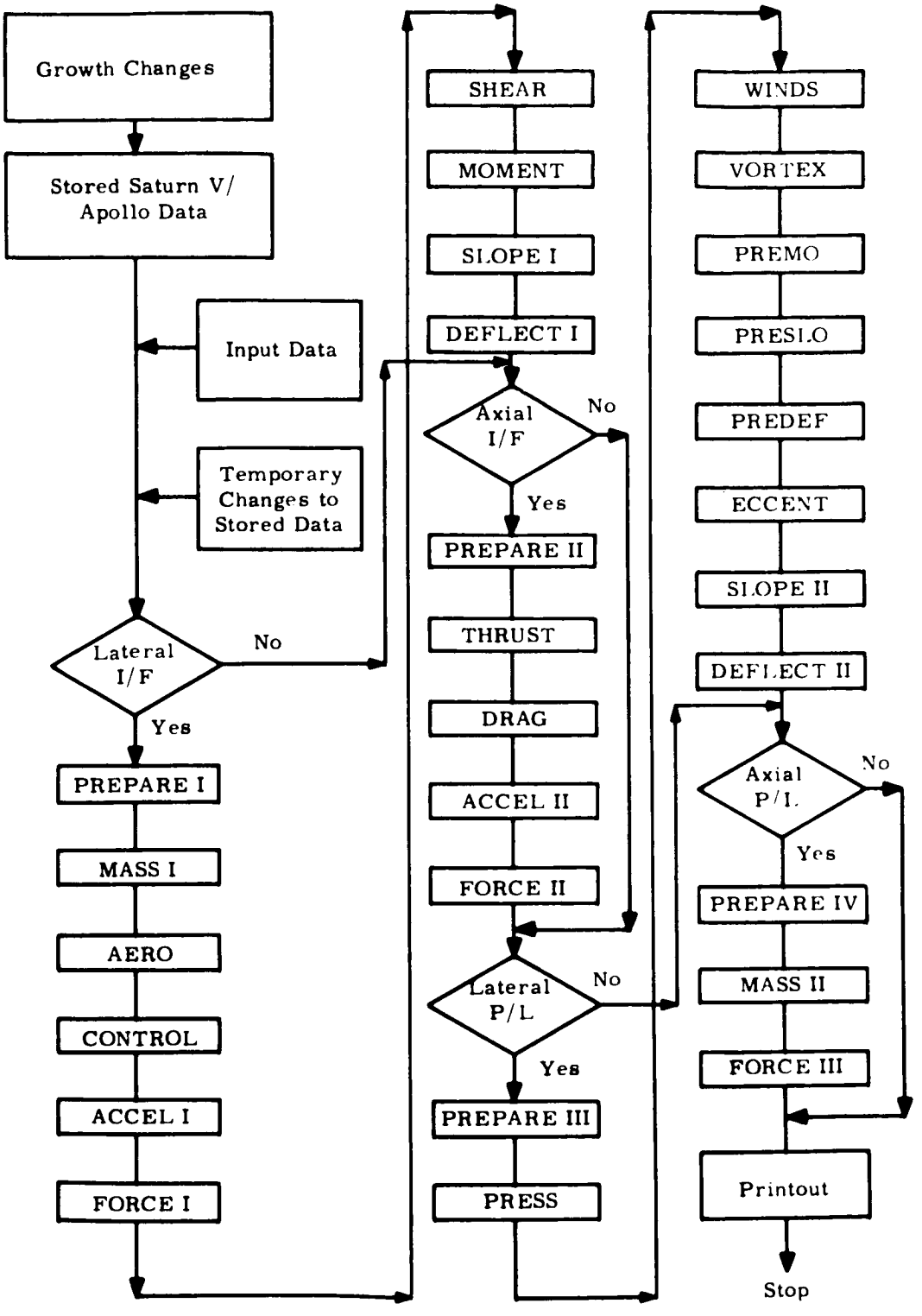

Figure C-1. LASS-1 Flow Diagram

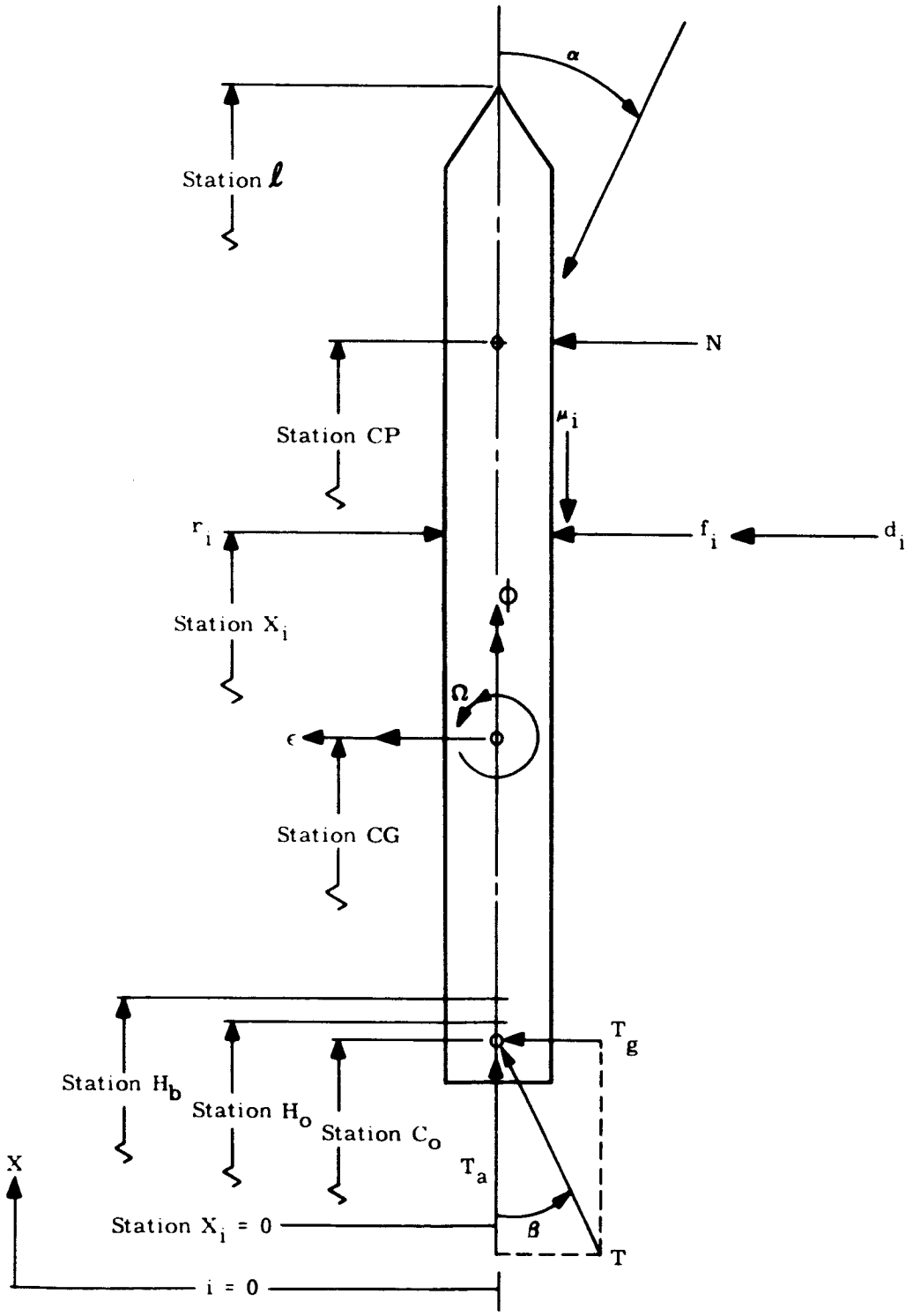

Figure C-2. Configuration Detail

b. Calculate station center of gravity (CG)

$$CG = \frac{\sum_i w_i x_i}{W}$$

c. Calculate pitch moment of inertia

$$I_p = \frac{1}{g} \sum_i (CG - x_i)^2 w_i$$

C.2.3 AERO

a. Calculate linear aero force distribution

$$f_i = SC_{z_{\alpha_i}} \alpha_i q_i$$

b. Calculate total linear aero force

$$\eta = \sum_i f_i$$

c. Calculate location of linear center of pressure (CP)

$$CP_l = \frac{\sum_i f_i x_i}{\eta}$$

d. Calculate nonlinear aero force distribution

$$d_i = SC_{z_{cf_i}} \sin^3 \alpha_i q_i$$

e. Calculate total nonlinear zero force

$$\Delta = \sum_i d_i$$

f. Calculate CP of nonlinear aero force

$$CP_d = \frac{\sum_i d_i x_i}{\Delta}$$

g. Calculate total normal aero force

$$N = \Delta + \eta$$

h. Calculate over-all CP

$$CP = \frac{CP_d \Delta + CP_l \eta}{N}$$

i. Calculate aero moment about CG

$$M_a = N(CP - CG)$$

C.2.4 CONTROL

a. Calculate engine control force

$$T_g = 0.8T \sin\beta$$

b. Calculate control moment about CG

$$M_c = (C_o - CG)\, T_g$$

C.2.5 ACCEL I

a. Calculate lateral acceleration

$$\epsilon = \frac{(N + T_g)\, g}{W}$$

b. Calculate angular acceleration

$$\Omega = \frac{M_c + M_a}{I_p}$$

c. Calculate lateral acceleration distribution

$$a_i = \epsilon + \Omega(x_i - CG)$$

C.2.6 FORCE I

a. Calculate resultant force distribution

$$r_i = -\frac{1}{g}(a_i w_i)$$

b. Calculate total equivalent force distribution

$$F_i = r_i + f_i + d_i + (T_g)_{i=C_o}$$

C.2.7 SHEAR

Calculate shear distribution

$$V_i = \sum_{j}^{i} F_j$$

C.2.8 MOMENT

Calculate bending moment distribution

$$M_i = \sum_{j}^{i} V_j \Delta x_j$$

C.2.9 SLOPE

Calculate relative slope

$$\Theta_i = \sum_{j}^{i} \frac{M_i}{(EI)_j} \Delta x_j$$

C.2.10 DEFLECT I

Calculate relative deflection

$$Y_i = \sum_{j}^{i} \Theta_j \Delta x_j$$

C.3 AXIAL - INFLIGHT

C.3.1 PREPARE II

a. Select and store axial weight distribution, Λ_i

b. Select and store drag coefficient distribution, C_{d_i}.

c. Select and store engine thrust, T.

d. Calculate and store dynamic pressure distribution, q_i.

e. Calculate total vehicle weight

$$W = \sum_i \Lambda_i$$

C.3.2 THRUST

Calculate axial thrust

$$T_a = (0.8 \cos\beta + 0.2)\, T$$

C.3.3 DRAG

a. Calculate drag force distribution

$$\mu_i = SC_{d_i} q_i$$

b. Calculate total drag force

$$D = \sum_i \mu_i$$

C.3.4 ACCEL II

Calculate axial acceleration

$$\phi = \frac{(T_a - D)\, g}{W}$$

C.3.5 FORCE II

Calculate axial force distribution

$$\delta_i = -\sum_{j}^{i} \left(\mu_j + \frac{\phi}{g} \Lambda_j \right) + (T_a)_{i=C_o}$$

C.4 LATERAL - PRELAUNCH

C.4.1 PREPARE III

Select and store lateral weight distribution, w_i

C.4.2 PRESS

Calculate dynamic pressure distribution

$$q_i = \frac{1}{2} \rho v_i^2$$

C.4.3 WINDS

a. Calculate aero wind force distribution

$$d_i = C_{z_{co_i}} q_i S$$

b. Calculate shear distribution

$$V_i = \sum_{j=1}^{i} d_j$$

c. Calculate moment distribution due to winds

$$M_{w_i} = \sum_{j=1}^{i} V_j \Delta x_{j-1}$$

C.4.4 VORTEX

Calculate vortex shedding moment distribution

$$M_{v_i} = \frac{0.25\left(M_{w_{i=H_b}}\right)}{(1 - H_b)^3}\left(x_i^3 - 3H_b x_i^2 + 6H_b l x_i - 3H_b l^2 + 2l^3\right)$$

C.4.5 PREMO

Calculate preliminary moment distribution due to winds and vortex shedding

$$M_{s_i} = M_{w_i} + M_{v_i}$$

C.4.6 PRESLO

Calculate preliminary slope distribution

$$\Theta_i = \sum_{j=1}^{i} \frac{M_{s_j}}{EI_j} \Delta x_j$$

C.4.7 PREDEF

Calculate preliminary deflection

$$y_i = \sum_{j=1}^{i} \Theta_j \Delta x_j$$

C.4.8 ECCENT

a. Calculate weight eccentricity moment at H_b

$$M_{e_{i=H_b}} = \sum_i w_i y_i$$

b. Calculate weight eccentricity moment distribution

$$M_{e_i} = M_{e_{i=H_b}} - \sum_{j}^{i} w_j y_j$$

c. Calculate total moment distribution

$$M_i = M_{s_i} + M_{e_i}$$

C.4.9 SLOPE II

Calculate slope distribution

$$\Theta_i = \sum_{j}^{i} \frac{M_j}{EI_j} \Delta x_j$$

C.4.10 DEFLECT II

Calculate deflection distribution

$$y_i = \sum_{j}^{i} \Theta_j \Delta x_j$$

C.5 AXIAL - PRELAUNCH

C.5.1 PREPARE IV

Select and store axial weight distribution, Λ_i

C.5.2 MASS II

Calculate total weight

$$W = \sum_{i} \Lambda_i$$

C.5.3 FORCE III

Calculate axial force distribution

$$\delta_i = W_{i=H_o} - \sum_{j}^{i} \Lambda_j$$

C.6 NOMENCLATURE

α	Angle of attack (degrees).
β	Engine gimbal angle (degrees).
N	Resultant aero force normal to vehicle axis (lbs).
T	Total thrust of all engines (lbs).
T_g	Control thrust (lbs).
T_a	Axial component of thrust (lbs).
CP	Station of center of pressure (inches).
CG	Station of center of gravity (inches).
C_o	Station of engine gimbal point (inches).
H_b	Station of hold-down point for restraining bending moments (inches).
H_o	Station of hold-down point for supporting vehicle weight on the launch pad (inches).
x	Dimension along vehicle centerline (inches).
i	Subscript denoting successive, discrete stations along vehicle axis.
ϵ	Lateral rigid body acceleration of vehicle (in/sec^2).
ϕ	Axial rigid body acceleration of vehicle (in/sec^2).
Ω	Angular rigid body acceleration of vehicle (rad/sec^2).
f_i	Linear normal aero force at station x_i (lbs).
d_i	Nonlinear normal aero force at station x_i (lbs).
μ_i	Axial drag force at station x_i (lbs).
w_i	Weight at station x_i - lateral distribution (lbs).

Λ_i Weight at station x_i - axial distribution (lbs).

I_p Pitch moment of inertia about CG (in-lb-sec^2).

g Acceleration of gravity on earth's surface (in/sec^2).

W Total weight of vehicle at a particular time (lbs).

Δ Resultant linear normal aero force (lbs).

η Resultant nonlinear normal aero force (lbs).

CP_l Station of center of pressure for linear aero forces (inches).

CP_b Station of center of pressure for nonlinear aero forces (inches).

M_a Aero moment about CG (in-lbs).

M_c Control moment about CG (in-lbs).

a_i Total lateral acceleration at station x_i (in/sec^2).

F_i Total equivalent lateral force at station x_i (lbs).

V_i Shear at station x_i (lbs).

M_i Bending moment at station x_i (in-lbs).

Θ_i Slope at station x_i (radians).

y_i Lateral deflection at station x_i (inches).

$(\Delta x)_i$ Equal to $x_{i+1} - x_i$ (inches).

D Total axial drag on vehicle (lbs).

C_{d_i} Drag coefficient at station x_i.

$C_{z_{\alpha_i}}$ Linear normal aero force coefficient at station x_i.

$C_{z_{cf_i}}$ Nonlinear normal aero force coefficient at station x_i.

v_i Wind velocity at station x_i (in/sec).

M_{w_i} Bending moment at station x_i due to winds (in-lbs).

l Station of most extreme position of vehicle (inches).

q_i Dynamic pressure at station x_i (lbs/in^2).

M_{v_i} Bending moment at station x_i due to vortex shedding (in-lbs).

M_{s_i} Equal to $M_{w_i} + M_{v_i}$ (in-lbs).

M_{e_i} Bending moment at station x_i due to weight eccentricity (in-lbs).

$(\Delta y)_i$ Equal to $y_{i+1} - y_i$ (inches).

$(EI)_i$ Bending stiffness at station x_i (lbs-in^2).

S Reference area (in^2).

$C_{z_{co_i}}$ Cross-flow coefficient for ground winds.

APPENDIX D

EXECUTIVE CONTROL PROGRAM

Since the executive control program is a logic controlling computer program rather than a program that performs scientific computations, a detailed description of engineering concepts is not applicable to this appendix.

A detailed description of the executive control program logic has been deferred to Volume 2 (the Programming Manual) of this document.

A general flow chart, however, is presented here (see Figure D-1) to aid in understanding Section 4 (Executive Control Program Description and Philosophy) of this document.

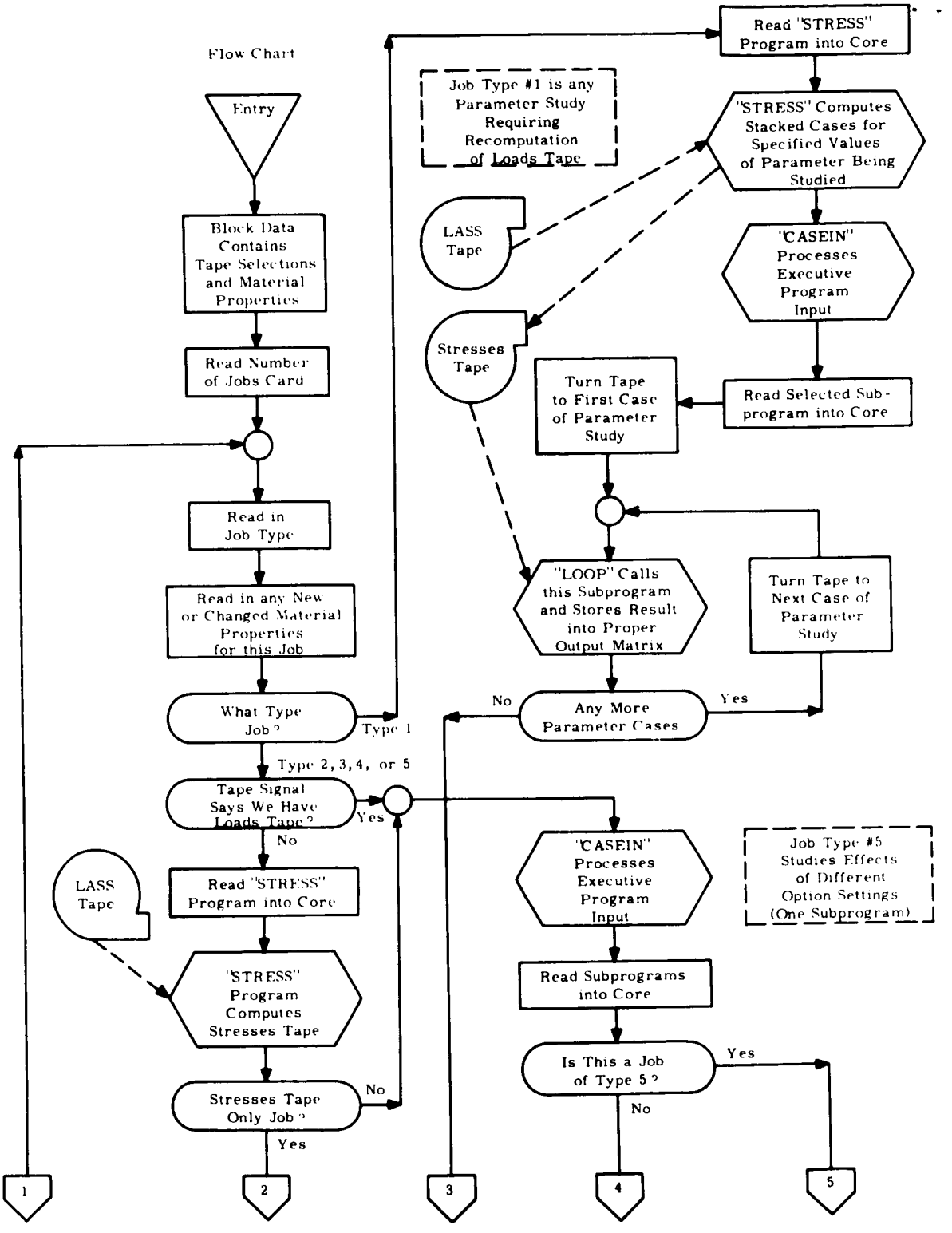

Figure D-1. Executive Control Program - Saturn V Structural Suboptimization

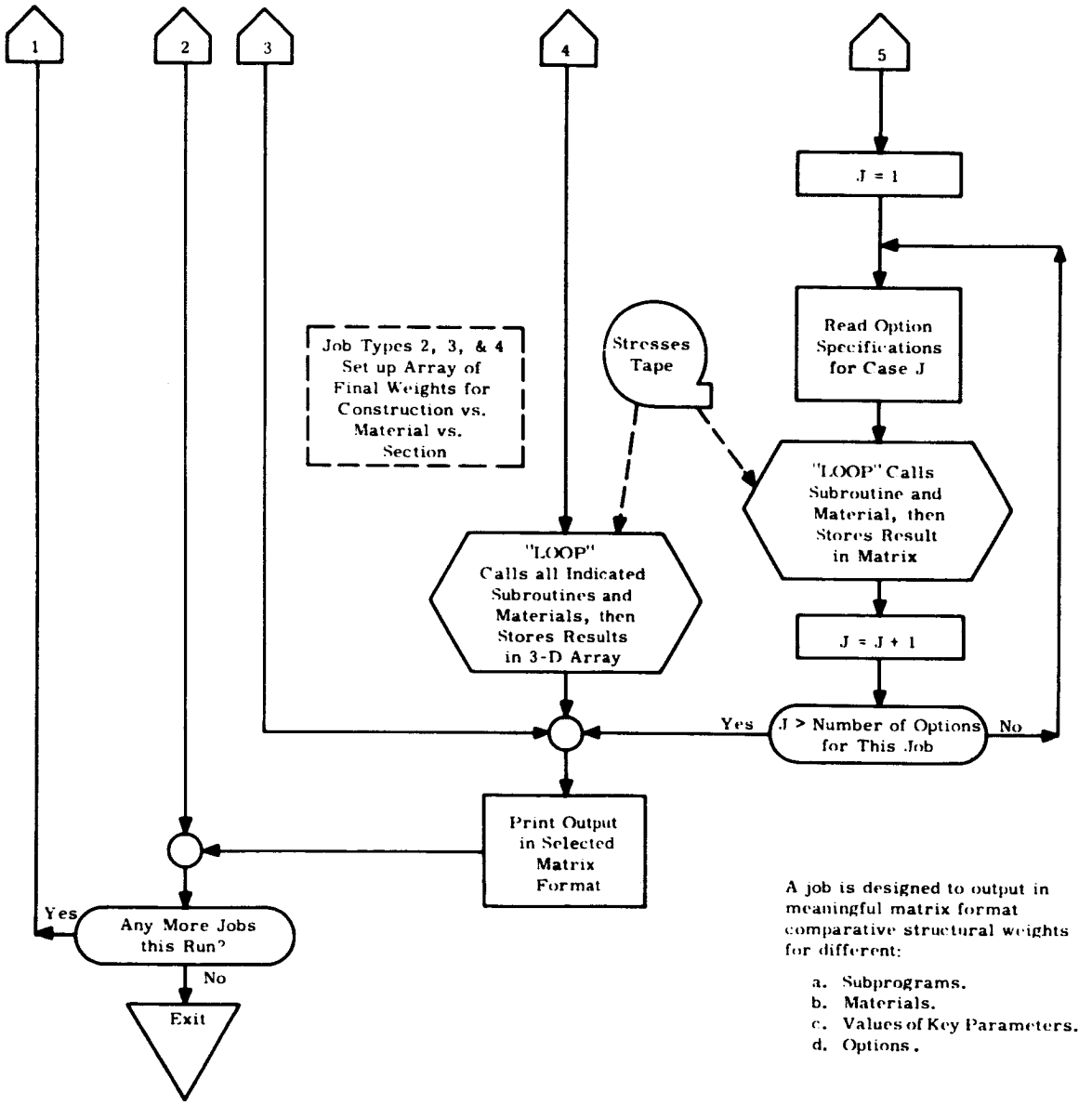

Figure D-1. Executive Control Program - Saturn V Structural Suboptimization (Cont.)

APPENDIX E

EQUATIONS USED IN STRESS PROGRAM

E.1 LIQUID LEVEL CALCULATION IN ELLIPTICAL HEADS

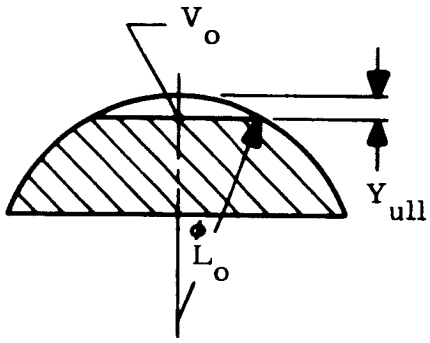

Figure E-1. Initial Liquid Level Arrangement in Upper Head

It is desirable that the input to the computer program be such that a "percent ullage" or ullage height can be used as input for calculating the liquid level in the tanks. Assuming a constant flow rate of the liquid, the empty volume can be expressed as

$$V_i = V_o + \sum_{j=1}^{i} \Delta V_j$$

where

$V_o = nV_T$

$\Delta V_i = G\Delta t_i$

G = flow rate (ft^3/sec)

V_T = total tank volume

n = percent ullage/100

V_i = empty tank volume at time t_i

Substituting for the quantities in the above equation gives

$$V_i = nV_T + G \sum_{j=1}^{i} \Delta t_j$$

The empty volume can also be expressed as

$$V_i = \pi a^2 \left(\frac{y_{ull}^2}{b} - \frac{y_{ull}^3}{3b^2} \right)$$

Equating expressions for V_i yields

$$y_{ull_i}^2 \left(3b - y_{ull_i} \right) = \frac{3b^2}{\pi a^2} \left(nV_T + G \sum_{j=1}^{i} \Delta t_j \right)$$

This is a cubic equation which will be solved by the Newton-Raphson iteration scheme for the liquid level in the head. Knowing the liquid level, the angle ϕ at the liquid level can be determined

$$y_{ull_i} = b - \frac{r}{k^2} \cot \phi_{L_i}$$

$$r = k \left[y_{ull_i} \left(2b - y_{ull_i} \right) \right]^{\frac{1}{2}}$$

Hence

$$\phi_{L_i} = \cot^{-1} \left\{ \frac{k \left(b - y_{ull_i} \right)}{\left[y_{ull_i} \left(2b - y_{ull_i} \right) \right]^{\frac{1}{2}}} \right\}$$

If the initial liquid height is known, it can be input directly and the angle of the liquid level can be determined immediately from the above equation. The initial empty volume, $V_o = nV_T$, can be calculated as previously shown and subsequent liquid levels determined by iteration on the equation for V_i as previously discussed. The liquid level calculation for the lower head is very similar and will not be discussed here.

E.2 STRESS RESULTANT EXPRESSIONS

The stress resultants for the meridional and circumferential directions of a general conical section are given by the equations shown in Figure E-2.

$$N_x = -\frac{\beta\gamma}{6r\cos\phi}(2r^3 - 3r\bar{r}^2 + r^3) + \frac{\beta\gamma d}{2r\sin\phi}(\bar{r}^2 - r^2) + \frac{Pr}{2\sin\phi} + \frac{F}{2\pi r\sin\phi} \pm \frac{M}{\pi r^2\sin\phi}$$

$$N_\theta = \frac{r}{\sin\phi}(\beta\gamma d + P)$$

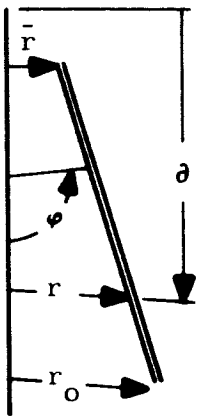

Figure E-2. Stress Resultant Expressions

These equations are valid for all conical shells. For shell segments above a propellant level, one must set the propellant density, γ, to zero.

It is more difficult to express a general set of equations for an elliptical head since the form of the equations depends upon the orientation. Consider first of all an elliptical head that is a lower dome of a separate bulkhead tank as shown in Figure E-3.

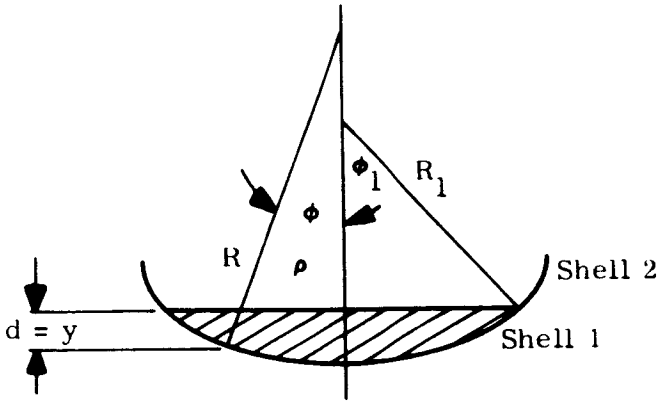

Figure E-3. Elliptical Lower Dome Head of Bulkhead Tank

For the shell below the liquid level, the stress resultants are given by

$$N_x = \frac{PR}{2} + \frac{\beta\gamma R}{2}\left\{d + \frac{R\sin\phi}{3}\left[\frac{2}{k}\left(1 + \frac{\cot^2\phi}{k^2}\right)^{\frac{3}{2}} - \frac{3}{k^2}\cot\phi - \frac{2}{k^4}\cot^3\phi\right]\right\}$$

$$N_\theta = \frac{PR}{2}\left(2 - \frac{R}{R_s}\right) + \beta\gamma d R$$

$$- \frac{\beta\gamma R^2}{2R_s}\left\{d + \frac{R\sin\phi}{3}\left[\frac{2}{k}\left(1 + \frac{\cot^2\phi}{k^2}\right)^{\frac{3}{2}} - \frac{3}{k^2}\cot\phi - \frac{2}{k^4}\cot^3\phi\right]\right\}$$

For the portion of the shell above the liquid level, the stress resultants become

$$N_x = \frac{PR}{2} + \frac{W(\phi_1)}{2\pi R\sin^2\phi}$$

$$N_\theta = \frac{PR}{2}\left(2 - \frac{R}{R_s}\right) - \frac{W(\phi_1)}{2\pi R_s\sin^2\phi}$$

where

$$W(\phi_1) = \frac{\beta\gamma\pi R^3\sin^3\phi_1}{3}\left[\frac{2}{k}\left(1 + \frac{\cot^2\phi_1}{k^2}\right)^{\frac{3}{2}} - \frac{2}{k^2}\cot\phi_1 - \frac{2}{k^4}\cot^3\phi_1\right]$$

The equations for an upper dome are somewhat different. The stress resultants for the shell shown in Figure E-4 are

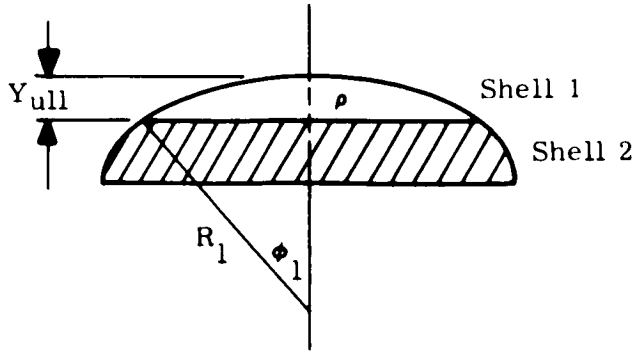

Figure E-4. Elliptical Upper Dome Head of Bulkhead Tank

For the portion of the shell below the liquid level

$$N_x = \frac{PR}{2} + \frac{V_u}{\sin \phi}$$

$$N_\theta = \frac{PR}{2}\left(2 - \frac{R}{R_s}\right) + \beta\gamma R\left(b - \frac{R}{k^2}\cos\phi - y_{ull}\right) - \frac{R}{R_s}\frac{V_u}{\sin\phi}$$

where

$$V_u = \frac{\beta\gamma k^2}{R \sin\phi}\left\{\frac{b + y_{ull}}{2}\left[\left(b - \frac{R}{k^2}\cos\phi\right)^2 - y_{ull}^2\right]\right.$$

$$+ \frac{1}{3}\left[y_{ull}^3 - \left(b - \frac{R}{k^2}\cos\phi\right)^3\right]$$

$$\left. + by_{ull}\left[y_{ull} - \left(b - \frac{R}{k^2}\cos\phi\right)\right]\right\}$$

The equations for the stress resultants of the portion of the shell above the liquid level are the same as those given above, with γ set equal to zero.

For a common bulkhead tank configuration, the equations are even more complex. Consider the general case in Figure E-5 where the liquid levels are as shown.

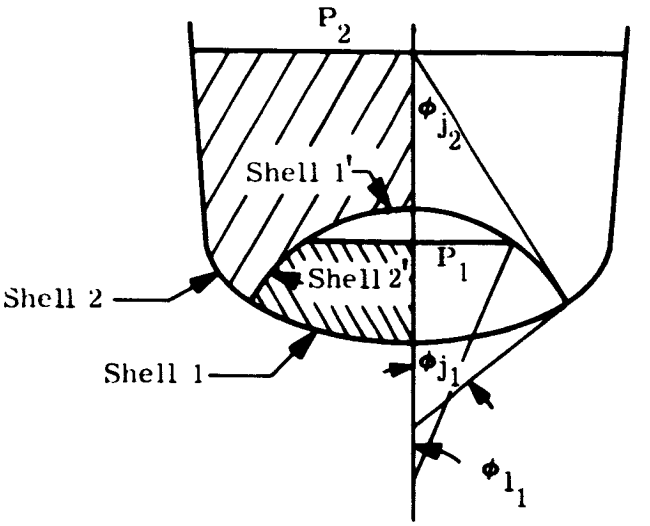

Figure E-5. Common Bulkhead Tank General Case

For shell 1'

$$N_x = (P_1 - P_2)\frac{R}{2} + \frac{W - C}{2\pi R \sin^2 \phi}$$

$$N_\theta = (P_1 - P_2)\left(2 - \frac{R}{R_s}\right)\frac{R}{2} - \beta\gamma dR - \frac{W - C}{2\pi R_s \sin^2 \phi}$$

For shell 2'

$$N_x = (P_1 - P_2)\frac{R}{2} + \frac{W - C}{2\pi R} + \frac{V_u}{\sin \phi}$$

$$N_\theta = (P_1 - P_2)\left(2 - \frac{R}{R_s}\right)\frac{R}{2} + \beta R(y_u\gamma_1 - d\gamma_2) - \frac{W - C}{2\pi R_s \sin^2 \phi} - \frac{R}{R_s}\frac{V_u}{\sin \phi}$$

where

$$V_u = \frac{\beta\gamma k^2}{R \sin \phi}\left\{\frac{b + y_{ull}}{2}\left[\left(b - \frac{R}{k^2}\cos \phi\right)^2 - y_{ull}^2\right]\right.$$

$$+ \frac{1}{3}\left[y_{ull}^3 - \left(b - \frac{R}{k^2}\cos \phi\right)^3\right]$$

$$\left. + by_{ull}\left[\left(-b + \frac{R}{k^2}\cos \phi\right) + y_{ull}\right]\right\}$$

$$y_u = b - \frac{R}{k^2}\cos \phi - y_{ull}$$

$$W = \frac{\beta\gamma\pi R^3 \sin^3 \phi}{3}\left[\frac{2}{k}\left(1 + \frac{\cot^2 \phi}{k^2}\right)^{\frac{3}{2}} - \frac{3}{k^2}\cot \phi - \frac{2}{k^4}\cot^3 \phi\right]$$

$$C = \pi\beta\gamma R^2 \sin^2 \phi d$$

For shell 1, the equations are as for the shell shown in Figure E-3, if the definition of d is changed to

$$d = \hat{y}(\phi_{l_1}) + y$$

where

$$\hat{y}(\phi_{l_1}) = b^2\left[\frac{\cos\phi_{l_1}}{\left(a^2\sin^2\phi_{l_1} + b^2\cos^2\phi_{l_1}\right)^{\frac{1}{2}}} - \frac{\cos\phi_{j_1}}{\left(a^2\sin^2\phi_{j_1} + b^2\cos^2\phi_{j_1}\right)^{\frac{1}{2}}}\right]$$

For shell 2, the equations are

$$N_x = \frac{C + W}{2\pi R\sin^2\phi} + \frac{W_{T_1} - \beta\gamma_2\left[V_{T_1} - V_\epsilon\left(\hat{\phi}_{l_2}\right)\right]}{2\pi R\sin^2\phi}$$

$$N_\theta = \beta\gamma_2 dR - \frac{R}{R_x}\left\{\frac{C + W}{2\pi R\sin^2\phi} + W_{T_1} - \beta\gamma_2\left[V_{T_1} - V_\epsilon\left(\hat{\phi}_{l_2}\right)\right]\right\}$$

where

$$V_\epsilon\left(\hat{\phi}_{l_2}\right) = \frac{\pi R^3\sin^3\hat{\phi}_{l_2}}{3}\left[\frac{2}{k}\left(1 + \frac{\cot^2\hat{\phi}_{l_2}}{k^2}\right)^{\frac{3}{2}} - \frac{3}{k^2}\cot\hat{\phi}_{l_2} - \frac{2}{k^4}\cot^3\hat{\phi}_{l_2}\right]$$

and C and W are as given before.

With a common bulkhead, the equations can change as the liquid level changes. Consider Figure E-6, which is the same as Figure E-5 with the exception of the liquid levels.

For shell 1, use the equations relating to Figure E-3, with $P = P_1$ for the equations below the liquid level.

For shell 2, use the equation relating to Figure E-3, with $\phi_l = \phi_{l_1}$ for the equations above the liquid level.

For shell 3, let $P = P_1 - P_2$ in the equations for the dome of Figure E-4 above the liquid level.

For shell 4, use the equations for shell 1' of Figure E-5, with the substitution

$$y = b^2\left[\frac{\cos\phi}{(a^2\sin^2\phi + b^2\cos^2\phi)^{\frac{1}{2}}} - \frac{\cos\phi_{j_1}}{\left(a^2\sin^2\phi_{j_1} + b^2\cos^2\phi_{j_1}\right)^{\frac{1}{2}}}\right]$$

For shell 5, use the equations for shell 2 of Figure E-5.

For shell 6, the equations for the stress resultants are

$$N_x = \frac{W_{T_2} + W_{T_1}}{2\pi R\sin^2\phi} + \frac{P_2 R}{2}$$

$$N_\theta = \frac{P_2 R}{2}\left(2 - \frac{R}{R_s}\right) - \frac{W_{T_2} + W_{T_1}}{2\pi R_s\sin^2\phi}$$

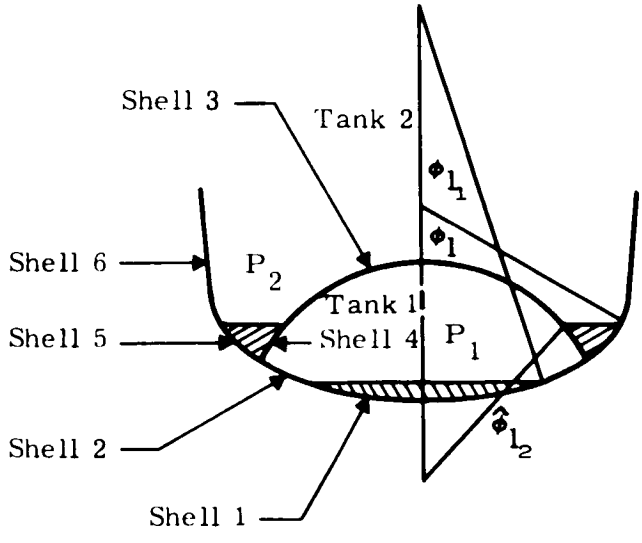

Figure E-6. Common Bulkhead Tank General Case with Different Liquid Levels

E.3 NOMENCLATURE

a	Semi-major axis of the elliptical head (inches).
b	Semi-minor axis of the elliptical head (inches).
d	Distance from the liquid level to the point in question on the elliptical head (inches).
d_1	Distance from the liquid level to the top of the elliptical head (inches).
y	Distance from the top of the elliptical head to the point in question on the elliptical head (inches); coordinate.
R	Distance from the normal to the shell middle surface to the point of interception with the shell centerline (inches).
R_s	Meridional radius of curvature of shell middle surface (inches).
r	Horizontal radius of shell middle surface (inches).
ϕ	Latitude angle, measured from shell centerline.
β	Number of g's acceleration.
γ	Specific weight of liquid ($lb/inch^3$).
V_ϵ	Volume of elliptical segment ($inch^3$).
$\overline{\phi}$	Edge value of ϕ.
ϕ_1	Value of ϕ at the liquid level.
y_{ull}	Ullage height in a tank.
E	Modulus of elasticity ($lb/inch^2$).
h	Shell thickness (inches).
k	Ratio of semi-major and semi-minor axes, a/b.
y_u	Distance below liquid level in upper head to point under consideration (inches).
μ	Poisson's ratio.
d_2	Distance from elliptical head - conical shell junction to the junction of the common bulkhead with the lower head.
W_{T_1}	Total weight of the liquid in tank number 1 (lb).
W_{T_2}	Total weight of liquid in tank 2 (lb).

V_{T_1}	Total volume of tank number 1.
$\hat{\phi}_{l_1}$	The latitude angle of the common bulkhead at the liquid level of tank 1 (radians).
$\hat{\phi}_{l_2}$	The latitude angle of the common bulkhead at the liquid level of tank 2 (radians).
V	Vertical force (lb/inch).
$N_{s,\theta}$	Meridional and hoop tension force (lb/inch).
P_z	Applied load normal to shell, acting inward (lb/inch^2).
P	Internal pressure (lb/inch^2).
δ	Radial (outward) displacement (inches).
χ	Increase in latitude angle (angle of rotation) (radians).
$\epsilon_{\theta,s}$	Strains in θ, s directions (inches/inch).
$\sigma_{\theta,s}$	Hoop and meridional stress (lb/inch^2).
P_{cr}	True axial buckling load of cone or cylinder (lb).
σ_{cr}	True critical buckling stress of cone or cylinder (lb/inch^2).
C	Correction factor.
t	Constant wall thickness of cone or cylinder (inches).
α	Semivertex angle of cone (radians).

APPENDIX F

AXIAL BUCKLING OF ORTHOTROPIC CYLINDERS

F.1 GENERAL

In the selection of orthotropic buckling criteria, the following requirements have to be fulfilled:

a. Generalized formulae that would be applicable for the various types of orthotropic structures being considered.

b. Selection of a theory that is substantiated with test data.

Based on these requirements, a generalized form of the Becker[9] equation is used, as follows

$$P_{cr} = 4\pi \left(\frac{\beta^2 D_{11} + D_{33}}{\frac{\beta^2}{A_{11}} + \frac{1}{2A_{33}}} \right)^{\frac{1}{2}}$$

where

$$\beta^2 = P_o + \left(P_o^2 + Q_o \right)^{\frac{1}{2}}$$

$$P_o = \frac{A_{33}}{A_{22}} \left(\frac{A_{22}D_{11} - A_{11}D_{22}}{A_{11}D_{22} - 2A_{33}D_{33}} \right)$$

$$Q_o = \frac{A_{11}}{A_{22}} \left(\frac{A_{22}D_{11} - 2A_{33}D_{33}}{A_{11}D_{22} - 2A_{33}D_{33}} \right)$$

By defining the stiffness parameters, the equation is adaptable for any type of orthotropic cylinder. In fact, by substituting the correct stiffness parameters for an isotropic cylinder, the equation reduces to the classical buckling solution for isotropic cylinders with the exception of Poisson's ratio, which has been assumed equal to zero. However, since we are dealing with the square of a very small number (Poisson's ratio), the difference is very slight.

In order to substantiate the theory, a literature survey was conducted to locate test data for axially loaded orthotropic cylinders. The theoretical buckling loads were calculated based on the generalized Becker equation and compared with the test results. The results of the study are shown on Figure F-1. As can be expected from past experience with the buckling of isotropic cylinders, the data shows considerable scatter. It can be concluded that a correction factor is required for each type of construction considered, as has been the case for isotropic cylinders.

F.2 NOMENCLATURE

A_{11} Extensional stiffness in longitudinal direction (lb/inch).

A_{22} Extensional stiffness in hoop direction (lb/inch).

A_{33} Shear stiffness (lb/inch).

D_{11} Flexural stiffness in longitudinal direction (inch-lb/radian).

D_{22} Flexural stiffness in hoop direction (inch-lb/radian).

D_{33} Torsional stiffness (inch-lb/radian).

P_{cr} Critical buckling load (pounds).

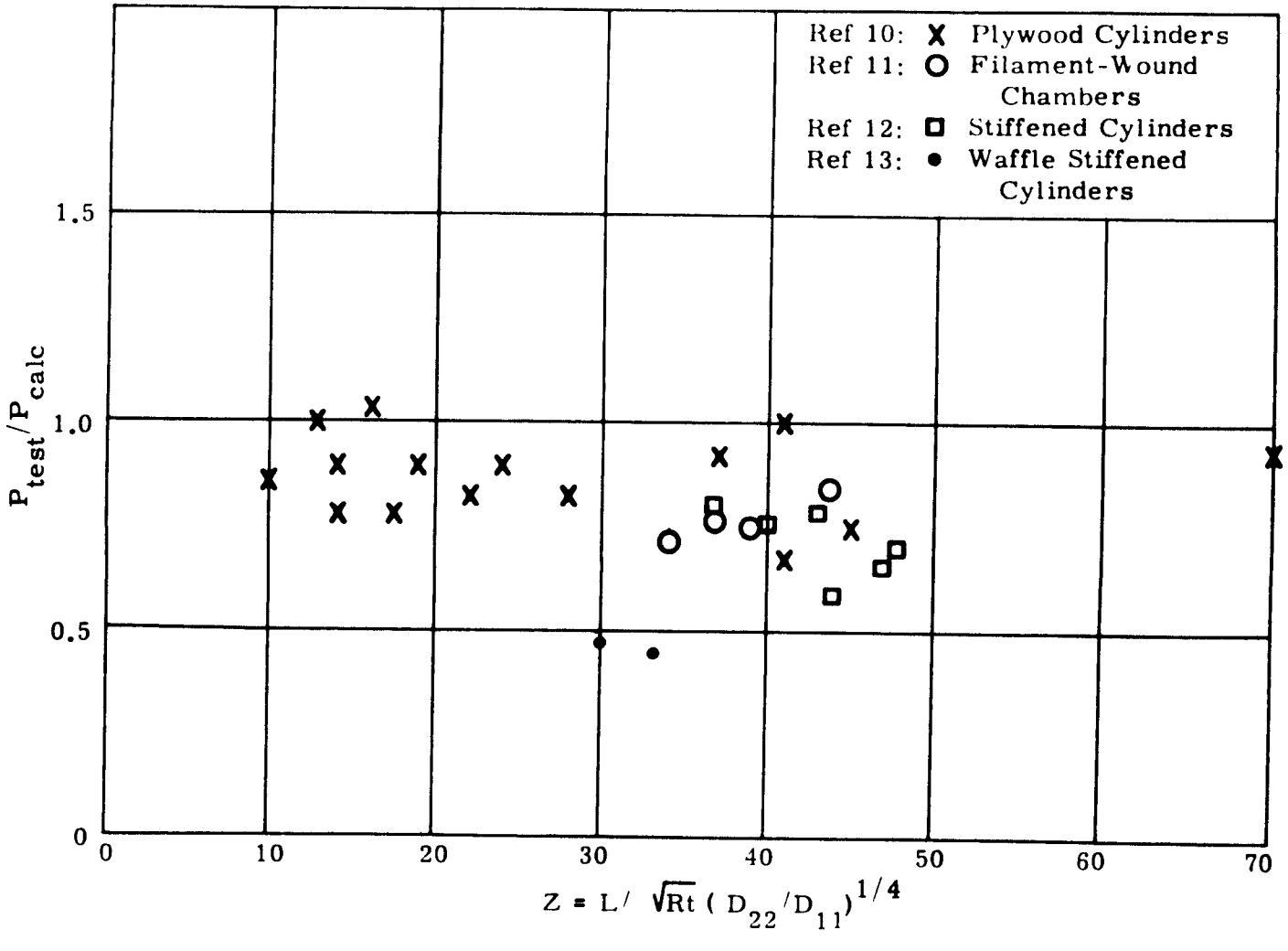

Figure F-1. Axially Loaded Orthotropic Cylinders

APPENDIX G

MONOCOQUE ANALYSIS

G.1 STRENGTH ANALYSIS

All of the loads acting on the launch vehicle, as calculated by the LASS-1 computer program, plus the pressure and hydrostatic loads, are resolved into stress resultants N_x and N_θ in the SWOP program. It is then necessary to apply some criterion to these stress resultants so that a skin thickness can be determined at each station of the vehicle which will support the most severe loading condition that occurs at that station throughout the flight. A question then arises about which strength criterion to use.

The common philosophy of all theories of strength is to predict the behavior of a material for generally complex stress states on the basis of experimental observations under particularly simple and well-duplicated conditions, e.g., uniaxial states of stress. For isotropic materials, the orientation of the principal axes is immaterial, and the values of the three principal stresses suffice to describe the state of stress uniquely.

Some of the older theories proposed through the years are:

a. The Lame'-Navier Theory.
b. Maximum-Normal-Strain Theory (Saint-Venant).
c. Beltrami's Energy Theory.
d. Maximum-Shearing-Stress Theory.
e. Mohr's Theory.

The first three of these theories conflict with experimental evidence, and Mohr's theory may be considered as a generalized version of the maximum-shearing-stress theory.

There are two theories available to predict yielding in ductile metals. Both require the knowledge of the "yield stress" in the uniaxial state of stress in order to predict the behavior under any given combination of principal stresses. The "yield stress" is assumed to be identical in tension and compression. These theories are:

a. The "maximum-shearing-stress" condition (Tresca and Saint-Venant) - This yield condition states that plastic yielding begins when the maximum shear

stress reaches a critical value. This condition can be stated as

$$\sigma_I - \sigma_{III} = \sigma_{eff}$$

for a uniaxial state of stress.

The principal stresses, σ_I and σ_{III}, are ordered from larger to smaller respectively, and σ_{eff} is the "yield stress."

b. The "energy-of-distortion" condition (von Mises and Hencky) - In terms of the principal normal stresses, this yield condition is stated as

$$2\,\sigma_{eff}^2 = (\sigma_1 - \sigma_2)^2 + (\sigma_2 - \sigma_3)^2 + (\sigma_3 - \sigma_1)^2$$

For this program, the von Mises-Hencky theory will be used. Under the assumptions of this analysis, the expression used to determine the skin thickness is

$$t_s = \left(N_x^2 + N_\theta^2 - N_x N_\theta\right)^{\frac{1}{2}} \frac{1}{\sigma_{all}}$$

where σ_{all} is the smaller of the two values: σ_{yield} and $\sigma_{ult}/1.4$.

The assumption has been made that the radial stress, σ_r, is negligible in comparison with σ_x and σ_θ.

The values of the stress resultants will change as a function of time at each station of the vehicle. Several time points will be selected during the vehicle flight at which to make an analysis and determine the stress resultants. From this catalog of stress resultants plus those due to the hydrostatic test conditions, the combination giving the largest value of

$$\left(N_x^2 + N_\theta^2 - N_x N_\theta\right)^{\frac{1}{2}}$$

for each station will be chosen, and the time at which this maximum occurs will be indicated.

Consideration of the practical aspect of design will probably prohibit the use of a monocoque shell section with a continuously varying skin thickness which the above calculation procedure gives. Actually, the vehicle will be manufactured by joining by several

sections, each having a constant thickness throughout. Therefore, this consideration has been built into the program in a manner such that the sections will not be longer than a preselected value and the largest required thickness in that section will govern the thickness of this section.

For instance, if a cylindrical tank is 485 inches long and the decision is made to manufacture the tank with cylindrical segments not more than 100 inches long, then the program will automatically select five sections of equal length to make up the tank. In each of these equal-length sections, the maximum thickness required to support the imposed loads is determined and the entire section is made with this thickness.

G.2 BUCKLING ANALYSIS

In addition to the strength analysis, the primary structural components of the launch vehicle must be subjected to a buckling criterion. Buckling occurs at a very low stress for monocoque shells with diameters of the magnitude considered here, and it is anticipated that buckling criteria will dictate a large portion of the design with monocoque construction.

The lowest critical buckling load for circular cones under axial compression has been determined in Reference 14 as

$$P = \frac{2Et^2\pi\cos^2\alpha}{3(1-\mu^2)^{\frac{1}{2}}}$$

It is well known that a considerable discrepancy exists between experimental and theoretical buckling loads of thin shells, particularly when calculations are based upon small deflection theory. In practice, this discrepancy is usually handled by multiplying the classical load by an experimental correction factor, C, using equations of the form

$$P_{cr} = 2\pi CEt^2\cos^2\alpha$$

$$\sigma_{cr} = \frac{CEt\cos\alpha}{r}$$

The buckling correction factor can be approximated by

$$C = 9\left(\frac{t\cos\alpha}{R}\right)^{0.6}$$

Substituting the required thickness for buckling into the allowable buckling stress equation

$$t_{buckling} = \left[\frac{N_x R^{1.6}}{9E(\cos\alpha)^{1.6}}\right]^{0.385}$$

Lackman and Penzien[14] have presented an experimentally determined curve for the correction coefficient for cones and cylinders as shown in Figure G-1.

The equations for P_{cr} and σ_{cr} discussed previously are applicable to cones and reduce to the equations generally used for cylinders when the semivertex angle, α, equals zero.

Designing a section of the launch vehicle for buckling requires that the maximum axial compressive stress resultant in that section be determined. This is easily done in the sense that the loads are all resolved into stress resultants in the planes of the shells. However, before this maximum can be chosen, the stress resultants must be examined for all stations in that section, for all times selected for calculation.

Once the maximum compressive stress resultant has been determined and the thickness calculated that is necessary to support this load, this thickness must then be compared with the thicknesses calculated at each station in the section by the strength criterion. The larger of the two thicknesses is, therefore, stored and an optimum thickness distribution of the launch vehicle is determined for the monocoque construction.

If this thickness is in the range that is allowable from practical considerations, the thickness is accepted. If, for instance, the thickness is less than the minimum gage allowed, then the minimum gage is used instead and the off-optimum design is used to calculate the section weight.

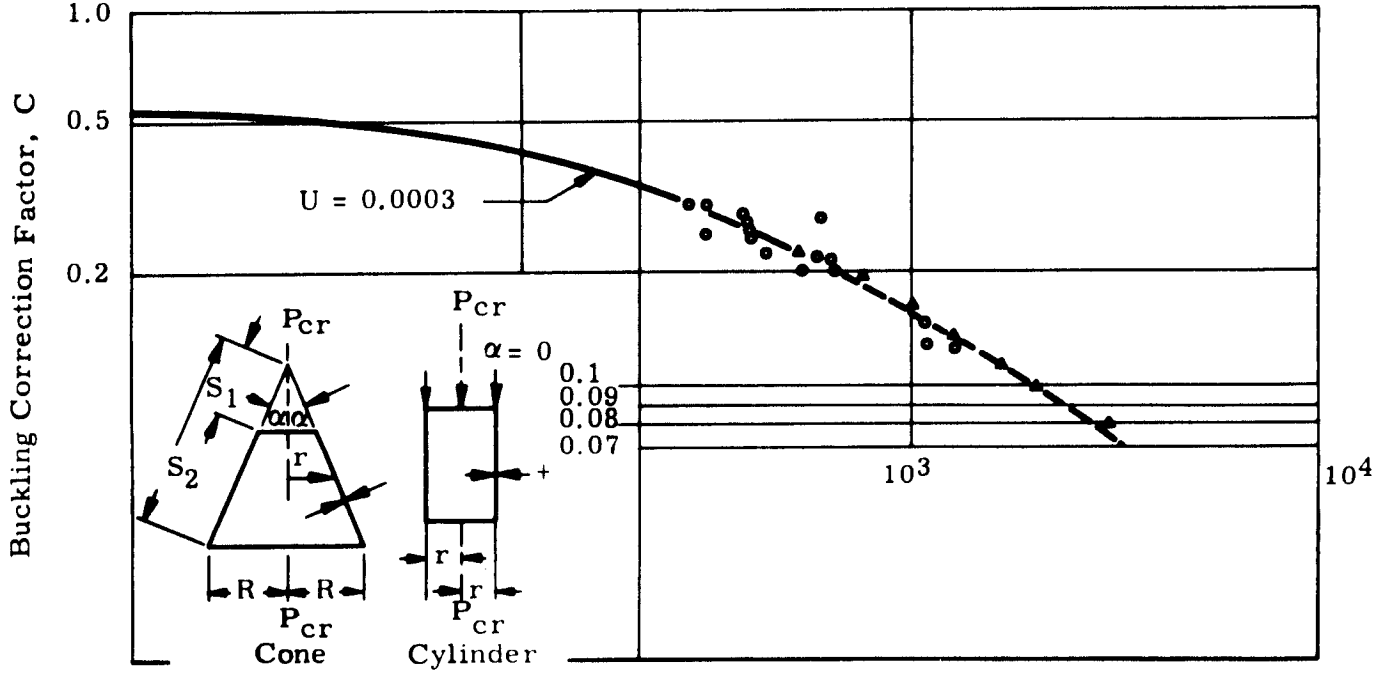

Figure G-1. Buckling Correction Factor, C, for Cylinders or Cones

APPENDIX H

HONEYCOMB SANDWICH

H.1 INTRODUCTION

A honeycomb sandwich cylinder consists of two high-density faces and a low-density core material. The purpose of this appendix is to establish a method for optimizing this type of structure when subjected to axial loading and/or internal pressure. Two modes of failure are considered: strength based on the von Mises yield criteria, and buckling which consists of both general and local instability. The local instability includes face wrinkling, monocell buckling, and shear instability.

In calculating the strength, i.e., the non-buckling requirements of the shell, it has been assumed that the faces resist all of the load and that these faces consist of equal thicknesses. The basic function of the low-density core is to provide the shell with overall stability, therefore, it has been assumed that the internal pressure has little or no effect on the buckling load carrying capacity.

The following formulae for honeycomb core properties have been developed[15] from Figure H-1.

$$\rho_c = \frac{8}{3} \frac{t}{d} \gamma_c$$

$$G_{lt} = \frac{5}{3} \frac{t}{d} G' = \frac{5}{8} \frac{\rho_c}{\gamma_c} G'$$

$$E_c = \frac{8}{3} \frac{t}{d} E' = \frac{\rho_c}{\gamma_c} E'$$

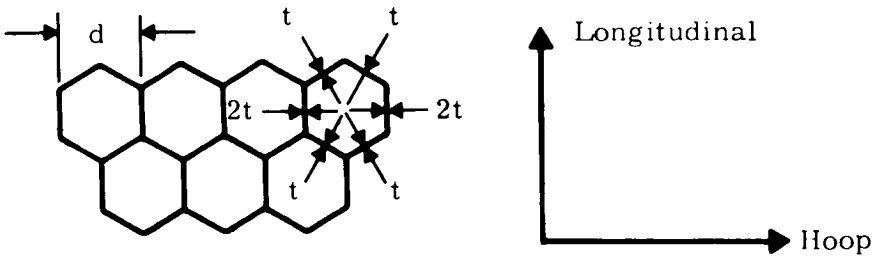

Figure H-1. Cross Section of Hexagonal Core

Evaluating the equations on the preceding page, it follows that

$$G_{lt} = C_1 \rho_c$$

$$E_c = C_1 \rho_c$$

The following formulae have been developed[15] from Figure H-2

$$\rho_c = 2\frac{t}{d}\gamma_c$$

$$G_{lt} = G_{nt} = \frac{t}{d} G' = \frac{\rho_c}{2\gamma_c} G'$$

$$E_c = 2\frac{t}{d} E' = \frac{\rho_c}{\gamma_c} E'$$

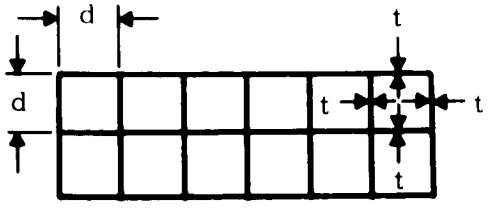

Figure H-2. Cross Section of a Square Cell

Evaluating the above equations, it follows that

$$G_{lt} = C_1 \rho_c$$

$$E_c = C_2 \rho_c$$

It can be concluded that the core shear modulus and the elastic modulus of the core material are directly proportional to the core density. The advantage of using C_1 and C_2 can be seen when attempting to establish a relationship for plastic honeycombs. It is very difficult to obtain values of G' and E' for plastic core materials.

Consequently, it is simpler to make a plot of modulus versus density using experimental values from the vendor and determine the slope of the resulting line.

For example[16], nylon modified phenolic resin using cloth type 21 gives the following criteria, which are plotted in Figure H-3.

Honeycomb Designation	G_{lt}	ρ_c
NP - 1/4 - 21 - 4	15,500	4
NP - 1/4 - 21 - 6	20,500	6
NP - 1/4 - 21 - 8	25,000	8
NP - 3/8 - 21 - 2.5	10,000	2.5
NP - 3/8 - 21 - 4.5	15,000	4.5

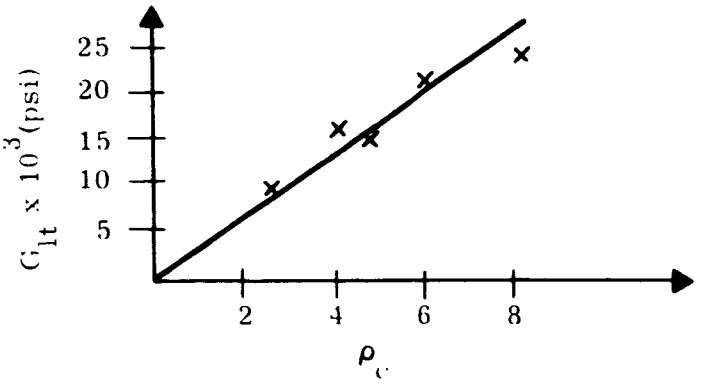

Figure H-3. Plot of Modulus versus Density

A determination of C_1 can be made from Figure H-3, i.e., for NP-1/4-21-6 hexcomb

$$C_1 = \frac{20,500}{6} = 3.42 \times 10^3 \ \frac{psi}{lb/ft^3}$$

The following is a list of some values of C_1 and C_2 for typical materials:

Material	Type of Core	C_1	C_2
2024-T3 Aluminum	Hex	14.4×10^3	57.8×10^3
7075-T6 Aluminum	Hex	14.1×10^3	60.7×10^3
PH-15-7Mo Steel	Square	11.5×10^3	63.0×10^3
PH-15-7Mo Steel	Hex	14.4×10^3	62.7×10^3

H.2 FAILURE MODES

H.2.1 GENERAL INSTABILITY[16]

Given a face working stress, it is required to determine the core thickness needed to stabilize the cylinder (see Figure H-4). The procedure is:

a. Assume t_c, then calculate

$$Z = \frac{2L^2}{D(t_c + t_f)}$$

$$U = G_{lt}(t_c + 2t_f)$$

$$D_f = \frac{1}{2} E_f t_f (t_c + t_f)^2$$

$$J = \frac{L^2 U}{\pi^2 D_f}$$

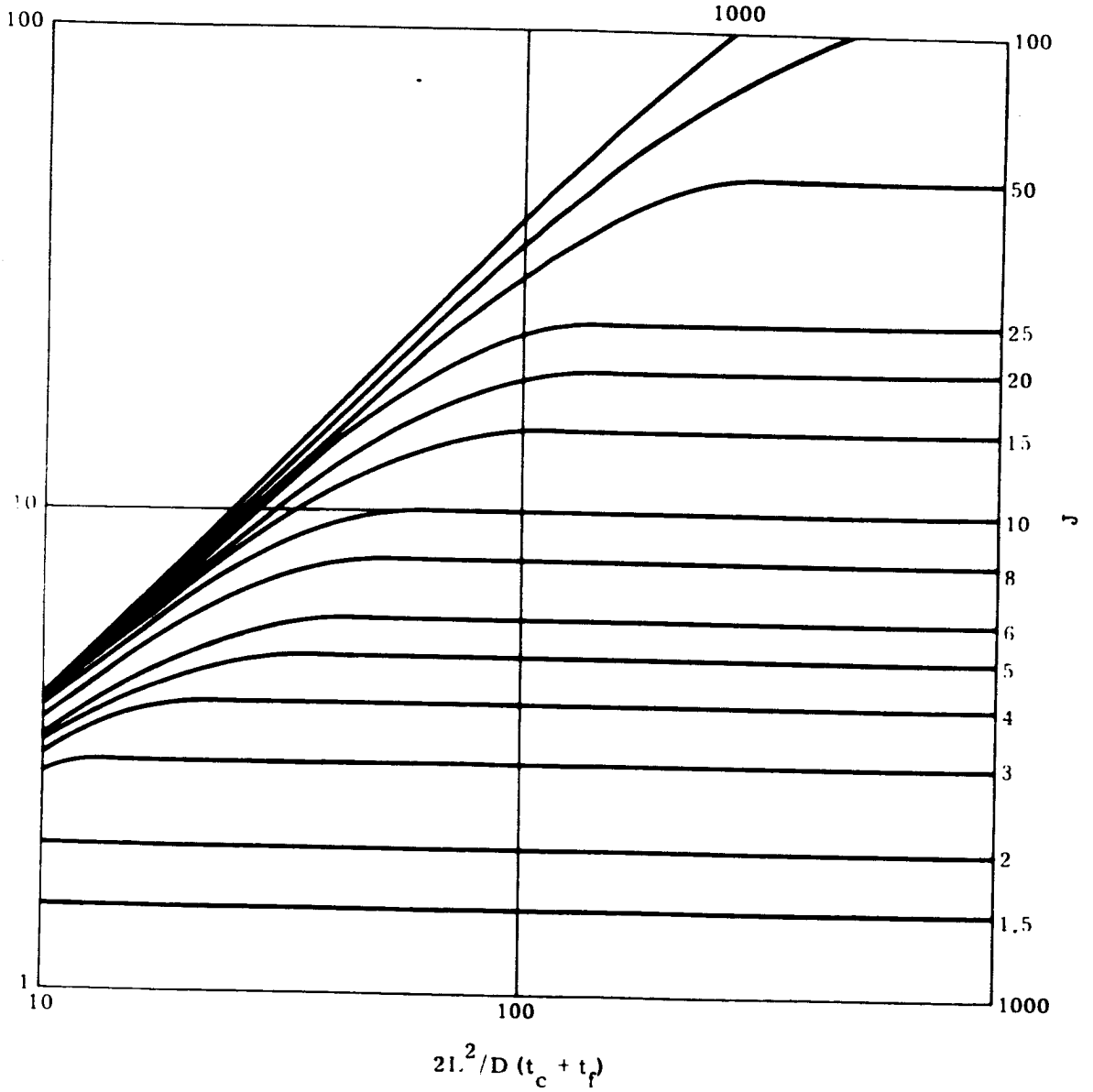

Figure H-4. Axial Compression of Honeycomb Sandwich Cylinders

b. Determine K_x, which is a function of J and Z, when

$$Z = \frac{2L^2}{D(t_c + t_f)}$$

The following equations[17], then, define K_x

$$K_x = \frac{J}{J + 1} + \frac{4Z^2}{\pi^4}$$

when

$$\frac{2Z}{\pi^2} \leq \frac{J}{J + 1}$$

and

$$K_x = \frac{2Z}{\pi^2}\left(2 - \frac{2Z}{\pi^2 J}\right)$$

when

$$\frac{J}{J + 1} \leq \frac{2Z}{\pi^2} \leq J$$

and

$$K_x = J$$

when

$$\frac{2Z}{\pi^2} \geq J$$

c. Make the following calculation check to see if it equals the known face stress

$$\sigma = \eta \frac{K_x U}{2t_f J}$$

d. If not, continue to assume values of t_c until the sandwich skin is stabilized, i.e., until σ equals the given face stress. For a comparison of test and theoretical figures, see Table H-1.

Table H-1

Comparison of Test and Theoretical Figures for 7075-T6 Aluminum Sandwich Cylinders with Face Thickness of 0.01 inch and a Core of Hexel Aluminum 3/16-5052-.001P*

Specimen	Core Thickness	Theoretical Buckling Stress	Actual Buckling Stress
1	0.125	55,000	61,000
2	0.188	67,200	69,000
3	0.188	67,200	62,000
4	0.400	70,000	74,000
5	0.400	70,000	78,000

*This material was obtained from Reference 18.

H.2.2 SHEAR INSTABILITY[19]

This mode of failure is a result of using a core that is "too soft" (one with a low core shear modulus). The faces slide with respect to one another since the shear deflections become large in magnitude. In order to preclude this type of failure, the core should be equal to or greater than the value described by

$$G_{lt} = \frac{2 E_f t_f}{D}$$

H.2.3 FACE WRINKLING[20]

This mode of failure is analogous to a beam on an elastic foundation. The elastic foundation consists of the spring rate of the core material perpendicular to the faces, with the beam being the faces themselves. The maximum allowable face stress based on face wrinkling is given by the following formula and is shown graphically in Figure H-5.

$$\sigma = 0.5 \sqrt{\eta_w E_f E_c G_{lt}}$$

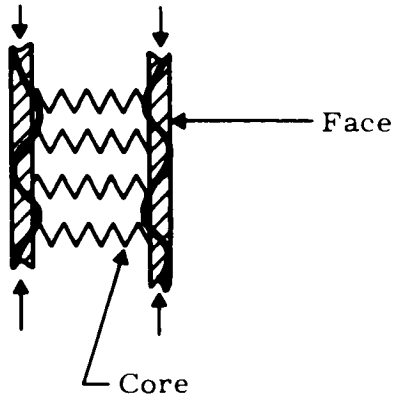

Figure H-5. Face Wrinkling Failure Mode

H.2.4 MONOCELL BUCKLING[20]

This mode of failure consists of buckling of the faces within the individual cells of the honeycomb core. The maximum allowable face stress based on monocell buckling is

$$\sigma = 0.9\,\eta_i\,E_f\left(\frac{t_f}{d}\right)^{\frac{3}{2}}$$

Substituting $\sigma = N_x/2t_f$ and rearranging terms results in

$$d_{max} = \frac{N_x(\eta_i E_f)^{\frac{2}{3}}}{2.15\,\sigma^{\frac{5}{3}}}$$

where d_{max} is the maximum allowable core diameter to preclude monocell buckling.

H.2.5 STRENGTH CRITERIA

In order to determine the required face thickness based on strength the von Mises yield equation is used

$$2t_f = \sqrt{\frac{N_x^2 - N_xN_y + N_y^2}{\sigma}}$$

with a sign convention having tension positive and compression negative.

H.3 OPTIMIZATION PROCEDURE

It is quite obvious that no optimization procedure can be developed based on the strength criteria, however the shell can be optimized based on axial buckling. Two parameters are optimized: the face working stress and the core shear modulus. For a constant load, the higher the allowable buckling face stress, the lighter are the resulting faces. However, increasing the face stress level results in a thicker and heavier core in order to stabilize the shell. Consequently, there exists an optimum face working stress where the total weight of the faces and core are a minimum, as shown in Figure H-6.

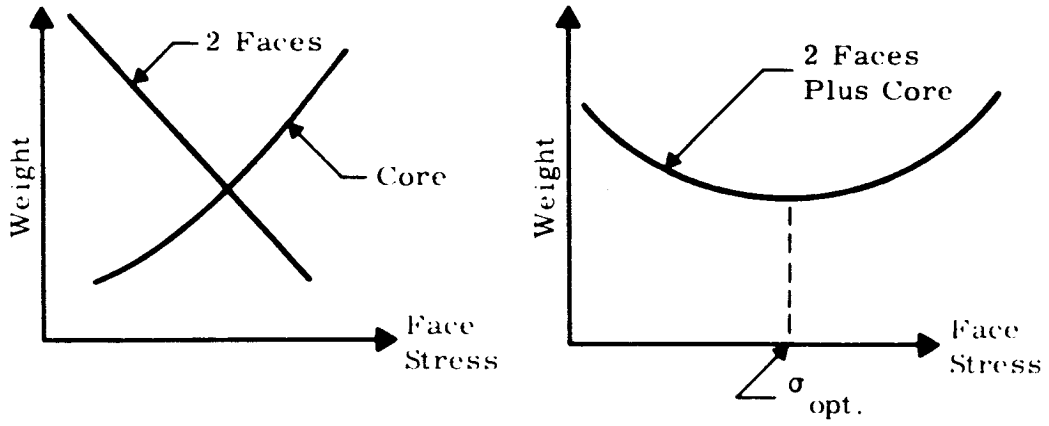

Figure H-6. Optimum Face Working Stress

Using the procedure for an optimum face stress a range of core shear moduli are investigated to determine the optimum core modulus that would result in a minimum weight. The procedure is developed in such a manner that any type of face material can be combined with any type of honeycomb core material. When using a hexagonal core material it is assumed that the core direction with the higher shear modulus is parallel to the longitudinal direction (axially loaded direction).

H.4 OPTION TO SPECIFY CORE THICKNESS

The option to specify the honeycomb core thickness is provided for in the optimization subroutine. This leaves only one design parameter to optimize, namely, the core shear modulus. The same basic equations are used to investigate general instability as have

been previously described in paragraph H.2. However, when investigating general instability since the core thickness is given, values of skin thickness, t_f, are assumed until the face working stress level equals the general instability buckling stress

$$\frac{N_x}{2t_f} = \eta \frac{K_x U}{2t_f J}$$

In order to optimize with respect to the core shear modulus, a range of values is investigated to determine the optimum modulus to be used.

H.5 WEIGHT CONSIDERATIONS

It is desired to develop a weight equation as a function of face working stress. Upon differentiation of this equation with respect to σ and setting it equal to zero to obtain a minimum weight, we obtain the optimum face working stress. However, due to the complexity of the general instability equations, an approximate formula will be used first to determine the core thickness, t_c. This formula is[21]

$$t_c' = 1.25\, D \left(\frac{\sigma}{\eta E_f}\right)$$

However, since this formula results in a higher required core thickness than the latest state-of-the-art method[20] a reduction factor will be applied to the preceding equation. The core thickness, t_c, at yield stress will be determined as described in paragraph H.2 of this appendix in order to determine a correction factor, which will then be used with the approximate formula. Calculations have shown that the ratio t_c'/t_c is approximately a constant at any stress level for a constant L/R, N_x/D, and G_{lt}. Therefore, it can be concluded that it will be the same for the optimum stress as well as yield

$$t_c' = K_1\, D \left(\frac{\sigma}{\eta E_f}\right)$$

Since t_c'/t_c is a constant, it follows that

$$\frac{K_1\, D \left(\frac{\sigma}{\eta E_f}\right)}{t_c} = \text{constant}$$

therefore

$$K_1 = \frac{t_c}{D\left(\frac{\sigma}{\eta E_f}\right)}$$

Let W equal the weight per surface area of a cylinder, and

$$K_2 = \frac{\rho_c}{\rho_f}$$

$$2t_f = \frac{N_x}{\sigma}$$

$$t_c = K_1 D\left(\frac{\sigma}{\eta E}\right)$$

The weight equation is

$$W = t_c \rho_c + 2t_f \rho_f$$

Substitution results with

$$W = \rho_f \left[K_1 K_2 D\left(\frac{\sigma}{\eta E_f}\right) + \frac{N_x}{\sigma}\right]$$

Substituting in the value of η (see Appendix A) in terms of the Ramberg-Osgood equation, we obtain

$$W = \rho_f \left\{\frac{K_1 K_2 D}{E_f}\left[\sigma^2 + \frac{3}{7}(n+1)\left(\frac{\sigma^{n+1}}{\sigma_o^{n-1}}\right) + \frac{9}{49} n \frac{\sigma^{2n}}{\sigma_o^{2n-2}}\right]^{\frac{1}{2}} + N_x \sigma^{-1}\right\}$$

To determine the stress level at which weight is a minimum, set $dW/d\sigma = 0$. Performing the differentiation and setting it equal to zero results with

$$\frac{N_x}{D} = \frac{K_1 K_2}{2E_f} \sigma^2 \left[1 + \frac{3}{7}(n+1)\left(\frac{\sigma}{\sigma_o}\right)^{n-1} + \frac{9n}{49}\left(\frac{\sigma}{\sigma_o}\right)^{2n-2}\right]^{-\frac{1}{2}}$$

$$\cdot \left[2 + \frac{3}{7}(n+1)^2\left(\frac{\sigma}{\sigma_o}\right)^{n-1} + \frac{18}{49}n^2\left(\frac{\sigma}{\sigma_o}\right)^{2n-2}\right]$$

Using this equation for the structural index, N_x/D, we can obtain the optimum face working stress that will result with a minimum weight structure.

In order to determine the true weight of any cylinder of sandwich type construction in lb/ft^2, the following formula is used

$$W = \left(\frac{\rho_c t_c + 2 t_f \rho_f}{12} F_b\right)$$

where $F_b = 1.25$ is a fabrication factor which takes into consideration non-calculated items such as core filler material, doublers, fasteners, etc.

H.6 CONICAL SECTIONS

Conical sections will be analysed using the equivalent cylinder method, where each section is transformed into an equivalent cylinder by

$$\overline{R} = \frac{R_{beg}\sqrt{L_c^2 + (R_{beg} - R_{end})^2}}{L_c}$$

$$\overline{L} = \left(\frac{R_{end} + 1.2 R_{beg}}{2.2 R_{beg}}\right) L_c$$

where

$\overline{R}$ = equivalent radius.

$\overline{L}$ = equivalent length.

R_{beg} = radius at beginning of section.

R_{end} = radius at end of section.

L_c = conical length.

H.7 NOMENCLATURE

N_x = Axial load per inch (lbs/inch).

N_y = Hoop load per inch (lbs/inch).

t_f = Face thickness (one) (inches).

t_c = Core thickness (inches).

D = Diameter of cylinder (inches).

D_f = Flexural rigidity of panel (lb-inches).

d = Diameter of circle inscribed within a honeycomb cell (inches).

σ = Face stress level (psi).

E_f = Modulus of elasticity of faces (psi).

G_{lt} = Shear modulus of core in longitudinal direction (psi).

E_c = Modulus of elasticity of core in direction perpendicular to the faces (psi).

ρ_c = Density of core (lbs/ft^3).

ρ_f = Density of faces (lbs/ft^3).

γ_c = Density of core material (lbs/ft^3).

G' = Shear modulus of core material (psi).

E' = Modulus of elasticity of core material (psi).

W = Weight of sandwich per surface area (lbs/ft^2).

C_1 = Specific shear modulus ($psi/lbs/ft^3$).

C_2 = Specific modulus of elasticity ($psi/lbs/ft^3$).

J = Rigidity parameter.

K_x = Buckling coefficient, axial compression.

L = Length of cylinder (inches).

U = Shear rigidity of panel.

η = Plasticity reduction factor for general instability.

η_i = Plasticity reduction factor for monocell buckling.

η_w = Plasticity reduction factor for face wrinkling.

APPENDIX I

45° WAFFLE STIFFENED CYLINDERS

I.1 INTRODUCTION

A 45° waffle stiffened cylinder consists of a thin skin with equally spaced stiffening ribs (see Figure I-1, Waffle Geometry). The purpose of this appendix is to establish a method for optimizing this type of structure subjected to axial loading and/or internal pressure. Two modes of failure are considered: strength based on the von Mises yield criteria, and buckling which consists of both general and local instability. The local instability includes panel buckling and rib crippling.

It is quite obvious that no optimization procedure can be developed based on the strength criteria, however the shell can be optimized based on axial buckling. Four parameters are to be optimized: skin thickness, overall waffle depth, rib thickness, and rib spacing. The following is a list of assumptions that are made in the optimization:

a. Internal pressure has no effect on the overall general instability, however it has been taken advantage of when considering panel buckling and rib crippling.
b. Rib spacing is sufficiently close so that the ribs and skin are equally stressed.
c. Curved panels between ribs are treated as flat plates when considering panel buckling since the radius of curvature is large.
d. Waffle is manufactured using the mechanical milling process.
e. Critical buckling stresses are within the elastic limit.

I.2 FAILURE MODES

I.2.1 GENERAL INSTABILITY

The following equation, which has previously been described in Appendix F, will be employed to describe failure in the general instability mode[9]:

$$N_{cr} = \frac{2}{R}\left(\frac{\beta^2 D_{11} + D_{33}}{\frac{\beta^2}{A_{11}} + \frac{1}{2A_{33}}}\right)^{\frac{1}{2}} C$$

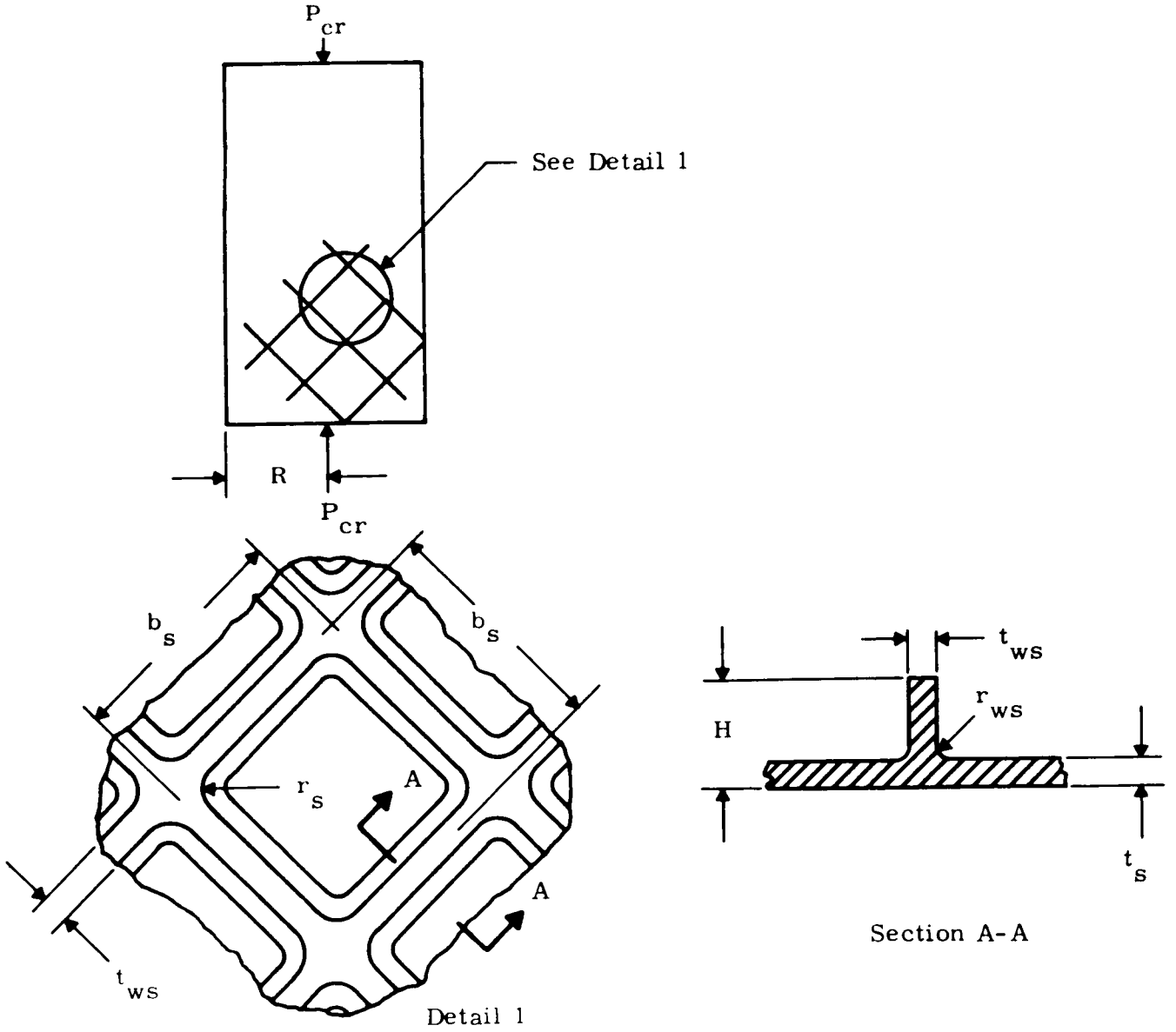

Figure I-1. 45° Waffle Stiffened Geometry

where

$$\beta^2 = P_o + \left(P_o^2 + Q_o\right)^{\frac{1}{2}}$$

$$P_o = \frac{A_{33}}{A_{22}}\left(\frac{A_{22}D_{11} - A_{11}D_{22}}{A_{11}D_{22} - 2A_{33}D_{33}}\right)$$

$$Q_o = \frac{A_{11}}{A_{22}}\left(\frac{A_{22}D_{11} - 2A_{33}D_{33}}{A_{11}D_{22} - 2A_{33}D_{33}}\right)$$

Letting the correction factor, C, equal 0.40 (based on experimental evidence shown in Appendix F) and for the type of construction being considered, $A_{11} = A_{22}$ and $D_{11} = D_{22}$, the equation reduces to

$$N_{cr} = \frac{0.8}{R}\left(\frac{D_{11} + D_{33}}{\frac{1}{A_{11}} + \frac{1}{2A_{33}}}\right)^{\frac{1}{2}}$$

It has been found advantageous from an optimization standpoint to express the design parameters all in terms of the overall depth, H. Letting $t_s = C_1$, $t_{ws} = C_2 H$, and $b_s = C_3 H$, the stiffness parameters can be expressed as[22]

$$A_{11} = A_x EH$$

$$A_{33} = A_{xy} EH$$

$$D_{22} = \left[I_x - \frac{A_s^2 A_x}{A_s^2}(\overline{K}_x - \overline{K}_s)^2\right] EH^3$$

$$D_{33} = \frac{1}{2} I_{xy} EH^3$$

where

$$I_{xy} = \frac{1}{1+\mu}\left(\frac{C_1^3}{6} + 2C_1\bar{K}_{xy}^2\right) + \frac{4C_2(1-C_1)}{C_3}\left[\frac{(1-C_1)^2}{6} + \frac{1}{2}\left(\frac{1}{2} - \bar{K}_{xy}\right)^2\right]$$

$$I_x = \frac{C_1^3}{12(1-\mu^2)} + \frac{C_2(1-C_1)^3}{24C_3} + \frac{C_1\bar{K}_x^2}{1-\mu^2} + \frac{C_2(1-C_1)}{2C_3}\left(\frac{1}{2} - \bar{K}_x\right)^2$$

$$A_x = \frac{C_1}{1-\mu^2} + \frac{(1-C_1)C_2}{2C_3}$$

$$A_{xy} = \frac{C_1}{2(1+\mu)} + \frac{(1-C_1)C_2}{2C_3}$$

$$A_s = \frac{\mu C_1}{1-\mu^2} + \frac{(1-C_1)C_2}{2C_3}$$

$$\bar{A}_s^2 = A_xA_y - A_s^2$$

$$\bar{K}_s = \frac{1}{A_s}\left[\frac{C_2(1-C_1)}{4C_3}\right]$$

$$\bar{K}_x = \frac{1}{A_x}\left[\frac{C_2(1-C_1)}{4C_3}\right]$$

$$\bar{K}_{xy} = \frac{1}{A_{xy}}\left[\frac{C_2(1-C_1)}{4C_3}\right]$$

Letting

$$f(C_1, C_2, C_3) = \left\{ \frac{\left[I_x - \frac{A_s^2 A_x}{\bar{A}_s^2} (\bar{K}_x - \bar{K}_s)^2 \right] + \frac{1}{2} I_{xy}}{\frac{1}{A_x} + \frac{1}{2A_{xy}}} \right\}^{\frac{1}{2}}$$

then

$$N_{cr} = \frac{0.8}{R} [f(C_1, C_2, C_3)] EH^2$$

I.2.2 PANEL AND RIB STRESS LEVELS

In order to investigate local panel buckling and rib crippling, the portion of the load resisted by the panels and ribs must be determined (see Figure I-2). The portion of the load resisted by each is a function of the stiffnesses (analogous to springs in parallel). Since a single panel is symmetrical about the x and y axes, the derivation will be done for the N_x loading only. The proportion of the load taken by the ribs and panel due to the hoop loading, N_y, is identical.

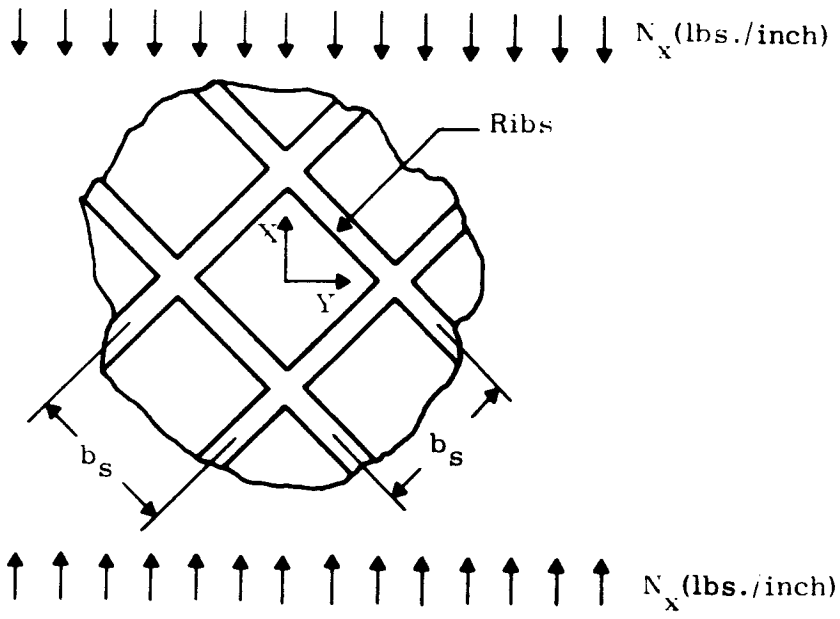

Figure I-2. Panel Detail

Letting the total axial load per panel plus ribs, L_T, equal $1.414b_sN_x$, the spring rate of the panel, K_p, equal Et_s, and the spring rate of the panel plus ribs, K_t, equal A_xEH, then proportioning the load in the panels and ribs according to the stiffnesses, we obtain

$$\text{load per panel, } L_p = \frac{t_s}{A_xH}(1.414b_sN_x)$$

$$\text{load per rib, } L_r = 0.707b_sN_x\left(1 - \frac{t_s}{A_xH}\right)$$

I.2.3 LOCAL PANEL BUCKLING

Having established the load level in the panels, a criterion will be determined for local panel buckling. Due to an axial load, N_x, the free-body diagram of the panel is as shown in Figure I-3.

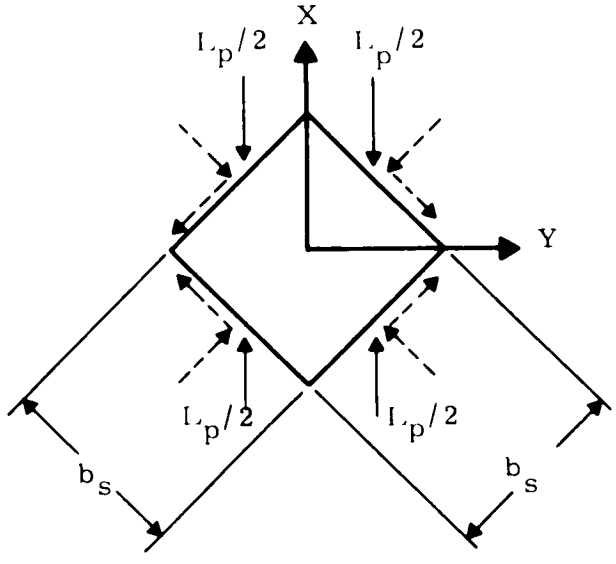

Figure I-3. Free-Body Diagram of the Panel

Re-orienting the forces on the free-body diagram, the element is as shown in Figure I-4, where $S_x = N_x/2A_xH$ and $f_s = -N_x/2A_xH$.

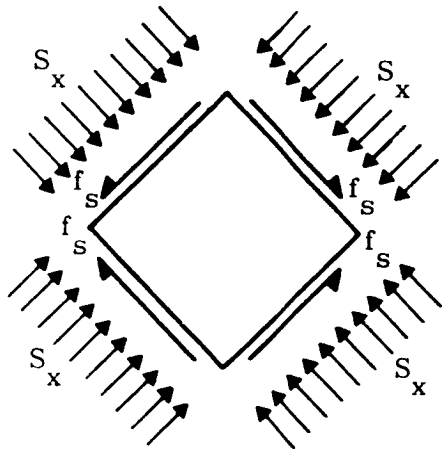

Figure I-4. Re-Oriented Forces on Free-Body Diagram

Similarly, due to hoop loading, N_y, the following is obtained, as shown in Figure I-5, where $S_y = N_y/2A_xH$ and $f_s' = N_y/2A_xH$.

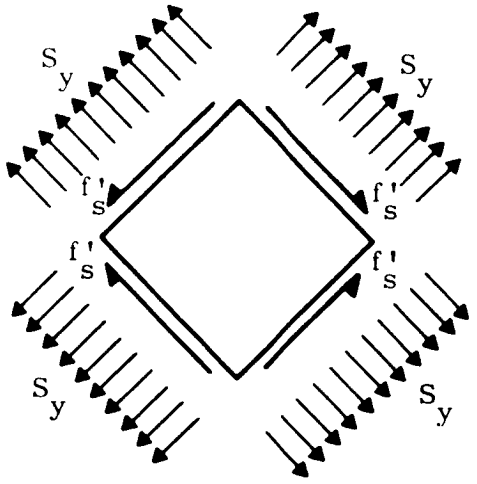

Figure I-5. Effect of Hoop Loading on Free-Body Diagram

Combining the effects of N_x and N_y results with Figure I-6 where $S^R = (N_x + N_y)2A_xH$ and $f_s^R = (-N_x + N_y)/2A_xH$.

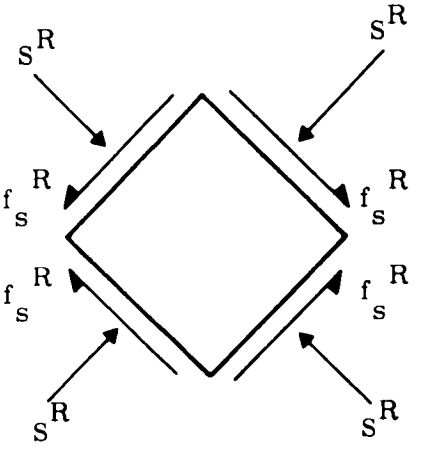

Figure I-6. Combined Effects on Free-Body Diagram

When S^R is negative (compression), the following interaction formula will be used for combined loading

$$\left|\frac{2S^R}{S_{cr}}\right| + \left(\frac{f_s^R}{f_{s_{cr}}}\right)^2 \leq 1$$

When S^R is positive (tension), the panel will be checked for shear instability only and the following formula will be used

$$\left|\frac{f_s}{f_{s_{cr}}}\right| \leq 1$$

For a square panel with simply supported edge conditions, use the following[23]

$$S_{cr} = 3.29 \frac{E}{1 - \mu^2}\left(\frac{C_1}{C_3}\right)^2$$

$$f_{s_{cr}} = 7.75 \frac{E}{1 - \mu^2} \left(\frac{C_1}{C_3}\right)^2$$

I.2.4 RIB CRIPPLING

Having established the load level in the ribs a criterion will be determined for rib crippling as shown in Figure I-7.

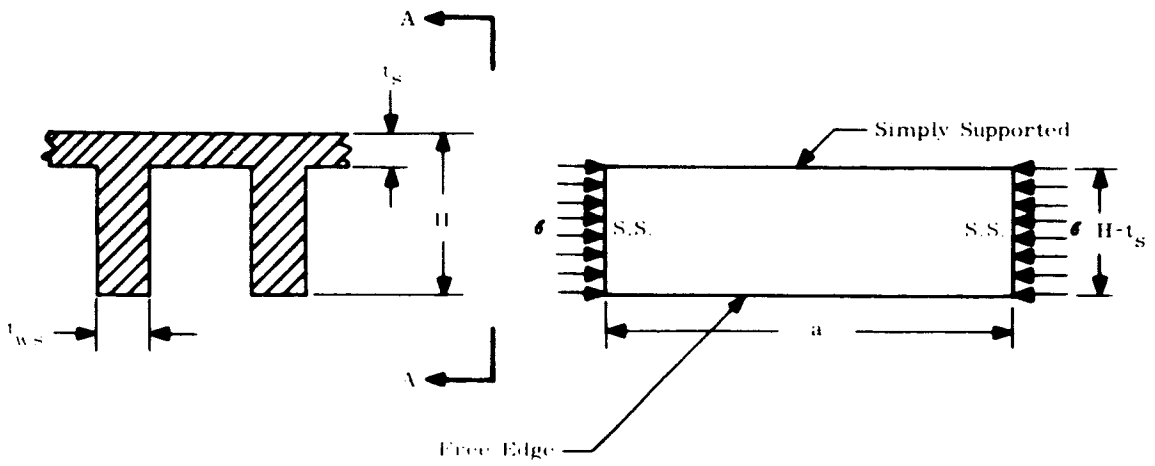

Figure I-7. Rib Crippling

It has been determined that the portion of the N_x load resisted by one rib is

$$L_r = 0.707 b_s N_x \left(1 - \frac{t_s}{A_x H}\right)$$

Applying the same principle in the hoop direction and letting $t_s = C_1 H$ and $b_s = C_3 H$, we obtain

$$\sigma = \frac{C_3 (N_x + N_y)}{(1 - C_1) C_2 H} \left(1 - \frac{C_1}{A_x}\right)$$

Assuming that $a/H - t_s$ approaches infinity (from Figure I-7), the critical buckling stress is given as

$$\sigma_{cr} = -3.85 \frac{E}{1 - \mu^2} \left(\frac{C_2}{1 - C_1} \right)^2$$

where $\sigma_{cr} \geq \sigma$ to preclude local rib crippling.

I.2.5 STRENGTH CRITERIA

Assuming that the skin and ribs are equally stressed, the von Mises yield criteria will be used to determine the stress level (where A_x is defined on page I-4)

$$\sigma = \frac{\sqrt{N_x^2 - N_x N_y + N_y^2}}{A_x H}$$

I.3 OPTIMIZATION PROCEDURE

It is desired to determine the optimum design parameters C_1, C_2, C_3, and H such that we arrive at a minimum weight configuration. The approach to be used is the concept of maximum strength-to-weight ratio based upon general instability. A logical range of C_1, C_2, and C_3 will be investigated and the resulting strength-to-weight ratios calculated. The configuration with the maximum ratio will be investigated for panel buckling and web crippling. If panel buckling and/or web crippling is not satisfied, the next highest value of strength-to-weight ratio is investigated until the local buckling criterion is satisfied. Having determined the optimum values of C_1, C_2, and C_3, the value of the overall depth can be calculated to satisfy general buckling by using

$$H = \sqrt{\frac{N_{cr} R}{0.8E\, f(C_1, C_2, C_3)}}$$

In order to determine the strength-to-weight ratios, the following equations are needed

$$N_{cr} = \frac{0.8}{R} f(C_1, C_2, C_3) E H^2$$

Average thickness, $t_{ave} = g(C_1, C_2, C_3)H$, so that

$$\frac{N_{cr}}{t_{ave}} = \frac{\frac{0.8}{R} f(C_1, C_2, C_3)EH}{g(C_1, C_2, C_3)}$$

Substituting the value of H results with

$$\frac{N_{cr}}{t_{ave}} = \frac{[f(C_1, C_2, C_3)]^{\frac{1}{2}}}{g(C_1, C_2, C_3)} \left(\frac{0.8N_{cr}E}{R}\right)^{\frac{1}{2}}$$

Since the terms N_{cr}, E, and R are the only given terms on the right-hand side of the equation, in order to obtain a maximum strength-to-weight ratio, the following term should be maximum

$$\frac{[f(C_1, C_2, C_3)]^{\frac{1}{2}}}{g(C_1, C_2, C_3)} = \text{maximum}$$

The first step in determining a logical range of C_1, C_2, and C_3 is to approximate the maximum value of C_3/C_1 that precludes panel buckling. Such a plot was made for $E = 10 \times 10^6$ and 30×10^6 and is shown on Figure I-8. The value of critical panel buckling stress approaches zero at a value of C_3/C_1 approximately equal to 130. Based upon this, it was decided to use a minimum value of $C_1 = 0.10$ and a maximum of $C_3 = 13$. The range of C_1 to be investigated was decided to be from 0.10 to 0.14 since this is sufficient to cover a wide range of strength-to-weight ratios (see Figure I-9). Similarly, it was decided to use a range of C_3/C_1 from 33 to 130. Based on Figures I-10 and I-11, the range of C_2 to be investigated is from 0.05 to 0.25 since the maximum values of strength-to-weight ratios occur within this range. In order to keep the number of calculations at a minimum, the following values of C_1, C_2, and C_3 were investigated with all possible combinations of each:

C_1 = 0.10, 0.11, 0.12, 0.13, 0.14

C_2 = 0.05, 0.10, 0.15, 0.20, 0.25

C_3 = 5, 7, 9, 11, 13

This would result with 125 combinations of C_1, C_2, and C_3.

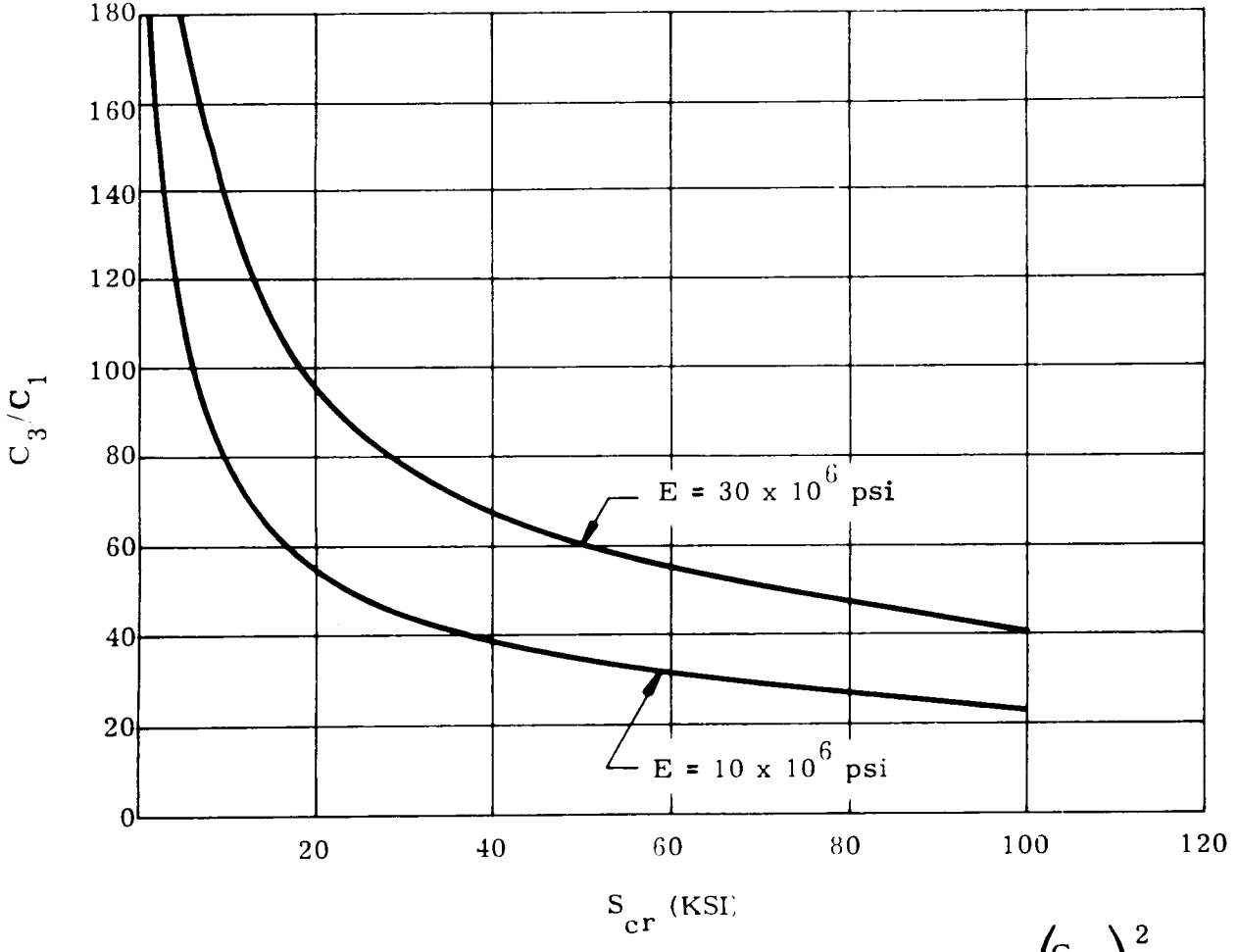

Panel Buckling Based on the Equation $S_{cr} = 5.5 \frac{E}{1-\mu^2} \left(\frac{C_3}{C_1}\right)^2$

Figure I-8. Maximum Value of C_3/C_1 that Precludes Panel Buckling

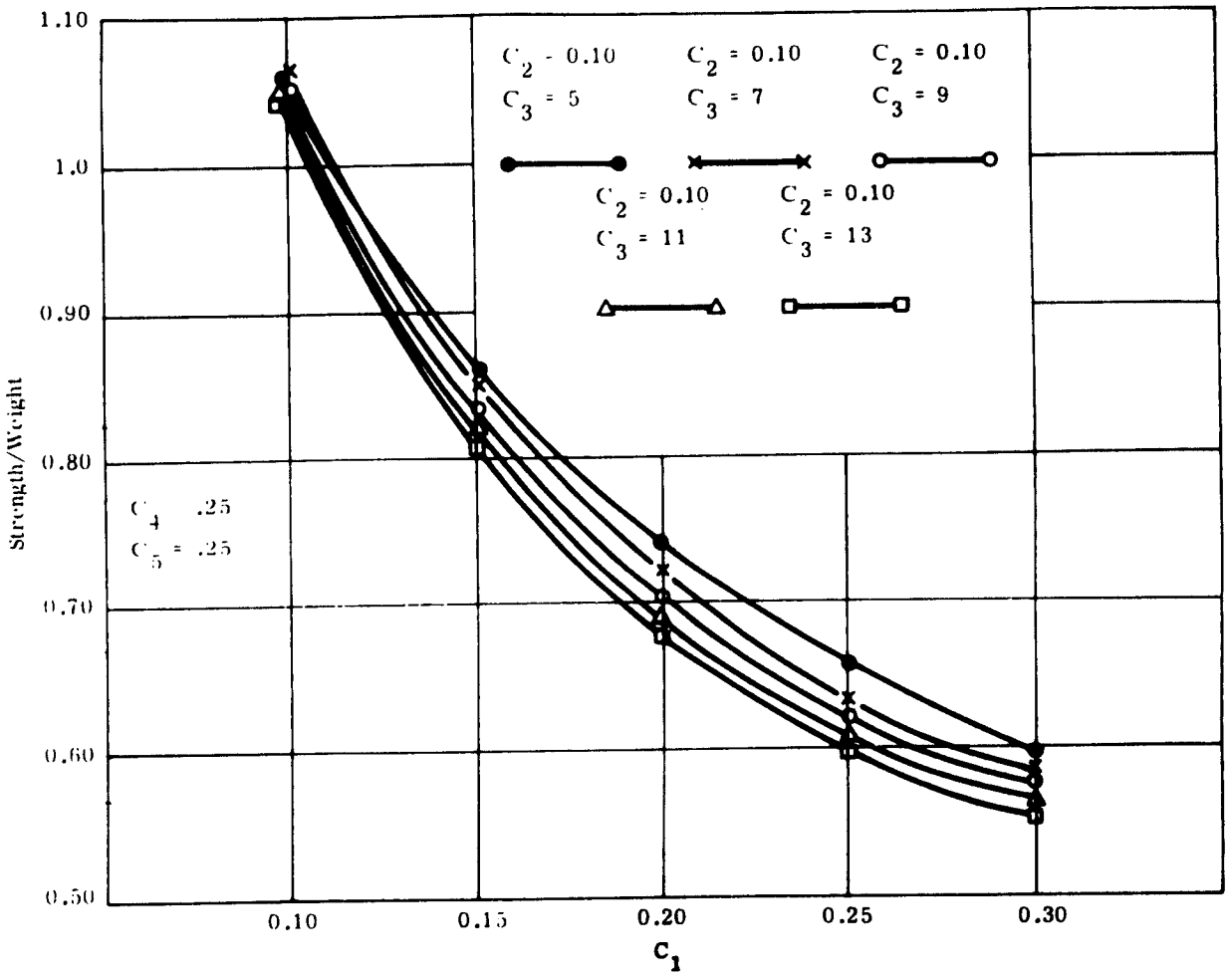

Figure I-9. Strength-to-Weight Ratio versus C_1 for C_2 = 0.10 and C_3 = 5 through 13

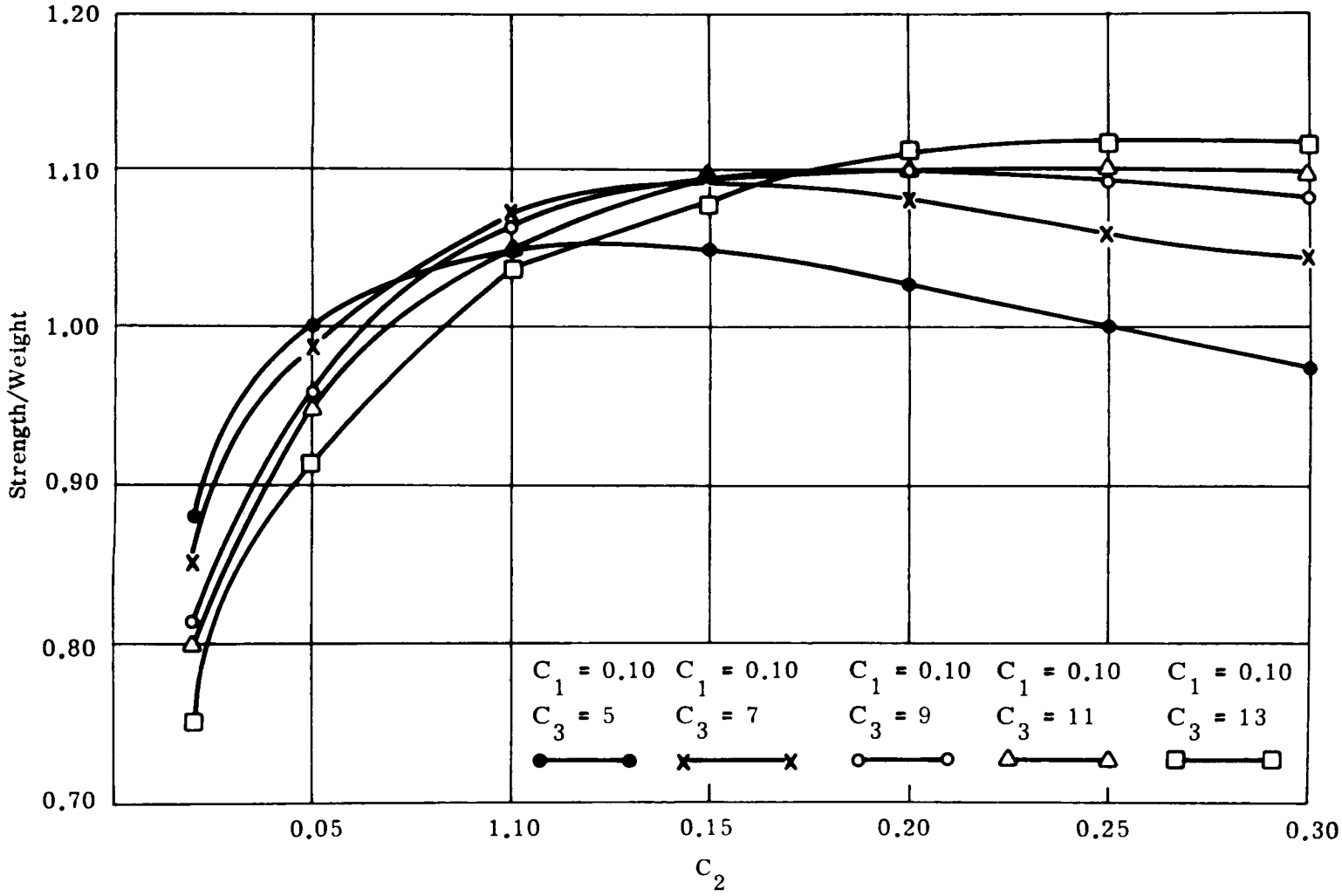

Figure I-10. Strength-to-Weight Ratio vs C_2 for C_1 = 0.10 and C_3 = 5 through 13

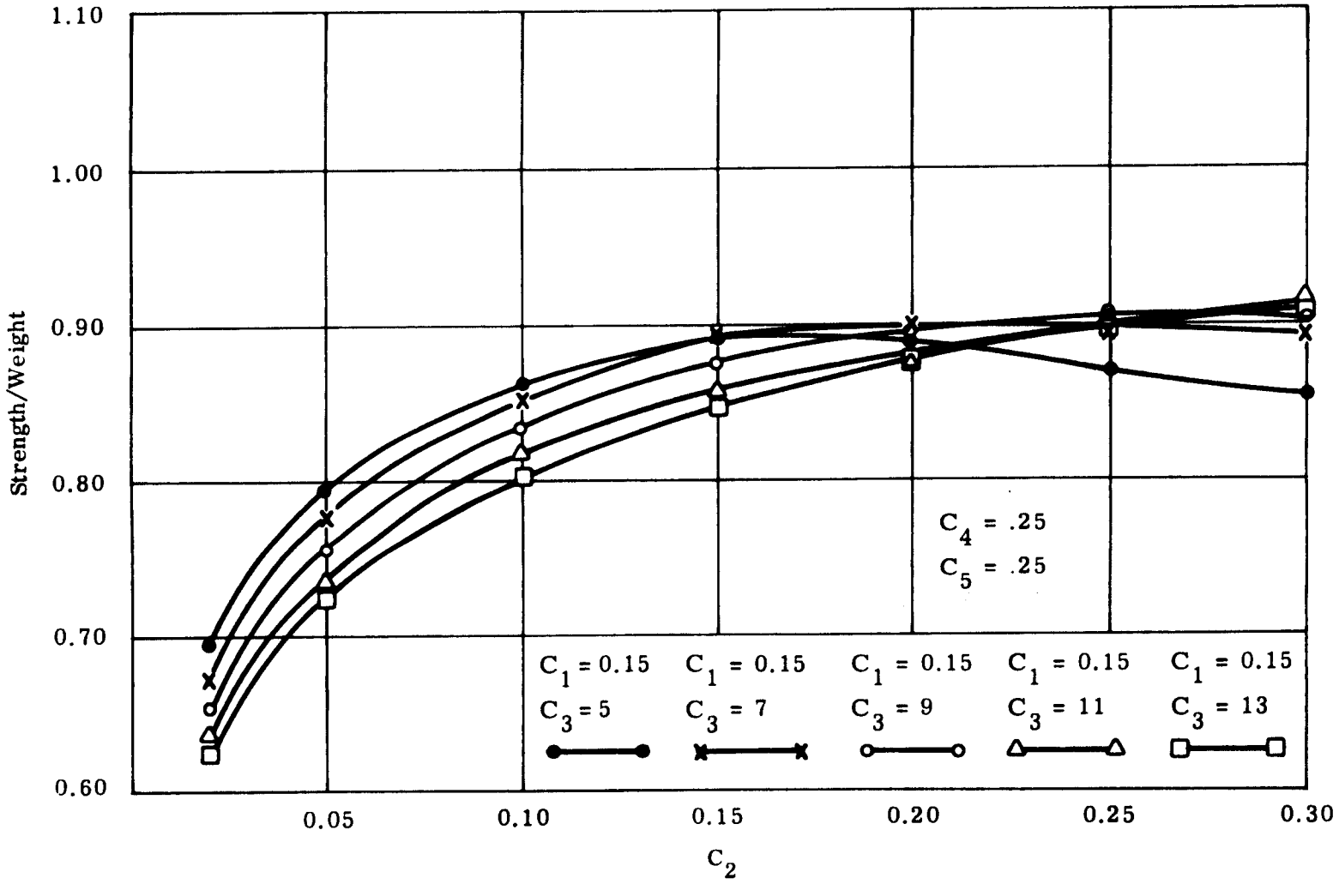

Figure I-11. Strength-to-Weight Ratio vs C_2 for C_1 = 0.15 and C_3 = 5 through 13

I.4 OPTIONS

I.4.1 OPTION TO SPECIFY OVERALL DEPTH

The purpose of this section is to determine an optimization procedure when given the value of the overall depth. The parameters that are considered for optimization are skin thickness, rib thickness, and rib spacing. As has been previously stated in paragraph I.3, the optimization will be considered for buckling governed cases only and not for strength.

Given the value of H, the value for $f(C_1, C_2, C_3)$ required to resist general instability is

$$f(C_1, C_2, C_3) = \frac{N_x R}{0.8EH^2}$$

However, due to the complexity of the $f(C_1, C_2, C_3)$, a method for simplifying the equation was sought. Assuming that the $f(C_1, C_2, C_3)$ is of the form $x = y^m$, values of $f(C_1, C_2, C_3)$ versus C_3 for various combinations of C_1 and C_2 are plotted on Figures I-12 through I-16. The plots on log-log paper consist of parallel straight lines thus verifying the assumed form of the equation $x = y^m$. Based on this equation, $C_3 = A[f(C_1, C_2, C_3)]^m$, where $m = -0.53$ and A is a function of C_2 and C_1. The values of A were determined for each combination of C_1 and C_2 and plotted on log-log paper against the value of C_2 (see Figure I-17). Here again, the results are straight parallel lines taking the same general form of the equation. Therefore, $A = BC_2^n$, where $n = 0.53$ and B is a function of C_1. The values of B are determined for each value of C_1 and plotted on log-log paper against the value of C_1 (see Figure I-18). The result is a straight line again taking the same general form of the equation. Therefore, $B = DC_1^p$, where $D = 0.545$ and $p = 0.443$. Substituting in the values of A and B, the following resulting equation is obtained and is accurate for the $0.05 \leq C_1 \leq 0.25$, $0.02 \leq C_2 \leq 0.25$, and $3 \leq C_3 \leq 13$

$$f(C_1, C_2, C_3) = 0.545\, C_1^{0.443} \left(\frac{C_2}{C_3}\right)^{0.53}$$

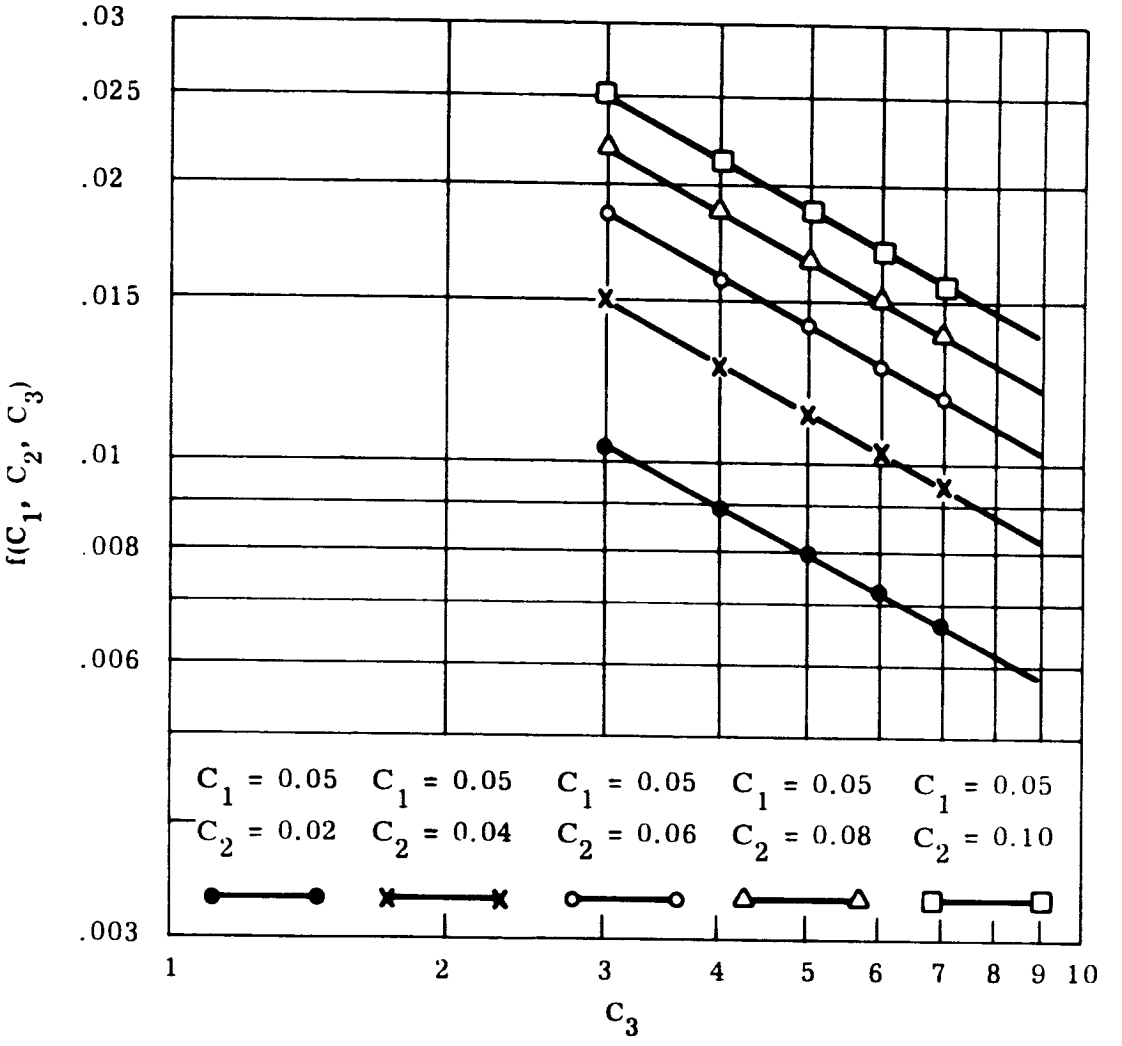

Figure I-12. Values of $f(C_1, C_2, C_3)$ vs C_3 for $C_1 = 0.05$

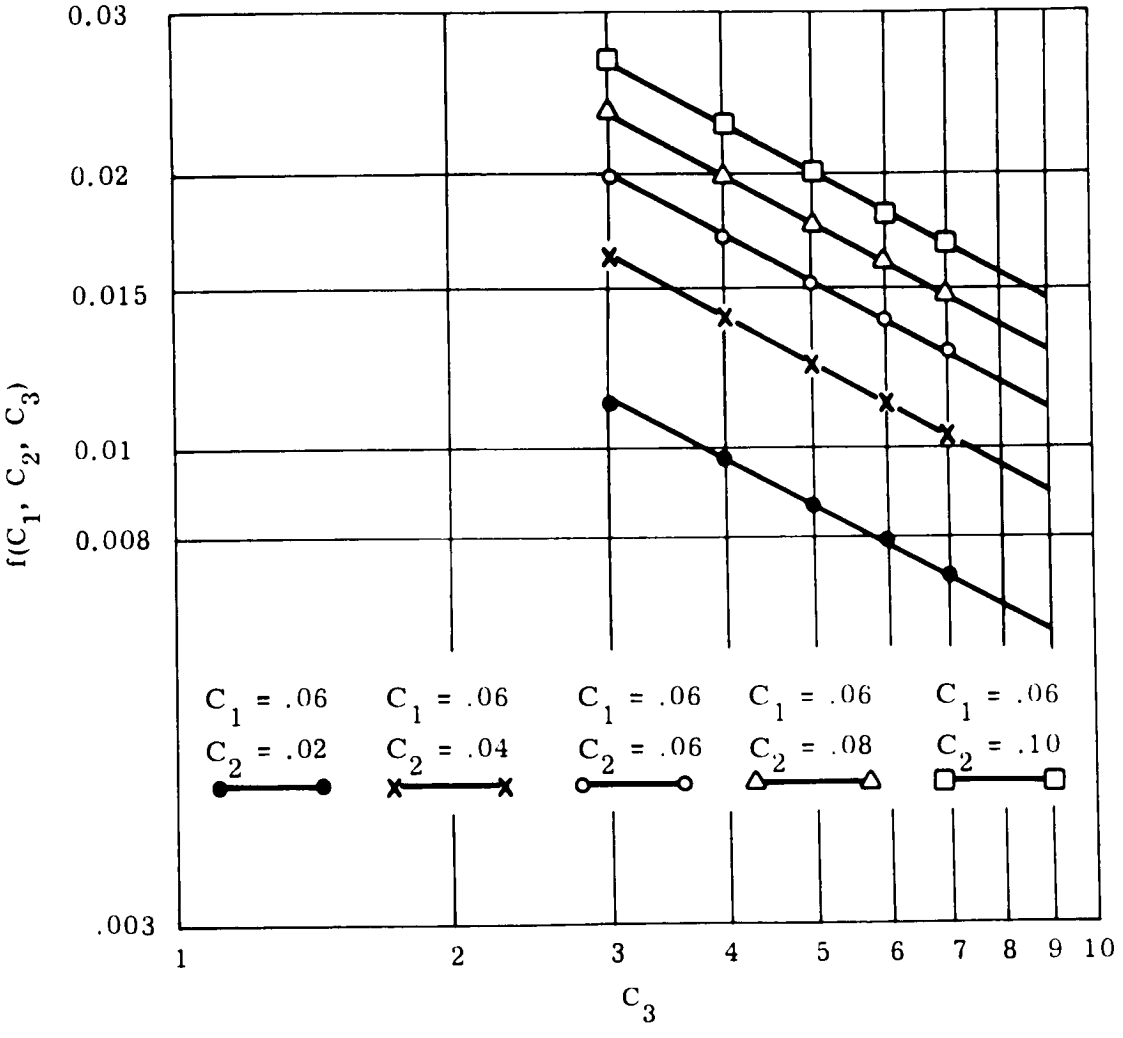

Figure I-13. Values of $f(C_1, C_2, C_3)$ vs C_3 for $C_1 = 0.06$

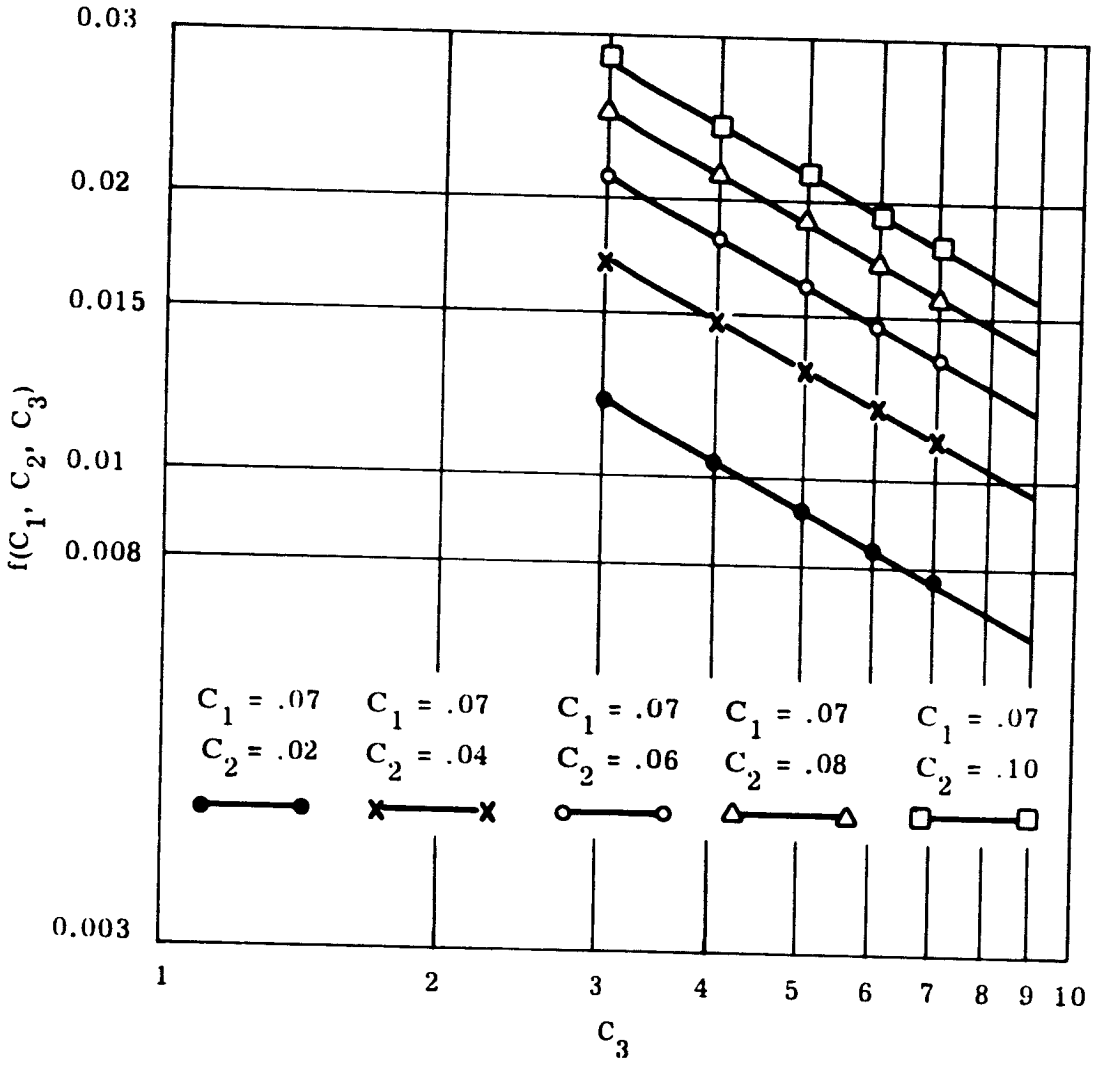

Figure I-14. Values of $f(C_1, C_2, C_3)$ vs C_3 for $C_1 = 0.07$

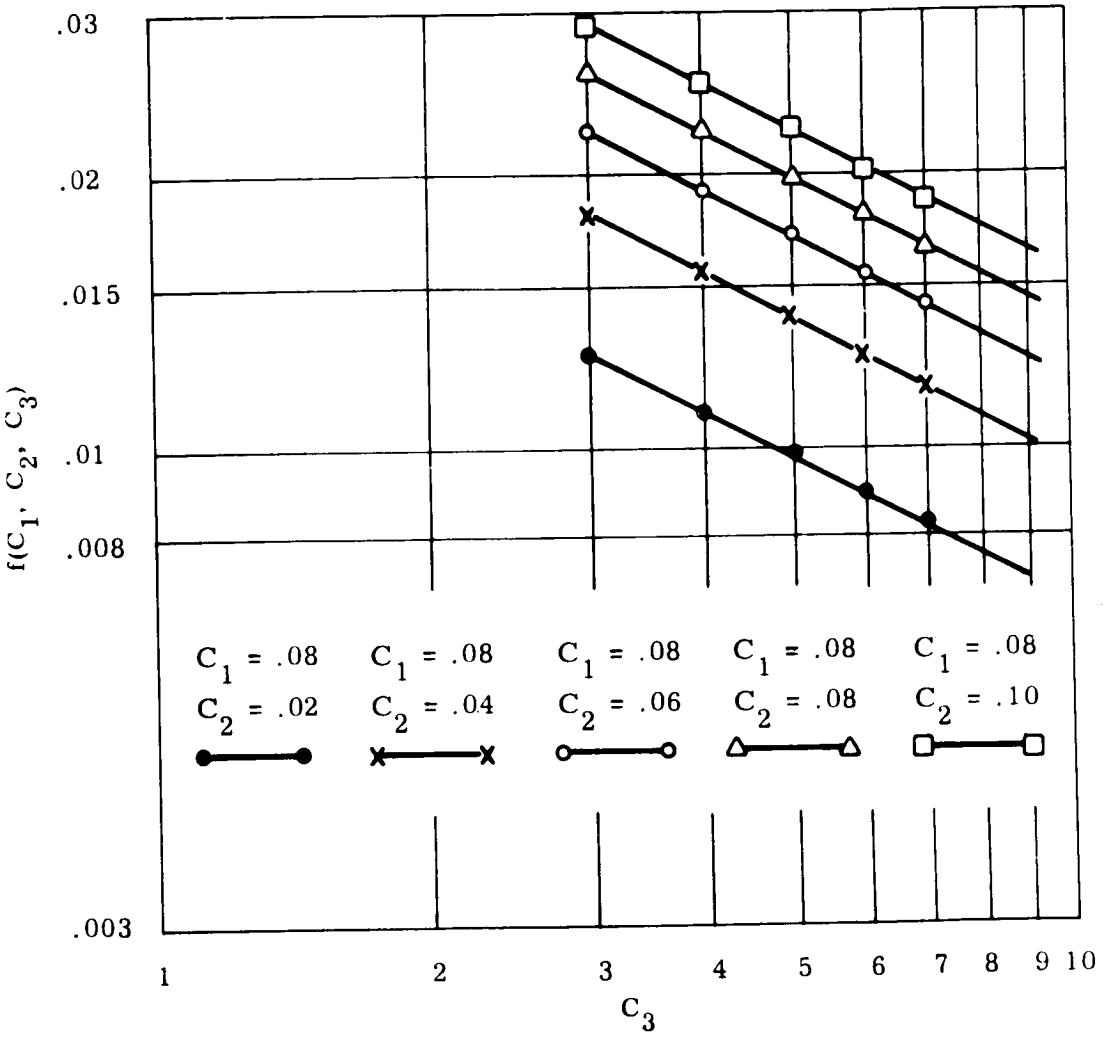

Figure I-15. Values of $f(C_1, C_2, C_3)$ vs C_3 for $C_1 = 0.08$

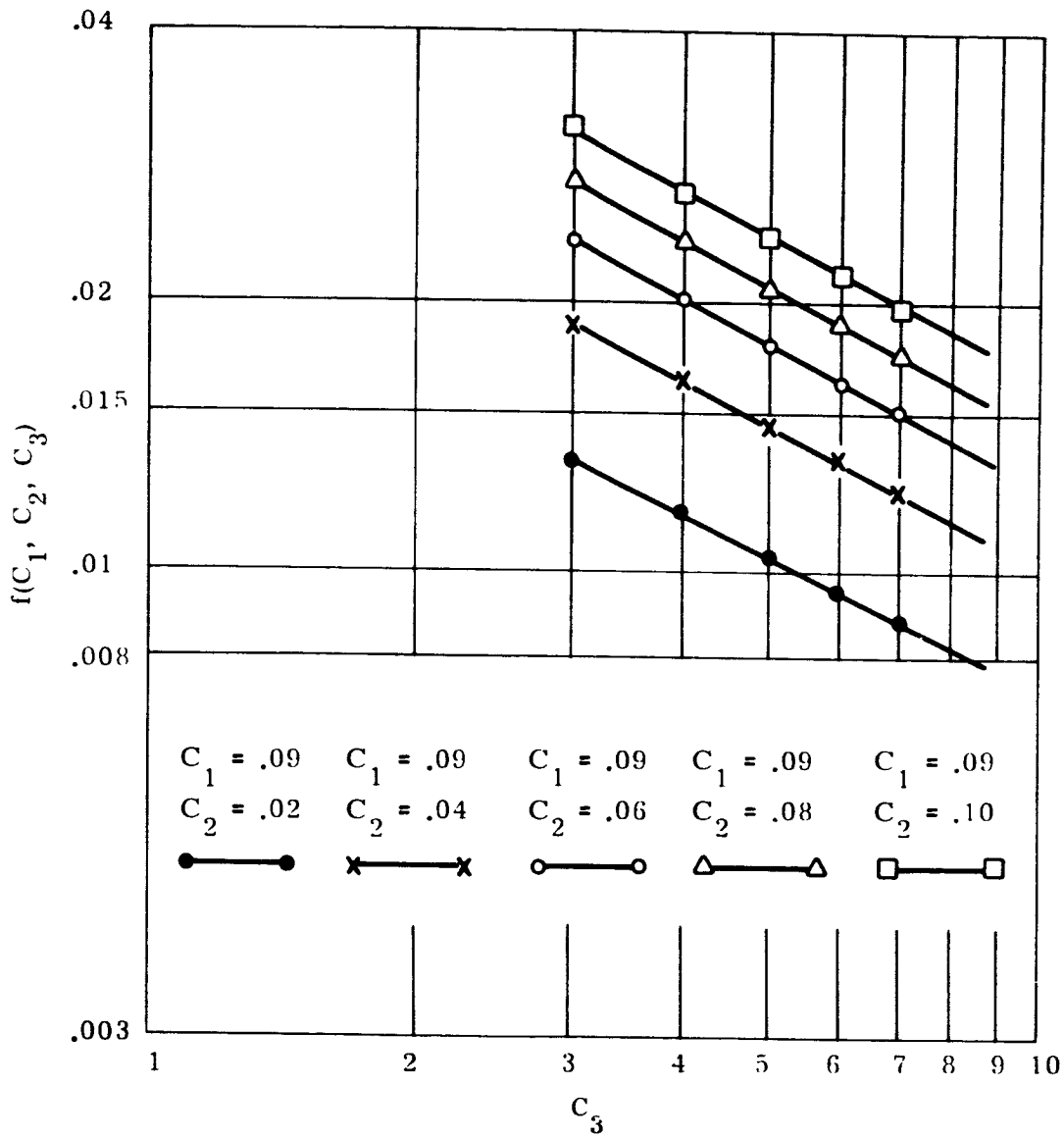

Figure I-16. Values of $f(C_1, C_2, C_3)$ vs C_3 for $C_1 = 0.09$

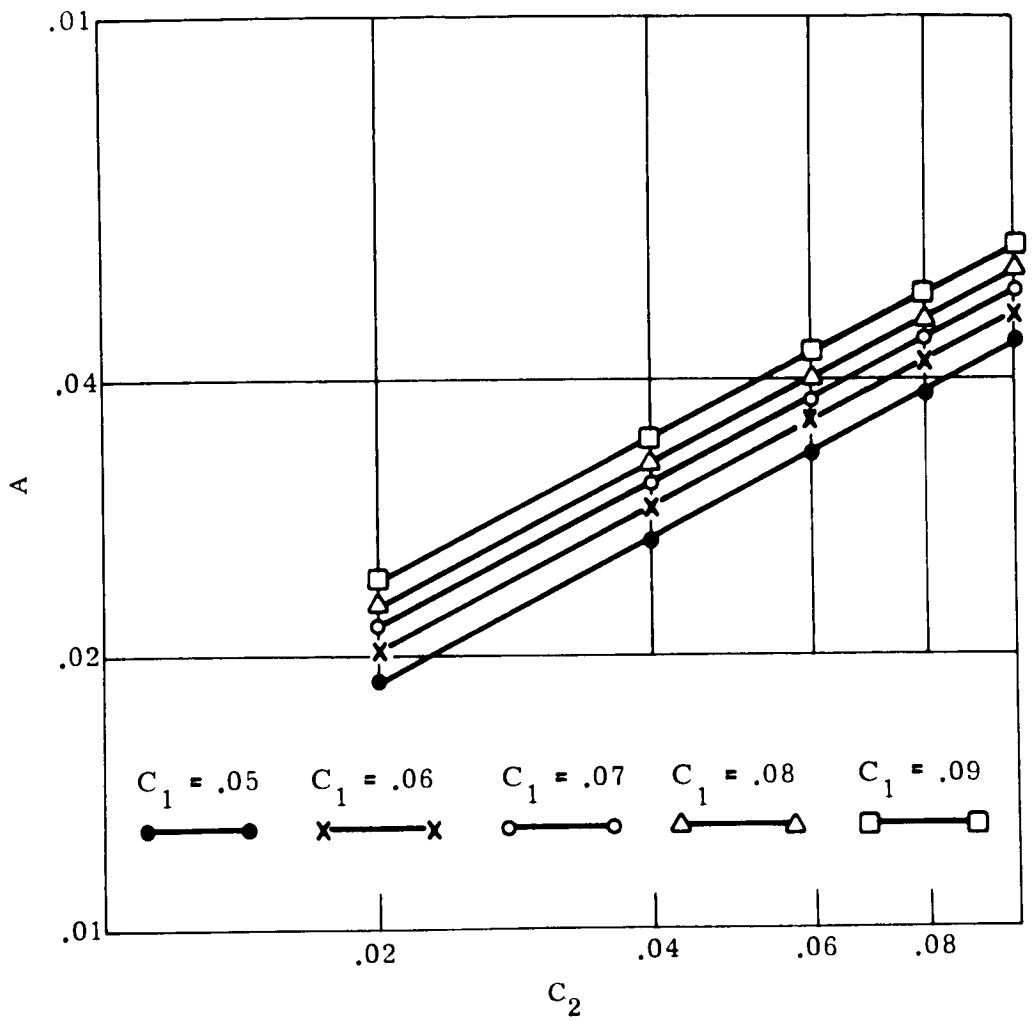

Figure I-17. Values of A vs C_2 for C_1 = 0.05 through 0.09

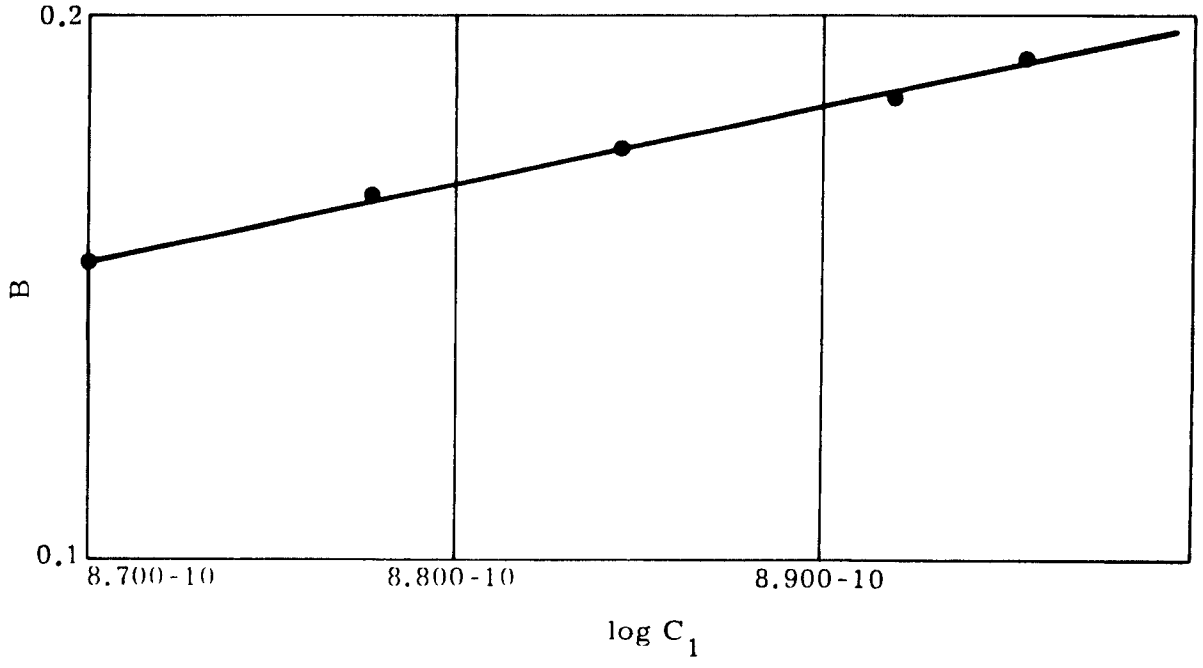

Figure I-18. Values of B vs Values of Log C_1

The logical range of C_1, C_2, and C_3 has already been determined in the general optimzation procedure, paragraph I.3. Knowing the required value of $f(C_1, C_2, C_3)$, the same range of C_1 and C_3 will be investigated and the corresponding values of C_2 will be calculated using the previously derived equation. This would result with 25 combinations of C_1, C_2, and C_3, with the following values of C_1 and C_3 being investigated

$$C_1 = 0.10, 0.11, 0.12, 0.13, 0.14$$

$$C_3 = 5, 7, 9, 11, 13$$

These 25 combinations are investigated for panel buckling and rib crippling. All design configurations that violate local instability will be eliminated. The average thickness for each of the remaining combinations is calculated as

$$t_{ave} = g(C_1, C_2, C_3)H$$

The design that yields the minimum average thickness is then chosen as the optimum.

I.4.2 OPTION TO SPECIFY RIB SPACING

The purpose of this paragraph is to determine an optimization procedure when given the value of rib spacing. The parameters that are considered for optimization are skin thickness, overall depth, and rib thickness. As has been previously stated in paragraph I.3, the optimization will be considered for buckling governed cases only and not for strength. The approximate formula developed for general instability is

$$N_{cr} = \frac{2C}{R}\left[0.545\, C_1^{0.443}\left(\frac{C_2}{C_3}\right)^{0.53}\right] EH^2$$

where

$$C = 0.40$$

$$C_1 = \frac{t_s}{H}$$

$$C_2 = \frac{t_{ws}}{H}$$

$$C_3 = \frac{b_s}{H}$$

Substituting the values of C_1, C_2, and C_3 results in

$$N_{cr} = \frac{2C}{R}\left[0.545\, t_s^{0.443}\left(\frac{t_{ws}}{b_s}\right)^{0.53}\right] EH^{1.557}$$

Letting

$$C_6 = \frac{t_s}{b_s}$$

$$C_7 = \frac{t_{ws}}{b_s}$$

$$C_8 = \frac{H}{b_s}$$

and substituting in these values results in

$$N_{cr} = \frac{2C}{R} f(C_6, C_7, C_8) E b_s^2$$

where

$$f(C_6, C_7, C_8) = 0.545\, C_6^{0.443} C_7^{0.53} C_8^{1.579}$$

Given the value of the rib spacing, b_s, the required value of $f(C_6, C_7, C_8)$ to resist general instability can be calculated using the above equation. In order to obtain an optimum design, the values of C_6, C_7, and C_8 must be chosen to satisfy the required $f(C_6, C_7, C_8)$ and also yield a minimum average thickness. Knowing the required $f(C_6, C_7, C_8)$, a logical range of C_6 and C_7 will be investigated, with the value of C_8 being calculated by

$$C_8 = \left[\frac{f(C_6, C_7, C_8)}{0.545\, C_6^{0.443}\, C_7^{0.53}}\right]^{0.635}$$

The range of C_6 and C_7 being investigated will be determined using the previously established range of the values of C_1, C_2, and C_3. The range of these values is

$$C_1 = 0.10, 0.11, 0.13, 0.13, 0.14$$

$$C_2 = 0.05, 0.10, 0.15, 0.20, 0.25$$

$$C_3 = 5, 7, 9, 11, 13$$

Since the range of $C_3 = b_s/H$ being investigated is from 5 to 13, the range of $C_8 = H/b_s$ is from 1/13 to 1/5. To establish the range of $C_6 = t_s/b_s$, substitute in the values of $b_s = H/C_8$ and $t_s = C_1 H$. This results with $C_6 = C_1 C_8$. Since the range of C_1 is from 0.10 to 0.14, and C_8 is from 1/13 to 1/5, the range of C_6 is

$$C_6 = 0.00772, 0.01279, 0.01786, 0.02293, 0.028$$

Similarly, the range of C_7 is

$$C_7 = 0.00384, 0.01538, 0.02692, 0.03846, 0.05$$

Having established the range of C_6 and C_7, the value of C_8 can be calculated for each of the 25 combinations of C_6 and C_7. Any combination that violates panel buckling or rib crippling will be eliminated. The average thickness of each of the remaining combinations is calculated and the configuration yielding the minimum average thickness will be chosen as the optimum. The average thickness is

$$t_{ave} = g(C_6, C_7, C_8)b_s$$

where

$$g(C_6, C_7, C_8) = C_6 + 4\left[\left(1 - \frac{C_7}{2}\right)\left(\frac{C_7}{2}\right)(C_8 - C_6) + C_4^2 C_8\left(1 - \frac{\pi}{4}\right)\right.$$
$$\cdot (1 - 2C_5 C_8 - C_7) + C_5^2 C_8^2\left(1 - \frac{\pi}{4}\right)(C_8 - C_6)$$
$$\left. + \pi(C_5 C_8 - 0.22\, C_4 C_8)\,(C_4^2 C_8^2)\left(1 - \frac{\pi}{4}\right)\right]$$

I.5 WEIGHT CONSIDERATIONS

Letting $r_{ws} = C_4 H$ and $r_s = C_5 H$, the weight per surface area of the cylinder is

$$w = g(C_1, C_2, C_3) \frac{H}{12} \rho$$

where

$$g(C_1, C_2, C_3) = \frac{C_3^2 C_1 + \left(C_3 - \frac{C_2}{2}\right)(C_2 - C_2 C_1)2}{C_3^2}$$

$$+ \frac{2\pi(C_5 - 0.22\, C_4)}{C_3^2}\left[C_4^2\left(1 - \frac{\pi}{4}\right)\right] + \frac{4C_5^2\left(1 - \frac{\pi}{4}\right)(1 - C_1)}{C_3^2}$$

$$+ \frac{4C_4^2\left(1 - \frac{\pi}{4}\right)(C_3 - 2C_5 - C_2)}{C_3^2}$$

In order to determine the true weight per surface area of any cylinder of waffle type construction, the following formula is used

$$w = g(C_1, C_2, C_3)\left(\frac{H}{12}\right)(\rho) F_b$$

where $F_b = 1.20$ is a fabrication factor which takes into consideration non-calculated items.

I.6 CONICAL SECTIONS

Conical sections will be analyzed using the equivalent cylinder method where each section is transformed into an equivalent cylinder by

$$\overline{R} = \frac{R_{beg}\sqrt{L_c^2 + (R_{beg} - R_{end})^2}}{L_c}$$

I.7 NOMENCLATURE

N_x	Axial load per inch (lbs/inch).
N_y	Hoop load per inch (lbs/inch).
R	Radius of cylinder (inches).
A_{11}	Extensional stiffness in longitudinal direction (lbs/inch).
A_{22}	Extensional stiffness in hoop direction (lbs/inch).
A_{33}	Shear stiffness (lbs/inch).
D_{11}	Flexural stiffness in longitudinal direction (inch-lbs).
D_{22}	Flexural stiffness in hoop direction (inch-lbs).
D_{33}	Torsional stiffness (inch-lbs).
N_{cr}	Critical buckling load per inch (lbs/inch).
H	Overall waffle depth (inches).
t_s	Thickness of skin (inches).
t_{ws}	Rib thickness (inches).
b_s	Rib spacing (inches).
μ	Poisson's ratio.
C_1	t_s/H
C_2	t_{ws}/H
C_3	b_s/H
E	Modulus of elasticity ($lbs/inch^2$).
w	Weight of waffle per surface area (lbs/ft^2).
r_s	Radius of intersection of ribs (inches).
r_{ws}	Fillet radius at intersection of ribs and skin (inches).
σ	Stress level ($lbs/inch^2$).
$\overline{R}$	Equivalent radius.

L_c Conical length.

R_{beg} Radius at beginning of section.

R_{end} Radius at end of section.

APPENDIX J

SEMI-MONOCOQUE CYLINDERS

J.1 INTRODUCTION

An analysis is made to determine the optimum cross-sectional dimensions of a surface loaded in compression, and stiffened by Z-section stringers. A method is presented whereby some of the dimensions may be chosen if necessary. This allows consideration of practical limitations such as minimum gage material. The following assumptions are made:

a. The skin and stringer sections behave as panels simply supported at the ends by the frames.

b. Thin-plate buckling theory is applicable.

c. "Strip theory" as described for general instability of wide panels is sufficiently accurate for application to orthotropic cylinders.

d. The most efficient designs are those in which the Euler instability and initial buckling occur simultaneously.

e. The frames do not restrain local buckling.

f. The effect of internal pressure and the transverse load produced is neglected when considering buckling failure.

g. The effect of plasticity can be considered by the use of a plasticity factor, η, related to the reduced modulus of the material.

J.2 RESULTS

By using the approach of equating initial and general instability, the optimum design of a semi-monocoque type of construction has been determined. The dimensions of the cross-section are interrelated such that they are all determined for the optimum design. If there are practical limitations on some of the dimensions, the optimum dimensions will not be allowable and a method is given whereby the structural efficiency can be kept as high as possible. For instance, if one of the dimensions of the skin or stringer is specified, Figure J-5 presents curves which determine the other panel dimensions if the frame spacing, axial load, and material modulus are known. Similarly, Figures J-6 through J-8 present curves whereby two of the dimensions may be specified and the

other dimensions may be determined while keeping the conditions of simultaneous initial and general instability.

If the optimum buckling stress is not in the elastic range of the material, then an iterative procedure is necessary to determine the material modulus and optimum stress.

J.3 ANALYSIS

J.3.1 GENERAL

The problem considered here is that of designing a large-diameter semi-monocoque shell of minimum weight. Figure J-1 shows a typical panel that is considered in the analysis. The axial compressive load is in the direction of the Z-section stringers, and L is the unsupported length between I-section frames.

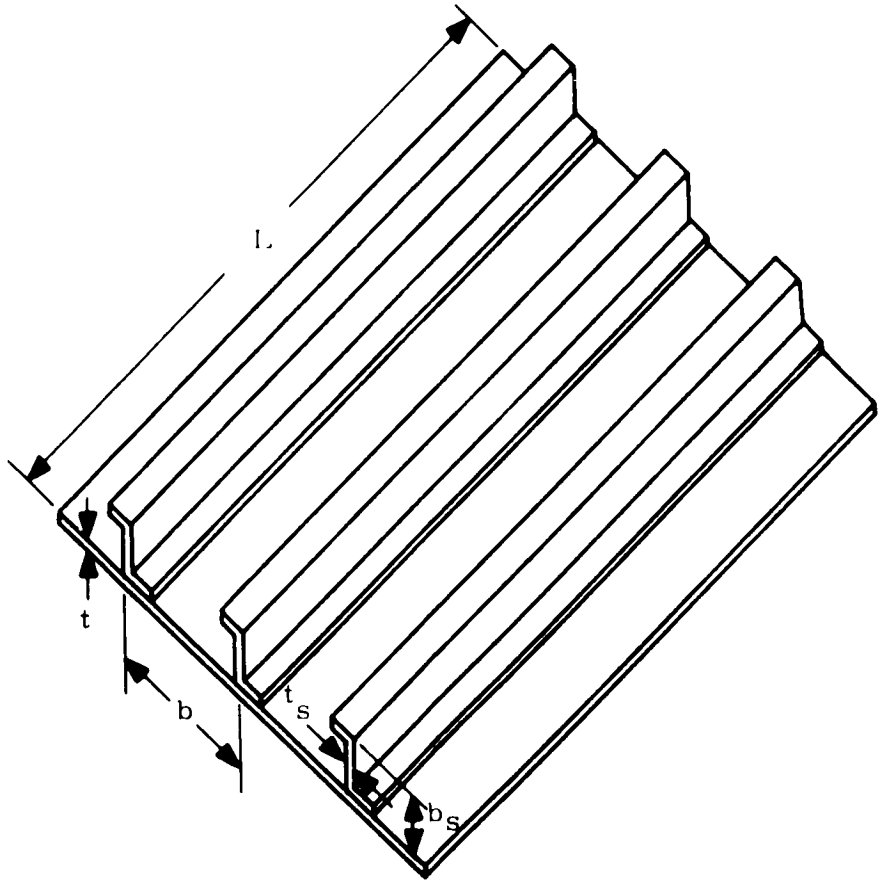

Figure J-1. Type of Construction Considered

In general, it has been found that the most efficient designs are those in which failure occurs simultaneously in all possible buckling modes. The local buckling stress is taken as that given by

$$\sigma_b = \left(\frac{\sigma_b}{\sigma_o}\right) K E_p \left(\frac{t}{b}\right)^2$$

where

$$E_p = C E \left(\frac{E_s}{E}\right)\left(\frac{E_t}{E_s}\right)^{\frac{1}{2}}$$

and K depends upon the type of end conditions. For a simply supported condition, K = 3.62.

The method used takes full account of the interaction between plate and stiffener buckling through the use of the factor (σ_b/σ_o), but the effect of the stiffener root fillet has been neglected. The results of the plate stiffener interaction are shown in Figure J-2 and were obtained from References 24 and 25. The upper portion of the curves correspond to a skin and stringer local type of instability, and the lower portion of the curves reflect a torsional type of instability. The two modes of failure coincide at the points of discontinuity. Note that σ_o is the buckling stress of the skin if the edges are pinned along the stringers and σ_b is the actual initial buckling stress.

The Euler general instability relation is used, where

$$\sigma_e = \frac{E_p \pi^2 \rho^2}{L^2}$$

The axial stress is related to the axial stress resultant, N_x, as follows

$$\sigma = \frac{N_x}{t}$$

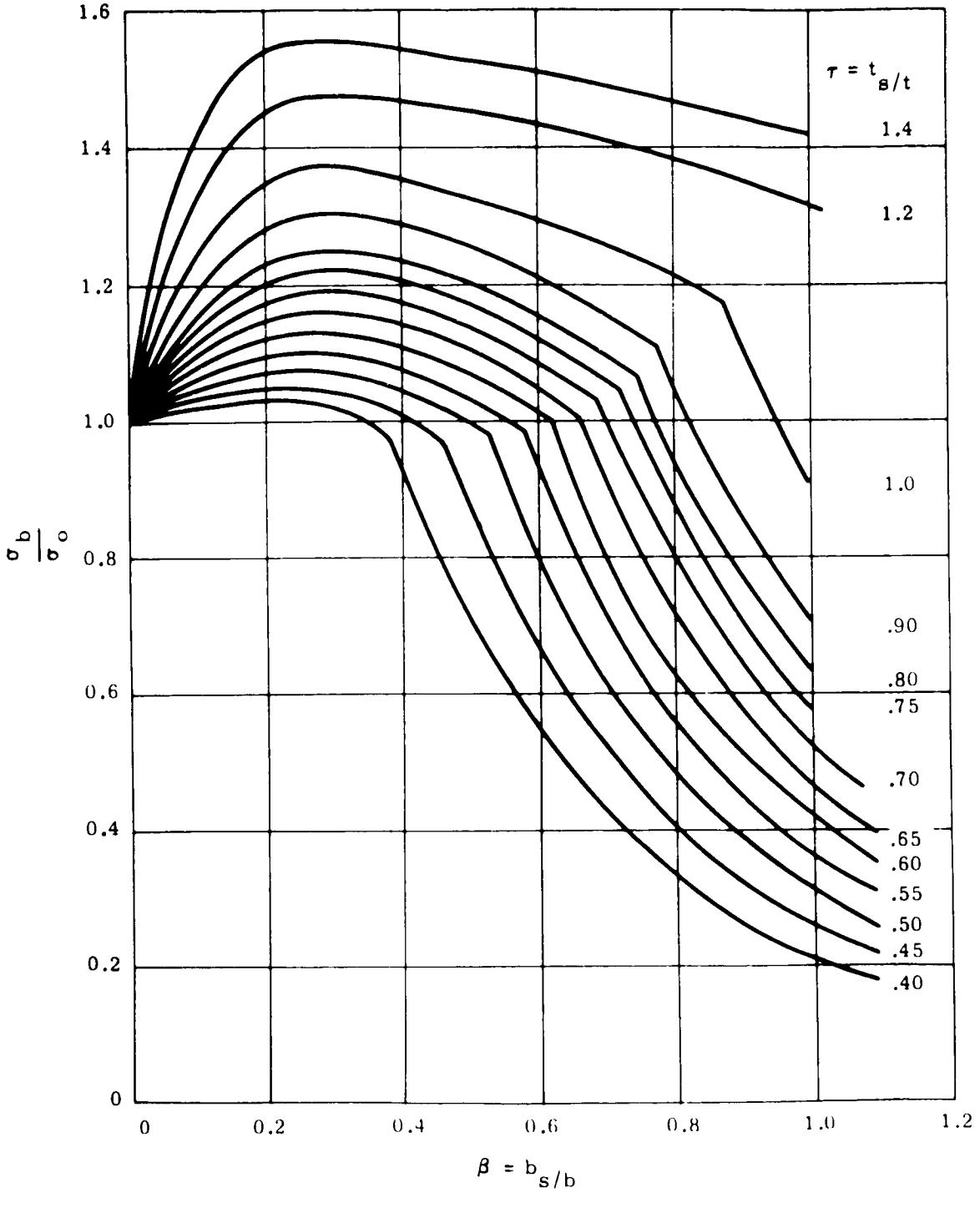

Figure J-2. Initial Buckling Stress of Flat Panels with Z-Section Stringers ($d_s/b_s = 0.3$)

The above expressions are combined in the following form

$$\sigma = F\left(\frac{N_x E \rho}{L}\right)^{\frac{1}{2}}$$

where F is Farrar's efficiency factor

$$F = \pi^{\frac{1}{2}} K^{\frac{1}{4}} \left(\frac{\rho}{E}\right)^{\frac{1}{2}} \left(\frac{t}{b}\right)^{\frac{1}{2}} \left(\frac{\sigma_b}{\sigma_o}\right)^{\frac{1}{4}}$$

For a given load, material, and effective panel length, the most efficient design occurs when F is maximum. The expression for ρ/E is

$$\frac{\rho}{E} = \frac{1}{(12)^{\frac{1}{2}}} \frac{b_s}{t} \left[\frac{1 + 6\alpha + \dfrac{3(1+2\alpha)}{\dfrac{b_s t_s}{bt}}}{\left(1 + 2\alpha + \dfrac{bt}{b_s t_s}\right)\left[(1+2\alpha)\dfrac{b_s t_s}{bt} + 1\right]^2} \right]^{\frac{1}{2}}$$

Substituting the above equation into that for F gives the general expression

$$F = \left(\frac{\pi^2 K}{12}\right)^{\frac{1}{4}} \left(\frac{b_s}{b}\right)^{\frac{1}{2}} \left[\frac{1 + 6\alpha + \dfrac{3(1+2\alpha)}{\dfrac{b_s t_s}{bt}}}{\left(1 + 2\alpha + \dfrac{tb}{b_s t_s}\right)\left[(1+2\alpha)\dfrac{b_s t_s}{bt} + 1\right]^2} \right]^{\frac{1}{4}} \left(\frac{\sigma_b}{\sigma_o}\right)^{\frac{1}{4}}$$

The expression for F is simplified by the following substitutions

$$K = 3.62$$

$$\frac{b_s}{b} = \beta$$

$$\frac{t_s}{t} = \tau$$

$$\alpha = 0.3$$

so that

$$F = 1.314 \frac{[\beta^3\tau(7.6 + 4.48\beta\tau)]^{\frac{1}{4}}}{1 + 1.6\beta\tau} \left(\frac{\sigma_b}{\sigma_o}\right)^{\frac{1}{4}}$$

F is plotted in Figure J-3 and has a maximum value of 0.96 at $\tau = 1.2$ and $\beta = 1.03$. The most efficient design for buckling is, therefore, given by the relationship

$$\sigma = 0.96\left(\frac{N_x E_p}{L}\right)^{\frac{1}{2}}$$

The equivalent panel-stringer thickness can be calculated as

$$\bar{t} = \left(\frac{1}{F}\right)\left(\frac{N_x L}{E_p}\right)^{\frac{1}{2}}$$

and the skin thickness is

$$t = \frac{\bar{t}}{(1 + 1.6\beta\tau)}$$

From Figure J-3 it is noticeable that the efficiency is very high along the line which represents simultaneous buckling in two modes at initial instability. In fact, this line is the extremum of the efficiency for the upper range of τ and β and is very close to the extremum in the lower range. If conditions are such that it is not possible to use the optimum design value of the efficiency, then the efficiency can be kept high by designing along this line. Figure J-4 gives the combination of τ and β which determines this line of high efficiency.

We may combine the preceding applicable equations to get a set of dimensionless equations as follows

$$T = t\left(\frac{E_p}{N_x L}\right)^{\frac{1}{2}} = \frac{1}{F(1 + 1.6\beta\tau)}$$

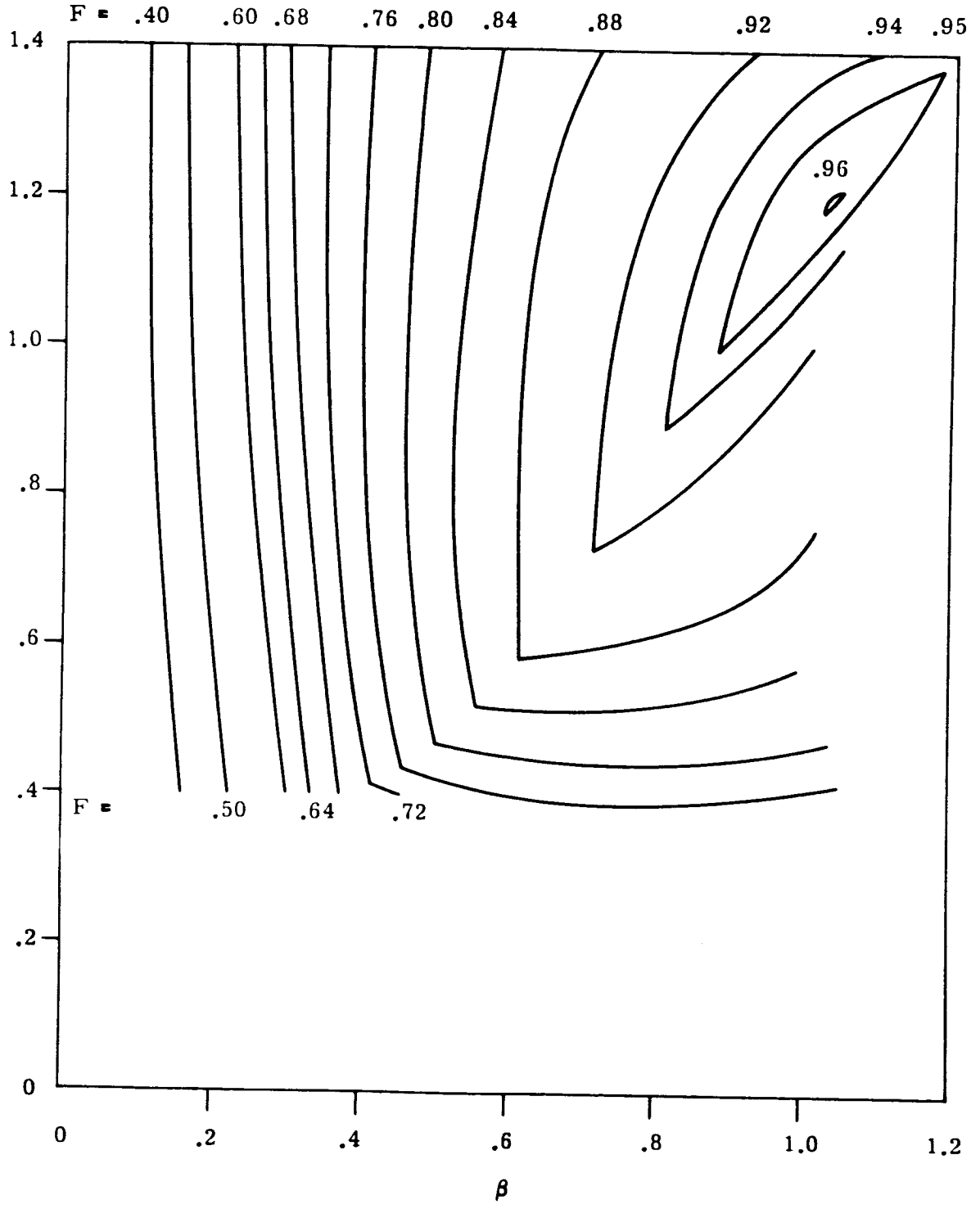

Figure J-3. Contours of the Efficiency, F, for Z-Section Stringers where Initial and General Instability Occur Simultaneously

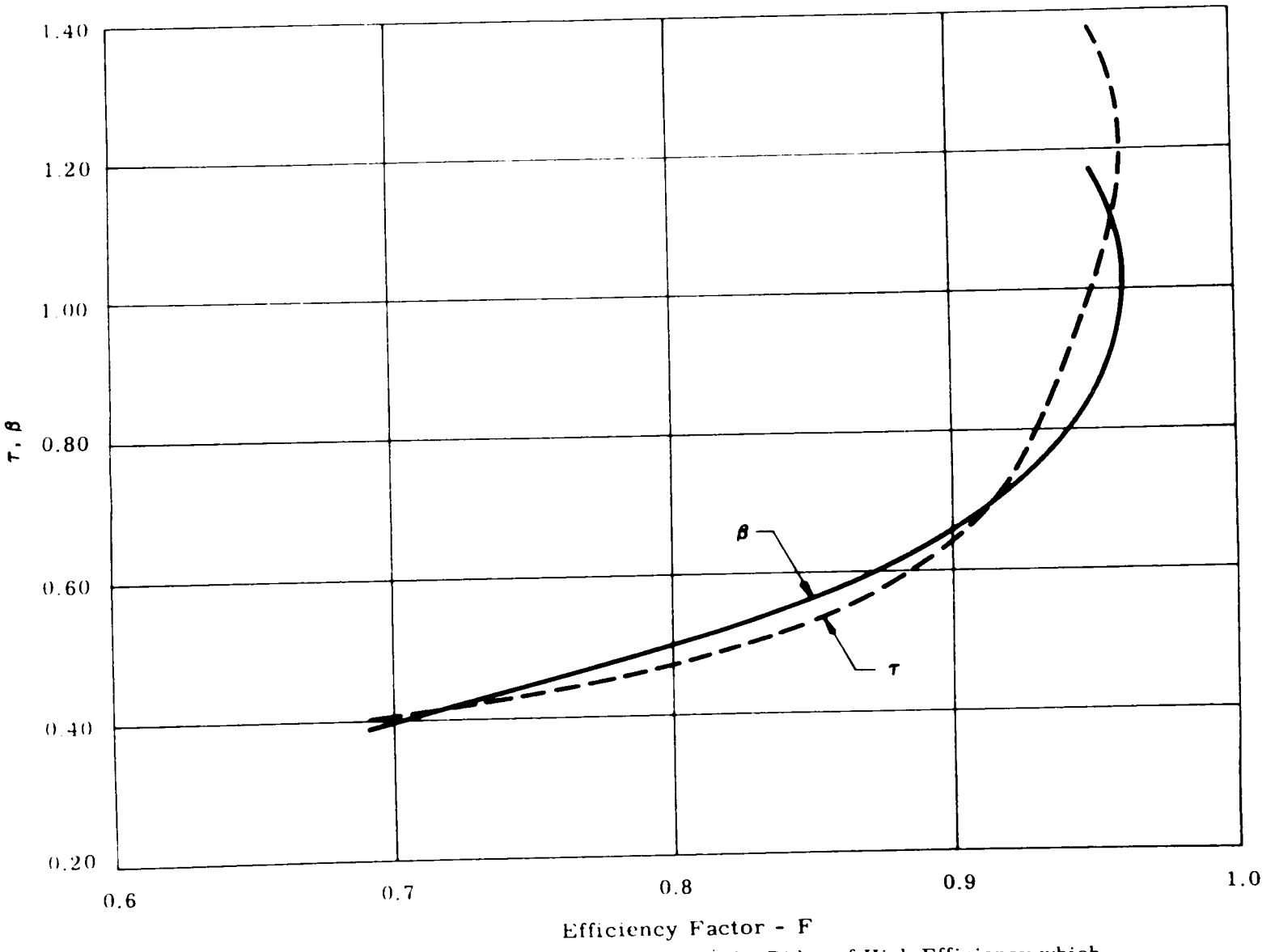

Figure J-4. Combinations of τ and β which Give the Ridge of High Efficiency which Represents Simultaneous Buckling in Two Modes at Initial Instability

$$T_s = t_s\left(\frac{E_p}{N_x L}\right)^{\frac{1}{2}} = \frac{\tau}{F(1 + 1.6\beta\tau)}$$

$$B = b\left(\frac{E_p}{N_x L^3}\right)^{\frac{1}{4}} = 1.103\, F^{\frac{1}{2}} \frac{1 + 1.6\beta\tau}{[\beta^3\tau(7.6 + 4.48\beta\tau)]^{\frac{1}{2}}}$$

$$B_s = b_s\left(\frac{E_p}{N_x L^3}\right)^{\frac{1}{4}} = 1.103\, F^{\frac{1}{2}} \frac{(1 + 1.6\beta\tau)}{[\beta\tau(7.6 + 4.48\beta\tau)]^{\frac{1}{2}}}$$

Using the values of F, β, and τ in Figure J-4, the above equations are plotted in Figure J-5. If one of the dimensions t, t_s, b, or b_s is specified, then for a given N_x, E_p, and L, all other dimensions can be determined from Figure J-5. This gives the flexibility of considering manufacturing limitations such as minimum gage material.

The weight penalty invoked by specifying one of the parameters can be seen immediately from Figure J-5 by comparing the efficiency with that for the optimum design.

When more than one parameter is specified, it is probable that a more severe penalty will result because it will not, in general, be possible to design on the ridge of high efficiency represented by the set of curves in Figure J-5. Figures J-6 through J-8 show contours of constant values of F and all combinations of T, B, and B_s plotted against τ and β. If two parameters are specified, then for given values of E_p, N_x, and L, two of the values of T, B, or B_s can be calculated. The intersection of these curves determines a value of F, τ, and β, so the other two parameters can be calculated.

J.3.2 FRAME EQUATIONS

The requirement for the frame stiffness will be taken as that given by Reference 26

$$E_f I_f = \frac{\pi C_f}{4} \cdot \frac{D^4 N_x}{L}$$

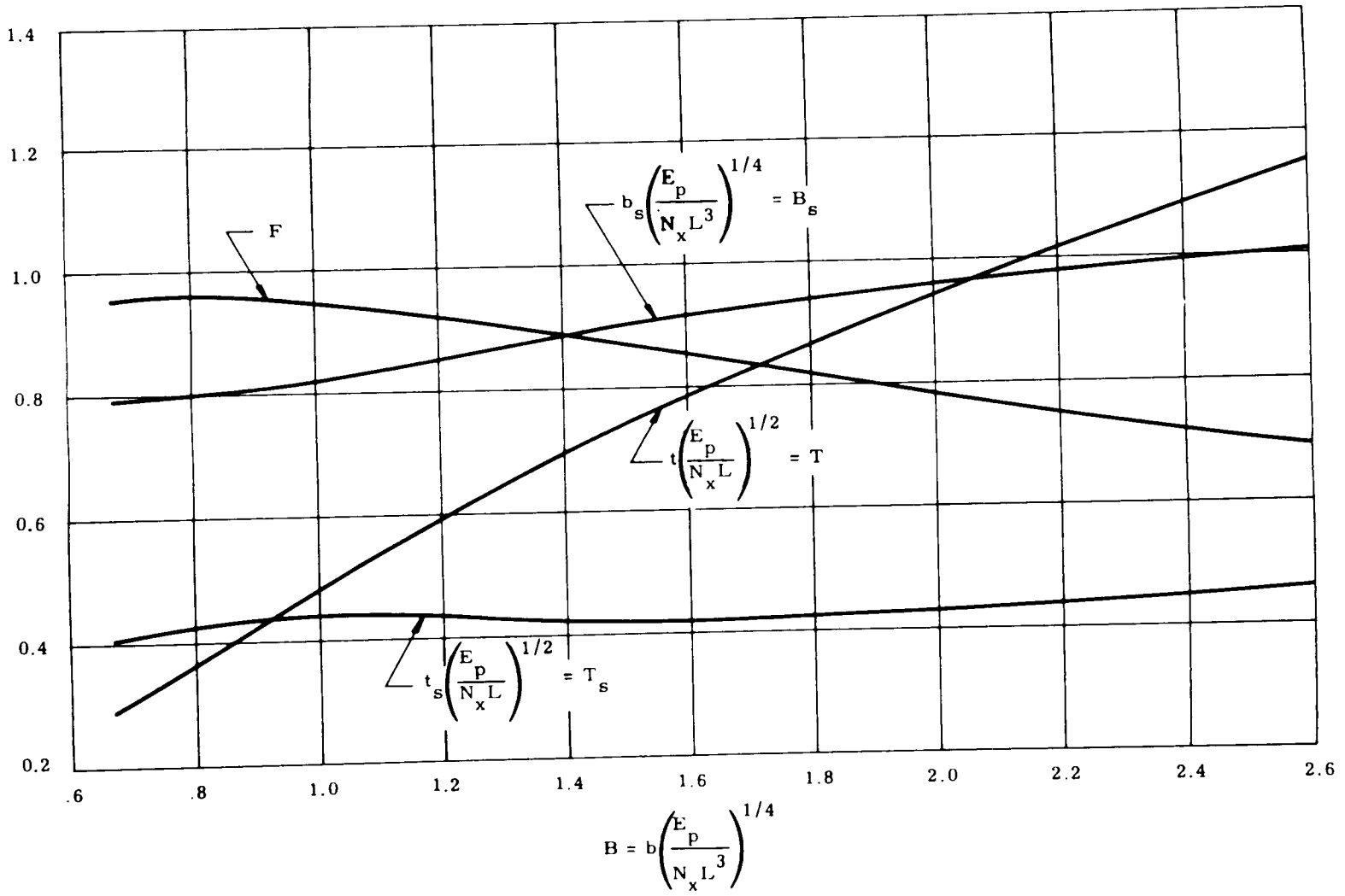

Figure J-5. Optimum Sizing Chart for Specifying One Parameter in Z-Section Stringer-Stiffened Panel

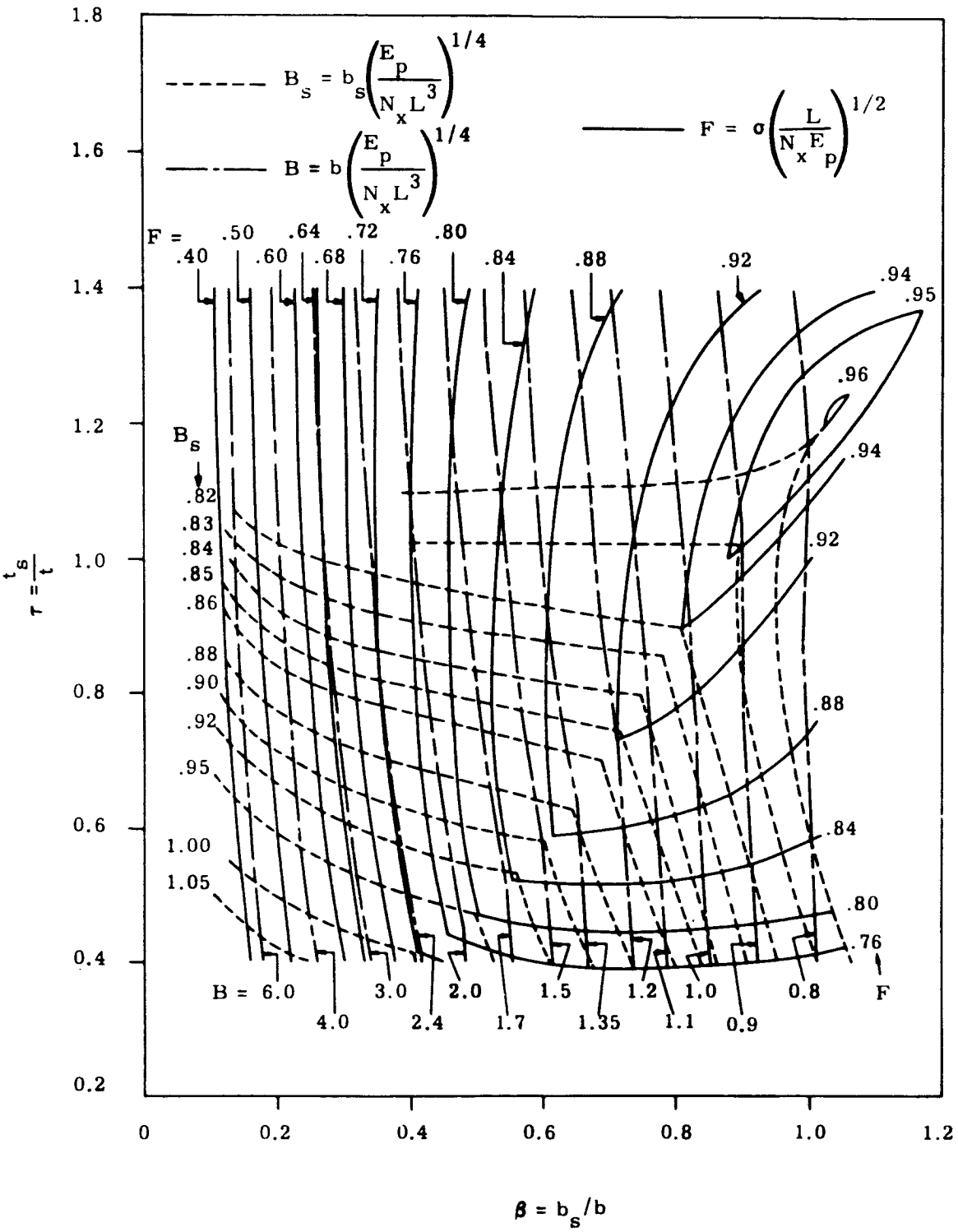

Figure J-6. Sizing Curves for Specified Values of Stringer Spacing and Height for Semi-Monocoque Construction with Z-Section Stringers

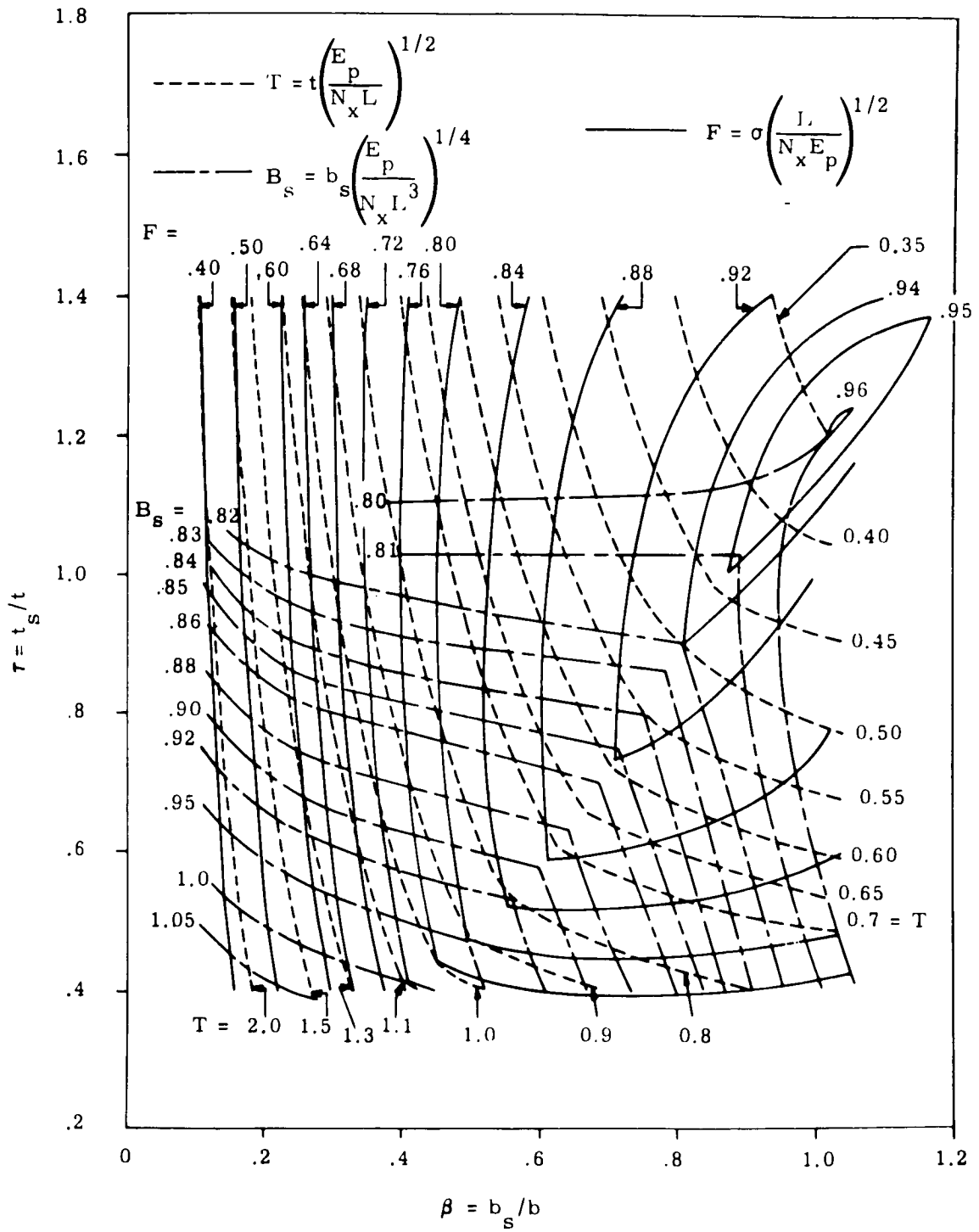

Figure J-7. Sizing Curves for Specified Values of Stringer Height and Skin Thickness for Semi-Monocoque Construction with Z-Section Stringers

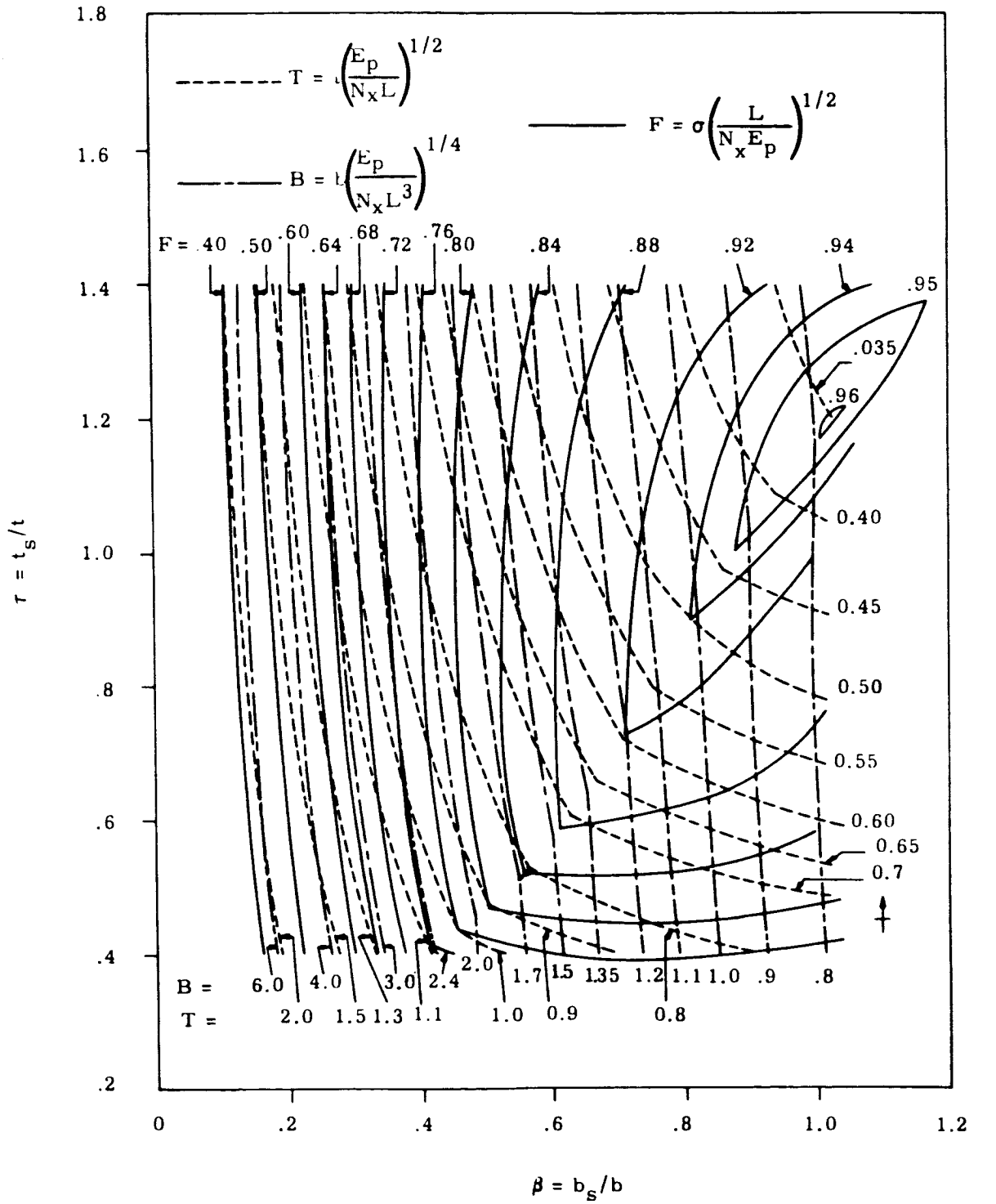

Figure J-8. Sizing Curves for Specified Values of Skin Thickness and Stringer Spacing for Semi-Monocoque Construction with Z-Section Stringers

Assuming the area-moment of inertia relationship

$$I_f = K_f A_f^2$$

results in an average frame thickness

$$\bar{t}_f = \left(\frac{4\pi C_f}{K_f}\right)^{\frac{1}{2}} \left(\frac{R}{L}\right)^2 \left(\frac{N_x L}{E_f}\right)^{\frac{1}{2}}$$

then the total equivalent skin-stringer-frame thickness is

$$\bar{t}_T = (LN_x)^{\frac{1}{2}} \left[\frac{1}{F(E_p)^{\frac{1}{2}}} + \left(\frac{4\pi C_f}{K_f}\right)^{\frac{1}{2}} \left(\frac{R}{L}\right)^2 \frac{1}{(E_f)^{\frac{1}{2}}} \right]$$

The frame spacing which gives the minimum total thickness can be determined by setting the derivative of the preceding equation to zero and solving for L

$$L_o = (3)^{\frac{1}{2}} \left(\frac{4\pi C_f}{K_f}\right)^{\frac{1}{4}} \left(\frac{E_p}{E_f}\right)^{\frac{1}{4}} F^{\frac{1}{2}} R$$

Making the substitutions

$$C_f = 6.25 \times 10^{-5}$$

$$K_f = 3.0875$$

the optimum frame spacing is found

$$L_o = 0.219 \left(\frac{E_p}{E_f}\right)^{\frac{1}{4}} F^{\frac{1}{2}} R$$

Substituting the optimum length, the total equivalent thickness corresponding to the optimum frame spacing can be determined

$$\bar{t}_T = (1.316 + 0.439) \left[\frac{\left(\frac{4\pi C_f}{K_f}\right)^2}{E_p^3 E_f} \right]^{\frac{1}{8}} \frac{(N_x R)^{\frac{1}{2}}}{(F)^{\frac{3}{4}}}$$

The two numerical values in parentheses show the relative weight of the panel and frame weights respectively. This indicates that the optimum frame spacing gives a three-to-one ratio for the panel (skin and stringer) -to-frame weight.

The above equation simplifies to

$$\bar{t}_T = 0.2216 \, (E_p E_f)^{-\frac{1}{8}} \, \frac{(N_x R)^{\frac{1}{2}}}{(F)^{\frac{3}{4}}}$$

The frame dimensions are essentially those recommended in Reference 25, i.e.,

$$\alpha_f = 0.65$$

$$\frac{b_f}{t_f} = 40$$

and the specific dimensions can be calculated from

$$\bar{t}_f = 0.01595 \left(\frac{R}{L}\right)^2 \left(\frac{N_x L}{E_f}\right)^{\frac{1}{2}}$$

$$t_f = 0.104 \, (\bar{t}_f L)^{\frac{1}{2}}$$

$$b_f = 4.17 \, (\bar{t}_f L)^{\frac{1}{2}}$$

$$d_f = 0.65 \, b_f$$

J.4 NOMENCLATURE

b_f	Frame height.
b	Stringer pitch.
b_s	Stringer height.
t	Skin thickness.
t_s	Stringer thickness.

t_f	Frame thickness.
d_f	Frame flange length.
d_s	Stringer flange length.
$\bar{t}$	Average thickness of stringer stiffened panel.
$\bar{t}_f$	A_f/L - Equivalent frame thickness per unit length.
$\bar{t}_T$	Average total thickness of frame and stringer stiffened panel.
t_v	Skin thickness necessary for direct strength requirements.
t_m	Minimum gage thickness for skin.
K_x	Ratio of skin thickness to the average stringer stiffened panel thickness, $t/\bar{t}$.
K_θ	Ratio of skin thickness to the average frame stiffened panel thickness, $t/t + \bar{t}_f$.
N_x	Axial stress resultant.
N_θ	Circumferential stress resultant.
σ	Stress.
σ_{ty}	Tensile yield stress.
σ_{tu}	Tensile ultimate stress.
C	Buckling correction factor.
η	Plasticity reduction factor.
F_y	Yield factor of safety.
F_u	Ultimate factor of safety.
F_b	Fabrication factor.
F	Efficiency factor.
E	Young's modulus of stringer stiffened panel.
E_s	Secant modulus of stringer stiffened panel.
E_t	Tangent modulus of stringer stiffened panel

E_f Young's modulus of frame.

E_p $CE(E_s/E)\,(E_t/E_s)^{\frac{1}{2}} = CE\eta$

L' Length of tank or interstage section.

L'_{input} Maximum length of sheet available commercially.

L Frame spacing.

l Length of sheets combined to make up L'.

R Radius of shell.

τ t_s/t.

β b_s/b.

γ Material density (lb/ft^3).

w Weight per unit surface area.

ϵ Arbitrarily small quantity.

σ_b Section initial buckling stress.

σ_o Initial buckling stress of a long plate of width b and thickness t, simply supported along its edges.

$\sigma_{0.7}$ Stress corresponding to the point of intersection of a line with a slope of 0.7 E drawn from the origin on the stress-strain diagram.

$\sigma_{0.85}$ Stress corresponding to the point of intersection of a line with a slope of 0.85 E drawn from the origin on the stress-strain diagram.

A Surface area.

APPENDIX K

90° WAFFLE STIFFENED CYLINDERS

K.1 INTRODUCTION

A 90° waffle stiffened cylinder consists of a thin skin with equally spaced longitudinal and circumferential stiffening ribs (see Figure K-1). The purpose of this appendix is to establish a method for optimizing this type of structure subjected to axial loading and/or internal pressure. Two modes of failure are considered: strength based on the von Mises yield criteria, and buckling which consists of both general and local instability. The local instability includes panel buckling and rib crippling.

It is quite obvious that no optimization procedure can be developed based on the strength criteria, however the shell can be optimized based on axial buckling. Four parameters are to be optimized: overall depth, rib thickness, rib spacing, and skin thickness. The following is a list of assumptions that are made in the optimization procedure:

a. Internal pressure has no effect on the overall general instability, however it has been considered when investigating panel buckling.
b. Rib spacing is sufficiently close that the ribs and skin are equally stressed.
c. Curved panels between ribs are treated as flat plates when considering panel buckling since the radius of curvature is large.
d. 90° waffle stiffened skin is manufactured using the mechanical milling process.
e. Critical buckling stresses are within the elastic limit.

K.2 FAILURE MODES

K.2.1 GENERAL INSTABILITY

The following equation, which has previously been described in Appendix F, will be employed to describe failure in the general instability mode[9]

$$N_{cr} = \frac{2}{R}\left(\frac{\beta^2 D_{11} + D_{33}}{\frac{\beta^2}{A_{11}} + \frac{1}{2A_{33}}}\right)^{\frac{1}{2}} C$$

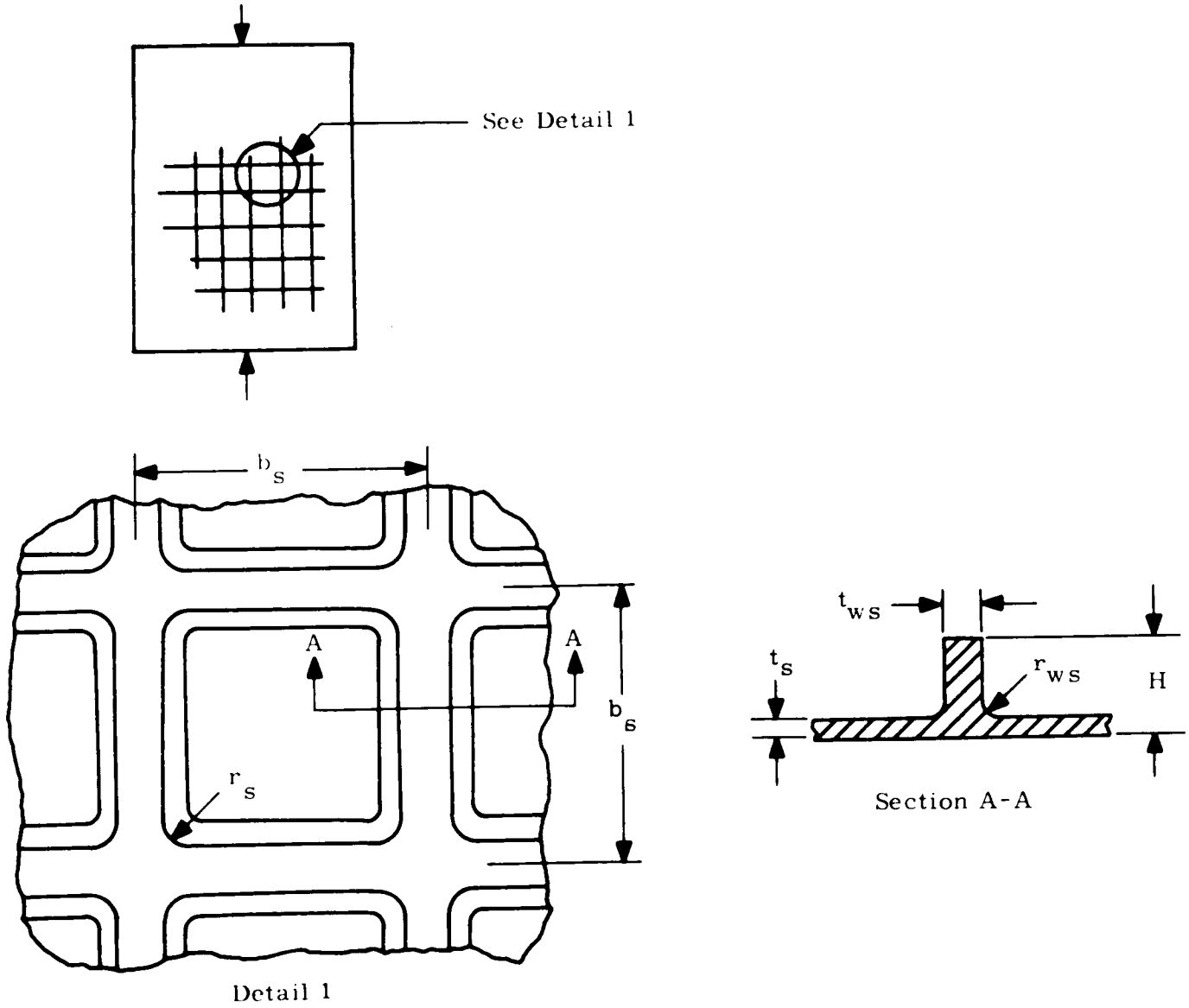

Figure K-1. 90° Waffle Stiffened Geometry

where

$$\beta^2 = P_o + \left(P_o^2 + Q_o\right)^{\frac{1}{2}}$$

$$P_o = \frac{A_{33}}{A_{22}}\left(\frac{A_{22}D_{11} - A_{11}D_{22}}{A_{11}D_{22} - 2A_{33}D_{33}}\right)$$

$$Q_o = \frac{A_{11}}{A_{22}}\left(\frac{A_{22}D_{11} - 2A_{33}D_{33}}{A_{11}D_{22} - 2A_{33}D_{33}}\right)$$

Letting the correction factor $C = 0.40$, based on experimental evidence shown in Appendix F for 45° waffle stiffened cylinders, and, for the type of construction being considered, $A_{11} = A_{22}$ and $D_{11} = D_{22}$, the equation reduces to

$$N_{cr} = \frac{0.8}{R}\left(\frac{D_{11} + D_{33}}{\frac{1}{A_{11}} + \frac{1}{2A_{33}}}\right)^{\frac{1}{2}}$$

It has been found advantageous from an optimization standpoint to express the design parameters all in terms of the overall depth, H. Letting $t_s = C_1H$, $t_{ws} = C_2H$, and $b_s = C_3H$, the stiffness parameters can be expressed as[22]

$$A_{11} = A_x EH$$

$$A_{33} = A_{xy} EH$$

$$D_{22} = \left[I_x - \frac{A_s^2 A_x}{\overline{A}_s^2}\left(\overline{K}_x - \overline{K}_s\right)^2\right] EH^3$$

$$D_{33} = \frac{1}{2} I_{xy} EH^3$$

where

$$I_{xy} = \frac{C_1^3}{6(1+\mu)}$$

$$I_x = \frac{C_1^3}{12(1-\mu^2)} + \frac{C_2(1-C_1)^3}{12C_3} + \frac{C_1}{1-\mu^2}\bar{K}_x^2 + \frac{C_2(1-C_1)}{C_3}\left(\frac{1}{2} - \bar{K}_x\right)^2$$

$$A_x = \frac{C_1}{1-\mu^2} + \frac{C_2(1-C_1)}{C_3}$$

$$A_{xy} = \frac{C_1}{2(1+\mu)}$$

$$A_s = \frac{\mu C_1}{(1-\mu^2)}$$

$$\bar{A}_s^2 = A_x^2 - A_s^2$$

$$\bar{K}_s = 0$$

$$\bar{K}_x = \frac{1}{A_x}\left[\frac{C_2(1-C_1)}{2C_3}\right]$$

letting

$$f(C_1, C_2, C_3) = \left\{ \frac{\left[I_x - \frac{A_s^2 A_x}{\bar{A}_s^2}\left(\bar{K}_x - \bar{K}_s\right)^2 + \frac{1}{2}I_{xy}\right]}{\frac{1}{A_x} + \frac{1}{2A_{xy}}} \right\}$$

$$N_{cr} = \frac{0.8}{R}\left[f(C_1, C_2, C_3)\right]EH^2$$

K.2.2 PANEL BUCKLING

Assuming that the stress level in the ribs and panels are equal, the stress in the hoop and longitudinal directions can be calculated as shown in Figure K-2 where σ_x equals N_x/A_xH and σ_y equals N_y/A_xH.

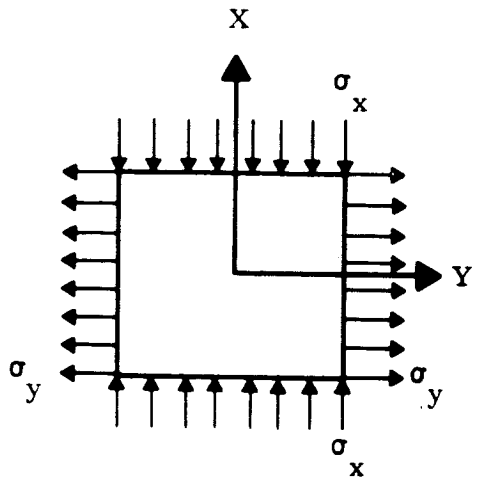

Sign Convention

Compression	positive
Tension	negative

Figure K-2. Free-Body Diagram of the Panel

Assuming simply supported edge conditions, the following formulae[27] will be employed to investigate panel buckling

$$\sigma_e = \frac{\pi^2 E C_1^2}{12(1-\mu^2) C_3^2}$$

If $-3\sigma_e < \sigma_y < 7\sigma_e$, the critical stress in the x direction is found as

$$S_{cr} = 4\sigma_e - \sigma_y$$

If $\sigma_y > 7\sigma_e$, vary m = 2, 3, 4.... until the following inequality holds

$$\sigma_e(2m^2 - 2m + 3) < \sigma_y < \sigma_e(2m^2 + 2m + 3)$$

After determining the integer m, the following is used to determine the critical stress in the x direction

$$S_{cr} = \sigma_e(m^2 + 1)^2 - m^2\sigma_y$$

If $\sigma_y < -3\sigma_e$, vary n = 2, 3, 4.... until the following inequality holds

$$\sigma_e\left[1 - n^2(n-1)^2\right] > \sigma_y > \sigma_e\left[1 - n^2(n+1)^2\right]$$

After determining the integer n, the following is used to determine the critical stress in the x direction

$$S_{cr} = \frac{\sigma_e(1+n^2)^2 - \sigma_y}{n^2}$$

In order that panel buckling is not critical, the following inequality must hold

$$\frac{\sigma_x}{S_{cr}} \geq 1$$

K.2.3 RIB CRIPPLING

Assuming that the stress level in the ribs and panels are equal, the stress in the longitudinal direction (as shown in Figure K-3) can be calculated as σ_x equals N_x/A_xH.

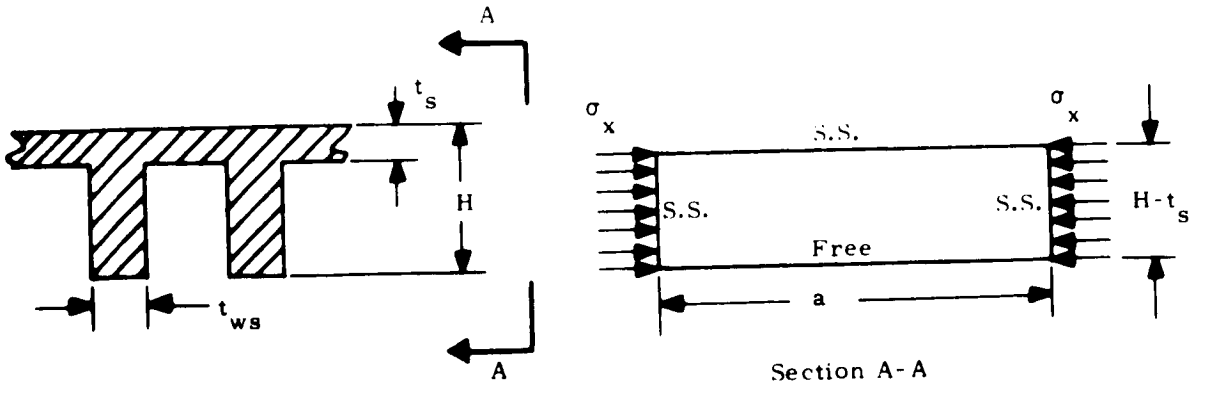

Figure K-3. Rib Crippling

Assuming $a/(H - t_s)$ approaches infinity, the critical buckling stress is given as[23]

$$S_{cr} = 0.385\left(\frac{E}{1-\mu^2}\right)\left(\frac{C_2}{1-C_1}\right)^2$$

where

$$\frac{\sigma_x}{S_{cr}} \geq 1$$

to preclude rib crippling.

K.2.4 STRENGTH CRITERIA

Assuming that the skin and ribs are equally stressed, the von Mises yield criteria will be used to determine the stress level

$$\sigma = \frac{\sqrt{N_x^2 - N_x N_y + N_y^2}}{A_x H}$$

K.3 OPTIMIZATION PROCEDURE

It is desired to determine the optimum design parameters, C_1, C_2, C_3, and H, such that we arrive at a minimum weight configuration. The approach to be used is the concept of maximum strength-to-weight ratio based upon general instability. A logical range of C_1, C_2, and C_3 will be investigated and the resulting strength-to-weight ratios calculated. The configuration with the maximum ratio will be investigated for panel buckling and web crippling. If panel buckling and/or web crippling is not satisfied, the next higher value of strength-to-weight ratio is investigated until the local buckling criteria is satisfied. Having determined the optimum values of C_1, C_2, and C_3, the value of the overall depth can be calculated to satisfy general instability by

$$H = \sqrt{\frac{N_{cr} R}{0.8\, E\, f(C_1, C_2, C_3)}}$$

In order to determine the strength-to-weight ratios, the following equations are needed

$$N_{cr} = \frac{0.8}{R} f(C_1, C_2, C_3) EH^2$$

Average thickness, $t_{ave} = g(C_1, C_2, C_3)H$, so that

$$\frac{N_{cr}}{t_{ave}} = \frac{\frac{0.8}{R} f(C_1, C_2, C_3) EH}{g(C_1, C_2, C_3)}$$

Substitution of the value of H results in

$$\frac{N_{cr}}{t_{ave}} = \frac{[f(C_1, C_2, C_3)]^{\frac{1}{2}}}{g(C_1, C_2, C_3)} \left(\frac{0.8 N_{cr} E}{R}\right)^{\frac{1}{2}}$$

Since the terms N_{cr}, E, and R are the only given terms on the right-hand side of the equation, in order to obtain a maximum strength-to-weight ratio, the following term should be maximum

$$\frac{[f(C_1, C_2, C_3)]^{\frac{1}{2}}}{g(C_1, C_2, C_3)} = \text{maximum}$$

The first step in determining a logical range of C_1, C_2, and C_3 is to approximate the maximum value of C_3/C_1 that precludes panel buckling. Considering a panel loaded uniaxially (loaded in the longitudinal direction with the hoop stress equal to zero) values of C_3/C_1 versus S_{cr} were plotted (see Figure K-4). The value of critical panel buckling stress approaches zero at approximately $C_3/C_1 = 140$. Based upon this, it was decided to use a minimum value of $C_1 = 0.05$ and a maximum value of $C_3 = 7$. In order to cover a wide range of critical panel buckling stresses, the maximum value of $C_1 = 0.09$ and minimum value of $C_3 = 3$ were chosen. This would result with the range of C_3/C_1 being from 33 to 140. Based on Figures K-5 and K-6, the range of C_2 to be investigated is from 0.02 to 0.10 since the maximum values of strength-to-weight ratios occur within this range. In order to keep the number of calculations at a minimum, the following values of C_1, C_2, and C_3 are investigated with all possible combinations of each:

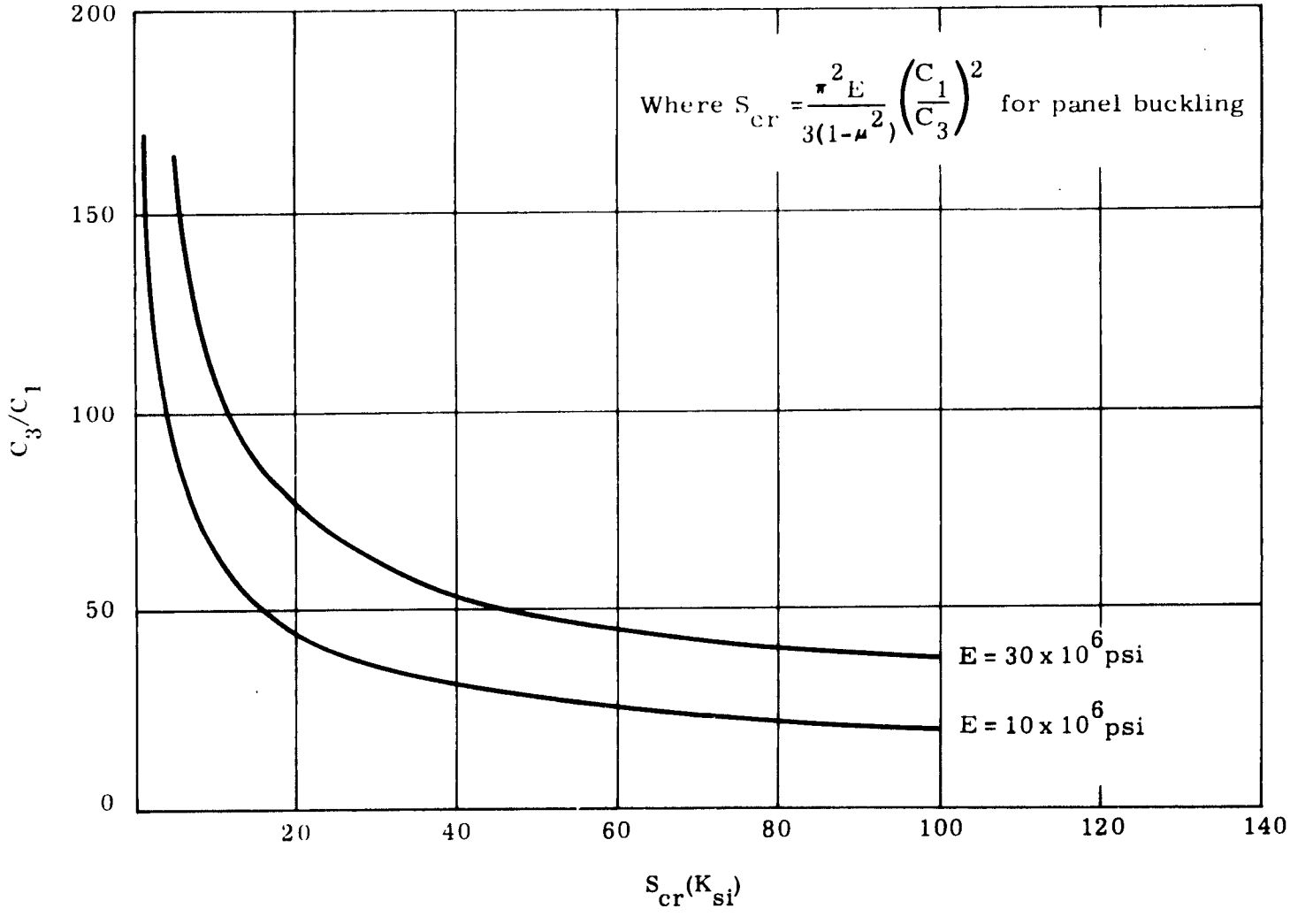

Figure K-4. Maximum Value of C_3/C_1 that Precludes Panel Buckling

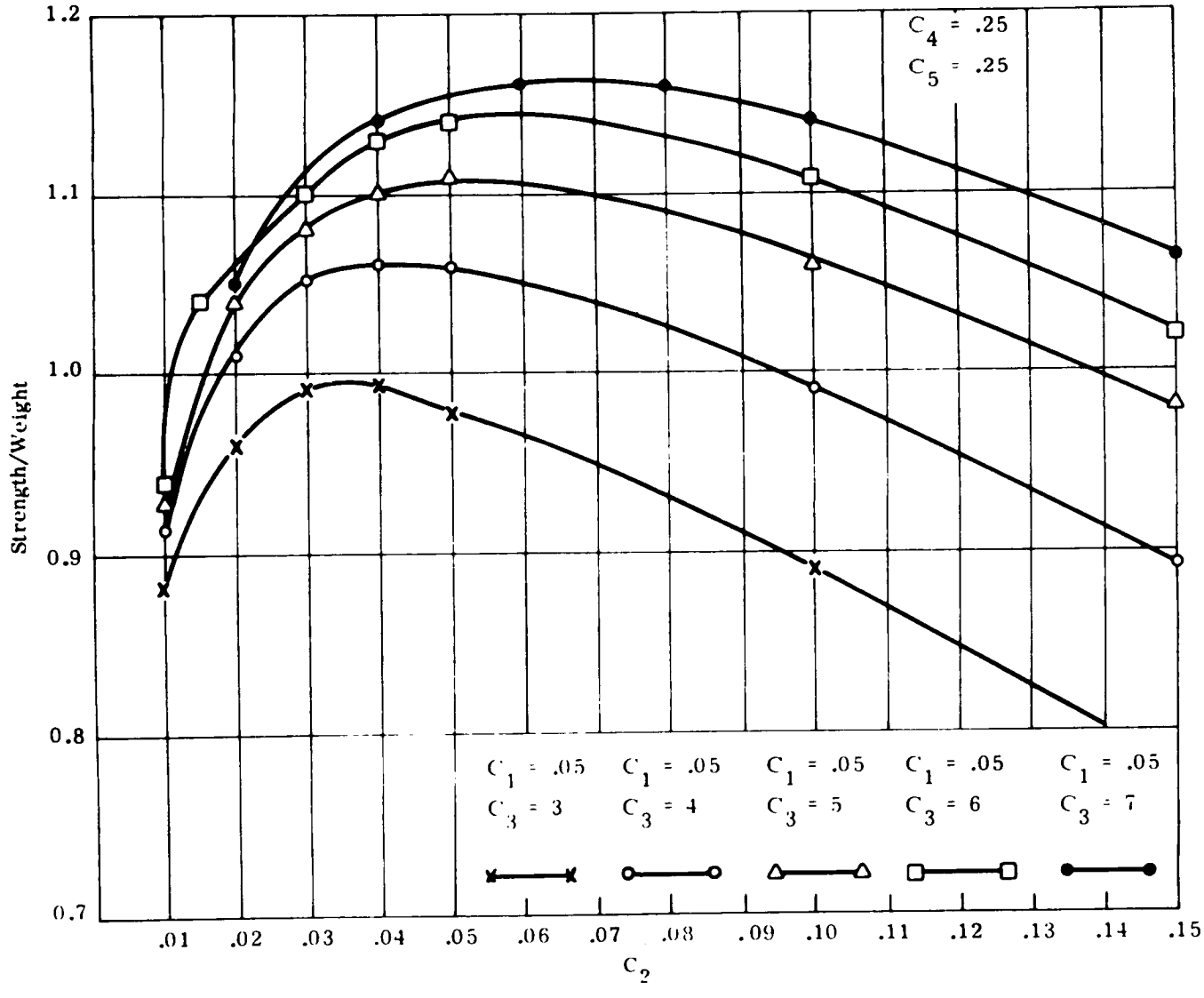

Figure K-5. Strength-to-Weight Ratio versus C_2 for C_1 = 0.05 and C_3 = 3 through 7

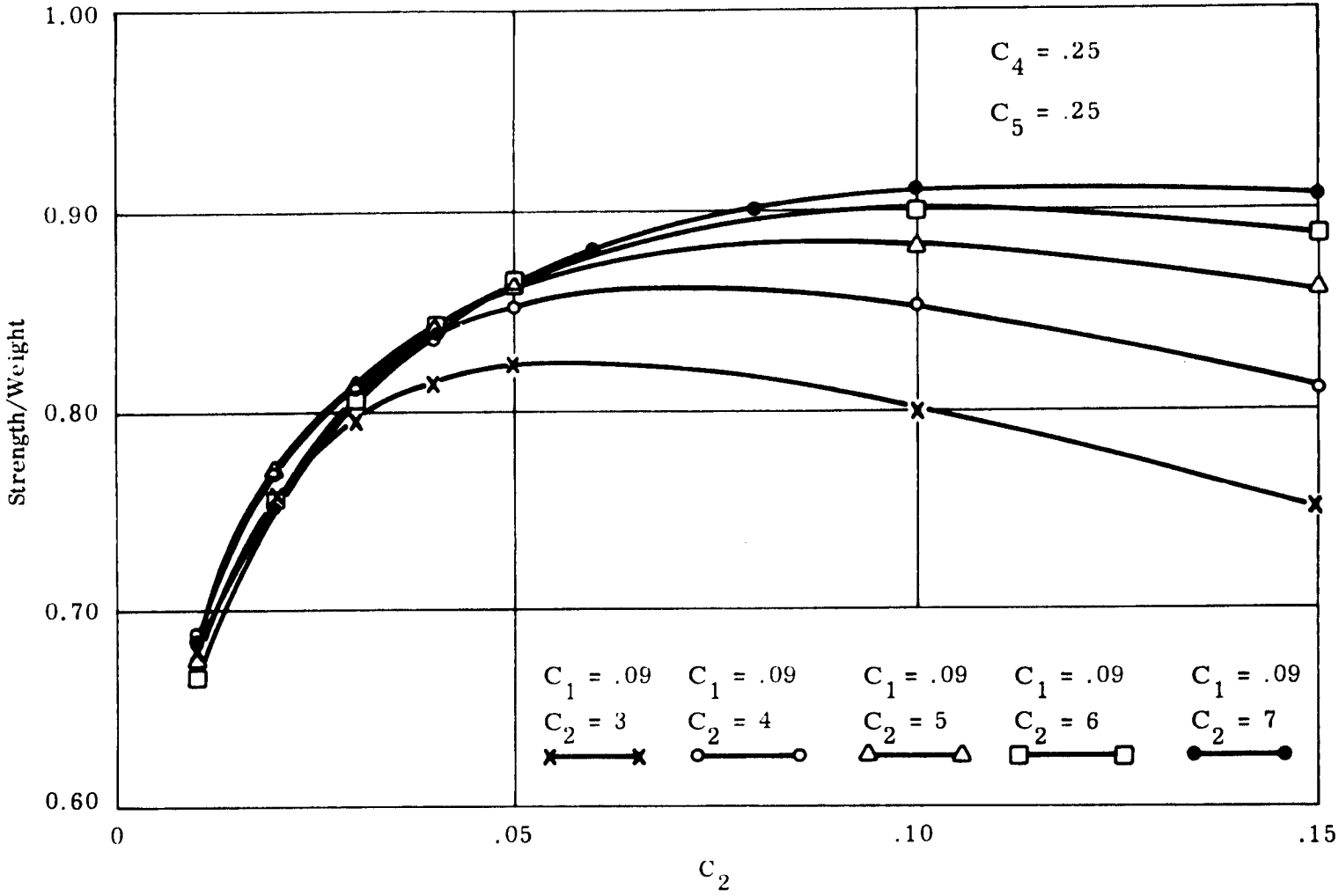

Figure K-6. Strength-to-Weight Ratio versus C_2 for C_1 = 0.09 and C_3 = 3 through 7

C_1 = 0.05, 0.06, 0.07, 0.08, 0.09

C_2 = 0.02, 0.04, 0.06, 0.08, 0.10

C_3 = 3, 4, 5, 6, 7

This would result in 125 combinations of C_1, C_2, and C_3.

K.4 OPTIONS

K.4.1 OPTION TO SPECIFY OVERALL DEPTH

The purpose of this section is to determine an optimization procedure when given the value of the overall depth. The parameters that are considered for optimization are skin thickness, rib thickness, and rib spacing. As has been previously stated in paragraph K.3, the optimization will be considered for buckling governed cases only and not for strength.

Given the value of H, the value for $f(C_1, C_2, C_3)$ required to resist general instability is

$$f(C_1, C_2, C_3) = \frac{N_x R}{0.8\, E H^2}$$

However, due to the complexity of the $f(C_1, C_2, C_3)$, a method for simplifying the equation was sought. Assuming that the $f(C_1, C_2, C_3)$ is of the form $x = y^m$, values of $f(C_1, C_2, C_3)$ versus C_2 for various combinations of C_1 and C_3 are plotted on Figures K-7 through K-11. The plots on log-log paper consist of parallel straight lines, thus verifying the assumed form of the equation $x = y^m$. Based on this equation, $C_2 = A\,[f(C_1, C_2, C_3)]^m$, where m = 2.18 and A is a function of C_3 and C_1. The values of A were determined for each combination of C_1 and C_3 and plotted on log-log paper against the value of C_3 (see Figure K-12). Here again, the results are straight parallel lines taking the same general form of the equation. Therefore, $A = BC_3^n$ where n = 0.97 and B is a function of C_1. The values of B are determined for each value of C_1 and plotted on log-log paper against the value of C_1 (see Figure K-13). The result is a straight line again taking the same general form of the equation. Therefore, $B = DC_1^p$ where D = 20.4 and p = -0.96. Substituting in the values of A and B, the following

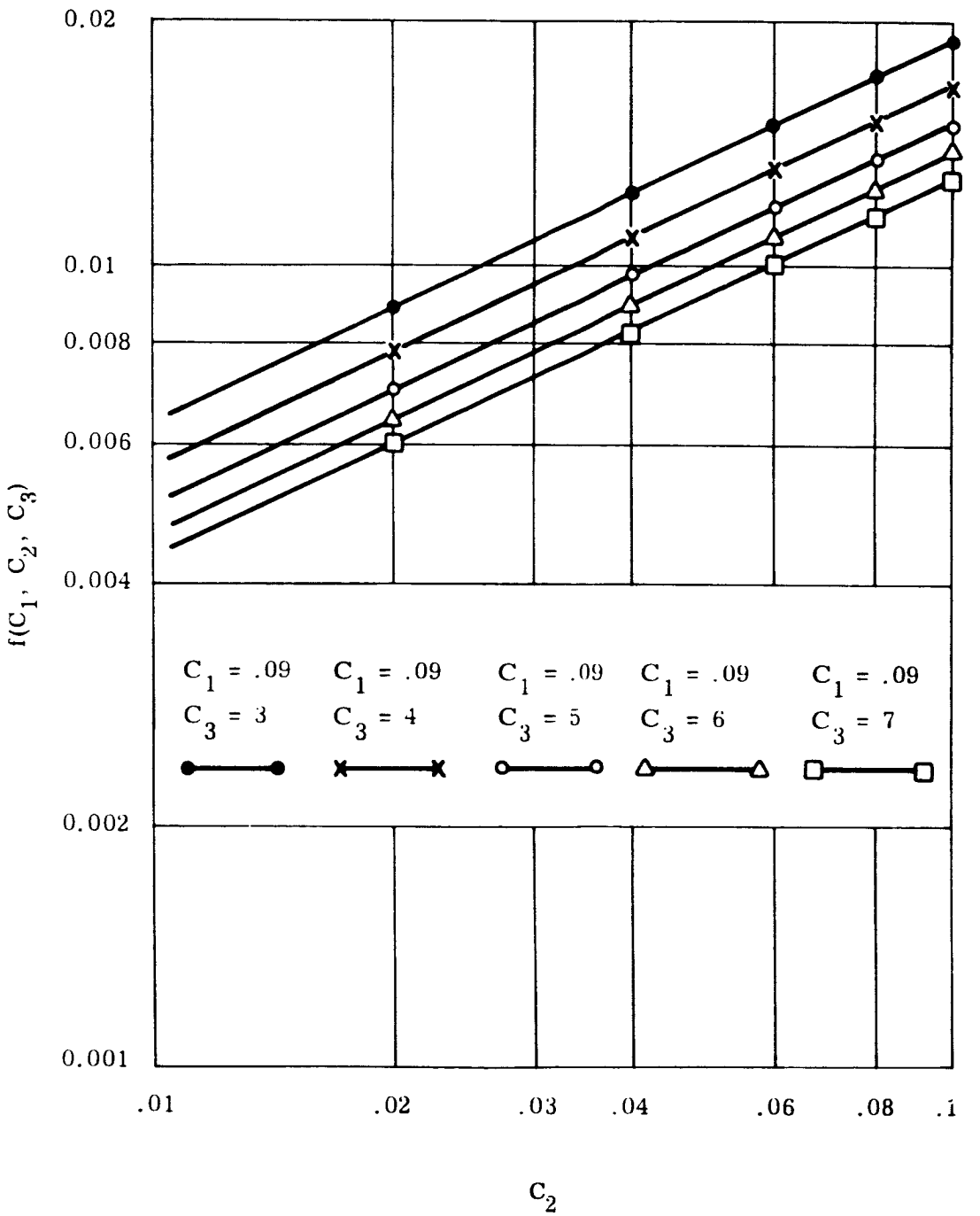

Figure K-7. Values of $f(C_1, C_2, C_3)$ versus C_2 for $C_1 = 0.09$

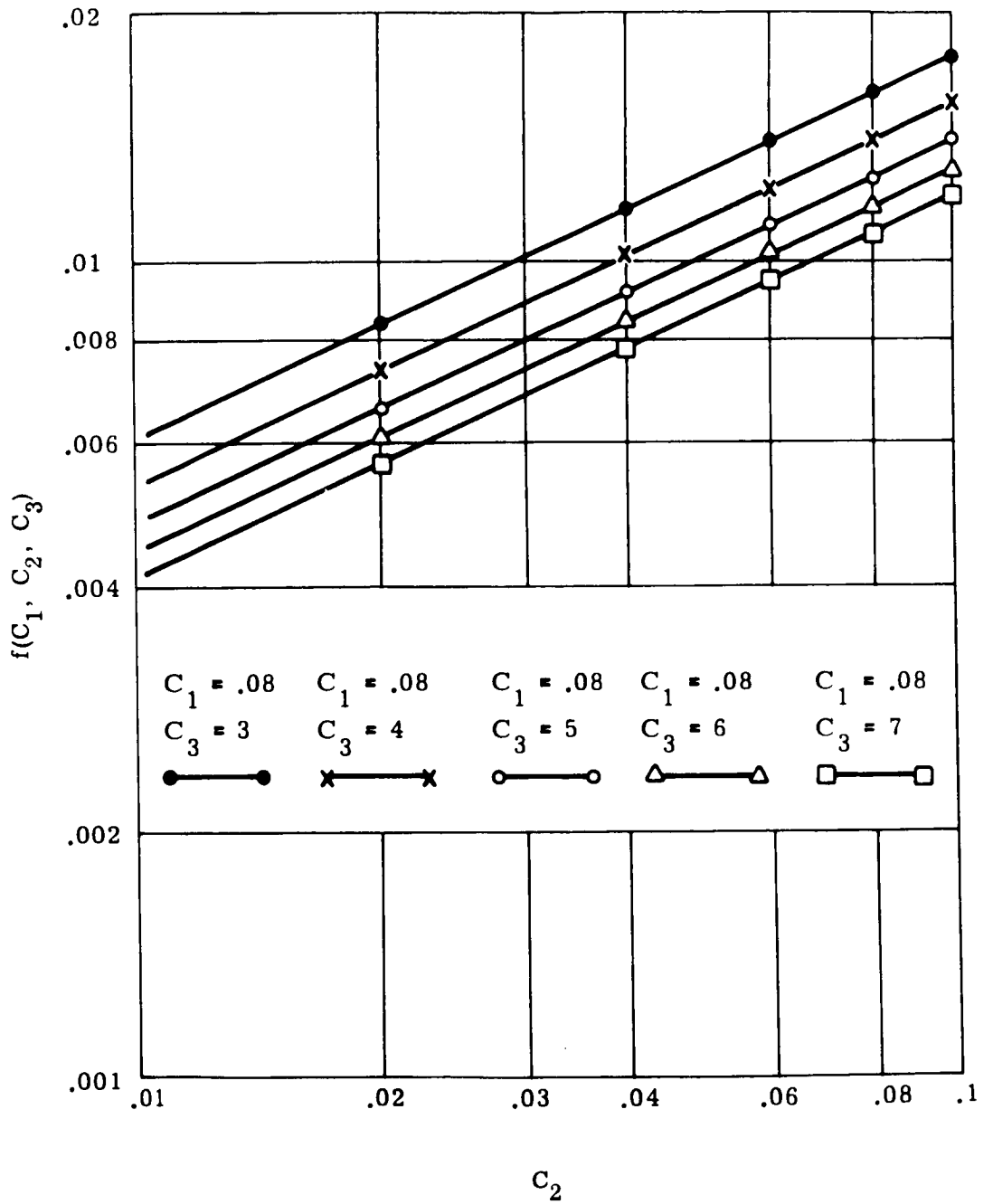

Figure K-8. Values of $f(C_1, C_2, C_3)$ versus C_2 for $C_1 = 0.08$

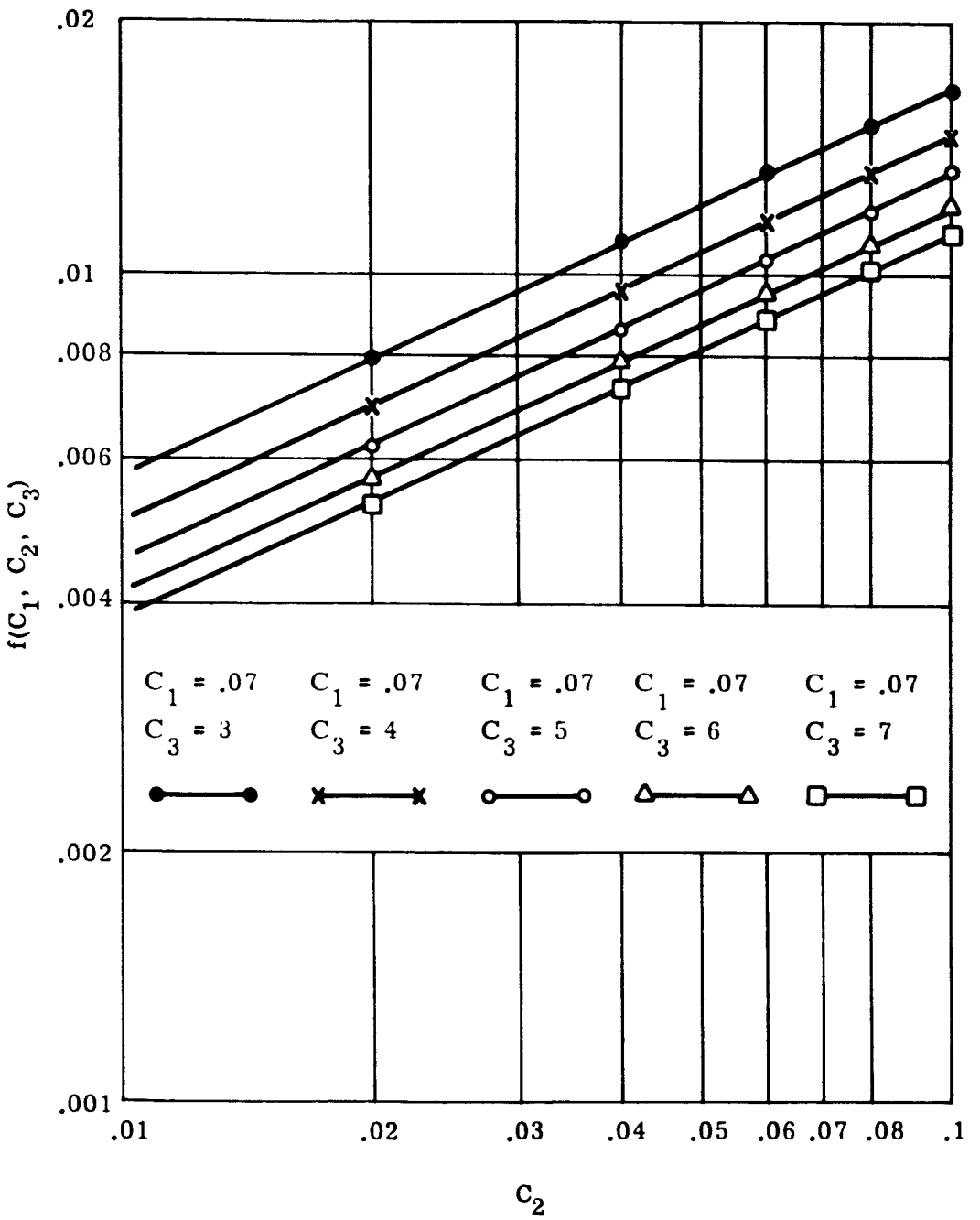

Figure K-9. Values of $f(C_1, C_2, C_3)$ versus C_2 for $C_1 = 0.07$

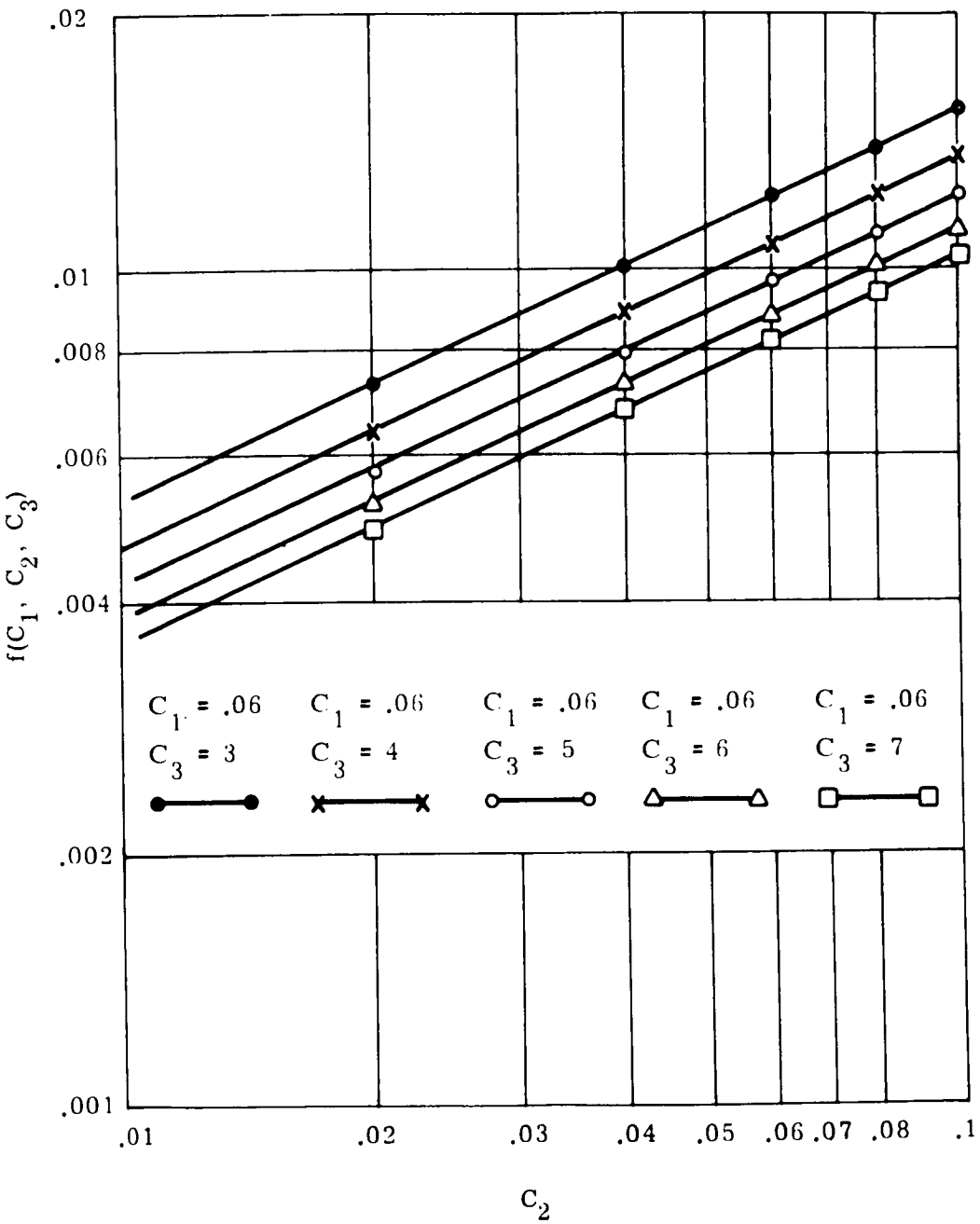

Figure K-10. Values of $f(C_1, C_2, C_3)$ versus C_2 for $C_1 = 0.06$

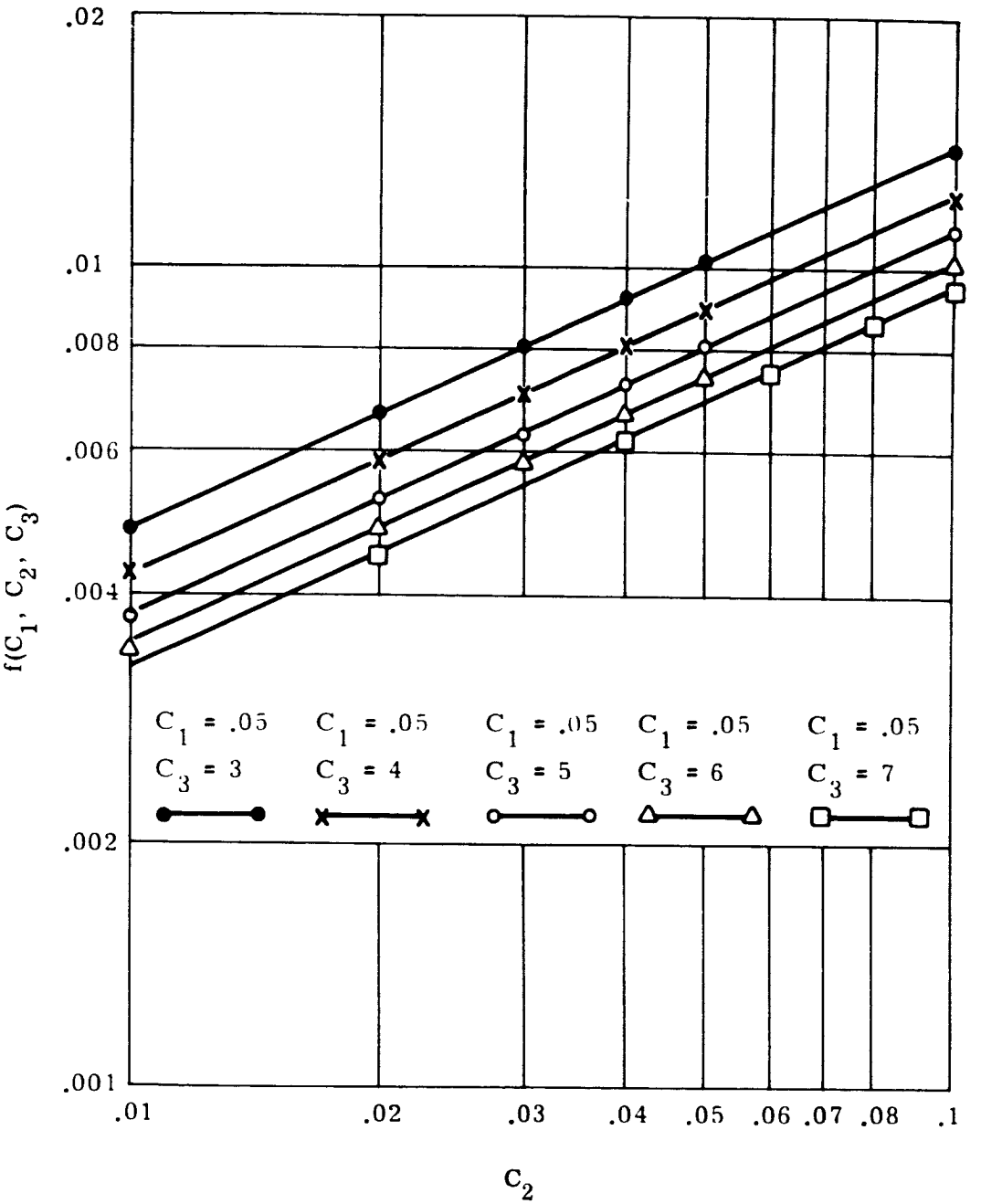

Figure K-11. Values of $f(C_1, C_2, C_3)$ versus C_2 for $C_1 = 0.05$

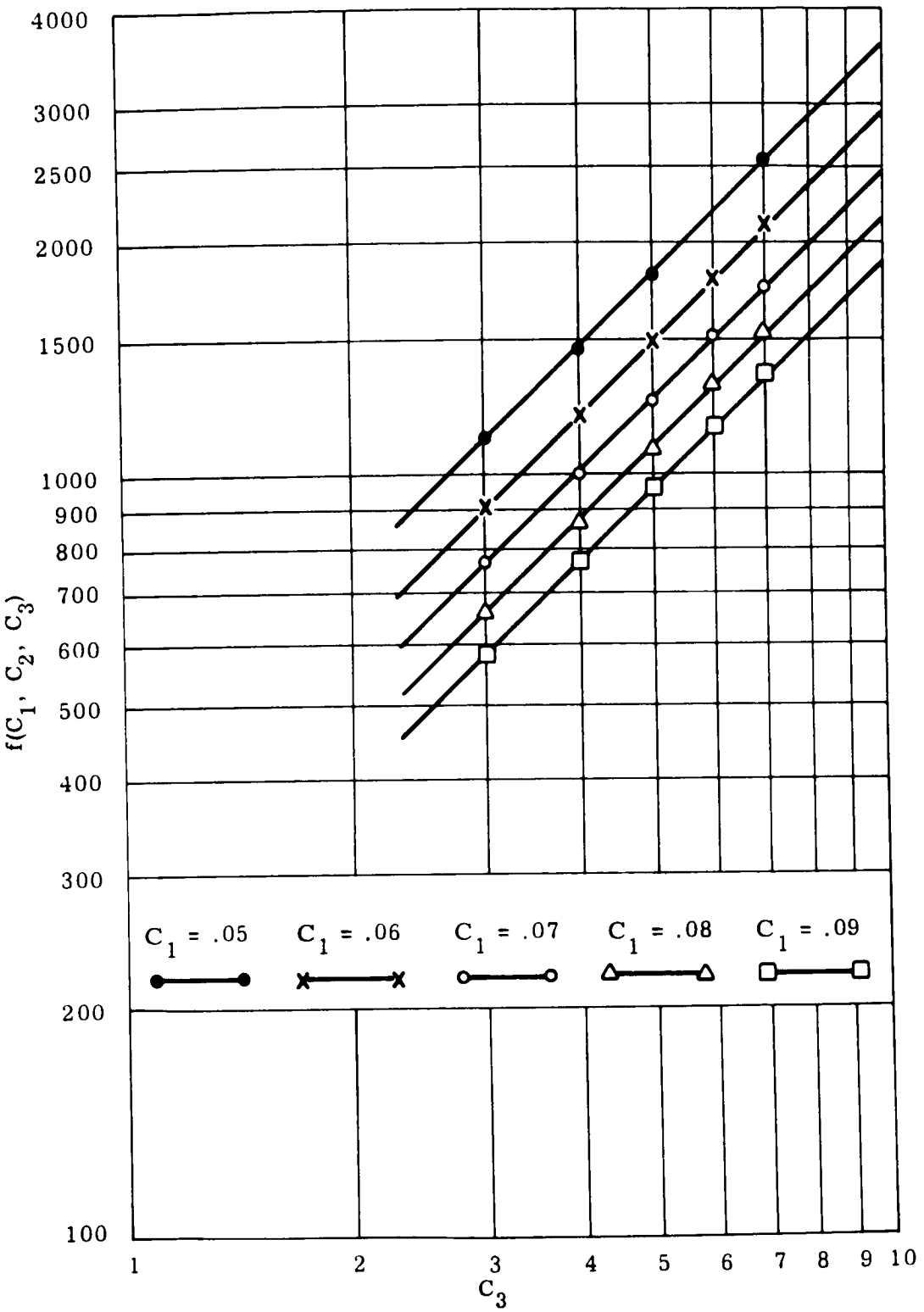

Figure K-12. Values of A versus C_3 for C_1 = 0.05 through 0.09

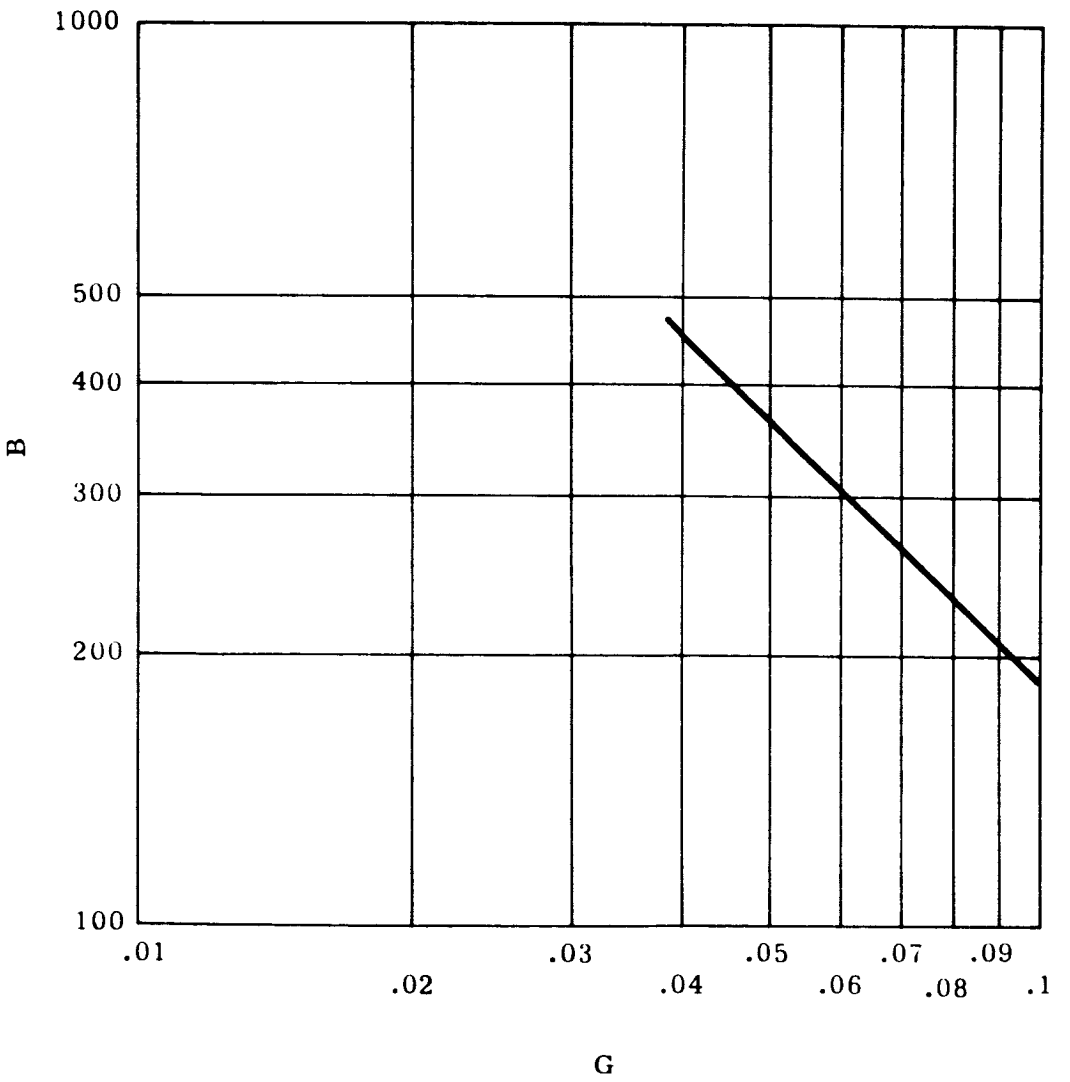

Figure K-13. Values of B versus C_1

resulting equation is obtained and is accurate for the $0.05 \leq C_1 \leq 0.15$, $0.02 \leq C_2 \leq 0.25$, and $3 \leq C_3 \leq 13$

$$C_2 = 20.4 \frac{C_3^{0.97}}{C_1^{0.96}} [f(C_1, C_2, C_3)]^{2.18}$$

The logical range of C_1, C_2, and C_3 has already been determined in the general optimization procedure (see paragraph K.3). Knowing the required value of $f(C_1, C_2, C_3)$, the same range of C_1 and C_3 will be investigated, and the corresponding values of C_2 will be calculated using the previously derived equation. This would result with 25 combinations of C_1, C_2, and C_3 with the following values of C_1 and C_3 being investigated

$$C_1 = 0.05, 0.06, 0.07, 0.08, 0.09$$

$$C_3 = 3, 4, 5, 6, 7$$

These 25 combinations are investigated for panel buckling and rib crippling. All design configurations that violate local instability will be eliminated. The average thickness for each of the remaining combinations is calculated as

$$t_{ave} = g(C_1, C_2, C_3) H$$

The design that yields the minimum average thickness is then chosen as the optimum.

K.4.2 OPTION TO SPECIFY RIB SPACING

The purpose of this section is to determine an optimization procedure when given the value of rib spacing. The parameters that are considered for optimization are skin thickness, overall depth, and rib thickness. As has been previously stated in paragraph K.3, the optimization will be considered for buckling governed cases only and not for strength. The approximate formula developed for general instability is

$$N_{cr} = \frac{0.8}{R} \left(\frac{C_2 C_1^{0.96}}{20.4 C_3^{0.97}} \right)^{0.459} EH^2$$

where C_1 equals t_s/H, C_2 equals t_{ws}/H, and C_3 equals b_s/H.

Substituting in the values of C_1, C_2, and C_3 results in

$$N_{cr} = \frac{0.8}{R}\left(\frac{t_{ws}\, t_s^{0.97}}{20.4\, b_s^{0.94}}\right)^{0.459} EH^{1.541}$$

Letting C_6 equal t_s/b_s, C_7 equal t_{ws}/b_s, and C_8 equal H/b_s, and substituting in the values of C_6, C_7, and C_8 results in

$$f(C_6, C_7, C_8) = \frac{N_{cr} R}{0.8\, E\, b_s^2}$$

where

$$f(C_6, C_7, C_8) = \left(\frac{C_7 C_6^{0.97}}{20.4}\right)^{0.459} C_8^{1.541}$$

Given the value of the rib spacing, b_s, the required value of $f(C_6, C_7, C_8)$ to resist general instability can be calculated using the above equation. In order to obtain an optimum design, the values of C_6, C_7, and C_8 must be chosen to satisfy the required $f(C_6, C_7, C_8)$ and also yield a minimum average thickness. Knowing the required $f(C_6, C_7, C_8)$, a logical range of C_6 and C_7 will be investigated, with the value of C_8 being calculated by

$$C_8 = \left(\frac{20.4}{C_7 C_6}\right)^{0.298} \left[f(C_6, C_7, C_8)\right]^{0.650}$$

The range of C_6 and C_7 being investigated will be determined using the previously established range of the values of C_1, C_2, and C_3. The range of these values is

C_1 = 0.05, 0.06, 0.07, 0.08, 0.09

C_2 = 0.02, 0.04, 0.06, 0.08, 0.10

C_3 = 3, 4, 5, 6, 7

Since the range of C_3 equals b_s/H being investigated is from 3 to 7, the range of C_8 equals H/b_s is from 1/7 to 1/3. To establish the range of C_6 equals t_s/b_s, substitute in the values of b_s equals H/C_8 and t_s equals $C_1 H$. This results with C_6 equals $C_1 C_8$. Since the range of C_1 is from 0.05 to 0.09, and C_8 is from 1/7 to 1/3, the range of C_6 is

$$C_6 = 0.00716,\ 0.01287,\ 0.01858,\ 0.02429,\ 0.030$$

Similarly, the range of C_7 is

$$C_7 = 0.00286,\ 0.010395,\ 0.017930,\ 0.025465,\ 0.033$$

Having established the range of C_6 and C_7, the value of C_8 can be calculated for each of the 25 combinations of C_6 and C_7. Any combination that violates panel buckling or rib crippling will be eliminated. The average thickness of each of the remaining combinations is calculated and the configuration yielding the minimum average thickness will be chosen as the optimum. The average thickness is

$$t_{ave} = g(C_6, C_7, C_8) b_s$$

where

$$g(C_6, C_7, C_8) = C_6 + 4\left[\left(1 - \frac{C_7}{2}\right)\left(\frac{C_7}{2}\right)(C_8 - C_6) + C_4^2 C_8\left(1 - \frac{\pi}{4}\right)\right.$$
$$\cdot (1 - 2C_5 C_8 - C_7) + C_5^2 C_8^2\left(1 - \frac{\pi}{4}\right)(C_8 - C_6)$$
$$\left. + \pi (C_5 C_8 - 0.22\, C_4 C_8)\left(C_4^2 C_8^2\right)\left(1 - \frac{\pi}{4}\right)\right]$$

K.5 WEIGHT CONSIDERATIONS

Letting r_{ws} equal $C_4 H$ and r_s equal $C_5 H$, the weight per surface area of the cylinder is

$$w = g(C_1, C_2, C_3)\frac{H}{12}\rho$$

where

$$g(C_1, C_2, C_3) = \frac{C_3^2 C_1 + \left(C_3 - \frac{C_2}{2}\right)\left(C_2 - C_2 C_1\right)2}{C_3^2}$$

$$+ \frac{2\pi\,(C_5 - 0.22\,C_4)}{C_3^2}\left[C_4^2\left(1 - \frac{\pi}{4}\right)\right]$$

$$+ \frac{4C_5^2\left(1 - \frac{\pi}{4}\right)\left(1 - C_1\right)}{C_3^2}$$

$$+ \frac{4C_4^2\left(1 - \frac{\pi}{4}\right)\left(C_3 - 2\,C_5 - C_2\right)}{C_3^2}$$

In order to determine the true weight of any cylinder of the 90° waffle stiffened type of construction, the following formula is used

$$w = g(C_1, C_2, C_3)\,\frac{H}{12}\,\rho\,F_b$$

where F_b equals 1.20 is a fabrication factor which takes into consideration non-calculated items.

K.6 CONICAL SECTIONS

Conical sections will be analyzed using the equivalent cylinder method where each section is transformed into an equivalent cylinder by

$$\overline{R} = \frac{R_{beg}\sqrt{L_c^2 + (R_{beg} - R_{end})^2}}{L_c}$$

K.7 NOMENCLATURE

N_x	Axial load per inch (lbs/inch).
N_y	Hoop load per inch (lbs/inch).
R	Radius of cylinder (inches).
A_{11}	Extensional stiffness in longitudinal direction (lbs/inch).
A_{22}	Extensional stiffness in hoop direction (lbs/inch).
A_{33}	Shear stiffness (lbs/inch).
D_{11}	Flexural stiffness in longitudinal direction (inch-lbs).
D_{22}	Flexural stiffness in hoop direction (inch-lbs).
D_{33}	Torsional stiffness (inch-lbs).
N_{cr}	Critical buckling load per inch (lbs/inch).
H	Overall depth (inches).
t_s	Thickness of skin (inches).
t_{ws}	Rib thickness (inches).
b_s	Rib spacing (inches).
μ	Poisson's ratio.
C_1	t_s/H.
C_2	t_{ws}/H.
C_3	b_s/H.
E	Modulus of elasticity ($lbs/inch^2$).
w	Weight per surface area (lbs/ft^2).
r_s	Radius of intersection of ribs (inches).
r_{ws}	Fillet radius of intersection of ribs and skin ($inches^2$).
σ	Stress level ($lbs/inch^2$).
$\overline{R}$	Equivalent radius.

R_{beg} Radius at beginning of section.

R_{end} Radius at end of section.

L_c Conical length.

APPENDIX L

60° NO-FACE CORRUGATION

1.1 INTRODUCTION

A 60° no-face corrugation consists of a constant-thickness sheet formed into a repeating series of equilateral corrugations. These are no-face sheets on the corrugation surfaces, however, equally spaced circumferential rings exist. The purpose of this appendix is to establish a method for optimizing this type of structure (see Figure L-1).

A corrugated sheet without face panels is essentially unidirectional as far as an efficient load path is concerned. In the intertank stage areas where pressure loads do not exist, the primary loading is axial. Thus, the subject corrugated structure with the corrugations running longitudinally can be considered for use in these interstage areas. Two modes of local instability are considered: buckling of the panels between rings, and local crippling of the corrugation. Due to the fact that the properties of the corrugation are uniaxial (flexural and axial stiffnesses in circumferential direction are, for all practical purposes, zero), it is feasible to treat buckling of the panels between rings as Euler columns. Three parameters are subject to optimization: skin thickness, corrugation depth, and ring spacing. The following assumptions have been made:

a. There is no lateral pressure.
b. The equilateral corrugation shape is optimum (all elements have the same critical stress).
c. General or panel instability occurs as column instability.
d. Stresses remain elastic.
e. Distortion effects due to curvature are negligible.
f. A typical ring geometry can be defined.
g. Wherever "optimization" is mentioned directly or in any of its forms, it connotes that a minimum weight has been effected.
h. For a given length, the optimum cross-section geometry has been achieved when the column stress and the crippling stress are equal.

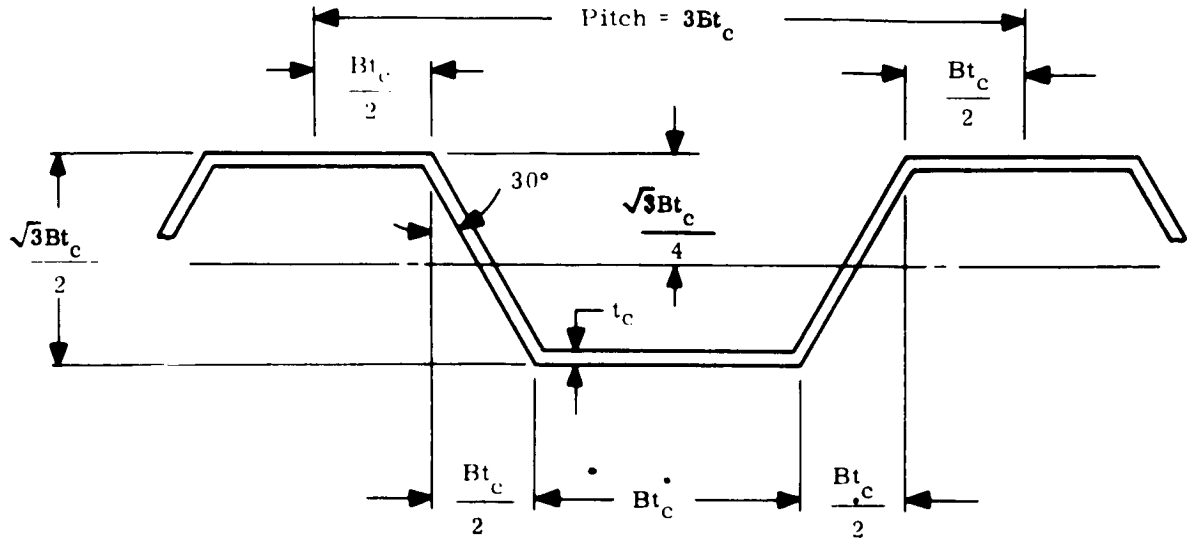

Figure L-1. 60° Corrugation Geometry

L.2 FAILURE MODES

L.2.1 LOCAL CRIPPLING

In order to predict the local crippling of the corrugation skin, it is assumed that the edge conditions are simply supported. The critical local crippling stress is[27]

$$\sigma_l = 3.62\,E\left(\frac{t_c}{b_c}\right)^2$$

L.2.2 PANEL BUCKLING

As has been previously described, panel buckling consists of Euler column buckling between rings. Assuming partially fixed end conditions, the following is used to predict the Euler buckling stress[27]

$$\sigma_e = \frac{C\pi^2 E}{\left(\frac{L}{\rho}\right)^2}$$

where $C = 2.05$.

L.3 OPTIMIZATION PROCEDURE

In order to arrive at an optimum corrugation configuration, the critical stress levels for Euler and local crippling are equated to one another. This, however, will determine only two design parameters, namely the corrugation skin and depth. The third parameter, the ring spacing, will be determined as will be seen later by another method.

Equating $\sigma_l = \sigma_e$ and letting $b_c = Bt_c$, then

$$3.62\,E\left(\frac{1}{B}\right)^2 = \frac{C\pi^2 E}{\left(\frac{L}{\rho}\right)^2}$$

where $\rho = 0.367\ Bt_c$ for the 60° corrugation being considered and

$$B^2 = \frac{1.194\,L}{t_c}$$

Equating the actual stress level with local crippling stress

$$\frac{N_x}{\frac{4}{3}t_c} = 3.62\,E\left(\frac{1}{B}\right)^2$$

$$B^2 = \frac{4.84\,E\,t_c}{N_x}$$

Equating both values of B^2

$$t_c = 0.496\sqrt{\frac{N_x L}{E}}$$

Therefore, given the value of ring spacing, the optimum corrugation skin thickness can be calculated. Knowing t_c, the other corrugation geometry can be calculated by

$$B = \sqrt{\frac{1.194\,L}{t_c}}$$

The weight for any given length of corrugated cylinder without rings is

$$\text{Weight} = 4.19\, D t_c L \gamma_c$$

L.4 OPTIONS

L.4.1 OPTION TO SPECIFY RING SPACING

The option to specify the ring spacing is provided. Since the unsupported length is given, there is no need to perform the iteration to determine the optimum number of rings. It is simply a matter of determining the corrugation geometry such that the Euler buckling stress is equal to the local crippling. Given the value of L, the corrugation geometry is determined by

$$t_c = 0.496 \sqrt{\frac{N_x L}{E}}$$

$$B = \sqrt{\frac{1.194\, L}{t_c}}$$

The ring weight is then found by using the equation derived in paragraph L.5.

L.4.2 OPTION TO SPECIFY CORRUGATION DEPTH

The option to specify the corrugation depth is also provided. Since there are two design parameters common to both modes of instability and one is being specified, the optimum design is not necessarily the one that yields equal Euler and local buckling stresses. In order to determine the optimum ring spacing, the iteration scheme outlined in paragraph L.5 will be used. In order to determine the corrugation skin thickness, it will be calculated based on both forms of instability, and the maximum of the two is chosen. Equating the actual stress level and the local crippling stress, the following is obtained

$$\frac{N_x}{\frac{4}{3} t_c} = 3.62\, E \left(\frac{t_c}{\frac{2}{\sqrt{3}} d_c} \right)^2$$

$$t_{c_1} = \left(\frac{N_x d_c^2}{3.62 E}\right)^{\frac{1}{3}}$$

where d_c = given depth

Equating the actual stress and the Euler buckling stress, the following is obtained

$$t_{c_E} = \frac{N_x L^2}{4.5 E d_c^2}$$

where L is a function of the number of rings.

L.4.3 OPTION TO SPECIFY CORRUGATION THICKNESS

Giving the value of the corrugation thickness automatically specifies the working stress level since the average thickness is dependent only on t_c

$$\sigma = \frac{N_x}{t_{ave}} = \frac{3 N_x}{4 t_c}$$

Here again, the optimum configuration is not necessarily the one in which the critical buckling stress levels are equal. Knowing the working stress level, the value of B can be calculated based on local crippling

$$\frac{3 N_x}{4 t_c} = 3.62 E \left(\frac{1}{B}\right)^2$$

$$B = \sqrt{\frac{4.815 E t_c}{N_x}}$$

Knowing t_c and B, the value of the unsupported length can be calculated letting the Euler buckling stress equal the known working stress

$$\frac{3 N_x}{4 t_c} = \frac{C \pi^2 E}{\left(\frac{L}{\rho}\right)^2}$$

$$L = \frac{t_c^{\frac{3}{2}} B}{1.71} \left(\frac{\pi^2 E}{N_x} \right)^{\frac{1}{2}}$$

After calculating the value of the unsupported length necessary to satisfy Euler buckling, it must be checked for compatibility with the overall cylinder length such that a condition of equal unsupported length exists. If compatibility does not exist, the unsupported length is reduced until the condition of equal lengths exists. Reducing the length allows a reduction of t_c since the Euler buckling stress is directly proportional to t_c and indirectly to the unsupported length squared. This reduction of t_c will have no effect on local buckling since the panel width is decreasing and, consequently, the local allowable crippling stress is increasing. It should be evident that, if the unsupported length is increased for equal length compatibility, the value of B will have to be increased to satisfy Euler buckling, and consequently local crippling would become critical.

L.5 RING GEOMETRY

Experimental evidence has indicated that a certain ring stiffness is required to force an inflection point of the buckling pattern at the ring support. This required ring stiffness is[28]

$$E_r I_r = 3 \times 10^{-5} \frac{\pi N_x D^4}{L}$$

Assuming a symmetrical I, [, or Z shape with 1/4 area in each cap, i.e.

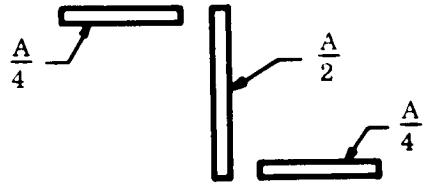

the moment of inertia of this shape is

$$I_r = \frac{A_r h_r^2}{6}$$

and we assume further that the ring depth is

$$h_r = 3h_c$$

But, h_c has been defined as $\sqrt{3}/2\, Bt_c$

therefore

$$h_r = 3\left(\frac{\sqrt{3}}{2} Bt_c\right) = 2.59\, Bt_c$$

$$h_r^2 = 6.75\, B^2 t_c^2$$

Substituting into the required stiffness equation results with the following ring area

$$A_r = 2.67 \times 10^{-5} \frac{\pi N_x D^4}{B^2 t_c^2 E_r L}$$

Writing a weight equation for the ring

$$W_{tr} = 8.37 \times 10^{-5} \frac{\pi N_x D^5 \gamma_r}{B^2 t_c^2 E_r L}$$

Combining the weight of the corrugation and the rings results in

$$W = N\left(4.19\, Dt_c L\gamma_c + \frac{N-1}{N}\, 8.37 \times 10^{-5} \frac{\pi N_x D^5 \gamma_r}{B^2 t_c^2 E_r L}\right) F_b$$

where N is the number of bays the cylinder is divided into by the added rings and F_b is a fabrication factor of 1.2 to account for non-calculated items.

To optimize the 60° no-face corrugation, the following procedure is used:

a. Design the corrugation without any intermediate rings to reduce the unsupported length and calculate the resulting weight.

b. Add one ring and design the corrugation based on the reduced value of unsupported length and calculate the resulting weight of the corrugation plus the ring.

c. Continue adding the rings until an increase in total weight is noted. At this point, the optimum ring spacing has been found.

L.6 NOMENCLATURE

t Corrugation thickness (inches).

d_c Corrugation depth (inches).

E Modulus of elasticity (psi).

σ Stress level (psi).

L Unsupported Euler column length (inches).

N_x Axial compressive loading (lbs/inch).

D Diameter of cylinder (inches).

ρ Radius of gyration of corrugation cross-section (inches).

I_r Moment of inertia of circumferential ring cross-section (inches).

A_r Area of circumferential ring cross-section (inches).

N Number of equal length bays.

γ Material density.

APPENDIX M

SINGLE-FACE CORRUGATION

M.1 INTRODUCTION

The purpose of this appendix is to establish a method for optimizing single-face corrugated cylinders subjected to axial loads and/or internal pressure. Two modes of failure are to be considered: strength based on the von Mises yield criteria, and elastic buckling. The elastic buckling consists of general instability, buckling of the unsupported panel lengths between rings, and local crippling of the corrugation and skin.

It is quite obvious that no optimization procedure can be developed based on the strength criteria, however, the shell can be optimized based on axial buckling. Four parameters are to be optimized: corrugation skin thickness, corrugation depth, ring spacing, and ring depth. The following assumptions have been made in the analysis:

a. Internal pressure has no effect on the overall general instability.
b. Ring spacing is sufficiently close so that the rings and skin are equally stressed.
c. Curved panels are treated as flat plates.
d. Critical buckling stresses are within the elastic range.

In order to minimize the number of design parameters, the following relationships have been established, as shown in Figure M-1:

a. A square corrugation pattern is used thereby equating the local crippling stresses of the webs and flanges.
b. Skin thickness is twice the corrugation thickness since the unsupported length of the skin is twice as much, thereby equating the local crippling stresses of the skin and corrugation. This is also compatible with manufacturing since the backup material should be at least twice as thick when welding the corrugation to the skin.
c. It has been assumed that the flange area of the rings represents 50 percent of the total ring area. Based on this consideration, the analysis is applicable for Z, C, or I rings since each have equal moments of inertia for a given depth and thickness.

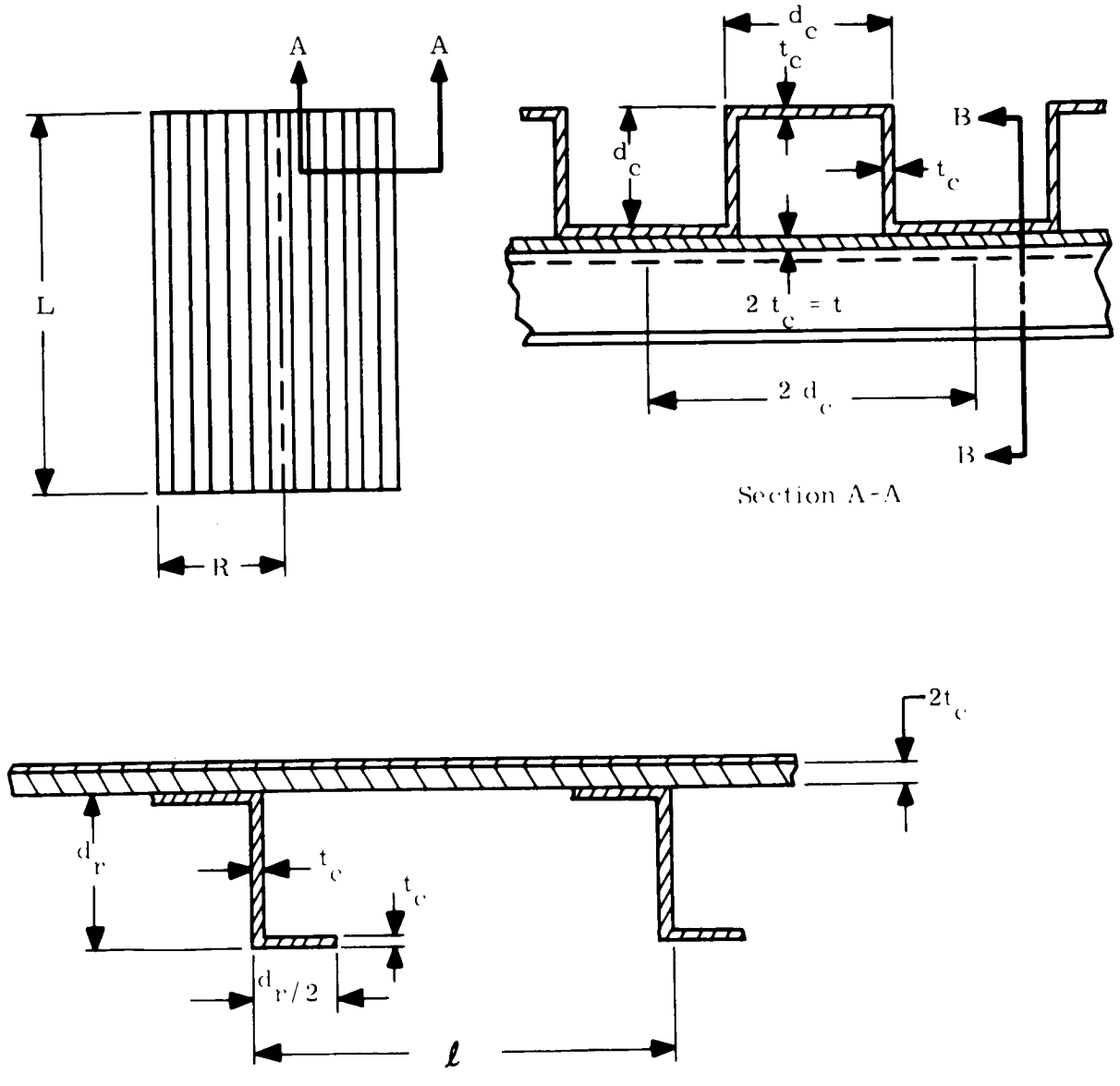

Figure M-1. Single-Face Corrugation Geometry

M.2 FAILURE MODES

M.2.1 GENERAL INSTABILITY[29]

In order to predict the general instability of axially loaded cylinders, the following equations are used. These equations represent the latest state of the art and take into consideration the effects of asymmetry, that is, the effect of whether the rings and stringers (corrugation in this case) are on the inside or outside of the skin.

$$N_x \frac{L^2}{\pi^2 D} = m^2(1 + \beta^2)^2 + m^2 \frac{EI_s}{dD} + m^2\beta^4 \frac{EI_r}{lD} + \left(\frac{G_s J_s}{dD} + \frac{G_r J_r}{lD}\right) m^2\beta^2$$

$$+ \frac{12Z^2}{m^2\pi^4}\left(\frac{1 + \bar{S}\Lambda_s + \bar{R}\Lambda_r + \bar{S}\bar{R}\Lambda_{rs}}{\Lambda}\right)$$

where

$$\Lambda_r = 1 + 2\alpha^2\beta^2(1 - \beta^2\mu)\frac{\bar{Z}_r}{R} + \alpha^4\beta^4(1 + \beta^2)^2\left(\frac{\bar{Z}_r}{R}\right)^2$$

$$\Lambda_s = 1 + 2\alpha^2(\beta^2 - \mu)\frac{\bar{Z}_s}{R} + \alpha^4(1 + \beta^2)^2\left(\frac{\bar{Z}_s}{R}\right)^2$$

$$\Lambda_{rs} = 1 - \mu^2 + 2\alpha^2\beta^2(1 - \mu^2)\left(\frac{\bar{Z}_r}{R} + \frac{\bar{Z}_s}{R}\right)$$

$$+ \alpha^4\beta^4[1 - \mu^2 + 2\beta^2(1 + \mu)]\left(\frac{\bar{Z}_r}{R}\right)^2$$

$$+ 2\alpha^4\beta^4(1 + \mu)^2\frac{\bar{Z}_r\bar{Z}_s}{R^2} + \alpha^4\beta^4[2(1 + \mu) + \beta^2(1 - \mu^2)]\left(\frac{\bar{Z}_s}{R}\right)^2$$

$$\Lambda = (1 + \beta^2)^2 + 2\beta^2(1 + \mu)(\bar{R} + \bar{S})$$

$$+ (1 - \mu^2)[\bar{S} + 2\beta^2\bar{R}\bar{S}(1 + \mu) + \beta^4\bar{R}]$$

with

$$Z^2 = \frac{L^4(1 - \mu^2)}{R^2t^2}$$

$$\overline{S} = \frac{A_s}{td}$$

$$\alpha = \frac{m\pi R}{L}$$

$$D = \frac{Et^3}{12(1 - \mu^2)}$$

$$\overline{R} = \frac{A_r}{tl}$$

$$\beta = \frac{nL}{m\pi R}$$

In order to utilize the above equation, it must be minimized with respect to m and n to obtain the theoretical buckling load. However, due to the complexity and time limitation involved, it is assumed that the stringer and ring eccentricities do not affect the buckling mode shape. Based on this assumption, the equations used to determine the buckling mode shape for the Becker equation (see Appendix F) are used. This assumption is valid and it will be shown later in this appendix that it does not affect the final buckling load. Utilizing the Becker equation and non-dimensionalizing the design parameters, the following equations are obtained. Let

$$d_c = C_1 t_c$$

$$d_r = C_2 t_c$$

$$l = C_3 t_c$$

$$N_x = f(C_1, C_2, C_3) \frac{2ECt_c^2}{R}$$

where

$$f(C_1, C_2, C_3) = \frac{1}{2\phi^{\frac{1}{2}}}\left[\frac{2(1+\beta^2)^2}{3(1-\mu^2)} + \frac{C_1^2}{3} + \beta^4\frac{C_2^3}{3C_3} + \beta^2\left(\frac{3}{16} + \frac{C_2}{4C_3}\right)\right] + \phi^{\frac{1}{2}}\left[\frac{1 + \Lambda_s + \frac{C_2}{C_3}(\Lambda_r + \Lambda_{rs})}{\Lambda}\right]$$

$$\phi = \left(d_{11} + 0.375\,\beta^2 d_{33} + \beta^4 d_{22}\right)\left(\frac{1}{a_{22}} + 1.33\,\beta^2 + \frac{\beta^4}{a_{11}}\right)$$

$$\beta^2 = P + (P^2 + Q)^{\frac{1}{2}}$$

If β^2 is negative, then $\beta^2 = 0$. If $P^2 + Q$ is negative, then $\beta^2 = 0$

$$P = \frac{a_{33}}{a_{22}}\left(\frac{a_{22}d_{11} - a_{11}d_{22}}{a_{11}d_{22} - 2a_{33}d_{33}}\right)$$

$$Q = \frac{a_{11}}{a_{22}}\left(\frac{a_{22}d_{11} - 2a_{33}d_{33}}{a_{11}d_{22} - 2a_{33}d_{33}}\right)$$

where

$$a_{11} = 4$$

$$a_{22} = 2\left(1 + \frac{C_2}{C_3}\right)$$

$$a_{33} = 0.75$$

$$d_{11} = \frac{7C_1^2}{12}$$

$$d_{22} = \frac{C_2^3}{3C_3}\left[1 + \frac{3}{2\left(1 + \frac{C_2}{C_3}\right)}\right]$$

$$d_{33} = 0.1875\left(\frac{C_1^2}{2} + \frac{2C_2^2}{3C_3} + \frac{8}{3}\right)$$

$$A_{11} = a_{11}\, Et_c$$

$$A_{22} = a_{22}\, Et_c$$

$$A_{33} = a_{33}\, Et_c$$

$$D_{11} = d_{11}\, Et_c^3$$

$$D_{22} = d_{22}\, Et_c^3$$

$$D_{33} = d_{33}\, Et_c^3$$

$$\Lambda_s = 1 + \frac{\psi C_1(\beta^2 - \mu)}{\phi^{\frac{1}{2}}} + \frac{(1 + \beta^2)^2 \psi_s^2 C_1^2}{4\phi}$$

$$\Lambda_{rs} = 1 - \mu^2 + \frac{\beta^2(1 - \mu^2)(\psi_r C_2 + \psi_s C_1)}{\phi^{\frac{1}{2}}} + \frac{\beta^4[1 - \mu^2 + 2\beta^2(1 + \mu)]\psi_r^2 C_2^2}{4\phi}$$

$$+ \frac{\beta^4(1 + \mu)^2 \psi_r C_2 \psi_s C_1}{2\phi} + \frac{\beta^2[2(1 + \mu) + \beta^2(1 - \mu^2)]\psi_s^2 C_1^2}{4\phi}$$

$$\Lambda_r = 1 + \frac{\beta^2(1 - \beta^2\mu)\,\psi_r C_2}{\phi^{\frac{1}{2}}} + \frac{(1 + \beta^2)^2 \psi_r{}^2 C_2{}^2}{4\phi}$$

$$\Lambda = (1 + \beta^2)^2 + 2\beta^2(1 + \mu)\left(\frac{C_2}{C_3} + 1\right)$$

$$+ (1 - \mu^2)\left[1 + 2\beta^2 \frac{C_2}{C_3}(1 + \mu) + \beta^4 \frac{C_2}{C_3}\right]$$

The following table is a comparison between the "hybrid" and exact methods for determining the buckling wave pattern and the critical buckling load.

Case	$\frac{1}{R}$	Exact[29]	"Hybrid"	Percent Difference
1	0.05	0.004111	0.00453	10
2	0.10	0.003826	0.00424	10
3	0.15	0.003720	0.00408	10
4	0.20	0.0003629	0.00399	10
5	0.25	0.003574	0.00389	10

As can readily be seen, the percent difference is not only small, but is consistent. Therefore, the method of using the Becker equation to determine the buckling wave pattern is justified.

Having established the validity of the hybrid method, it was compared with actual test results to determine the accuracy of the theory. The following table shows such a comparison, where

$$N_{test} = \frac{\text{Critical Moment}}{\pi R^2}$$

Group	Cylinder	Ring Spacing (inches)	Stiffener Spacing (inches)	Test Critical Moment	Critical Load (lbs/inch)		$\frac{N_{test}}{N_{calc.}}$
					N_{test} [12]	$N_{calc.}$	
I	1	6	2.48	5.32×10^6	1135	1987	0.57
	2	9	2.48	4.68×10^6	1000	1869	0.535
	3	12	2.48	4.44×10^6	950	1763	0.54
II	1	6	4.04	3.4×10^6	725	1216	0.60
	2	9	4.04	3.05×10^6	650	1071	0.61
	3	12	4.04	2.88×10^6	615	966	0.635

As can be expected from past experience with the buckling of isotropic monocoque cylinders, a correction factor is required to correlate the test results and theory. Therefore, the buckling correction factor to be used for the single-face corrugated cylinders is C = 0.58.

M.2.2 PANEL BUCKLING[29]

To predict the buckling of the unsupported panel lengths between rings (see Figure M-2), the following equation is used

$$\frac{N_x p_1^2}{\pi^2 D} = m^2(1 + \beta^2)^2 + m^2 \frac{EI_s}{dD} + m^2\beta^2 \frac{GJ_s}{dD}$$

$$+ \frac{12Z^2}{m^2\pi^4}\left[\frac{1 + \bar{S}\Lambda_s}{(1 + \beta^2)^2 + 2\bar{S}\beta^2(1 + \mu) + \bar{S}(1 - \mu^2)}\right]$$

Once again, in order to predict the theoretical buckling load, the above equation must be minimized with respect to m and n. To simplify the minimization, a value of one will be used for m, the number of half wavelengths in the longitudinal direction. Physically, this defines the buckling pattern as one-half wavelength between rings. To minimize with respect to n, we begin by assuming a value equal to one and iterate with respect to n until a minimum value is reached.

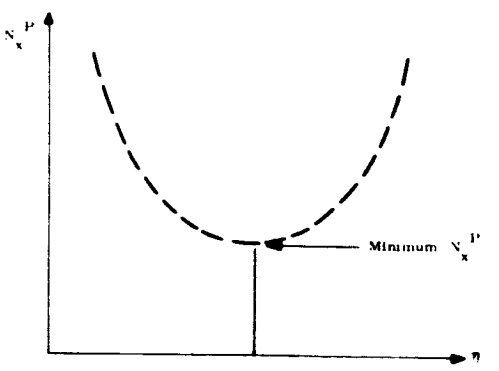

Figure M-2. Panel Buckling

Letting m = 1 and $d_c = C_1 t_c$ then

$$N_x^p = \left\{ \frac{2Et_c \pi^2 (1 + \beta)^2}{3(1 - \mu^2) C_3^2} + \frac{E\pi^2 t_c}{3} + \frac{2EC_3^2 t_c^3}{R^2 \pi^2} \left[\frac{1 + \Lambda_s}{(1 + \beta^2)^2 + 2\beta^2(1 + \mu) + (1 - \mu^2)} \right] \right\} C_p$$

where

$$\Lambda_s = 1 + \frac{\pi^2 R}{C_3^2 t_c} (\beta - \mu) \psi_s C_1 + \frac{\pi^4 R^2 (1 + \beta^2)^2 \psi_s^2 C_1^2}{C_3^4 t_c^2}$$

$$\beta = \frac{nC_3 t_c}{\pi R}$$

and C_p equals 0.58, the buckling correction factor. It has been assumed that the same factor is required as that used for overall instability.

M.2.3 LOCAL CRIPPLING[23]

To predict local crippling of the corrugation material, the following equation is used

$$\sigma_{cr} = 3.29 \frac{E}{1 - \mu^2} \left(\frac{t_c}{d_c} \right)^2$$

Letting

$$d_c = C_1 t_c$$

then

$$\sigma_{cr} = 3.29 \frac{E}{1 - \mu^2} \left(\frac{1}{C_1}\right)^2$$

M.2.4 STRENGTH CRITERIA

To determine the maximum stress level in the skin, a modified form of the von Mises yield equation is used. The skin is only investigated since its resultant stress level will always be greater than or equal to that of the corrugation

$$\sigma = \sqrt{\left(\frac{N_x}{A_x}\right)^2 - \left(\frac{N_x N_y}{A_x A_y}\right) + \left(\frac{N_y}{A_y}\right)^2}$$

where

$$A_x = 4t_c$$

$$A_y = 2t_c \left(1 + \frac{C_2}{C_3}\right)$$

M.3 OPTIMIZATION PROCEDURE

It is required to determine the optimum design parameters, C_1, C_2, C_3, and t_c, such that a minimum weight configuration is obtained. The approach to be taken is the concept of maximum strength-to-weight ratios. A logical range of C_1, C_2, and C_3 will be investigated, and the resulting strength-to-weight ratios calculated. The configuration with the maximum ratio will be investigated for panel buckling and local crippling. If panel buckling and/or local crippling is not satisfied, the values of C_1, C_2, and C_3 with the next highest strength-to-weight ratio is investigated.

This process is continued until panel buckling and local crippling are satisfied. Having determined the optimum values of C_1, C_2, and C_3, the value of the corrugation thickness,

t_c, can be calculated to satisfy general instability by

$$t_c = \sqrt{\frac{N_x R}{2CE[f(C_1, C_2, C_3)]}}$$

In order to determine the strength-to-weight ratios, the following equations are required

$$t_{ave} = g(C_1, C_2, C_3)\, t_c$$

Substituting the value of t_c into the average thickness equation results in

$$t_{ave} = \frac{g(C_1, C_2, C_3)}{[f(C_1, C_2, C_3)]^{\frac{1}{2}}} \left(\frac{N_x R}{2CE}\right)^{\frac{1}{2}}$$

In order for the average thickness and, consequently, the weight to be a minimum, the following ratio must be a maximum

$$\frac{[f(C_1, C_2, C_3)]^{\frac{1}{2}}}{g(C_1, C_2, C_3)} = \text{maximum}$$

Since $f(C_1, C_2, C_3)$ and $g(C_1, C_2, C_3)$ are indicative of the strength and weight respectively, the ratio is termed the strength-to-weight ratio.

The first step in determining a logical range of C_1, C_2, and C_3 is to investigate the range of values for C_1, which is a measure of the corrugation depth. Since local crippling is a function of the corrugation depth, values of critical local crippling stress are plotted against C_1 for various values of the modulus of elasticity (see Figure M-3). Upon investigating the curve, it was concluded that the critical buckling stresses are of a sufficient magnitude if the range of C_1 is from 20 to 40. The buckling curves approach an assymtope at approximately $C_1 = 20$ and 40 for values of the modulus of elasticity equal to 10^7 and 30×10^6, respectively.

Since C_3 is a measure of ring spacing, panel buckling must be investigated to determine a logical range for C_3. However, due to the complexity of the panel buckling equation, this form of instability will be simplified by considering the corrugation to be a Euler

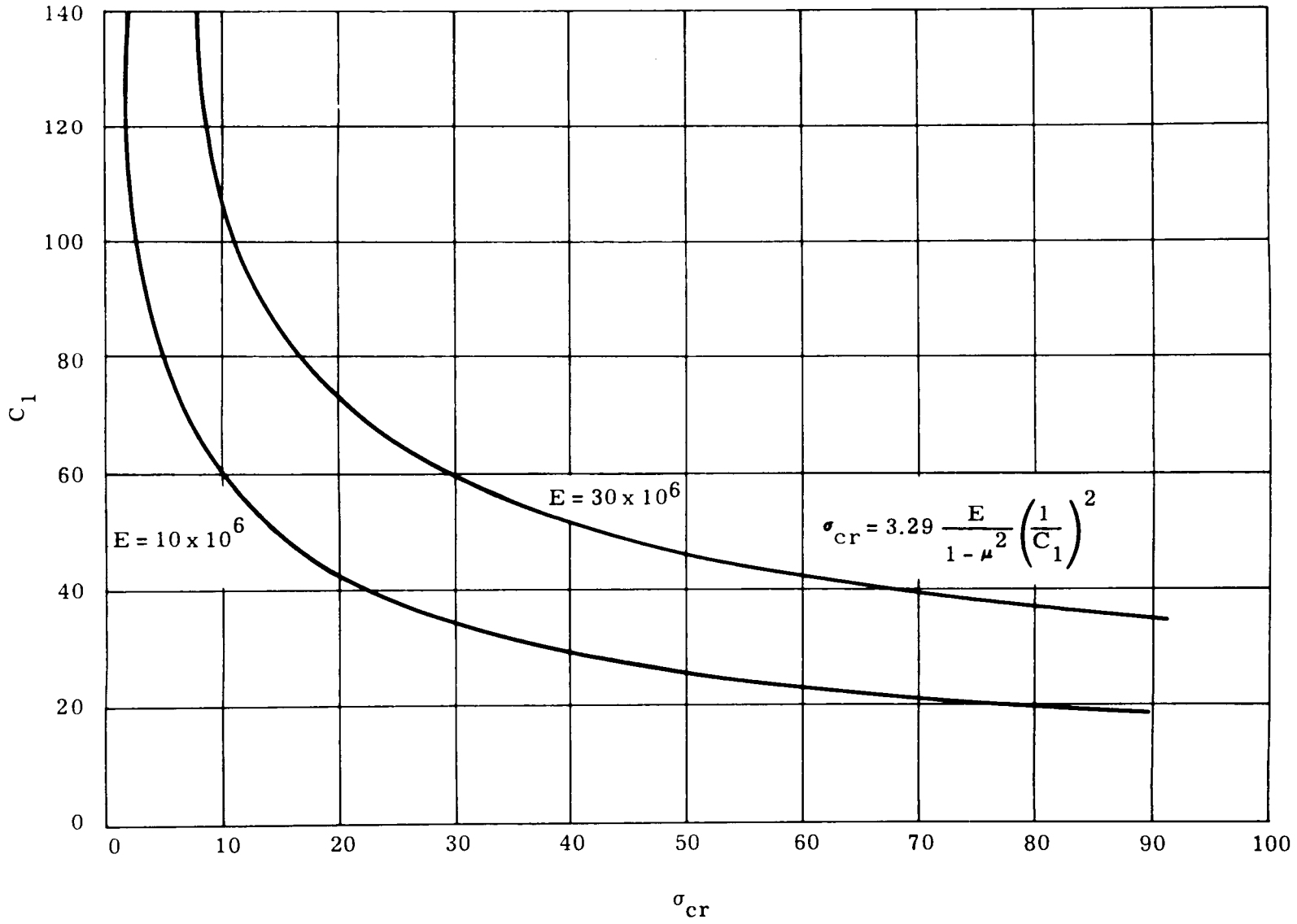

Figure M-3. Critical Local Crippling Stress versus C_1 for Various Values of Modulus of Elasticity

column simply supported between rings. It must be pointed out that panel buckling in the structural optimization computer program is still being investigated using the sophisticated equations, whereas the simplified Euler approximation is being used only to determine a logical range of C_3 to investigate. Values of the critical Euler buckling stresses are plotted against the l/ρ ratios (see Figure M-4). Upon investigating the curve, it was concluded that a range of l/ρ from 40 to 120 is sufficient to cover a wide range of critical panel buckling stresses for the range of values of modulus of elasticity. For the square corrugation pattern being studied, the radius of gyration, including the skin, can be expressed as

$$\rho = 0.68\, C_1 t_c$$

Since $l = C_3 t_c$, the ratio l/ρ is

$$\frac{l}{\rho} = 1.47\, \frac{C_3}{C_1}$$

Having already determined the ranges of C_1 and l/ρ, to investigate it is simply a matter of substituting in the values of the upper and lower bounds of these ranges into the preceding equation to determine the range of C_3. This results with values of C_3 from 500 to 3300.

Since no mode of local buckling failure is governed by C_2 (ring depth), the same range of values will be investigated as for C_1. There are several reasons why this is justified: (1) since the corrugation and ring are constructed of the same gage material, it is practical to have the same depth/skin thickness ratios, and (2) from a practical standpoint it is necessary that the ring and corrugation depth be approximately equal. Therefore, the range of C_2 is also from 20 to 40.

In order to minimize the number of possible design configurations, the following values of C_1, C_2, and C_3 are investigated as a possible optimum design:

C_1 = 20, 25, 30, 35, 40
C_2 = 20, 25, 30, 35, 30
C_3 = 500, 1200, 1900, 2600, 3300

This would result with 125 combinations of C_1, C_2, and C_3.

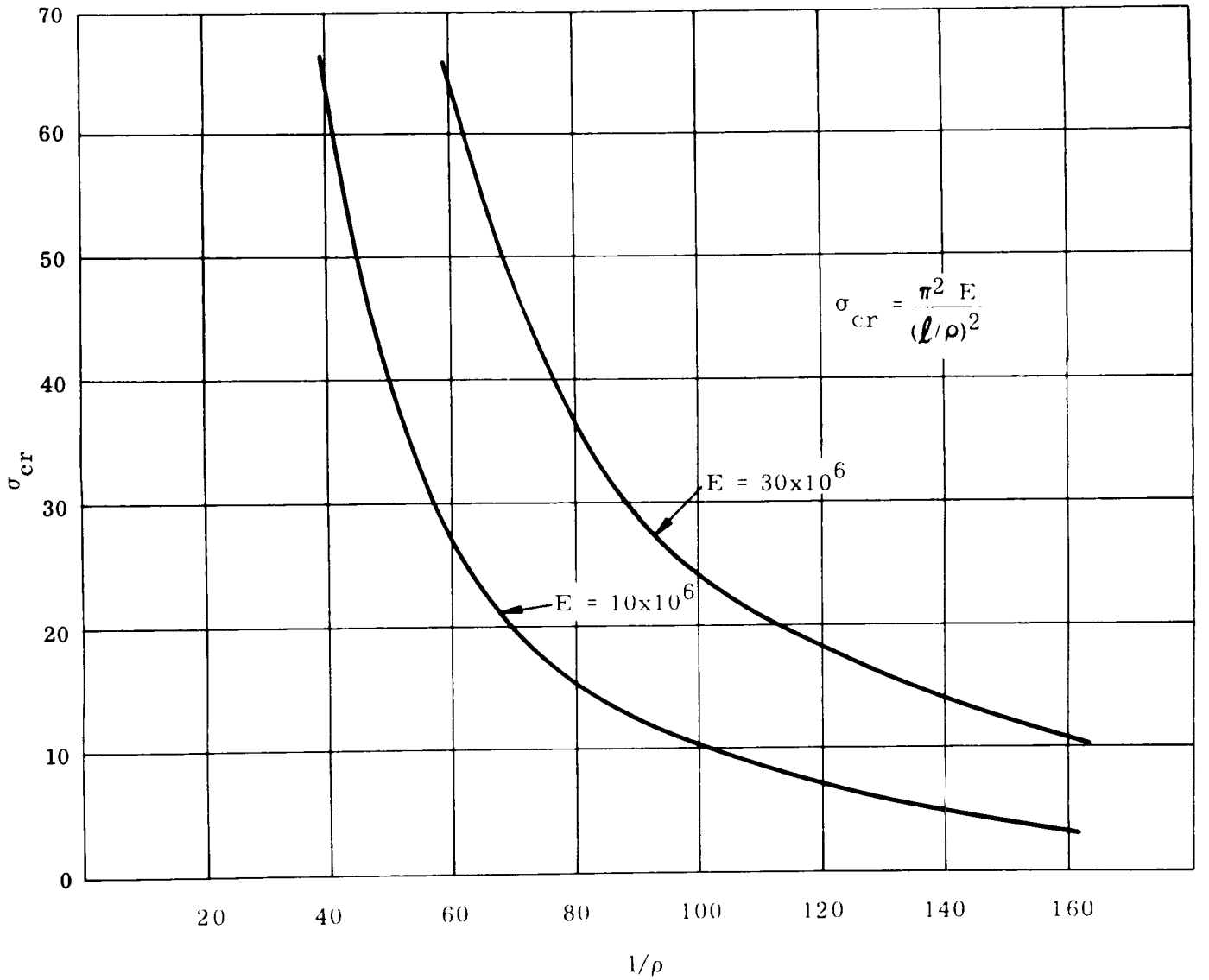

Figure M-4. Values of Critical Euler Buckling versus l/ρ Ratios

M.4 WEIGHT CONSIDERATIONS

In order to calculate the weight of the cylinder, the average "smeared out" thickness, including the circumferential rings, is

$$t_{ave} = 4t_c + \frac{2C_2 t_c^2 (i - 1)}{L}$$

The first term in the equation represents the weight of the corrugation and skin, where the second term represents the circumferential rings. In calculating the weight of the rings, only the intermediate rings are considered. The rings at the cylinder ends are included in the fabrication factor, F_b, which accounts for non-calculated items. Figure M-5 illustrates the criteria used for weight calculation.

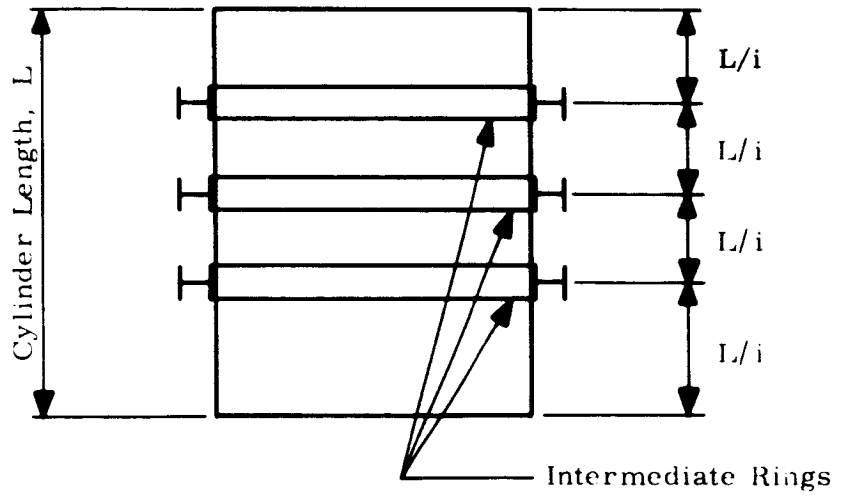

where i designates the number of equal unsupported lengths.

Figure M-5. Weight Equation Criteria

To calculate the weight per surface area, the following is used

$$w = \frac{t_{ave}}{12} \rho F_b$$

where F_b equals 1.2 to account for non-calculated items.

M.5 NOMENCLATURE

N_x	Axial load per inch (lbs/inch).
N_y	Hoop load per inch (lbs/inch).
R	Radius of cylinder (inches).
L	Length of cylinder (inches).
d_c	Corrugation depth (inches).
t_c	Corrugation skin thickness (inches).
d_r	depth of ring (inches).
l	Ring spacing (inches).
t	Thickness of cylinder shell wall (inches).
d	Corrugation pitch (inches).
J_r	Torsional constant for ring (inches^4).
J_s	Torsional constant for stringer (inches^4).
G	Shear modulus (psi).
E	Modulus of elasticity (psi).
μ	Poisson's ratio.
A_s	Area of stringer (inches^2).
A_r	Area of ring (inches^2).
I_s	Moment of inertia of stringer (inches^4).
I_r	Moment of inertia of ring (inches^4).
$\overline{Z}_r$	Distance from centroid of stiffener to middle surface of shell, positive if stiffener lies on external surface of shell (inches).
$\overline{Z}_s$	Distance from centroid of ring to middle surface of shell, positive if ring lies on external surface of shell (inches).
ψ_s	Indicates whether stringers are external or internal to the skin surface, -1 if internal, +1 if external.
ψ_r	Indicates whether rings are external or internal to skin surface, -1 if internal, +1 if external.
m	Number of half waves in cylinder buckle pattern in longitudinal direction.

n	Number of full waves in cylinder buckle pattern in circumferential direction.
C	Buckling correction factor.
A_{11}	Extensional stiffness in longitudinal direction (lbs/inch).
A_{22}	Extensional stiffness in circumferential direction (lbs/inch).
A_{33}	Shear stiffness (lbs/inch).
D_{11}	Flexural stiffness in longitudinal direction (inch-lbs).
D_{22}	Flexural stiffness in circumferential direction (inch-lbs).
D_{33}	Torsional stiffness (inch-lbs).
σ	Stress level (psi).
w	Weight per unit surface area (lbs/ft^2).

APPENDIX N

INTEGRAL STRINGER AND RING STIFFENED CYLINDERS

N.1 INTRODUCTION

The purpose of this analysis is to establish a procedure for optimizing an integral stringer and ring stiffened shell subjected to axial load (see Figure N-1). Two modes of failure are to be considered: strength based on the von Mises yield criteria and elastic instability. The elastic instability consists of general instability (overall collapse of the cylinder), buckling of the unsupported panel lengths between rings, buckling of the skin bounded by the ring and stringers, and crippling of the outstanding stringer rib.

The optimization procedure will be based on elastic buckling with the following parameters being optimized: depth of rib, skin thickness, rib thickness, rib spacing, and ring spacing. The following assumptions have been made:

a. Internal pressure has no effect on the overall general instability.
b. Ring spacing is sufficiently close that the rings and skin are equally stressed.
c. Curved panels are treated as flat plates since the ribs are closely spaced.
d. Critical buckling stresses are within the elastic limit.

In order to minimize the number of design parameters, the following relationships have been established:

a. The depth of the ring is two and one-half times that of the longitudinal stringer. This is arrived at by equating the local crippling stress of the outstanding leg of the longitudinal stringer with that of the web of the ring

$$k_s \frac{E}{1-\mu^2}\left(\frac{t_w}{b_s}\right)^2 = k_r \frac{E}{1-\mu^2}\left(\frac{t_w}{K_1 b_w}\right)^2$$

where

k_s = 0.385 (one edge free).

k_r = 3.29 (both edges simply supported).

and K_1 equals 2.92, but, since one of the edge conditions of the web is actually elastically supported, use $K_1 = 2.5$. Therefore, depth of ring equals $2.5\, b_w$.

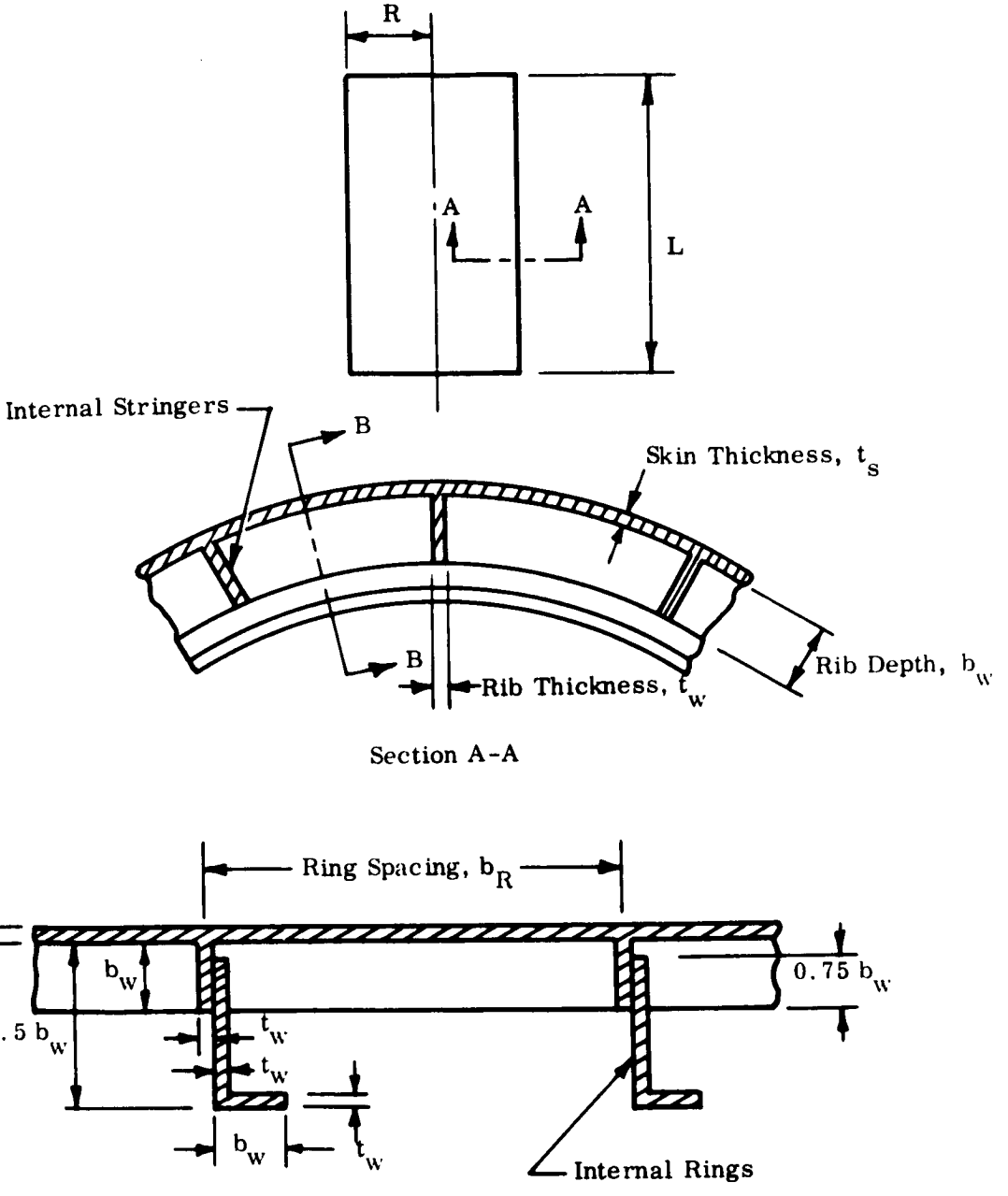

Figure N-1. Integral Stringer and Ring Stiffened Cylinder Geometry

b. Equating the local crippling stresses of the outstanding leg of the longitudinal stringer with that of the flange of the ring, we obtain a flange width equal to that of the stringer depth.

N.2 FAILURE MODES

N.2.1 GENERAL INSTABILITY

In order to predict general instability, the equations developed by Block, Card, and Mikulas[29] will be used. These equations represent the latest state of the art in buckling of orthotropic cylinders and take into consideration the effects of asymmetry, i.e., the effect of whether the rings and stringers are located on the inside or outside of the skin. The equations are

$$N_x \frac{L^2}{\pi^2 D} = m^2 (1 + \beta^2)^2 + m^2 \frac{E I_s}{d D} + m^2 \beta^4 \frac{E I_r}{l D} + \left(\frac{G_s J_s}{dD} + \frac{G_r J_r}{lD} \right) m^2 \beta^2$$

$$+ \frac{12 Z^2}{m^2 \pi^4} \left(\frac{1 + \bar{S} \Lambda_s + \bar{R} \Lambda_r + \bar{S} \bar{R} \Lambda_{rs}}{\Lambda} \right)$$

where

$$\Lambda_r = 1 + 2\alpha^2 \beta^2 (1 - \beta^2 \mu) \frac{\bar{Z}_r}{R} + \alpha^4 \beta^4 (1 + \beta^2)^2 \left(\frac{\bar{Z}_r}{R} \right)^2$$

$$\Lambda_s = 1 + 2\alpha^2 (\beta^2 - \mu) \frac{\bar{Z}_s}{R} + \alpha^4 (1 + \beta^2)^2 \left(\frac{\bar{Z}_s}{R} \right)^2$$

$$\Lambda_{rs} = 1 - \mu^2 + 2\alpha^2 \beta^2 (1 - \mu^2) \left(\frac{\bar{Z}_r}{R} + \frac{\bar{Z}_s}{R} \right)$$

$$+ \alpha^4 \beta^4 \left[1 - \mu^2 + 2\beta^2 (1 + \mu) \right] \left(\frac{\bar{Z}_r}{R} \right)^2 + 2\alpha^4 \beta^4 (1 + \mu)^2 \frac{\bar{Z}_r \bar{Z}_s}{R^2}$$

$$+ \alpha^4 \beta^2 \left[2 (1 + \mu) + \beta^2 (1 - \mu^2) \right] \left(\frac{\bar{Z}_s}{R} \right)^2$$

$$\Lambda = \left(1 + \beta^2\right)^2 + 2\beta^2 (1 + \mu)(\overline{R} + \overline{S}) + (1 - \mu^2) \cdot \left[\overline{S} + 2\beta^2 \overline{R}\,\overline{S} (1 + \mu) + \beta^4 \overline{R}\right]$$

with

$$Z^2 = \frac{L^4(1 - \mu^2)}{R^2 t^2}$$

$$\overline{S} = \frac{A_s}{td}$$

$$\alpha = \frac{m\pi R}{L}$$

$$D = \frac{Et^3}{12(1 - \mu^2)}$$

$$\overline{R} = \frac{A_r}{tl}$$

$$\beta = \frac{n L}{m\pi R}$$

In order to utilize the previously defined equations, it must be minimized with respect to m and n to obtain the minimum allowable loading. However, due to the complexity and time limitation involved, it will be assumed that the ring and stringer eccentricities do not affect the buckling mode shape. Based on this assumption, the equations used to determine the buckling mode shape for the Becker equation (see Appendix F) are used. This assumption has been proved valid and has been proven in Appendix M. Utilizing the Becker equation to determine the buckling mode shape and nondimensionalizing the design parameters, the following equations are obtained, letting

$$t_s = C_1 b_w$$

$$t_w = C_2 b_w$$

$$b_s = C_3 b_w$$

$$b_r = C_4 b_w$$

$$N_x = f(C_1, C_2, C_3, C_4) \frac{2ECb_w^2}{R}$$

where

$$f(C_1, C_2, C_3, C_4) = \frac{1}{2\phi^{\frac{1}{2}}} \left[\frac{(1 + \beta^2)^2 C_1^3}{12(1 - \mu^2)} + \frac{C_2}{12C_3} + \beta^4 \frac{2.92\, C_2}{C_4} + 0.375\, \beta^2 \left(\frac{C_2^3}{3C_3} + \frac{1.166 C_2^3}{3C_4} \right) \right] + \frac{\phi^{\frac{1}{2}}}{2} \left(\frac{1 + \bar{S}\Lambda_s + \bar{R}\Lambda_r + \bar{S}\bar{R}\Lambda_{rs}}{\Lambda} \right)$$

$$\phi = \left(d_{11} + 0.375\, \beta^2 d_{33} + \beta^4 d_{22} \right) \left(\frac{1}{a_{22}} + \frac{0.375\, \beta^2}{a_{33}} + \frac{\beta^4}{a_{11}} \right)$$

$$\beta^2 = P + (P^2 + Q)^{\frac{1}{2}}$$

$$P = \frac{a_{33}}{a_{22}} \left(\frac{a_{22} d_{11} - a_{11} d_{22}}{a_{11} d_{22} - 2a_{33} d_{33}} \right)$$

$$Q = \frac{a_{11}}{a_{22}} \left(\frac{a_{22} d_{11} - 2a_{33} d_{33}}{a_{11} d_{22} - 2a_{33} d_{33}} \right)$$

If β^2 is negative, set $\beta^2 = 0$

If $(P^2 + Q)$ are negative, set $\beta^2 = 0$

$$\bar{S} = \frac{C_2}{C_3 C_1}$$

$$\bar{R} = \frac{4.25\, C_2}{C_4 C_1}$$

$$\Lambda_s = 1 + \frac{2(\beta^2 - \mu)\,\bar{\zeta}_s \psi_s}{\phi^{\frac{1}{2}}} + \frac{(1 + \beta^2)^2\,\bar{\zeta}_s^2\,\psi_s^2}{\phi}$$

$$\Lambda_r = 1 + \frac{2\beta^2\,(1 - \beta^2\mu)\,\psi_r \bar{\zeta}_r}{\phi^{\frac{1}{2}}} + \frac{\beta^4\,(1 + \beta^2)^2 \bar{\zeta}_r^2}{\phi}$$

$$\Lambda_{rs} = 1 - \mu^2 + \frac{2\beta^2\,(1 - \mu^2)}{\phi^{\frac{1}{2}}}\,(\psi_r \bar{\zeta}_r + \psi_s \bar{\zeta}_s)$$

$$+ \frac{\beta^4\,[1 - \mu^2 + 2\beta^2\,(1 + \mu)]\,\bar{\zeta}_r^2 \psi_r^2}{\phi} + \frac{2\beta^4\,(1 + \mu)^2\,\psi_r \bar{\zeta}_r \psi_s \bar{\zeta}_s}{\phi}$$

$$+ \frac{\beta^2\,[2(1 + \mu) + \beta^2\,(1 - \mu^2)]\,\bar{\zeta}_s^2 \psi_s^2}{\phi}$$

$$\Lambda = (1 + \beta^2)^2 + 2\beta^2\,(1 + \mu)\,(\bar{R} + \bar{S})$$

$$+ (1 - \mu^2)\quad [\bar{S} + 2\beta^2\,\bar{R}\,\bar{S}\,(1 + \mu) + \beta^4\,\bar{R}]$$

$$d_{11} = \frac{1}{C_3}\left[\frac{C_2}{3} + \frac{C_1 C_2}{2} + \frac{C_1^2 C_2}{4} - \frac{C_2^2\,(1 + C_1)^2}{4\,(C_2 + C_3 C_1)}\right]$$

$$d_{22} = \frac{i_r + a_r\,(\bar{\zeta}_r - \bar{Y})^2 + C_1 C_4\,(\bar{Y})^2}{C_4}$$

$$a_r = 4.25\,C_2$$

$$i_r = 2.92\,C_2$$

$$\bar{\zeta}_r = 1.44$$

$$\bar{\zeta}_s = \frac{1 + C_1}{2}$$

$$\bar{Y} = \frac{6.11\,C_2}{4.25\,C_2 + C_1 C_4}$$

$$d_{33} = \frac{C_2^3}{16C_3} + \frac{0.219C_2^3}{C_4} + \frac{C_1^3}{16}$$

$$a_{11} = C_1 + \frac{C_2}{C_3}$$

$$a_{22} = \frac{4.25\,C_2 + C_1C_4}{C_4}$$

$$a_{33} = \frac{3\,C_1}{8}$$

$$D_{11} = d_{11}\,E\,b_w^3$$

$$D_{22} = d_{22}\,E\,b_w^3$$

$$D_{33} = d_{33}\,E\,b_w^3$$

$$A_{11} = a_{11}\,E\,b_w$$

$$A_{22} = a_{22}\,E\,b_w$$

$$A_{33} = a_{33}\,E\,b_w$$

C, the buckling correction factor, equals 0.58.

Presently, there is no test data available for this type of construction. Therefore, the same buckling correction factor will be used as for the single-face corrugation (see Appendix M).

N.2.2 PANEL BUCKLING

To predict the buckling of the unsupported panel lengths between rings, the same equation used for general instability will be used, with, of course, the stiffnesses of the

circumferential rings being taken as zero. The equation is

$$\frac{N_x^p \ell^2}{\pi^2 D} = m^2 (1 + \beta^2)^2 + m^2 \frac{E I_s}{dD} + m^2 \beta^2 \frac{G J_s}{dD}$$

$$+ \frac{12 Z^2}{m^2 \pi^4} \left[\frac{1 + \bar{S} \Lambda_3}{(1 + \beta^2)^2 + 2 \bar{S} \beta^2 (1 + \mu) + \bar{S} (1 - \mu^2)} \right]$$

In order to predict the theoretical panel buckling load, the above equation must be minimized with respect to m and n. To simplify the minimization, a value of one will be used for m, the number of buckling half wavelengths between rings. This is analogous to the buckling wave pattern of a simply supported Euler column between rings. To minimize with respect to n, a numerical iteration scheme is used to obtain the minimum value of N_x^p (see Figure N-2).

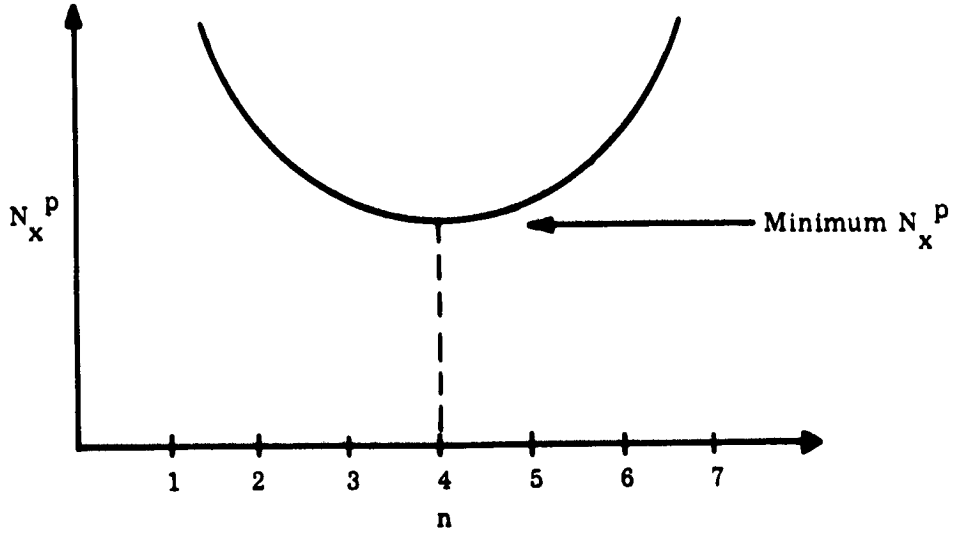

Figure N-2. Minimum Value of N_x^p

To do this, let

$m = 1$

$\ell = C_4 b_w$

$d = C_3 b_w$

so that

$$N_x^p = \left\{ \frac{\pi^2 D (1 + \beta^2)^2}{C_4^2 b_w^2} + \frac{\pi^2 C_2 E b_w}{12 C_4^2} + \beta^2 \frac{\pi^2 C_2^3 E b_w}{8 C_4^2 C_3} + \frac{12 D Z^2}{C_4^2 \pi^2 b_w^2} \left[\frac{1 + \bar{S} \Lambda_s}{(1 + \beta^2)^2 + 2\bar{S}\beta^2 (1 + \mu) + \bar{S}(1 - \mu^2)} \right] \right\} C_p$$

$$\beta = \frac{n C_4 b_w}{\pi R}$$

$$\alpha = \frac{\pi R}{C_4 b_w}$$

$$\bar{S} = \frac{C_2}{C_1 C_3}$$

$$\bar{R} = \frac{4.25 C_2}{C_4 C_1}$$

$$D = \frac{C_1^3 E b_w^3}{12 (1 - \mu^2)}$$

$$Z^2 = \frac{C_4^4 (1 - \mu^2) b_w^2}{C_1^2 R^2}$$

$$\Lambda_s = 1 + \frac{\pi^2 R}{C_4^2 b_w} (\beta^2 - \mu)(1 + C_1)\psi_s + \frac{\pi^4 R^2}{C_4^4 b_w^2} (1 + \beta^2)^2 \frac{(1 + C_1)^2}{4} \psi_s^2$$

C_p, the buckling correction factor, equals 0.58, which is the same factor used for general instability.

N.2.3 RIB CRIPPLING[23]

Assuming simply supported edge conditions and an aspect ratio of infinity, the critical rib crippling stress is

$$\sigma_{cr} = 0.385 \frac{E}{1 - \mu^2} C_2^2$$

N.2.4 SKIN BUCKLING[23]

Assuming simply supported edge conditions and an aspect ratio of infinity, the critical skin buckling stress is

$$\sigma_{cr} = 3.29 \frac{E}{1 - \mu^2} \left(\frac{C_1}{C_3}\right)^2$$

N.2.5 STRENGTH CRITERIA

To determine the maximum stress level in the skin, a modified form of the von Mises yield equation is used. The skin is investigated only since its resultant stress will always be greater than or equal to that of the stiffening elements

$$\sigma = \sqrt{\left(\frac{N_x}{a_{11} b_w}\right)^2 - \left(\frac{N_x N_y}{a_{11} a_{22} b_w^2}\right) + \left(\frac{N_y}{a_{22} b_w}\right)^2}$$

N.3 OPTIMIZATION PROCEDURE

It is necessary to determine the optimum design parameters C_1, C_2, C_3, C_4, and b_w such that a minimum weight configuration is obtained. The approach to be taken is the concept of maximum strength-to-weight ratio. A logical range of C_1, C_2, C_3, and C_4 will be investigated and the corresponding strength-to-weight ratios calculated. The configuration with the maximum ratio will be investigated for panel buckling and the local forms of instability (skin buckling and rib crippling). If any of these forms of instability are violated, the values of C_1, C_2, C_3, and C_4 with the next highest strength-to-weight ratio are investigated. This process is continued until all forms of instability are satisfied. Having determined the optimum values of C_1, C_2, C_3, and C_4, the value

of the rib depth can be calculated to satisfy general instability using

$$b_w = \sqrt{\frac{N_x R}{2 C E [f(C_1, C_2, C_3, C_4)]}}$$

In order to determine the strength-to-weight ratios, the following equations are required

$$\text{Average thickness, } t_{ave} = g(C_1, C_2, C_3, C_4)\, b_w$$

where

$$g(C_1, C_2, C_3, C_4) = C_1 + \frac{C_2}{C_3} + 4.25\,\frac{C_2}{C_4}$$

Substituting the value of b_w into the average thickness equation results with

$$t_{ave} = \frac{g(C_1, C_2, C_3, C_4)}{[f(C_1, C_2, C_3, C_4)]^{\frac{1}{2}}} \left(\frac{N_x R}{2 C E}\right)^{\frac{1}{2}}$$

In order for the average thickness, and consequently the weight, to be a minimum, the following ratio must be maximum

$$\frac{[f(C_1, C_2, C_3, C_4)]^{\frac{1}{2}}}{g(C_1, C_2, C_3, C_4)} \longrightarrow \text{maximum}$$

The first step in determining a logical range of C_1, C_2, C_3, and C_4 is to investigate skin buckling, which is dependent on the ratio C_3/C_1. A plot of critical skin buckling versus C_3/C_1 was constructed and is shown on Figure N-3. Based on this plot, it was found that a range of C_3/C_1 from 20 to 120 was sufficient to cover a wide range of allowable stress levels. Using C_1 from 0.05 to 0.09 and C_3 from 2 to 6 will result with the desired range of C_3/C_1. Similarly, a plot of C_2 versus critical rib crippling (see Figure N-4) stress was constructed to determine the range of C_2 to investigate. This results with C_2 from 0.05 to 0.15.

Since C_4 is a measure of ring spacing, panel buckling must be investigated to determine the range of values. However, due to the complexity of the panel buckling equation, this

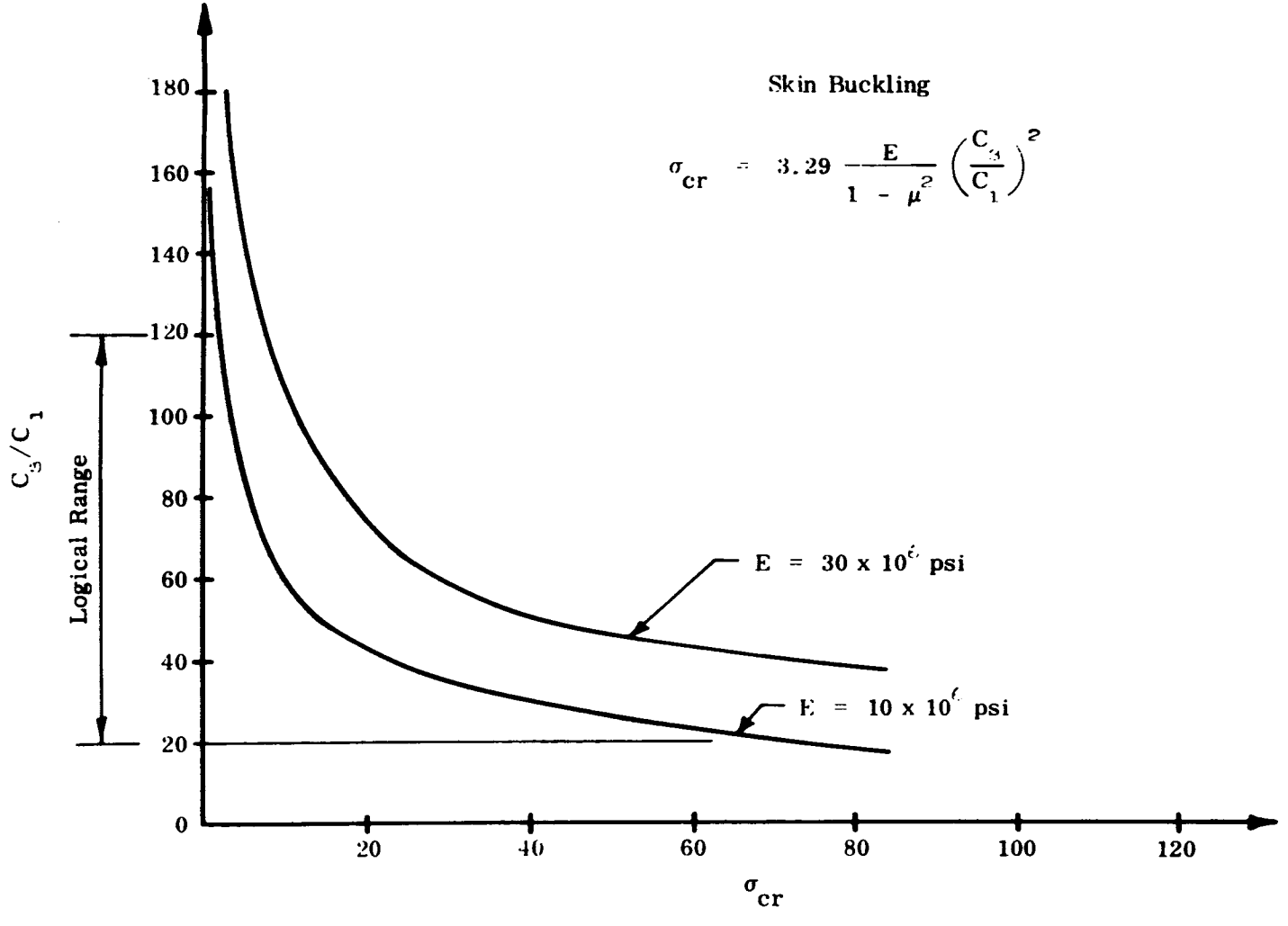

Figure N-3. Critical Skin Buckling versus C_3/C_1

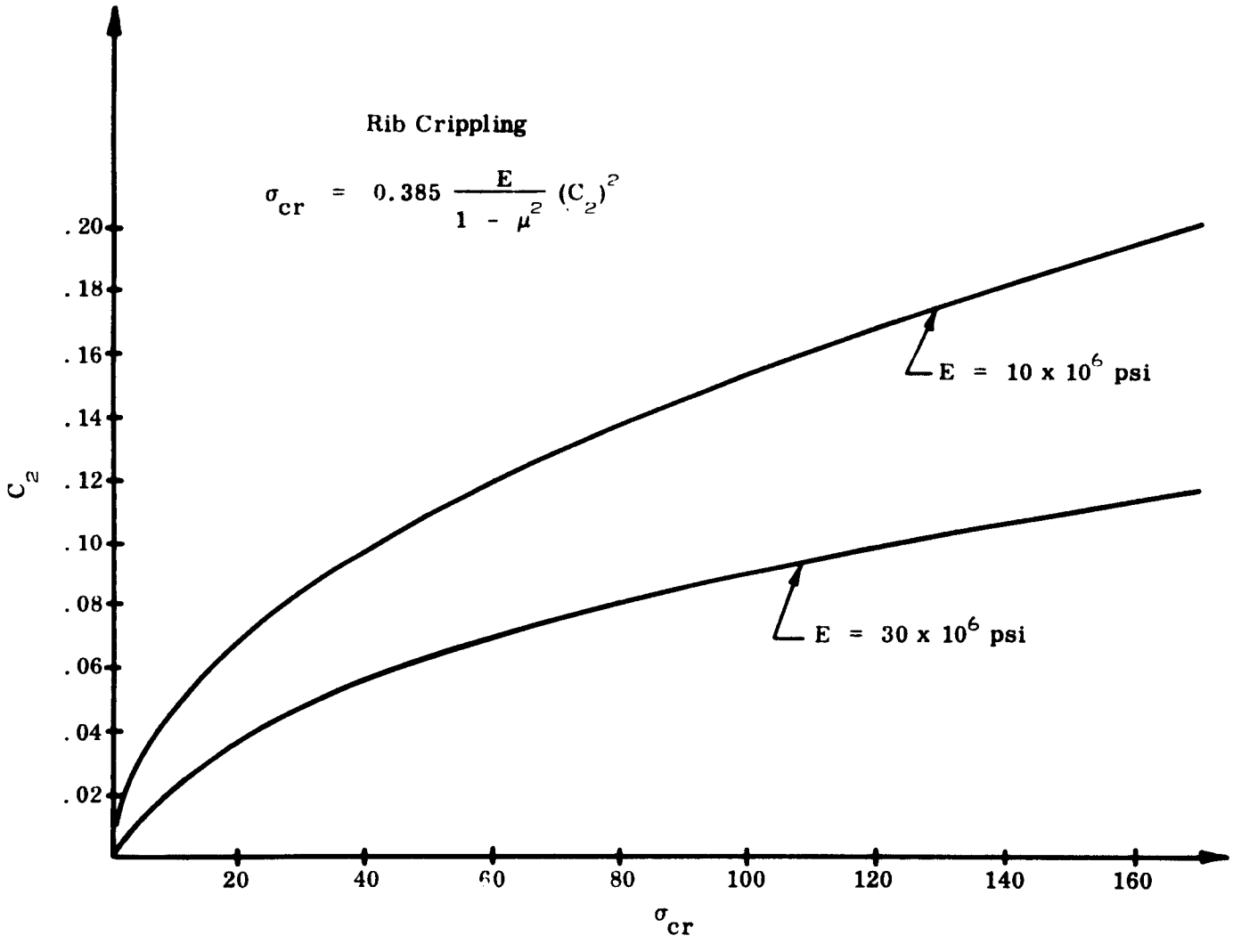

Figure N-4. C_2 versus Critical Rib Crippling

form of instability will be simplified by considering the stringers as Euler columns simply supported between rings. It must be pointed out that panel buckling in the structural optimization computer program is still being investigated using the sophisticated equations, whereas the simplified Euler approximation is being used only to determine a logical range of C_4. Values of the critical Euler stress levels versus C_4 are plotted on Figure N-5. The value of $\ell/\rho = C_4$ was arrived at as follows

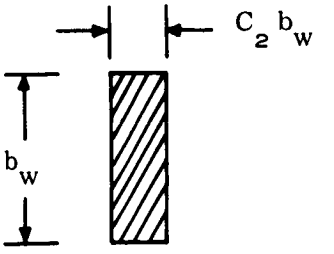

Stringer
Cross Section

$$\rho^2 = \frac{I}{A} = \frac{C_2 b_w^4}{12 C_2 b_w^2}$$

$$\rho = \frac{1}{\sqrt{12}} b_w$$

$$\ell = C_4 b_w \text{ (ring spacing)}$$

Therefore, $\ell/\rho = 3.42\ C_4$. Upon investigating the curve, it was concluded that the logical range of C_4 was from 10 to 30.

In order to minimize the number of design configurations, the following values are built in to the computer program

C_1 = 0.05, 0.06, 0.07, 0.08, 0.09

C_2 = 0.05, 0.075, 0.10, 0.125, 0.15

C_3 = 2, 3, 4, 5, 6

C_4 = 10, 15, 20, 25, 30

This would result with 625 combinations of C_1, C_2, C_3, C_4.

N.4 DEVELOPMENT OF WEIGHT EQUATION

In order to calculate the weight of the cylinder, the average "smeared out" thickness, including the circumferential rings, is

$$t_{ave} = \left(C_1 + \frac{C_2}{C_3} + 4.25\ \frac{C_2}{C_4}\right) b_w$$

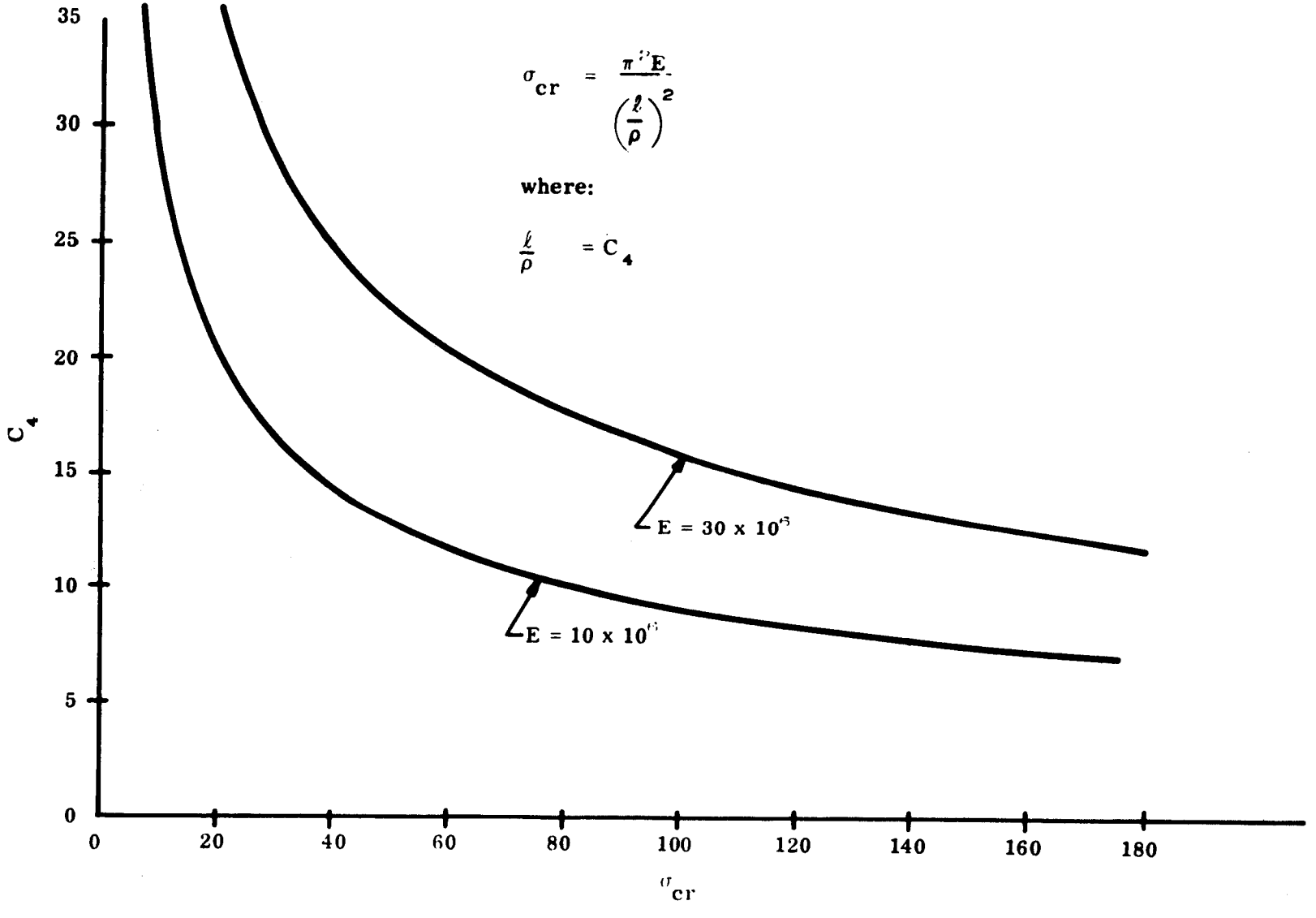

Figure N-5. Critical Euler Stress Levels versus C_4

The weight per surface area equals $t_{ave} \rho F_b$, where F_b, which is a fabrication factor accounting for noncalculated items, equals 1.20.

N.5 NOMENCLATURE

N_x	Axial load per inch (lbs/inch).
N_y	Hoop load per inch (lbs/inch).
R	Radius of cylinder (inches).
L	Length of cylinder (inches).
b_w	Depth of rectangular stringers (inches).
t_s	Skin thickness (inches).
t_{ws}	Thickness of rectangular stringers (inches).
b_s	Spacing of rectangular stringers (inches).
b_r	Spacing of circumferential rings (inches).
t	Thickness of cylinder shell wall (inches).
d	Stringer spacing (inches).
ℓ	Ring spacing (inches).
J_r	Torsional constant for ring (inches^4).
J_s	Torsional constant for stringer (inches^4).
G	Shear modulus (psi).
E	Modulus of elasticity (psi).
μ	Poisson's ratio.
A_s	Area of stringer (inches^2).
A_r	Area of ring (inches^2).
I_s	Moment of inertia of stringer (inches^4).
I_r	Moment of inertia of ring (inches^4).
$\overline{Z}_r$	Distance from centroid of stiffener to middle surface of shell, positive if stiffener lies on external surface of shell (inches).

$\bar{Z}_s$ Distance from centroid of ring to middle surface of shell, positive if ring lies on external surface of shell (inches).

ψ_s Indicates whether stringers are external or internal to the skin surface, -1 if internal, +1 if external.

ψ_r Indicates whether rings are external or internal to the skin surface, -1 if internal, +1 if external.

m Number of half waves in cylinder buckle pattern in longitudinal direction.

n Number of full waves in cylinder buckle pattern in circumferential direction.

C Buckling correction factor.

A_{11} Extensional stiffness in longitudinal direction (lbs/inch).

A_{22} Extensional stiffness in circumferential direction (lbs/inch).

A_{33} Shear stiffness (lbs/inch).

D_{11} Flexural stiffness in longitudinal direction (inch-lbs).

D_{22} Flexural stiffness in circumferential direction (inch-lbs).

D_{33} Torsional stiffness (inch-lbs).

σ Stress level (psi).

APPENDIX O

MONOCOQUE ELLIPSOIDAL HEADS

O.1 INTRODUCTION

The purpose of this appendix is to establish a method for analyzing monocoque ellipsoidal shells subjected to a uniform external collapsing pressure. Since only one design parameter exists (skin thickness), no optimization can be performed. Two failure criteria will be investigated: buckling and strength. The criteria that result with the maximum required thickness is used to design the shell.

O.2 FAILURE MODES

O.2.1 BUCKLING

Since there are no known methods of analysis for ellipsoidal shells subject to uniform external pressure, it is necessary to convert the ellipsoidal shell to an equivalent spherical shell and use the classic von Karmen-Tsien formula to predict buckling of monocoque spherical shells. The classical equation is

$$\sigma_{cr} = 0.606\ CE \frac{t}{R\ (\sin \beta)^{\frac{1}{3}}}$$

where C = 25 percent, the buckling correction factor required to correlate theoretical with experimental results.

In order to convert the ellipsoid to an equivalent spheriod, the following equations are used (see Figure O-1)

$$\beta = \pi - 2 \arctan\left(\frac{a}{b}\right)$$

$$R = \frac{a}{\sin \beta}$$

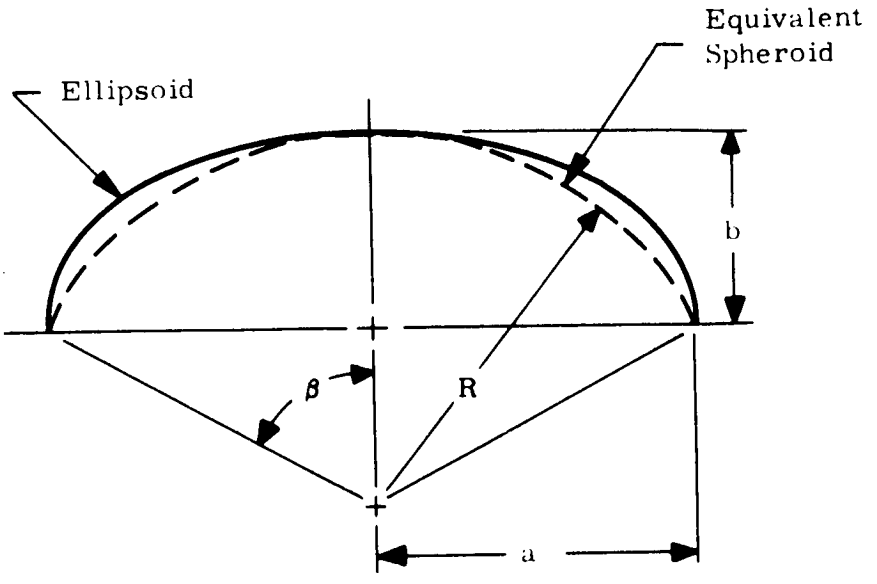

Figure O-1. Converting Ellipsoid to Equivalent Spheroid

In order that the stress levels at the apex of the ellipsoid and the equivalent shells are equal, an equivalent pressure loading must be determined. Setting

$$\frac{pa^2}{2b} = \frac{p_{eq} R}{2}$$

$$p_{eq} = \frac{pa^2}{Rb}$$

$$\sigma_{cr} = 0.606\ CE \frac{t}{R\ (\sin \beta)^{\frac{1}{2}}}$$

but

$$\sigma_{cr} = \frac{p_{eq} R}{2t}$$

and

$$C = 0.25$$

The required thickness to satisfy buckling is

$$t_{buckling} = 1.82\ R\ (\sin \beta)^{\frac{1}{6}} \left(\frac{p_{eq}}{E}\right)^{\frac{1}{2}}$$

O.2.2 STRENGTH

To calculate the required thickness based on strength, the von Mises yield equation is used

$$t_{strength} = \frac{\sqrt{N_x^2 - N_x N_y + N_y^2}}{\sigma_{all}}$$

where N_x and N_y are the actual meridional and hoop loadings that act on the ellipsoidal shell.

O.3 WEIGHT CONSIDERATIONS

To determine the true weight, in lbs/ft^2, of any ellipsoidal shell of monocoque construction (see Figure O-2), the following is used

$$w = \left(\frac{\rho t}{12}\right) F_b$$

where F = 1.09 is a fabrication factor which accounts for non-calculated items.

The total weight is calculated as w times the surface area, where the surface area is

$$\text{Surface Area} = \frac{\pi a}{144 b^2} \left\{ y \sqrt{(a^2 - b^2) y^2 + b^4} + \right.$$

$$+ \frac{b^4}{\sqrt{a^2 - b^2}} \ln \left[y \sqrt{a^2 - b^2} + \right.$$

$$\left. \left. + \sqrt{(a^2 - b^2) y^2 + b^4} \right] \right\}_{y_n}^{y_{n+1}}$$

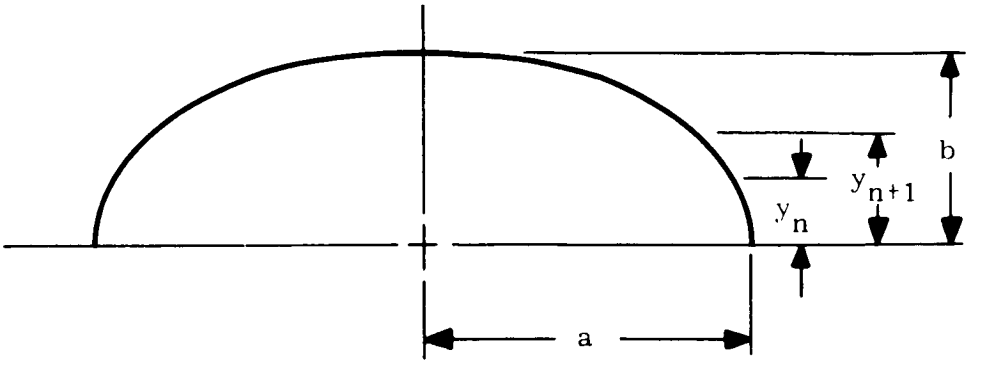

Figure O-2. Determination of Weight

O.4 NOMENCLATURE

t	Monocoque skin thickness (inches).
σ_{cr}	Critical buckling stress (psi).
E	Modulus of elasticity (psi).
β	Central angle (radians).
R	Equivalent radius of curvature (inches).
a	Major radius of ellipsoid (inches).
b	Minor radius of ellipsoid (inches).
p	Uniform external pressure (psi).
p_{eq}	Equivalent external pressure (psi).
N_x	Meridional load per inch (lbs/inch).
N_y	Hoop load per inch (lbs/inch).
ρ	Density of material (lbs/ft^3).

APPENDIX P

HONEYCOMB ELLIPSOIDAL SHELLS

P.1 INTRODUCTION

An ellipsoidal shell of honeycomb construction consists of two high-density faces and a low-density core material. The basic function of the faces is to carry the load, whereas the function of the core is to provide stability for the faces and transmit any shear that is developed. The purpose of this appendix is to establish a method for optimizing this type of construction subjected to a uniform pressure loading.

Two modes of failure are considered: strength based on the von Mises yield criteria, and buckling which consists of general and local instability. The modes of local instability include face wrinkling and monocell buckling. No optimization can be developed based on the strength criteria, however the shell can be optimized based on buckling. Two parameters are to be optimized; the face working stress and the core shear modulus. For a constant loading, the higher the allowable buckling stress, the lower is the resulting weight of the faces. However, increasing the face stress level results in a thicker and heavier core in order to stabilize the shell. Consequently, there exists an optimum face working stress where the total weight of the faces and the core are a minimum (see Figure P-1).

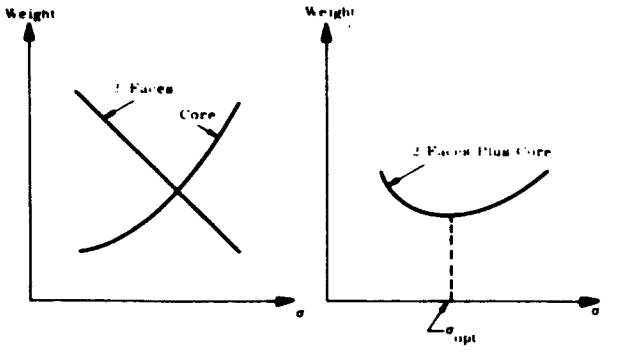

Figure P-1. Optimum Face Working Stress

It has been previously established (see Appendix H) that the shear modulus and elastic modulus of the core are directly proportional to the core density

$$G_c = C_1 \rho_c$$

$$E_c = C_2 \rho_c$$

P.2 FAILURE MODES

P.2.1 MONOCELL BUCKLING[19]

This mode of failure consists of buckling of the faces within the individual cells of the honeycomb core. The empirical formula presented is identical to that used for monocell buckling of axially loaded cylinders. Although this formula is for an element loaded uniaxially without a lateral pressure, it will be used to check monocell buckling for ellipsoidal shells. It is realized that a single cell of the facings is loaded biaxially plus a lateral pressure, however the lack of experimental data for this type of loading necessitates the use of the available formula. As more data becomes available, the formula can be modified to fit the loading condition, but for now the following formula will be used to predict monocell buckling

$$\sigma = 0.9 \eta_i E_f \left(\frac{t_f}{d}\right)^{\frac{3}{2}}$$

P.2.2 FACE WRINKLING [19]

This mode of failure is analagous to a beam on an elastic foundation. Once again, the formula presented is identical to that used for face wrinkling of axially loaded cylinders. Although this formula is for an element loaded uniaxially, it will be used to check face wrinkling for ellipsoidal shells. It is realized the skin is loaded biaxially, however the lack of experimental data for this type of loading necessitates the use of the available formula. As more data becomes available, the formula can be modified to fit the loading condition but for now the following formula will be used to predict face wrinkling

$$\sigma = 0.5 \sqrt[3]{\eta_w E_f E_c G_c}$$

When using a nonisotropic core (hexcell), use the smaller of the two values of core shear modulii.

P.2.3 GENERAL INSTABILITY

Since there are no known methods of analysis for ellipsoidal shells subject to uniform external pressure, it is necessary to convert the ellipsoidal shell to an equivalent spherical shell and use the equations derived for buckling of honeycomb spherical shells.

The following[30] is the formula used to predict buckling of a spherical shell of honeycomb sandwich construction subjected to a uniform external pressure

$$\sigma_{cr} = 0.606\, C\, \eta \frac{E_f\, t_{eff}}{R\, (\sin \beta)^{\frac{1}{3}}}$$

where

$$t_{eff} = \sqrt[3]{6 t_c t_f (2t_f + t_c)}$$

C = buckling correction factor

The equation used is a modified form of the von Karmen-Tsien formula used to predict buckling for monocoque spherical shells. Since a correction factor of 25 percent is required to correlate the classical solution with experimental results for monocoque shells, the same correction factor will be used for honeycomb shells until test results are obtained to dictate otherwise. The effect of the value of core shear modulus, G_c, upon the buckling strength of spherical shells of sandwich construction is not presently known. It is expected that for metal cores having[30] $G_c > 20,000$ psi, no reduction in calculated buckling allowable need be considered; however, test results will be required to establish the effects of low core shear modulus. In order to convert the ellipsoid to an equivalent spheroid, the following equations are used (see Figure P-2)

$$\beta = \pi - 2 \arctan\left(\frac{a}{b}\right)$$

$$R = \frac{a}{\sin \beta}$$

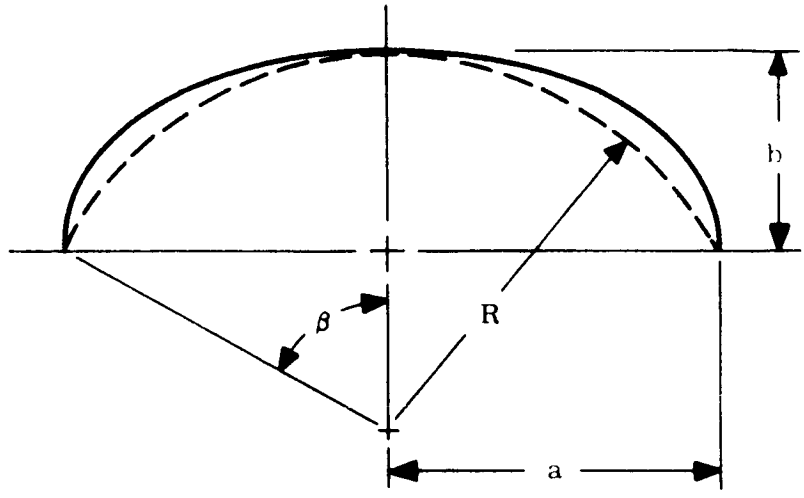

Figure P-2. Converting Ellipsoid to Equivalent Spheroid

In order that the stress levels at the apex of the ellipsoid and the equivalent shell are equal, the same meridional and hoop loading is assumed to act at the apex of the equivalent shell. The loading at the apex of an ellipsoid is

$$N_x = N_y = \frac{pa^2}{2b}$$

P.2.4 STRENGTH CRITERIA

In order to determine the required face thickness based on strength, the von Mises yield equation is used

$$2t_f = \frac{\sqrt{N_x^2 - N_x N_y + N_y^2}}{\sigma}$$

P.3 WEIGHT CONSIDERATIONS

P.3.1 DEVELOPMENT OF MINIMUM WEIGHT EQUATION

It is desired to develop a weight equation as a function of the face working stress. Upon differentiation of this equation with respect to the face stress and setting it equal to zero,

an expression is obtained for determining the optimum face working stress. The weight equation is

$$w = 2t_f\rho_f + 2t_c\rho_c$$

and letting

$$k_2 = \frac{\rho_c}{\rho_f}$$

then

$$w = (t_c k_2 + 2t_f)\rho_f$$

It has been previously established that the equation for general instability is

$$\sigma_{cr} = 0.606\, C\eta \frac{E_f t_{eff}}{R\,(\sin\beta)^{\frac{1}{3}}}$$

where

$$t_{eff} = \sqrt[3]{6t_c t_f (2t_f + t_c)}$$

Letting $2t_f + t_c = k_1 t_c$, where for all practical purposes $k_1 = 1$, and solving for t_c, the following is obtained

$$t_c = \frac{\sigma^{\frac{3}{2}} R^{\frac{3}{2}} (\sin\beta)^{\frac{1}{2}}}{1.15 C^{\frac{3}{2}} \eta^{\frac{3}{2}} t_f^{\frac{1}{2}} k_1^{\frac{1}{2}} E_f}$$

where η is defined in Appendix A.

Substituting the value of t_c, $t_f = N_x/2\sigma$, and η in terms of the Ramberg-Osgood equation, the following is obtained

$$w = \left\{ \frac{1.15\sigma^{\frac{5}{4}} R^{\frac{3}{2}} (\sin\beta)^{\frac{1}{2}} k_2 \left[1 + \frac{3}{7} n \left(\frac{\sigma}{\sigma_o}\right)^{n-1}\right]^{\frac{3}{4}} \left[\sigma + \frac{3}{7}\sigma_o \left(\frac{\sigma}{\sigma_o}\right)^{n}\right]^{\frac{3}{4}}}{C^{\frac{3}{2}} E_f^{\frac{3}{2}} N_x^{\frac{1}{2}} k_1^{\frac{1}{2}}} + \frac{N_x}{\sigma} \right\} \rho_f$$

Setting $dw/d\sigma = 0$ to obtain a minimum weight results in

$$\left(\frac{N_x}{R}\right)^{\frac{3}{2}} = \frac{0.86\,(\sin\beta)^{\frac{1}{2}}\,k_2}{E_f^{\frac{3}{2}}\,k_1^{\frac{1}{2}}\,C^{\frac{3}{2}}}\,\sigma^3 \cdot \left\{ \frac{\frac{8}{3} + \frac{3}{7}\left(n + \frac{5}{3}\right)\left(n + 1\right)\left(\frac{\sigma}{\sigma_o}\right)^{n-1} + \frac{9}{49}\left(2n + \frac{2}{3}\right) n \left(\frac{\sigma}{\sigma_o}\right)^{2n-2}}{\left[1 + \frac{3}{7}(n + 1)\left(\frac{\sigma}{\sigma_o}\right)^{n-1} + \frac{9}{49}\,n\left(\frac{\sigma}{\sigma_o}\right)^{2n-2}\right]^{\frac{1}{4}}} \right\}$$

Given the structural index and a value of the core density, the above equation can be used to determine the optimum face working stress that would result with a minimum weight. Knowing the face working stress, it is a simple matter of calculating the core thickness required to stabilize the skin. In order to optimize with respect to the core shear modulus, a practical range of modulii are investigated, each being optimized for the face working stress, and the value chosen that results with the minimum weight.

P.3.2 WEIGHT EQUATION

In order to determine the true weight in lbs/ft^2, ellipsoidal shell of sandwich construction (see Figure P-3) the following is used

$$w = \left(\frac{\rho_c t_c + 2t_f \rho_f}{12}\right) F_b$$

where $F_b = 1.25$ is a fabrication factor which takes into consideration non-calculated items such as core filler material, doublers, fasteners, etc.

The total weight is calculated as w times the surface area, where the surface area is

$$\text{Surface Area} = \frac{\pi a}{144\, b^2}\left[y\sqrt{(a^2 - b^2)\, y^2 + b^4} + \frac{b^4}{\sqrt{a^2 - b^2}} \ln\left(y\sqrt{a^2 - b^2} + \sqrt{(a^2 - b^2)\, y^2 + b^4} \right) \right]_{y_n}^{y_{n+1}}$$

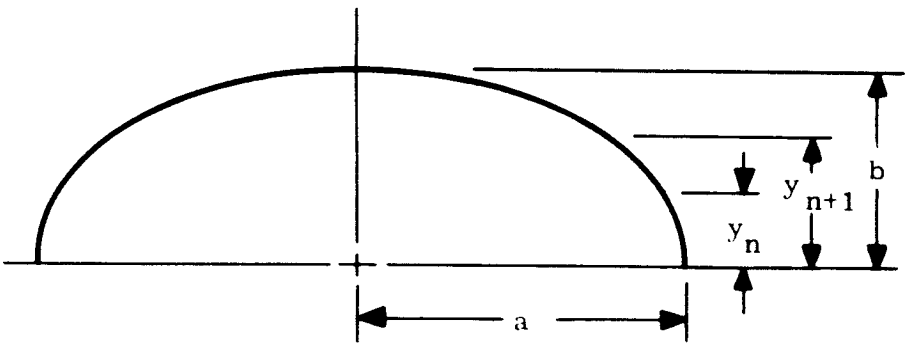

Figure P-3. Determination of Weight

P.4 NOMENCLATURE

N_x	Meridional load per inch (lbs/inch).
N_y	Hoop load per inch (lbs/inch).
p	External pressure (psi).
d	Diameter of circle inscribed within a honeycomb cell (inches).
t_f	Face thickness (one) (inches).
t_c	Core thickness (inches).
a	Major radius of ellipsoid (inches).
b	Minor radius of ellipsoid (inches).
σ	Face stress level (psi).

E_f Modulus of elasticity of faces (psi).

G_c Shear modulus of core (psi).

E_c Modulus of elasticity of the core perpendicular to the faces (psi).

ρ_c Density of core (lbs/ft^3).

ρ_f Density of face material (lbs/ft^3).

w Weight of sandwich per surface area (lb/ft^2).

C_1 Specific shear modulus ($psi/lbs/ft^3$).

C_2 Specific modulus of elasticity ($psi/lbs/ft^3$).

η Tangent-secant modulus plasticity reduction factor.

η_w Tangent modulus plasticity reduction factor.

η_i Secant modulus plasticity reduction factor.

APPENDIX Q

WAFFLE STIFFENED ELLIPSOIDAL SHELLS

Q.1 INTRODUCTION

A waffle stiffened ellipsoidal shell consists of a thin skin stiffened with equally spaced rectangular ribs (see Figure Q-1). The purpose of this appendix is to present a means for optimizing the shell subjected to an external collapsing pressure. The method used for the optimization routine was developed as shown in Reference 31. This work was adapted to suit the specific needs of the optimization routine. Four parameters are to be optimized: skin thickness, rib depth, rib spacing, and rib thickness. In determining the design configuration, the following modes of failure are considered: general instability, panel buckling of the skin, and crippling of the ribs. The following assumptions have been made:

a. Rib spacing is sufficiently close so that the ribs and skin are equally stressed.
b. Panels between ribs are treated as flat plates when considering panel buckling.
c. Waffle stiffened skin is manufactured using the mechanical milling process.
d. Critical buckling stresses are within the elastic limit.
e. External collapsing pressure is uniform.
f. Optimization procedure neglects the weight of the fillet radii.

Q.2 FAILURE MODES

Q.2.1 PANEL BUCKLING

In order to investigate this mode of local failure of the shell elements bounded by the stiffeners, it is assumed that the edge conditions for the biaxially loaded square plates are simply supported. The critical buckling stress level[27] is

$$\sigma_{cr_p} = k_p \frac{\pi^2 D_s}{b_s^2 t_s}$$

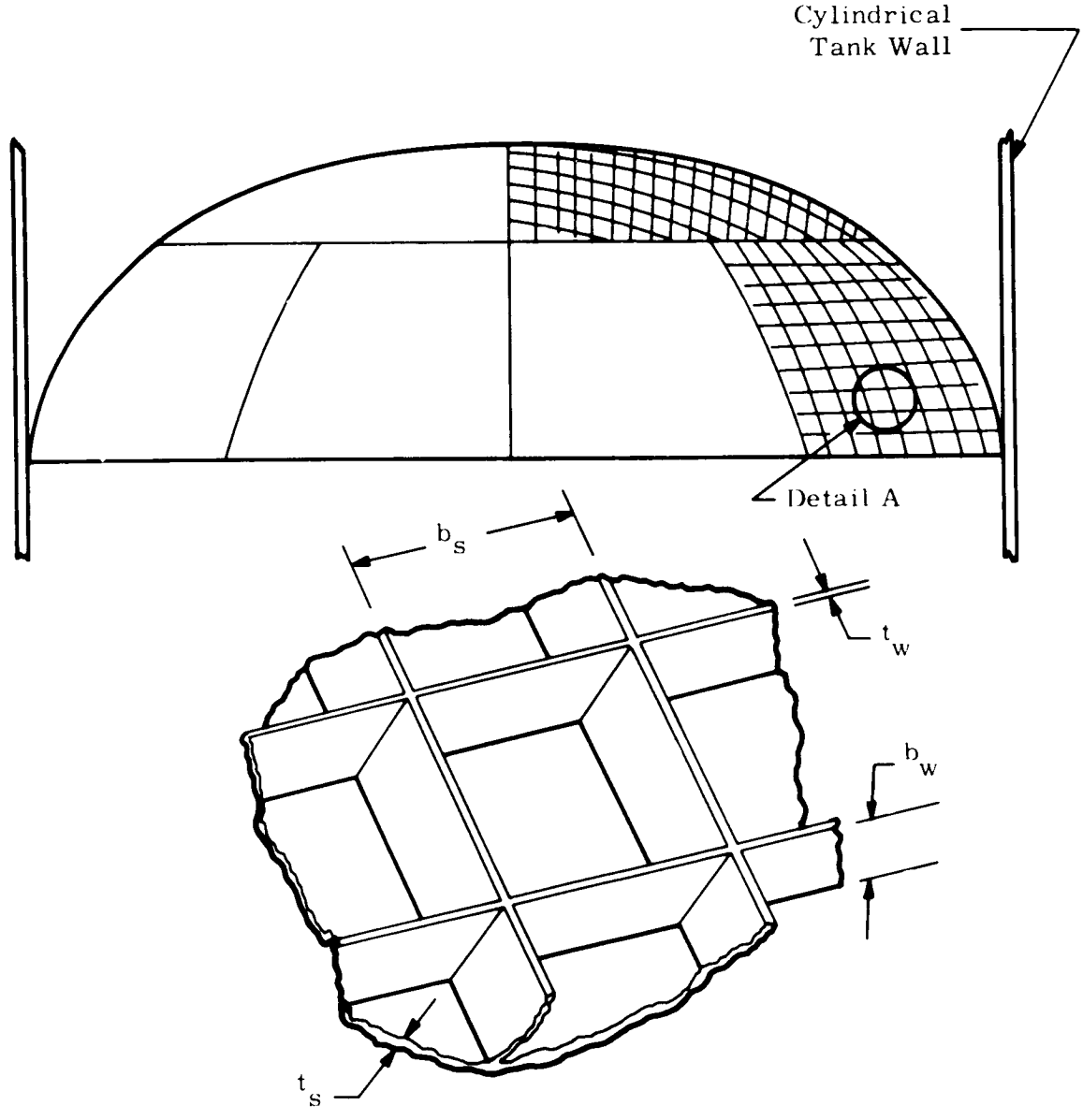

Detail A

Figure Q-1. Waffle-Stiffened Ellipsoidal Shell Geometry

where

$$k_p = 2$$

$$D_s = \frac{Et_s^3}{12(1 - \mu^2)}$$

To determine the allowable critical buckling pressure based on the local buckling of the panels, it is assumed that the panels are stressed as though only the shell participates in carrying the applied pressure. This results in

$$p_{cr_p} = 2 k_p \pi^2 E \left(\frac{D_s}{ER^3}\right) \frac{R^2}{b_s^2}$$

Q.2.2 RIB CRIPPLING

To investigate this local mode of failure, simply supported edge conditions are again assumed. The following equations depict the critical buckling stress level in the ribs[27]

$$\sigma_{cr_w} = k_w \frac{\pi^2 D_w}{b_w t_w}$$

where

$$D_w = \frac{Et_w^3}{12(1 - \mu^2)}$$

$$k_w = 0.50$$

But

$$\sigma_{cr_w} = \frac{p_{cr_w} R}{2\bar{t}}$$

where

$$\bar{t} = t_s \left[1 + \left(\frac{b_w}{b_s}\right)\left(\frac{t_w}{t_s}\right)\right]$$

Therefore,

$$p_{cr_w} = 2k_w \pi^2 E \left(\frac{R}{b_w}\right)^2 \frac{\bar{t}}{t_w} \frac{D_w}{ER^3}$$

Q.2.3 GENERAL INSTABILITY

Since there are no known methods of analysis for predicting the buckling of an ellipsoidal head subjected to external pressure, it is necessary to convert the ellipsoidal shell to an equivalent spherical shell and use the spherical shell buckling equations. The following formula[31] is used to predict the critical collapsing pressure

$$p_{cr_g} = 4CE \left[\frac{\bar{t}}{R} \frac{D}{D_s} \frac{D_s}{ER^3} \left(\frac{1 + \frac{D_3}{D}}{1 + \frac{\bar{E}}{G_3}} \right) \right]^{\frac{1}{2}}$$

where

$$\bar{t} = t_s \left[1 + \left(\frac{b_w}{b_s}\right)\left(\frac{t_w}{t_s}\right) \right]$$

$$\bar{E} = \frac{E\bar{t}}{(1 - \mu^2)}$$

$$D_s = \frac{Et_s^3}{12(1 - \mu^2)}$$

The ratios in the previous equation are closely approximated by the following formula when, as in the present case, $(b_s/t_s) >>> 1$ and only the skin carries in-plane shear

$$\frac{D}{D_s} = (1 - \mu^2)\left(\frac{b_w}{b_s}\right)^3 \left(\frac{t_w}{t_s}\right)\left(\frac{b_s}{t_s}\right)^2 \left[\frac{4 + \left(\frac{b_w}{b_s}\right)\left(\frac{t_w}{t_s}\right)}{1 + \left(\frac{b_w}{b_s}\right)\left(\frac{t_w}{t_s}\right)} \right]$$

$$\frac{D_3}{D} \approx 0$$

$$\frac{\bar{E}}{G_3} = (1 + \mu)\left(\frac{\bar{t}}{t_s}\right) - \mu$$

$$\frac{D_s}{ER^3} = \frac{\left(\frac{t_s}{R}\right)^3}{12(1 - \mu^2)}$$

$$\frac{\bar{t}}{R} = \frac{t_s}{b_s}\left(\frac{b_s}{R}\right)\left(1 + \frac{b_w t_w}{b_s t_s}\right)$$

In order to convert the ellipsoid to an equivalent spherical shell, it is assumed that the ellipsoid can be replaced by a spherical shell that intersects the replaced shell at the apex and the base (see Figure Q-2). The following equations will result with an equivalent shell

$$\beta = \pi - 2 \arctan\left(\frac{a}{b}\right)$$

$$R = \frac{a}{\sin \beta}$$

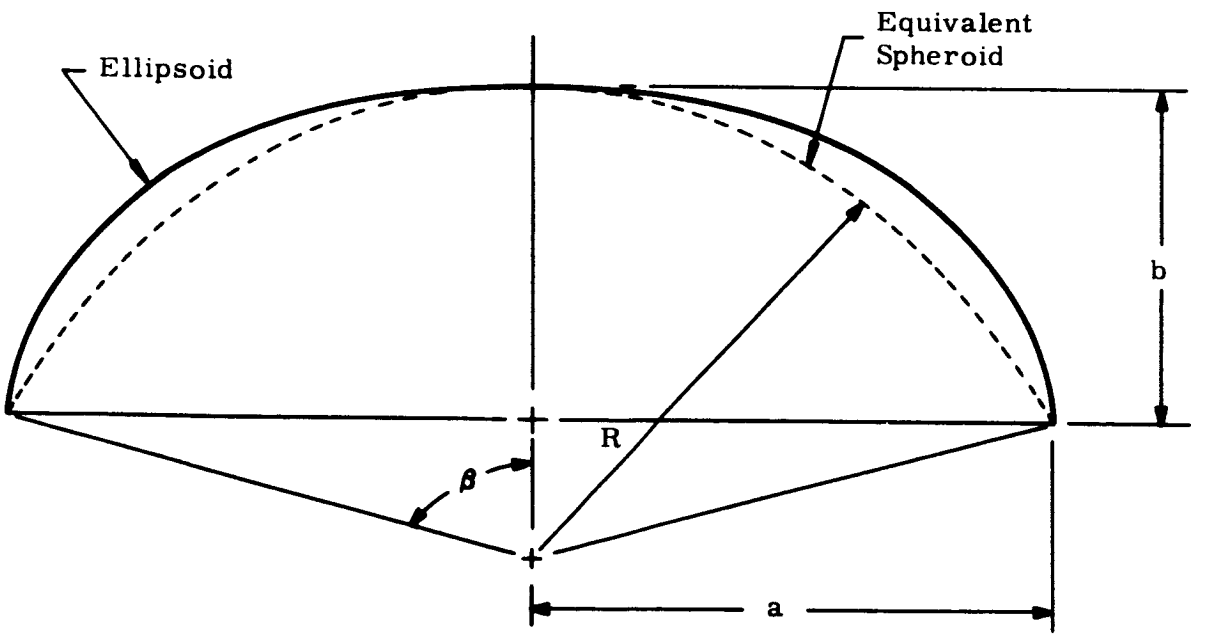

Figure Q-2. Converting Ellipsoid to Equivalent Spheriod

In order that the stress levels at the apex of the ellipsoidal and equivalent shells are equal, the same meridional and hoop loading is assumed to act at the apex of the equivalent shell. The loading at the apex of an ellipsoid is

$$N_x = N_y = \frac{pa^2}{2b}$$

To calculate the equivalent pressure loading, the following equation is used

$$p_{eq} = \frac{2N_x}{R}$$

To determine the buckling correction factor, C, a literature survey was made to locate test data for waffle stiffened spherical shells. Since no data could be found for ellipsoidal shells, it will be assumed that the same correction factor applies to the equivalent shell. The following shell test data presented[32] yielded a critical buckling pressure of 9.48 psi

b_s = 1.16 inches.

t_w = 0.0287 inch.

t_s = 0.0576 inch.

R = 20 inches.

E = 0.465×10^6 psi.

Based on the theoretical equations presented for general instability, the theoretical critical buckling pressure was calculated as 12.1 psi. Therefore, in order to correlate the test data and theory, a buckling correction of C = 0.785 is required.

Q.2.4 STRENGTH CRITERIA

Depending upon the intensity of the pressure loading, the shell may be strength governed rather than buckling governed. To determine the stress level, it is assumed that the skin and ribs are equally stressed, thereby permitting use of the von Mises yield equation

$$\sigma = \frac{\sqrt{N_x^2 - N_x N_y + N_y^2}}{\bar{t}}$$

where

$$\bar{t} = t_s\left(1 + \frac{b_w t_w}{b_s}\right)$$

Q.3 OPTIMIZATION PROCEDURE

In order to optimize the shell, the design parameters t_s, t_w, b_w, and b_s must be chosen such that a minimum weight configuration is obtained. The same basic concept of maximum strength-to-weight ratio is used; however, since the equations are all reduced to a workable form, the minimum weight equation will include panel buckling and rib crippling. Equating the critical buckling pressures of all the forms of instability will constitute a minimum weight design. The critical buckling and weight equations are summarized and are

$$p_{cr_g} = 4CE\left[\frac{\bar{t}}{R}\,\frac{D}{D_s}\,\frac{D_s}{ER^3}\left(\frac{1 + \frac{D_3}{D}}{1 + \frac{\bar{E}}{G_3}}\right)\right]^{\frac{1}{2}}$$

$$p_{cr_p} = 2k_p\pi^2 E\left(\frac{D_s}{ER^3}\right)\frac{R^2}{b_3^2}$$

$$p_{cr_w} = 2k_w\pi^2 E\left(\frac{R}{b_w}\right)^2 \cdot \frac{\bar{t}}{t_w} \cdot \frac{D_w}{ER^3}$$

$$t_{ave} = t_s\left(1 + 2\,\frac{b_w t_w}{b_s t_s}\right)$$

Equating the first two equations above and utilizing the last, results with the following weight equation

$$\frac{t_{ave}}{R} = F\left(\frac{p_{eq}}{E}\right)^{\frac{3}{5}}$$

where F is the following efficiency factor

$$F = \left(1 + 2\frac{b_w t_w}{b_s t_s}\right)\left[\frac{3\left\{2 + (1+\mu)\left[\left(\frac{b_w}{b_s}\right)\left(\frac{t_w}{t_s}\right)\right]\right\}}{\left(\frac{b_w}{b_s}\right)^3\left(\frac{t_w}{t_s}\right)\left[4 + \left(\frac{b_w}{b_s}\right)\left(\frac{t_w}{t_s}\right)\right]}\ \frac{12(1-\mu^2)}{2^3 k_s \pi^2}\right]^{\frac{1}{5}}\ \frac{1}{C^{\frac{2}{5}}}$$

Equating the critical stresses in the two local modes of instability leads to the following relationship between b_w/b_s and t_w/t_s

$$\left(\frac{b_w}{b_s}\right)\left(\frac{t_w}{t_s}\right) = 2r\left\{1 + \left[1 + \left(\frac{1}{r}\right)\right]^{\frac{1}{2}}\right\}$$

where

$$r = \left[\frac{1}{2}\left(\frac{t_w}{t_s}\right)\right]^4$$

Substituting the above equation into the preceding equation results in

$$F = \frac{0.636\ r^{\frac{1}{10}}}{C^{\frac{2}{5}}}\ \frac{\left\{1 + 4r\left[1 + \left(1 + \frac{1}{r}\right)^{\frac{1}{2}}\right]\right\}}{\left\{r\left[1 + \left(1 + \frac{1}{r}\right)^{\frac{1}{2}}\right]\right\}^{\frac{3}{5}}}\ x\left\{\frac{1 + 1.3r\left[1 + \left(1 + \frac{1}{r}\right)^{\frac{1}{2}}\right]}{2 + r\left[1 + \left(1 + \frac{1}{r}\right)^{\frac{1}{2}}\right]}\right\}^{\frac{1}{5}}$$

In order for the weight to be minimum and, consequently, the strength-to-weight ratio to be maximum, the efficiency factor, F, must be minimized with respect to t_w/t_s. Figure Q-3 shows a plot of F versus t_w/t_s. The efficiency factor is a minimum of 1.88 when $t_w/t_s = 0.80$, for C = 1.0. Regardless of the value of C, the design will always be minimum at $t_w/t_s = 0.80$ but, of course, the value of efficiency factor will be dependent upon the correction factor. Therefore,

$$F = \frac{1.88}{C^{\frac{2}{5}}}$$

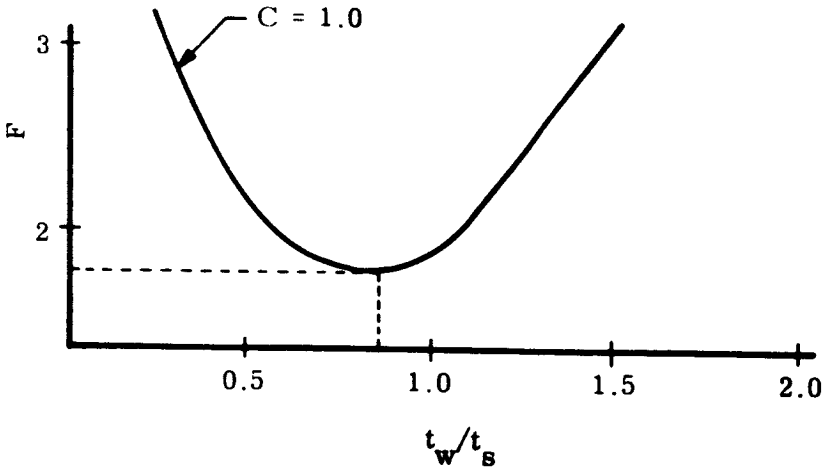

Figure Q-3. Efficiency Factor, F, versus t_w/t_s

The auxiliary equations necessary for design are

$$t_s = \frac{t_{ave}}{\left[1 + 2\left(\frac{b_w}{b_s}\right)\left(\frac{t_w}{t_s}\right)\right]}$$

$$b_s = \left(\frac{3.62\, E\, t_s^{\,3}}{p_{eq}\, R}\right)^{\frac{1}{2}}$$

The following is a list of steps required to obtain an optimum design for a given loading condition:

a. Knowing the correction factor, C, determine F.
b. Determine t_{ave}.
c. Knowing $t_w/t_s = 0.80$, calculate b_w/b_s.
d. Calculate t_s.
e. Calculate b_s.

Q.4 DEVELOPMENT OF WEIGHT EQUATION

The weight equation previously used considered only the weight of the skin and ribs and not that of the fillet radii between the ribs and skin. Neglecting this small portion of weight will have little or no effect upon the optimum configuration, however it should be included when calculating the final weight. Letting $C_4 = r_{w_s}/H$ and $C_5 = r_s/H$, the

following equations are obtained

$$w = \frac{t_{ave}}{12}\rho$$

where

$$t_{ave} = t_s\left[1 + 2\left(\frac{b_w}{b_s}\right)\left(\frac{t_w}{t_s}\right)\right] + \frac{2\pi[C_5(b_w + t_s) - 0.22\,C_4(b_w + t_s)]}{b_s^2}$$

$$\cdot\left[C_4^2(b_w + t_s)^2\left(1 - \frac{\pi}{4}\right)\right] + \frac{4\,C_5^2(b_w + t_s)^2\left(1 - \frac{\pi}{4}\right)(H - t_s)}{b_s^2}$$

$$+ \frac{4\,C_4^2(b_w + t_s)^2\left(1 - \frac{\pi}{4}\right)[b_s - 2\,C_5(b_w + t_s) - t_w]}{b_s^2}$$

The total weight is calculated as w x surface area x F_b, where $F_b = 1.20$ is a fabrication factor which takes into consideration non-calculated items, and (see Figure Q-4)

$$\text{surface area} = \frac{\pi a}{144\,b^2}\left\{y\sqrt{(a^2 - b^2)y^2 + b^4} + \frac{b^4}{\sqrt{a^2 - b^2}}\right.$$

$$\left.\cdot \ln\left[y\sqrt{a^2 - b^2} + \sqrt{(a^2 - b^2)y^2 + b^4}\right]\right\}_{y_n}^{y_{n+1}}$$

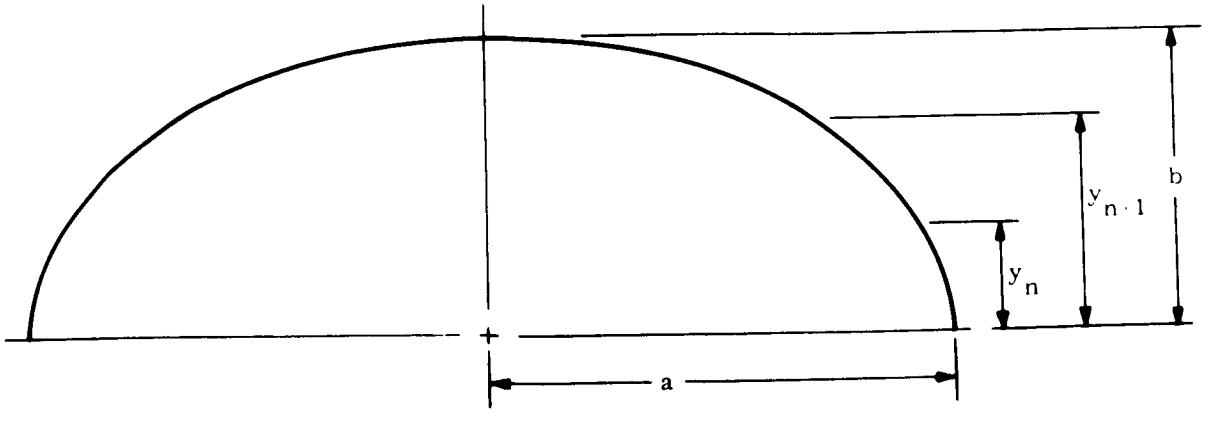

Figure Q-4. Determination of Weight

Q.5 NOMENCLATURE

N_x	Meridional load per inch (lbs/inch).
N_y	Hoop load per inch (lbs/inch).
p	External pressure (psi).
b_s	Rib spacing (inches).
b_w	Rib depth (inches).
t_w	Rib thickness (inches).
t_s	Skin thickness (inches).
H	Overall waffle depth (inches).
μ	Poisson's ratio.
E	Young's modulus of elasticity (psi).
R	Equivalent spherical radius of curvature (inches).
C	Buckling correction factor.
a	Major radius of ellipsoid (inches).
b	Minor radius of ellipsoid (inches).
ρ	Density of material (lbs/ft^3).
D	Flexural stiffness of the skin and ribs in the hoop and meridional directions.
p_{cr_g}	Critical buckling pressure (psi).
r_{w_s}	Fillet radius at intersection of ribs and skin (inches).
r_s	Radius of intersection of ribs (inches).

REFERENCES

1. Saturn V Launch Vehicle Design Data, MSFC IN-P&VE-62-2, 17 December 1962, Reissued 15 July 1964 (Confidential).

2. F.R. Shanely, Strength of Materials, McGraw-Hill Book Company, New York, 1957.

3. Metallic Materials and Elements for Flight Vehicle Structures, MIL-HDBK-5, August 1962.

4. Properties of Missile Materials at Cryogenic Temperatures, The Martin Company, May 1960.

5. Cryogenic Materials Data Handbook, Technical Document Report No. ML-TDR-64-280, August 1964.

6. Structural Materials Data Manual, Volume I, General Electric Company Missile and Space Division.

7. Aerospace Structural Metals Handbook, Volume II, "Non-Ferrous Alloys," ASD-TDR-63-741, March 1963.

8. Progress Report of the NASA Special Committee on Materials Research for Supersonic Transports, NASA TN-D-1798, May 1963.

9. H. Becker, General Instability of Stiffened Cylinders, NACA TN 4237, July 1958.

10. E.W. Kuenzi, Effect of Length on the Buckling Stresses of Thin-Walled, Plywood Cylinders in Axial Compression, Forest Products Laboratory, U.S. Dept. of Agriculture, Report No. 1514, January 1959.

11. R. Ravenhall, Designing for Stiffness and Buckling in Filament-Wound Rocket Case Structures, Hercules Powder Company, Rocky Hill, New Jersey.

12. M.F. Card, Bending Tests of Large Diameter Stiffened Cylinders Susceptible to General Instability, NASA TN-D-2200, April 1964.

13. P. Seide, The Effectiveness of Integral Waffle-Like Stiffening for Long, Thin Circular Cylinders Under Axial Compression, The Ramo-Woolridge Corp., Report No. AM6-10.

14. L. Lackman and J. Penzien, Buckling of Circular Cones Under Axial Compression, ASME Paper No. 60-APM-17, 18 June 1959.

15. L.E. Kaechele, Minimum Weight Design of Sandwich Panels, ASTIA Document No. AD 133011, 22 March 1957.

16. Mechanical Properties of Hexcel Honeycomb Materials, Hexcel Products Inc. Bulletin No. TSB120, February 1964.

17. M. Stein and J. Mayers, Compressive Buckling of Simply Supported Curved Plates and Cylinders of Sandwich Construction, NACA Technical Note 2601, January 1952.

18. J.H. Cunningham and M.J. Jacobson, Design and Testing of Honeycomb Sandwich Cylinders Under Axial Compression, Engineering Paper No. 1393, Missile and Space Division, Douglas Aircraft Co., August 1962.

19. J.H. Cunningham and M.J. Jacobson, Design and Testing of Honeycomb Sandwich Cylinders Under Axial Compression, NASA TN-D-1510, December 1962.

20. T.E. Hess, Analysis of Honeycomb Shells, PIR SM-8156-561, Missile and Space Division, General Electric Company, December 1963.

21. A. Krivetsky, Approximate Core Thickness Required for Sandwich Plates and Shells in Compression, Report No. 7-58-0252-1, Bell Aircraft Corp., August 1958.

22. T.E. Hess and J.R. Vinson, Behavior of Orthotropic Structures, Document No. 61SD46, General Electric Company, March 1961.

23. R.J. Roark, Formulas for Stress-Strain, McGraw-Hill Book Company, Inc., New York, 1954.

24. Structures Data Sheet No. 02.01.25, Royal Aeronautical Society.

25. D.J. Farrar, "The Design of Compression Structures for Minimum Weight," Journal of the Royal Aeronautical Society, November 1949.

26. F.R. Shanley, Weight-Strength Analysis of Aircraft Structures, Second Edition, Dover Publications, New York.

27. S. Timoshenko, Theory of Elastic Stability, McGraw-Hill Book Company, New York, 1936.

28. Zophres, Voce, and Striekler, Design Buckling Criteria for Cylinders and Truncated Cones of Small Semi-Vertex Angle in the Low R/t and Z Parameter Ranges, S-TL Document No. 6120-J280-RV000.

29. D.L. Block, M.F. Card, and M.M. Mikulas, Jr., Buckling of Eccentrically Stiffened Orthotropic Cylinders, NASA TN-D-2960, August 1965.

30. F.A. Dittoe and A.H. Hausrath, Estimated Design [for] Allowable Buckling Stresses for the Stability of Spherical Shells of Conventional Sandwich Construction Under Uniform External Pressure, AS-D-690, Convair Aviation, General Dynamics Corp., December 1960.

31. R. F. Crawford and D. B. Schwartz, "General Instability and Optimum Design of Grid-Stiffened Spherical Domes," AIAA Journal, Volume 3, No. 3, March 1965.

32. R. R. Meyer and R. J. Bellifante, Fabrication and Experimental Evaluation of Common Domes Having Waffle-Like Stiffening, Part I, Report No. SM-47742, Douglas Aircraft Corp., November 1964.

ERRATA

NASA SP-6008 and SP-6008-01

Volumes I and II

STRUCTURAL SYSTEMS AND PROGRAM DECISIONS

Prepared by

Apollo Program Office

Please replace the foreword in Volumes I and II of NASA SP-6008 and SP-6008-01 with the attached new forewords.

Issued 9-6-66

FOREWORD

This document, though an official release of the Apollo Program Office, is furnished for information purposes only. Its purpose is to present an automated methodology that provides the user with a tool to rapidly assess the effect that structural systems have upon launch vehicle weight and performance as a result of changes in design criteria, materials, and manufacturing.

This book is primarily intended for those in the administration, design, development, manufacture, and test of Apollo System. The text emphasizes the importance of the structural system to overall space vehicle performance which results from the trade-off between launch vehicle hardware weight and payload capability. The need for such a rapid assessment tool results from the frequent recommendations made to improve stage capability on a basis of structural design criteria refinements.

The text provides to those who wish to apply the developed methodology, all details necessary to do so, and includes the mathematical development, computer program user's manuals and necessary instructions and procedures.

Launch Vehicle Structural System Assessments is intended to be a constructive aid to the NASA Apollo Team in assisting them in the weight and performance area.

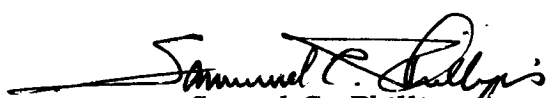

Samuel C. Phillips
Major General, USAF
Director, Apollo Program